frontiers | Research Topics

Multiple sclerosis and related disorders: Challenges and approaches to mechanisms, biomarkers, and therapeutic targets

Edited by
Jinzhou Feng, Philippe Monnier, Shougang Guo and Cong-Cong Wang

Published in
Frontiers in Immunology
Frontiers in Neurology

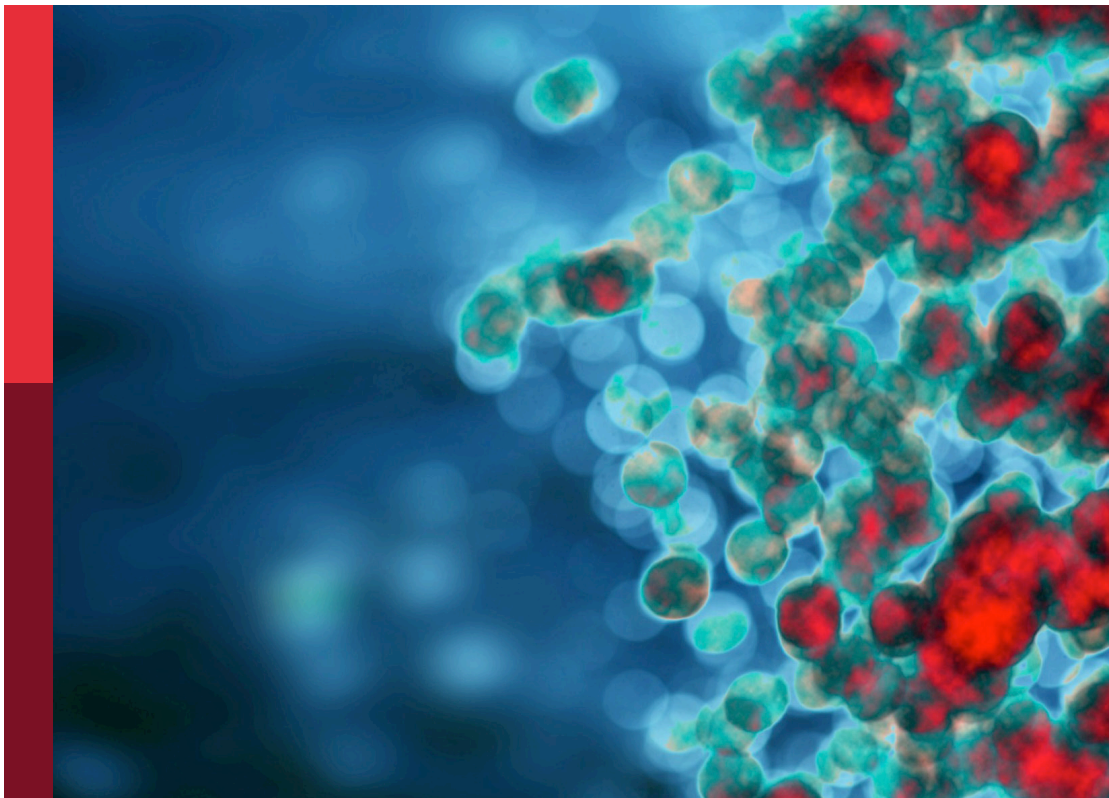

ISSN 1664-8714
ISBN 978-2-8325-4955-1
DOI 10.3389/978-2-8325-4955-1

About Frontiers

Frontiers is more than just an open access publisher of scholarly articles: it is a pioneering approach to the world of academia, radically improving the way scholarly research is managed. The grand vision of Frontiers is a world where all people have an equal opportunity to seek, share and generate knowledge. Frontiers provides immediate and permanent online open access to all its publications, but this alone is not enough to realize our grand goals.

Frontiers journal series

The Frontiers journal series is a multi-tier and interdisciplinary set of open-access, online journals, promising a paradigm shift from the current review, selection and dissemination processes in academic publishing. All Frontiers journals are driven by researchers for researchers; therefore, they constitute a service to the scholarly community. At the same time, the *Frontiers journal series* operates on a revolutionary invention, the tiered publishing system, initially addressing specific communities of scholars, and gradually climbing up to broader public understanding, thus serving the interests of the lay society, too.

Dedication to quality

Each Frontiers article is a landmark of the highest quality, thanks to genuinely collaborative interactions between authors and review editors, who include some of the world's best academicians. Research must be certified by peers before entering a stream of knowledge that may eventually reach the public - and shape society; therefore, Frontiers only applies the most rigorous and unbiased reviews. Frontiers revolutionizes research publishing by freely delivering the most outstanding research, evaluated with no bias from both the academic and social point of view. By applying the most advanced information technologies, Frontiers is catapulting scholarly publishing into a new generation.

What are Frontiers Research Topics?

Frontiers Research Topics are very popular trademarks of the *Frontiers journals series*: they are collections of at least ten articles, all centered on a particular subject. With their unique mix of varied contributions from Original Research to Review Articles, Frontiers Research Topics unify the most influential researchers, the latest key findings and historical advances in a hot research area.

Find out more on how to host your own Frontiers Research Topic or contribute to one as an author by contacting the Frontiers editorial office: frontiersin.org/about/contact

Multiple sclerosis and related disorders: Challenges and approaches to mechanisms, biomarkers, and therapeutic targets

Topic editors

Jinzhou Feng — First Affiliated Hospital of Chongqing Medical University, China
Philippe Monnier — University Health Network (UHN), Canada
Shougang Guo — Department of Neurology, Shandong Provincial Hospital, China
Cong-Cong Wang — The First Affiliated Hospital of Shandong First Medical University, China

Citation

Feng, J., Monnier, P., Guo, S., Wang, C.-C., eds. (2024). *Multiple sclerosis and related disorders: Challenges and approaches to mechanisms, biomarkers, and therapeutic targets*. Lausanne: Frontiers Media SA. doi: 10.3389/978-2-8325-4955-1

Table of contents

frontiers | Frontiers in Neurology

TYPE Editorial
PUBLISHED 17 May 2024
DOI 10.3389/fneur.2024.1427299

OPEN ACCESS

EDITED AND REVIEWED BY
Robert Weissert,
University of Regensburg, Germany

*CORRESPONDENCE
Philippe Patrick Monnier
✉ Philippe.Monnier@uhnresearch.ca
Jin-Zhou Feng
✉ fengjinzhou@hotmail.com
Shou-Gang Guo
✉ guoshougang1124@163.com
Cong-Cong Wang
✉ skyfly_32633@126.com

RECEIVED 03 May 2024
ACCEPTED 09 May 2024
PUBLISHED 17 May 2024

CITATION
Zhou Y, Monnier PP, Feng J-Z, Guo S-G and Wang C-C (2024) Editorial: Multiple sclerosis and related disorders: challenges and approaches to mechanisms, biomarkers, and therapeutic targets.
Front. Neurol. 15:1427299.
doi: 10.3389/fneur.2024.1427299

Editorial: Multiple sclerosis and related disorders: challenges and approaches to mechanisms, biomarkers, and therapeutic targets

Yang Zhou[1], Philippe Patrick Monnier[2]*, Jin-Zhou Feng[3]*, Shou-Gang Guo[4]* and Cong-Cong Wang[1,5]*

[1]Department of Neurology, The First Affiliated Hospital of Shandong First Medical University, Shandong Provincial Qianfoshan Hospital, Jinan, China, [2]Department of Physiology, University of Toronto, Toronto, ON, Canada, [3]Department of Neurology, The First Affliated Hospital of Chongqing Medical University, Chongqing, China, [4]Department of Neurology, Shandong Provincial Hospital Affiliated to Shandong First Medical University, Shandong Academy of Medical Sciences, Jinan, China, [5]Shandong Institute of Neuroimmunology, Jinan, China

KEYWORDS

MS, NMOSD, MOGAD, molecular mechanisms, biomarkers, therapeutic

Editorial on the Research Topic
Multiple sclerosis and related disorders: challenges and approaches to mechanisms, biomarkers, and therapeutic targets

Multiple sclerosis (MS)-related disorders are chronic autoimmune disease of the central nervous system (CNS) characterized by inflammation, demyelination, and neurodegeneration. Common MS-related disorders include MS, neuromyelitis optica spectrum disorder (NMOSD), myelin oligodendrocyte glycoprotein-antibody-associated disorders (MOGAD), and other diseases, which have relatively independent clinical features and diagnostic markers. In addition, biomarkers of MS-related disorders are employed in clinical diagnosis, estimation of disease risk or prognosis, assessment of disease staging, and monitoring of disease progression or response to therapy (1). However, at present, there is no cure for MS-related disorders. Disease-modifying therapies (DMTs) represent the mainstay of treatment, and patients are generally required to undergo lifelong treatment. In order to facilitate the dissemination of the latest research findings in this field, we have organized this Research Topic. The Research Topic comprises 10 manuscripts that expand contemporary knowledge and understanding of the mechanisms, biomarkers, and therapeutic targets of MS and related diseases.

MS is a CNS inflammatory demyelinating disease that involves white matter. The pathogenesis of MS is mainly due to auto-reactive lymphocytes (T and B cells), innate immune and microglial cells, which synergistically mediate myelin loss, secondary axonal injury, and astrocyte reactive hyperplasia (2). The disease may be related to genetic, environmental, viral infection, and other factors. Neurofilament light (NfL) has been identified as a marker of axonal damage. Mi et al. conducted a study in which they analyzed NfL levels in the plasma of MS patients in conjunction with clinical and magnetic resonance imaging (MRI) assessments. The level of plasma NfL is correlated with the activity and severity of MS, and is therefore anticipated to become a novel biomarker

for the assessment of MS activity and disease status. The protein growth arrest specific 6 (Gas6) and its tyrosine kinase receptors Tyro-3, Axl, Mer (TAMs) have been linked to the remyelination of neurons and the stimulation of oligodendrocyte survival. D'Onghia et al. assessed the soluble levels of Gas6-TAMs in serum and cerebrospinal fluid (CSF), at the time of MS diagnosis, and to evaluate their possible correlations with short-term disease severity. The serum levels of Axl were found to be higher in patients with lower disability at the time of onset, while the serum levels of Gas6 were higher in patients with lower disability over time. These findings suggest that serum Gas6 may be a reliable prognostic biomarker. Zhang X. et al. reported that the nationwide prevalence of CSF-OCB in Chinese MS patients was 76.4%, and demonstrated that their diagnostic approach is effective in differentiating MS from other CNS diseases. The prevalence of CSF-OCB demonstrated an association with high latitude and altitude in Chinese MS patients. Dorsch et al. conducted a study to examine disease progression in patients with MS, defined using an objective, home-based assessment of motor functions, compared to 3-month confirmed disease progression (3-mCDP) as defined by the EDSS. It may be beneficial to reduce the length of observation periods during clinical trials, which would enhance confidence in the ability to identify progression events associated with MS. Zhang L. et al. proposed that lacune may serve as a potential MRI biomarker in MS. In this study, they sought to elucidate the relationship between small vessel disease (CSVD) and MS using lacune as a biomarker. Arisi et al. identified drug-dependent alterations in miRNA profiles in patients with relapsing-remitting MS (RRMS) and proposed a series of candidate miRNAs that they believe may be involved in the corresponding pharmacological mechanisms.

NMOSD is a rare relapsing neuroinflammatory autoimmune disease that primarily affects the optic nerves and spinal cord. Most cases exhibit aquaporin-4-antibody positivity. The pathological mechanism of NMOSD differs from that of MS, primarily involving autoimmune injury of astrocytes, secondary demyelinating changes, and perivascular inflammation, including neutrophil and eosinophilic infiltration (3). The most common associations of MOGAD include central nervous system demyelination, which manifests as acute disseminated encephalomyelitis in children, optic neuritis (ON) and transverse myelitis (TM) in children and adults. Unlike MS, MOGAD does not typically present with radiographic white matter changes (4). Wang et al. demonstrated that an elevated systemic immune-inflammation index (SIRI) may serve as a distinguishing indicator for differentiating MOGAD from AQP4-IgG-positive NMOSD. Additionally, they observed that decreased MLR levels may be associated with an increased probability of MOGAD recurrence. Ma et al. demonstrated that patients with mild disability NMOSD exhibited compensatory increases in local network properties to maintain stability at the system level. Additionally, they observed that alterations in the morphological network nodal properties of NMOSD patients were more relevant for clinical assessments when compared with functional network nodal properties. Furthermore, they found that these alterations exhibited predictive values of worsening in the Expanded Disability Status Scale (EDSS) scores. Asseyer et al. found that lower cervical spinal cord volume was associated with increased pain in patients with AQP4-IgG-positive NMOSD. Furthermore, regional spinal cord MRI measures have been identified as being crucial for monitoring disease-related changes within the spinal cord of individuals diagnosed with AQP4-IgG-positive NMOSD and MOGAD.

Finally, autoimmune encephalitis is defined as a non-infectious, immune-mediated inflammatory process that affects the brain parenchyma. It is characterized by the presence of neural antibodies in a significant proportion of patients (5). Anti-NMDA receptor (NMDAR) encephalitis is a prevalent autoimmune encephalitis, with GluN1 antibodies as a key causal factor. Prompt identification is of critical consequence. Iizuka et al. demonstrated that the severity of the disease in patients and the presence of four key symptoms were associated with higher levels of GluN1-ab antibodies in CSF samples taken at the time the disease was first diagnosed. The results may indicate a potential link between the presence of these antibodies and the subsequent one-year functional status of patients.

In conclusion, the articles in this Research Topic expand current knowledge regarding the mechanisms, biomarkers, and therapeutic targets of MS and related diseases. The findings of these studies offer novel scientific evidence and provide insights into the latest advances in this rapidly developing field.

Author contributions

YZ: Writing – original draft. PM: Writing – review & editing. J-ZF: Writing – review & editing. S-GG: Writing – review & editing. C-CW: Writing – review & editing.

Funding

The author(s) declare that financial support was received for the research, authorship, and/or publication of this article. This work was supported by grants from the National Natural Science Foundation of China (82371356) and the China Postdoctoral Science Foundation (2023M732135).

Conflict of interest

The authors declare that the research was conducted in the absence of any commercial or financial relationships that could be construed as a potential conflict of interest.

Publisher's note

References

1. Lleo A. Biomarkers in neurological disorders: a fast-growing market. *Brain Commun.* (2021) 3:fcab086. doi: 10.1093/braincomms/fcab086

2. Kuhlmann T, Moccia M, Coetzee T, Cohen JA, Correale J, Graves J, et al. Multiple sclerosis progression: time for a new mechanism-driven framework. *Lancet Neurol.* (2023) 22:78–88. doi: 10.1016/S1474-4422(22)00289-7

3. Siriratnam P, Huda S, Butzkueven H, van der Walt A, Jokubaitis V, et al. A comprehensive review of the advances in neuromyelitis optica spectrum disorder. *Autoimmun Rev.* (2023) 22:103465. doi: 10.1016/j.autrev.2023.103465

4. Rinaldi S, Davies A, Fehrni J, Beadnall HN, Wanh J, Hardy T, et al. Overlapping central and peripheral nervous system syndromes in MOG antibody-associated disorders. *Neurol Neuroimmunol Neuroinflamm.* (2021) 8:924. doi: 10.1212/NXI.0000000000000924

5. Abbatemarco JR, Yan C, Kunchok A, Rae-Grant A. Antibody-mediated autoimmune encephalitis: a practical approach. *Cleve Clin J Med.* (2021) 88:459–71. doi: 10.3949/ccjm.88a.20122

frontiers | Frontiers in Neurology

TYPE Original Research
PUBLISHED 08 August 2023
DOI 10.3389/fneur.2023.1224748

OPEN ACCESS

EDITED BY
Jinzhou Feng,
First Affiliated Hospital of Chongqing Medical University, China

REVIEWED BY
Honghao Wang,
Guangzhou First People's Hospital, China
Philippe Monnier,
University Health Network (UHN), Canada
Qinming Zhou,
Shanghai Jiao Tong University, China

*CORRESPONDENCE
Ning Wang
ningwang@fjmu.edu.cn
Ying Fu
fuying@fjmu.edu.cn

†These authors have contributed equally to this work

RECEIVED 18 May 2023
ACCEPTED 25 July 2023
PUBLISHED 08 August 2023

CITATION
Zhang L, Yu X, Zheng Y, Lin A, Zhang Z, Li S, Wang N and Fu Y (2023) Lacunes are associated with late-stage multiple sclerosis comorbidities.
Front. Neurol. 14:1224748.
doi: 10.3389/fneur.2023.1224748

Lacunes are associated with late-stage multiple sclerosis comorbidities

Lijie Zhang[1,2†], Xintong Yu[1,2†], Yexiang Zheng[1,2], Aiyu Lin[1,2], Zaiqiang Zhang[3], Shaowu Li[4], Ning Wang[1,2*] and Ying Fu[1,2,3*]

[1]Department of Neurology and Institute of Neurology of The First Affiliated Hospital, Institute of Neuroscience, Fuzhou, China, [2]Fujian Key Laboratory of Molecular Neurology, Fujian Medical University, Fuzhou, China, [3]Department of Neurology, China National Clinical Research Center for Neurological Diseases, Beijing Tiantan Hospital, Capital Medical University, Beijing, China, [4]Department of Neuroimaging, Beijing Neurosurgical Institute, Beijing Tiantan Hospital, Capital Medical University, Beijing, China

Multiple sclerosis (MS) is a condition that affects the veins and small blood vessels. Previous research suggests that individuals with MS have an increased risk of vascular events and higher mortality rates. However, the relationship between MS and cerebral small vessel disease (CSVD) remains uncertain. This study aims to investigate the association between MS and lacunes. A prospective observational study was conducted, including a total of 112 participants, of which 46 had MS and 66 had CSVD. All participants underwent an MRI scan and a battery of neurological functional assessments. The presence of definite lacunes and black holes was determined through the analysis of T2-weighted, T1-weighted, and FLAIR images. The occurrence of lacunes in MS patients was found to be 19.6%. Notably, the duration of MS was identified as the sole risk factor for the development of lacune lesions in MS patients [odds ratio (OR) = 1.3, 95% confidence interval (CI) = 1.1–1.6, $p = 0.008$]. Comparatively, MS patients with lacunes exhibited a higher frequency of attacks and larger volumes of T2 lesions compared to MS patients without lacunes. Further analysis using receiver operating characteristic (ROC) curves showed that lacune lesions had limited ability to discriminate between MS and CSVD when disease duration exceeded 6 years. The presence of small arterial lesions in the brain of individuals with MS, along with the duration of the disease, contributes to the development of lacunes in MS patients.

KEYWORDS

multiple sclerosis (MS), cerebral small vessel disease (CSVD), lacune, disease duration, arteriolar damage

Introduction

Black holes in multiple sclerosis (MS) are characterized by T1 hypointense and T2 hyperintense lesions on MRI (1). These lesions can be categorized as either acute black holes, which may either progress to permanent black holes or transform into transient black holes (2). The exact etiology and pathogenesis of black holes remain uncertain. Some studies have proposed that CD8-mediated immune damage may contribute to the formation of black holes (3–5).

While MS primarily affects veins and venules, cerebral small vessel disease (CSVD) primarily affects small arteries. Aging, vascular risk factors (VRFs), and chronic inflammation are known to cause damage to the microvascular system, including the small arteries, resulting

in hypoperfusion and tissue hypoxia that can influence the extent and distribution of MS-related pathology (6).

Lacunes, which are residual lesions of lacunar infarction or small hemorrhagic foci, serve as prominent imaging features of CSVD, reflecting intracranial arteriole lesions (7). Therefore, in this study, we focused on monitoring lacunar lesions to explore potential associations between CSVD and MS. We aimed to investigate the incidence of lacunes in an MS cohort and evaluate the related risk factors based on demographic and clinical characteristics, shedding light on the potential clinical significance of lacunes in MS patients.

Materials and methods

Patients

In this ongoing study, we prospectively collected clinical, demographic, and imaging data from patients diagnosed with MS and CSVD. The patients were hospitalized at Tian Tan Hospital of Capital Medical University in Beijing, China, between 2015 and 2017. MS diagnosis was made according to the 2010 McDonald MS standard (8) while CSVD diagnosis followed the 2013 European "Neuroimaging standards for research into small vessel disease" (9). Patients who fell into both categories of MS and CSVD were explicitly excluded from this study. All participants completed a structured questionnaire (10) and underwent physical and neurological assessments during their hospital stay (11).

Criteria for patient selection in our investigation were as follows:

1. Undergoing an MRI examination at least 2 days after the completion of physical and/or neurological examinations during hospitalization.
2. Having a fully documented medical record including information on hypertension, hyperlipidemia, diabetes, atrial fibrillation, current smoking, alcohol use, age at onset, age at baseline, disease duration at baseline, number of attacks, annual recurrence rate (ARR), number of relapses, and the use of any form of disease-modifying therapy (DMT).
3. Undergoing a comprehensive neurological examination, including the Expanded Disability Status Scale (EDSS) and modified Rankin scale (mRS).

Patients were excluded based on the following criteria: (a) MS patients who experienced relapse and receive steroid treatment within 30 days before study entry, (b) Pre-existing medical conditions associated with brain pathologic processes such as cerebrovascular disease or a history of alcohol abuse, (c) Confirmation of ischemic or hemorrhagic infarcts in the brain as observed in MRI, and (d) Pregnancy.

MRI protocol

All patients underwent brain MRI using a 3.0-T scanner (Magnetom Trio Tim; Siemens) equipped with a 32-channel head coil. The imaging protocol included diffusion-weighted imaging (DWI), T2-weighted imaging, fluid-attenuated inversion recovery (FLAIR), and T1-weighted imaging (12).

MR imaging analysis

During the analysis, the MR imaging experts were blinded to the physical and neurological conditions of the subjects. Two experienced neuroimagers, also blinded to MR images obtained through other analytical sequences, assessed lacune lesions on T2-, T1-weighted, and FLAIR images. Lacunes were defined as a round or ovoid subcortical fluid-filled cavity (CSF-like signal) between 3 mm and approximately 15 mm in diameter, consistent with a previous acute small subcortical infarct or haemorrhage in the territory of a perforating arteriole. The diameter of the involved perforating arteriole varies from 40 to 850 μm, and the diameter of the associated infarct ranges from 2 to 3 mm to 15 mm or larger (9). Importantly, we distinguished these lesions from "black holes" (13, 14), which were round or elliptical in shape with neat edges and showed a liquid or near-liquid low signal on the T1 image. In addition, there is rarely a low signal on the FLAIR image due to the presence of myelin regeneration in the lesion. T2-, T1-weighted, and FLAIR images (Figure 1) were used to identify definite lacune lesions and black holes. To determine the volumes of individual white matter hyperintensity (WMH) lesions, manual segmentation was performed using MRIcro software based on the T2 images.[1]

Reproducibility of lacune assessment

To ensure accuracy in identifying lacune lesions, two raters independently assessed their presence. Both raters were blinded to each other's evaluations and their own previous assessments. Interclass correlation coefficients were calculated, and the values exceeded 0.8. Where there was discrepancy between the two raters, a third rater's assessment was used.

Statistical analysis

All statistical analyses were conducted using SPSS 17.0 (SPSS Inc., Chicago, IL). Differences between MS patients with and without lacune lesions were assessed using chi-square and Mann–Whitney tests. We used chi-square tests for gender, hypertension, hyperlipidemia, diabetes, atrial fibrillation, current smoking, and alcohol between MS patients with and without lacune lesions, as well as to compare the frequency of lacune in different groups of patients. Binary logistic regression analysis was performed to adjust for potential confounding factors. The diagnostic value of lacune lesions was determined using receiver operating characteristic (ROC) curves, with stratified evaluation at a time point of 6 years.

Results

We enrolled a total of 46 patients with MS and 66 patients with CSVD through a meticulous selection process. Among the MS patients, the median age was 32 years (range: 25–56 years), and the

1 http://www.cabiatl.com/mricro/mricro/

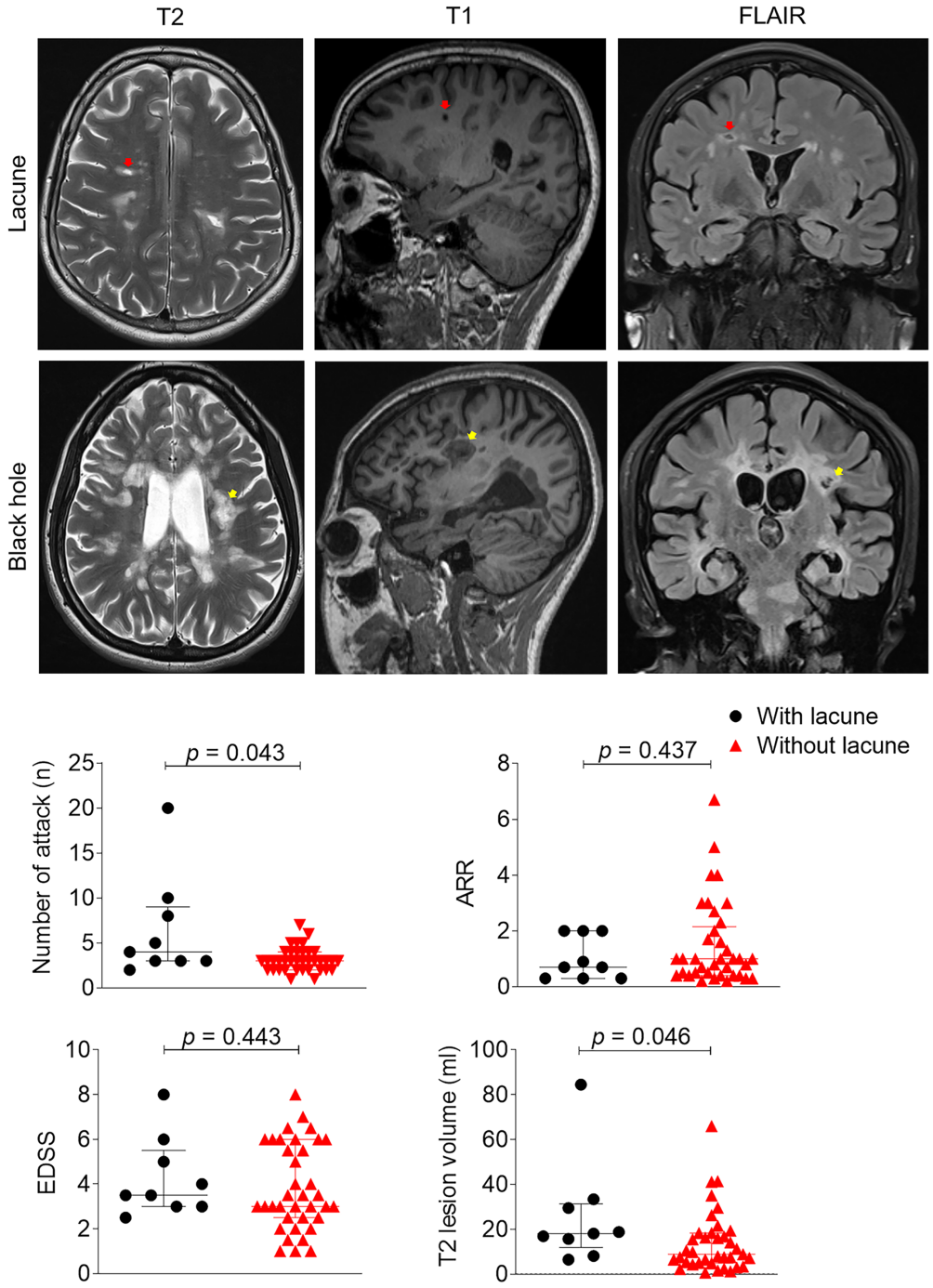

FIGURE 1
Clinical and imaging differences between patients with or without lacune. Example of lacune (red arrow) and black hole lesion (yellow arrow) in this study: Lacunas defined as round or ovoid, subcortical, fluid-filled cavities 3–15 mm in diameter in the territory of 1 perforating arteriole, specifically, lesions were round or elliptical in shape, and edges were neat, showing a liquid or near-liquid low signal on the T1 image. EDSS, expanded disability status scale, ARR, annual relapse rate; inferential statistical analysis was performed with Mann–Whitney tests.

median disease duration was 5 years (range: 2–7 years). Fifteen (33%) of the MS patients were male (Table 1). Nine out of the 46 MS patients met the imaging threshold for lacune lesions (19.6%) (Supplementary Figure S1). We performed Mann–Whitney tests to examine the clinical and demographic characteristics of patients with and without lacune lesions. No significant differences were observed in age or vascular risk factors between the two groups (Table 1). However, there was a significant difference in disease duration [median (IQR), 4 (1.8–6.0) vs. 10 (4.3–13.5), $p = 0.016$]. To adjust for age, we conducted binary logistic regression analysis, which revealed a significant association between disease duration (OR = 1.3, 95% CI = 1.1–1.6, $p = 0.008$) and the presence of lacune lesions. MS patients with lacune lesions exhibited a higher frequency of attacks (6 vs. 3, $p = 0.043$) and larger T2 lesion volumes (19 vs. 23 mL, $p = 0.046$)

TABLE 1 Demographic and clinical characteristics of patients.

Characteristic	MS without lacuna (*N* = 37)	MS with lacuna (*N* = 9)	*P1-value*	MS (*N* = 46)	CSVD (*N* = 66)	*P2-value*
Age, year, median (IQR)	29 (24–36)	36 (29–52)	0.074	32 (25–36)	54 (47–61)	<0.001
Male sex, *n* (%)	12 (32)	3 (33)	1.000	15 (33)	31 (47)	0.129
Hypertension, *n* (%)	0 (0)	1 (11.1)	0.196	1 (2)	42 (64)	<0.001
SBP, mmHg, median (IQR)	115 (105–120)	120 (113–123)	0.233	115 (109–120)	133 (122–144)	<0.001
DBP, mmHg, median (IQR)	75 (67–80)	75 (70–80)	0.387	75 (70–80)	80 (73–86)	<0.001
Hyperlipidemia, *n* (%)	7 (19)	4 (44)	0.24	11 (24)	30 (46)	0.020
Diabetes, *n* (%)	1 (2.7)	0 (0)	1.000	1 (2)	11 (17)	0.033
Atrial fibrillation, *n* (%)	0 (2.7)	0 (0)	1.000	0 (0)	1 (2)	1.000
Current smoking, *n* (%)	1 (2.7)	0 (0)	1.000	1 (2)	23 (35)	<0.001
Alcohol, *n* (%)	1 (2.7)	0 (0)	1.000	1 (2%)	17 (26)	0.001
Disease duration, year, (median, IQR)	4 (1.8–6.0)	10 (4.3–13.5)	0.016	5 (2–7)	2 (1–5)	0.001

Hypertension, systolic blood pressure > 140 mmHg and/or diastolic blood pressure > 90 mmHg; Diabetes, fasting plasma glucose ≥ 7.0 millimoles per liter and/or plasma glucose after a meal for two hours ≥ 11.1 millimoles per liter; Hyperlipidemia, serum total cholesterol levels > 5.72 millimoles per liter and/or triglycerides > 1.7 millimoles per liter. MS, multiple sclerosis; CSVD, cerebral small vessel disease; IQR, inter quartile range. χ^2 test and Mann–Whitney test for differences between patient with lacuna and without (*P1*) or for differences between CSVD patient and MS patient (*P2*).

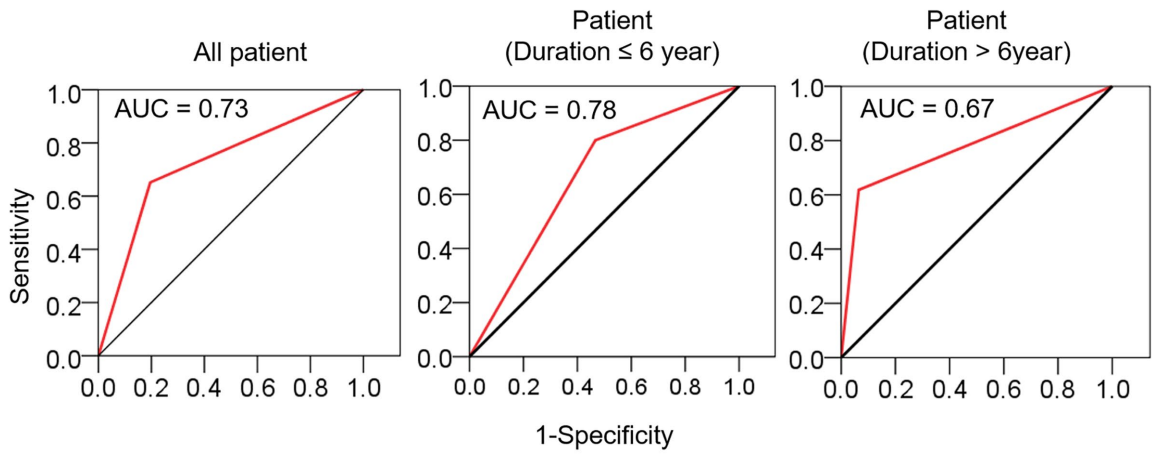

FIGURE 2
The sensitivity and specificity of lacune in distinguishing MS from CSVD. ROC curves were used to evaluate the diagnostic value of lacune, and the stratified evaluation was performed at a time point of 6 years. AUC, area under curve.

compared to those without lacune lesions (Figure 1). No differences were observed in ARR (0.7 vs. 1.0, $p = 0.437$), EDSS (3.5 vs. 3.0, $p = 0.443$) and mRS (1.0 vs. 1.0, $p = 0.482$).

Comparison between the MS and CSVD groups revealed a higher incidence of traditional VRFs among CSVD patients (Table 1). There was a significant difference in the incidence of lacunes between the CSVD and MS groups (65.1% vs. 19.6%, $p < 0.001$), with an area under the ROC curve (AUC) of 0.73. However, when stratified by disease duration at a time point of 6 years, the AUC values decreased for patients with a disease course of >6 years (AUC = 0.67) (Figure 2), suggesting a diminishing ability to discriminate lacunar lesions with prolonged disease duration. Notably, the frequency of lacune lesions in MS patients with a disease duration over 6 years was comparable to that of CSVD patients (46.7 vs. 65.1%, $p = 0.184$).

Discussion

Our study aimed to investigate the frequency and clinical significance of lacune lesions in individuals diagnosed with MS. By comparing the clinical features of MS patients with and without such lesions and analyzing the ROC curve after age stratification, we found that disease duration was the only significant risk factor for the occurrence of lacune lesions in MS patient. Furthermore, these findings suggest that the duration of MS increases the risk of CSVD, highlighting the time sensitivity and the importance of initiating preventive treatments at an appropriate time.

To the best of our knowledge, there are no existing reports exploring the potential relationship between lacune lesions and MS. Classical descriptions of lacunae can include lacune lesions (9), which can be challenging to distinguish from "black holes" in images

(13, 14). To overcome this challenge, we further defined the distinguishing characteristics of lacune lesions in the imaging data of our study cohort. Based on our assessment criteria, we determined that the incidence of lacune lesions in the study population was 19.6%. It is important to note that the actual incidence is expected to be higher than the reported value we detected.

Traditional VRFs such as hypertension, diabetes, hyperlipidemia, and smoking were not significant factors in MS patients (with incidence rates of 2.2%, 2.2%, 23.9%, and 2.2% respectively). This could be attributed to the younger age [median (IQR): 31.5 (24.8–36.3)] of the enrolled population in our study compared to the aforementioned study. Several publications have shown an increased rate of ischemic stroke (IS) in MS patients (15, 16). Similarly, CSVD patients also exhibit a higher incidence of IS. Therefore, we were interested in exploring the differences in the development and causal influences of lacunes in MS patients compared to CSVD patients. The level of VRFs was higher in the CSVD cohort compared to the MS cohort, and the overall incidence of lacunes was also higher. When drawing ROC curves using lacune lesions, age-stratified analysis revealed that when the disease duration exceeded 6 years, lacune lesions had limited discriminatory capability between MS and CSVD. This further emphasizes the association between lacune lesions and MS disease duration, suggesting that intervention therapy for CSVD should be initiated at an appropriate time in the MS population.

There are several limitations to our study that should be acknowledged. First, the sample size was relatively small and should be expanded to further support our conclusions. Additionally, the mechanism underlying the increased risk of cerebral small vessel disease in MS patients remains unclear. It is hypothesized that MS disease creates a chronic inflammatory environment that damages small arterioles in the brain (6), but empirical confirmation is needed.

Data availability statement

The original contributions presented in the study are included in the article/Supplementary material, further inquiries can be directed to the corresponding authors.

Ethics statement

The studies involving human participants were reviewed and approved by Tian Tan Hospital of Capital Medical University. The patients/participants provided their written informed consent to participate in this study.

Author contributions

YF formulated the study concept. YF and AL acquired funding for the study. YF and NW designed the study. LZ, YZ, ZZ, XY, and SL collected data. SL, YF, LZ, and YZ analyzed the data. YF and YZ wrote the manuscript. All authors contributed to the article and approved the submitted version.

Funding

This work was supported by the grants U21A20360 (YF) and 82271375 (AL) from the National Natural Science Foundation of China; the grant 2020Y9129 (YF) from the Joint Funds for the innovation of science and Technology of Fujian Province.

Acknowledgments

The authors thank our patients for participating in this study, the clinical neuroimmunology team for recruiting the patients.

Conflict of interest

The authors declare that the research was conducted in the absence of any commercial or financial relationships that could be construed as a potential conflict of interest.

Publisher's note

Supplementary material

The Supplementary material for this article can be found online at: https://www.frontiersin.org/articles/10.3389/fneur.2023.1224748/full#supplementary-material

References

1. Barkhof F, McGowan JC, van Waesberghe JH, Grossman RI. Hypointense multiple sclerosis lesions on T1-weighted spin echo magnetic resonance images: their contribution in understanding multiple sclerosis evolution. *J Neurol Neurosurg Psychiatry*. (1998) 64:S77–9.

2. Sahraian MA, Radue EW, Haller S, Kappos L. Black holes in multiple sclerosis: definition, evolution, and clinical correlations. *Acta Neurol Scand*. (2010) 122:1–8. doi: 10.1111/j.1600-0404.2009.01221.x

3. Fazekas F, Strasser-Fuchs S, Schmidt H, Enzinger C, Ropele S, Lechner A, et al. Apolipoprotein E genotype related differences in brain lesions of multiple sclerosis. *J Neurol Neurosurg Psychiatry*. (2000) 69:25–8. doi: 10.1136/jnnp.69.1.25

4. Enzinger C, Ropele S, Smith S, Strasser-Fuchs S, Poltrum B, Schmidt H, et al. Accelerated evolution of brain atrophy and "black holes" in MS patients with APOE-epsilon 4. *Ann Neurol*. (2004) 55:563–9. doi: 10.1002/ana.20027

5. Pirko I, Nolan TK, Holland SK, Johnson AJ. Multiple sclerosis: pathogenesis and MR imaging features of T1 hypointensities in a (corrected) murine model. *Radiology*. (2008) 246:790–5. doi: 10.1148/radiol.2463070338

6. Geraldes R, Esiri MM, DeLuca GC, Palace J. Age-related small vessel disease: a potential contributor to neurodegeneration in multiple sclerosis. *Brain Pathol*. (2017) 27:707–22. doi: 10.1111/bpa.12460

7. Wardlaw JM, Smith C, Dichgans M. Mechanisms of sporadic cerebral small vessel disease: insights from neuroimaging. *Lancet Neurol*. (2013) 12:483–97. doi: 10.1016/S1474-4422(13)70060-7

8. Polman CH, Reingold SC, Banwell B, Clanet M, Cohen JA, Filippi M, et al. Diagnostic criteria for multiple sclerosis: 2010 revisions to the McDonald criteria. *Ann Neurol*. (2011) 69:292–302. doi: 10.1002/ana.22366

9. Wardlaw JM, Smith EE, Biessels GJ, Cordonnier C, Fazekas F, Frayne R, et al. Neuroimaging standards for research into small vessel disease and its contribution to ageing and neurodegeneration. *Lancet Neurol*. (2013) 12:822–38. doi: 10.1016/S1474-4422(13)70124-8

10. Dolic K, Weinstock-Guttman B, Marr K, Valnarov V, Carl E, Hagemeier J, et al. Risk factors for chronic cerebrospinal venous insufficiency (CCSVI) in a large cohort of volunteers. *PLoS One*. (2011) 6:e28062. doi: 10.1371/journal.pone.0028062

11. Zivadinov R, Marr K, Cutter G, Ramanathan M, Benedict RH, Kennedy C, et al. Prevalence, sensitivity, and specificity of chronic cerebrospinal venous insufficiency in MS. *Neurology*. (2011) 77:138–44. doi: 10.1212/WNL.0b013e318212a901

12. Pichler A, Khalil M, Langkammer C, Pinter D, Ropele S, Fuchs S, et al. The impact of vascular risk factors on brain volume and lesion load in patients with early multiple sclerosis. *Mult Scler*. (2019) 25:48–54. doi: 10.1177/1352458517736149

13. van Walderveen MA, Kamphorst W, Scheltens P, van Waesberghe JH, Ravid R, Valk J, et al. Histopathologic correlate of hypointense lesions on T1-weighted spin-echo MRI in multiple sclerosis. *Neurology*. (1998) 50:1282–8. doi: 10.1212/WNL.50.5.1282

14. van den Elskamp IJ, Lembcke J, Dattola V, Beckmann K, Pohl C, Hong W, et al. Persistent T1 hypointensity as an MRI marker for treatment efficacy in multiple sclerosis. *Mult Scler*. (2008) 14:764–9. doi: 10.1177/1352458507087842

15. Allen NB, Lichtman JH, Cohen HW, Fang J, Brass LM, Alderman MH. Vascular disease among hospitalized multiple sclerosis patients. *Neuroepidemiology*. (2008) 30:234–8. doi: 10.1159/000128103

16. Zoller B, Li X, Sundquist J, Sundquist K. Risk of subsequent ischemic and hemorrhagic stroke in patients hospitalized for immune-mediated diseases: a nationwide follow-up study from Sweden. *BMC Neurol*. (2012) 12:41. doi: 10.1186/1471-2377-12-41

frontiers | Frontiers in Neurology

TYPE Study Protocol
PUBLISHED 10 October 2023
DOI 10.3389/fneur.2023.1258635

OPEN ACCESS

EDITED BY
Jinzhou Feng,
First Affiliated Hospital of Chongqing Medical University, China

REVIEWED BY
Dirk Schriefer,
University Hospital Carl Gustav Carus, Germany
Philipp Albrecht,
Heinrich Heine University of Düsseldorf, Germany

*CORRESPONDENCE
Tanja Schmitz-Hübsch
✉ tanja.schmitz-huebsch@charite.de

RECEIVED 14 July 2023
ACCEPTED 26 September 2023
PUBLISHED 10 October 2023

CITATION
Dorsch E-M, Röhling HM, Zocholl D, Hafermann L, Paul F and Schmitz-Hübsch T (2023) Progression events defined by home-based assessment of motor function in multiple sclerosis: protocol of a prospective study.
Front. Neurol. 14:1258635.
doi: 10.3389/fneur.2023.1258635

Progression events defined by home-based assessment of motor function in multiple sclerosis: protocol of a prospective study

Eva-Maria Dorsch[1,2,3,4,5], Hanna Marie Röhling[1,2,3,6], Dario Zocholl[7], Lorena Hafermann[7], Friedemann Paul[1,2,3,4,5] and Tanja Schmitz-Hübsch[1,2,3,5]*

[1]Experimental and Clinical Research Center, a Cooperation between the Max-Delbrück-Center for Molecular Medicine in the Helmholtz Association and the Charité—Universitätsmedizin Berlin, Berlin, Germany, [2]Experimental and Clinical Research Center, Charité—Universitätsmedizin Berlin, Corporate Member of Freie Universität Berlin and Humboldt-Universität zu Berlin, Berlin, Germany, [3]Max-Delbrück-Center for Molecular Medicine in the Helmholtz Association (MDC), Berlin, Germany, [4]Department of Neurology, Charité—Universitätsmedizin Berlin, Corporate Member of Freie Universität Berlin and Humboldt Universität zu Berlin, Berlin, Germany, [5]Neuroscience Clinical Research Center, Charité—Universitätsmedizin Berlin, Corporate Member of Freie Universität Berlin and Humboldt Universität zu Berlin, Berlin, Germany, [6]Motognosis GmbH, Berlin, Germany, [7]Institute of Biometry and Clinical Epidemiology, Charité—Universitätsmedizin Berlin, Corporate Member of Freie Universität Berlin and Humboldt-Universität zu Berlin, Berlin, Germany

Background: This study relates to emerging concepts of appropriate trial designs to evaluate effects of intervention on the accumulation of irreversible disability in multiple sclerosis (MS). Major starting points of our study are the known limitations of current definitions of disability progression by rater-based clinical assessment and the high relevance of gait and balance dysfunctions in MS. The study aims to explore a novel definition of disease progression using repeated instrumental assessment of relevant motor functions performed by patients in their home setting.

Methods: The study is a prospective single-center observational cohort study with the primary outcome acquired by participants themselves, a home-based assessment of motor functions based on an RGB-Depth (RGB-D) camera, a camera that provides both depth (D) and color (RGB) data. Participants are instructed to perform and record a set of simple motor tasks twice a day over a one-week period every 6 months. Assessments are complemented by a set of questionnaires. Annual research grade assessments are acquired at dedicated study visits and include clinical ratings as well as structural imaging (MRI and optical coherence tomography). In addition, clinical data from routine visits is provided semiannually by treating neurologists. The observation period is 24 months for the primary endpoint with an additional clinical assessment at 27 month to confirm progression defined by the Expanded Disability Status Scale (EDSS). Secondary analyses aim to explore the time course of changes in motor parameters and performance of the novel definition against different alternative definitions of progression in MS. The study was registered at Deutsches Register für Klinische Studien (DRKS00027042).

Discussion: The study design presented here investigates disease progression defined by marker-less home-based assessment of motor functions against 3-month confirmed disease progression (3 m-CDP) defined by the EDSS. The technical approach was chosen due to previous experience in lab-based settings. The observation time per participant of 24, respectively, 27 months is commonly

conceived as the lower limit needed to study disability progression. Defining a valid digital motor outcome for disease progression in MS may help to reduce observation times in clinical trials and add confidence to the detection of progression events in MS.

KEYWORDS

multiple sclerosis, disease progression, outcome measures, gait, balance, motor performance, Kinect, digital biomarker

1. Introduction

Multiple sclerosis (MS) as a neuroinflammatory disease features a chronic course with recurrent relapses of inflammatory activity as well as chronic disability in the long-term. Accumulation of disability in multiple sclerosis may occur as relapse-associated worsening (RAW) or steady progression independent of relapse activity (PIRA) (1). While a number of MS therapies were approved to reduce the frequency of relapses, capturing disease progression in MS still poses a major challenge and an urgent scientific need. A sufficient 'gold standard' of clinical outcome measures in MS research and clinical practice is lacking (2) but highly desirable to assess the effectiveness of novel interventions that target chronic processes rather than relapse in this disorder (3).

A recent review reported on outcomes in phase III clinical trials of secondary progressive multiple sclerosis since 1990 (4). Among the studies reviewed, the Expanded Disability Status Scale (EDSS) (5) was by far the most frequently used outcome measure employed by 16 out of 17 trials. Increase in EDSS ratings confirmed after 3 months was most commonly used to define confirmed disability progression (CDP) events as an endpoint (6). However, there is no clear consensus on this concept and protocols diverge with respect to the time frame used to confirm EDSS progression and the cut-offs used to define increase in EDSS ratings as a function of baseline EDSS score (7, 8). The most important determinant for robust definitions of progression was the length of the confirmation period, as confirmation of the EDSS after 3 or even 6 months provided only imprecise estimates of the long-term disease course (9). Despite its extensive use in MS research, the EDSS as an ordinal scale has several limitations in terms of reliability and sensitivity (10) specifically in the early course of MS (11, 12). Another important source of variability are short-term fluctuations in performance known to occur to a relevant degree in MS (13) as well as in other chronic neurological conditions (14). Furthermore, motor performance may differ between clinical and home-based assessments (15). Thus, some of the limitations of current operational definitions of CDP are related to the fact that they rely on infrequent single-point rater-based assessments in the clinical setting. The concept of 'No evidence of disease activity' (NEDA) has been introduced as a potential endpoint for the evaluation of disease-modifying therapies' (DMTs) effectiveness in relapsing remitting MS (16, 17).

Within this concept events of CDP or lack thereof within a given timeframe, respectively, represent one component. Other components are the absence of clinical relapses and absence of radiological signs of inflammatory disease activity. Recently, predictive value has been shown for total brain volume loss (BVL) on disability progression. Thus, measures of decline in brain volume have been added as a fourth component (NEDA-4) (18). Still, this concept circumvents the challenge to reliably quantify and compare the degrees of disability accumulation between subjects or treatment arms. Further, not all components can be applied in the progressive forms of MS (19).

At a time when chronic disease processes represent the target for future interventions in MS, improving the operational definitions of disability progression remains a key priority of MS research (20). Technical measures to quantify specific functions have been explored in this respect. Walking impairments are reported in up to 75% by people with MS (pwMS) (21) and thus pose a good candidate for quantitative assessment in this disorder. Consequently, the instrumental assessment of gait, mobility or other specific functions has received attention in MS research (15, 22–26). Interestingly, instrumental gait analysis has shown dysfunctional walking patterns despite clinically normal gait function even in early stage disease (27). Technical methods of remote assessment such as commercial activity trackers have a part in recent MS trials protocols (28). However, sources of variance and appropriate definitions of relevant change still need to be established for emerging digital biomarkers (29, 30).

Following this strategy, this investigation aims to devise and evaluate an instrumental definition of CDP in early RRMS by episodic patient self-assessment of motor symptoms at home. Among the various technologies available, we chose a visual-perceptive technology based on commercial RGB-D cameras. As a marker-free method this study applies a consumer-grade RGB-Depth (RGB-D) camera (Microsoft Azure Kinect®) combined with customized software (Motognosis Amsa) for motion capture at home as the primary outcome. As a marker-free method, it has high potential for clinical utility and RGB-D technology has been explored for the purpose of task-based motor assessment in various neurological conditions in research settings (31–34). As a novelty, we here turn the patient into the central operator and home-based application into the primary outcome. This enables data acquisition at higher frequency compared to conventional protocols that rely on in-patient research visits.

Primary endpoint is the accuracy of detection of progression events at 24 month compared to progression events defined as 3-month CDP in EDSS. Relation of such definitions to patients' reports of function and impairment as well as structural change on MR imaging and optical coherence tomography (OCT) will complement the final analysis.

2. Methods

2.1. Study design

The study is a single-center prospective observational cohort study. Study data combines observations from different sources:

patients' remote self-assessment, data from treating neurologists obtained in routine clinical care—both performed semiannually—and data from annual in-person study visits at an academic clinical research center. The primary outcome consists of home-based recordings of short motor tests (Amsa, Motognosis GmbH, Berlin, Germany) performed twice a day for a period of 1 week every 6 months. Patient-reported outcomes is acquired every 6 months using validated questionnaires on specific functions, impairments and quality of life.

Data requested from treating neurologists comprise the Multiple Sclerosis Functional Composite (MSFC-3) (35), the global assessment of the change since last observation [clinical global impression of change (CGI) (36)] and information on relapse events/relapse therapy including recovery, change of therapy or comorbidity since prior visit.

Annual study visits at the research site comprise clinical and functional assessment including Motognosis Labs as well as imaging of brain (MRI) and retina (OCT) detailed below.

The observation period is 24 months for the primary endpoint with an additional clinical assessment at 27 months to confirm progression defined by EDSS.

2.2. Participants

The study targets a sample size of 150 people with a diagnosis of relapsing–remitting MS according to revised McDonald criteria (37) in their earlier disease course defined as <10 years since diagnosis in order to allow some heterogeneity in disability stage. Inclusion was restricted to those able to walk at least short distances with unilateral assistance at baseline—equivalent to ≤6.0 EDSS—in accordance with the requirements of the primary outcome measure. To enhance generalizability of results, study recruitment aims for at least 20% aged 55 or older and for at least 33% of EDSS ≥ 3.5 (moderately affected).

Inclusion further allows use of any intervention for MS or other morbidity as long as this is not considered to affect compliance with the study protocol. Comorbidities are not excluded as long as not considered to interfere with motor performance.

Prior disease activity or other known predictors of disease progression were implemented as additional inclusion criteria to increase expected CDP observations at 24 months while at the same time trying to maintain generalizability of our findings for the target population of early RRMS.

2.2.1. Inclusion criteria

- Written informed consent to participate in this study.
- Participant's age is ≥18 years.
- Participant resides within reasonable range from study center to allow supervision of technical set-up at home and provision of technical back-up.
- Diagnosis of relapsing–remitting multiple sclerosis according to 2017 diagnostic criteria (37).
- AND
  Disease duration of <10 years since diagnosis.
- AND
  EDSS ≤ 6.0 (ability to perform short walking tests with only unilateral assistance).
- AND
  fulfillment of one or more of the following criteria:
  - o history of recent disease activity: ≥ 1 relapse or ≥ 1 new T2 lesion or ≥ 1 Gd + enhancing lesion on MRI over the past 2 years.
  - o OR
    Findings on routine brain MRI from within 6 months prior to screening: total T2 lesion load of ≥10.
  - o OR
    Findings on routine brain MRI from within 6 months prior to screening: any Gd + enhancing lesion.
  - o OR
    Findings on routine MRI from within 6 months prior to screening: ≥ 1 spinal or brainstem lesion.
  - o OR
    Finding on optical coherence tomography performed at screening: Peripapillary retinal nerve fiber layer (pRNFL) < 92 µm in a non-optic neuritis eye.

2.2.2. Exclusion criteria

- Relapse within 3 months prior to baseline visit.
- Other disease or condition with suspected effect on motor performance.
- Any condition foreseen to prevent compliance with protocol.
- The patient is pregnant at screening.
- Any contra-indications for MRI investigation at screening.

2.3. Data acquisition

An overview of the visit schedule is provided in Table 1.

2.3.1. Primary outcome: self-assessment of motor functions at home (Motognosis Amsa)

Measurements are recorded with a markerless motion analysis system consisting of the measurement software (Amsa V 1.2.0, Motognosis GmbH, Berlin, Germany) running on an All-in-One PC (Optiplex 5,480, Dell GmbH, Frankfurt am Main, Germany) and a single RGB-Depth camera (Azure Kinect, Microsoft Corporation, Redmond, WA, United States).

The device is delivered to the patient's home and set-up appropriately by qualified staff along with oral instruction of the testing protocol which includes assessment of six specified short motor tasks within the recording space of the camera. All data are stored on the system hardware only.

Participants are instructed to use Motognosis Amsa twice a day—preferably morning and later afternoon/evening—for a period of 7 days for each visit. Participants start by preparing the measuring area (e.g., removal of clutter). When the measurement area is cleared, they can start the software. The software can be controlled with gestures, i.e., lifting of the left or right arm. Assessments start with a positioning phase, where participants will see themselves on the computer screen and will be guided to the correct starting location with visual and auditory cues. Subsequently assessment-specific video instructions are provided. After execution of an assessment a result page is shown. If a measurement error occurred, a notification will be shown with the request to rerecord. Otherwise, the participant can proceed to the next assessment. If a specific task was not recorded, the participant is supposed to enter the reason for the omission in a free text field.

TABLE 1 Overview study assessments and visit schedule.

Assessment	Rater	Screening	Baseline visit (V) 1	Visit 2	Visit 3	Visit 4	Visit 5	Visit 6
			Month 1	Month 6	Month 12	Month 18	Month 24	Month 27
Written informed consent	Investigator	□						
Assessment of in- and exclusion criteria/confirmation of in and exclusion criteria	Investigator	□	□		□		□	□
Assessment/Follow up of patients' characteristics (diagnosis ascertainment, comorbidities, age, height, weight, relapses in past 24 months/since last visit, current symptoms, treatment: current treatment at baseline, change of treatment at follow-up)	Investigator		□		□		□	□
EDSS	Investigator	□	□		□		□	□
MSFC-4	Study assistant		□		□		□	□
6-min walk test	Study assistant		□		□		□	□
PASS-MS assessment of motor functions			□		□		□	□
PRO PGIC	Patient		□	●	□	●	□	□
PRO MSWS-12	Patient		□	●	□	●	□	□
PRO FSMC	Patient		□	●	□	●	□	□
PRO NRS	Patient		□	●	□	●	□	□
PRO HAQUAMS	Patient		□	●	□	●	□	□
PRO PHQ-9	Patient		□	●	□	●	□	□
PRO GLTEQ	Patient		□	●	□	●	□	□
PRO EQ-5D-5L	Patient		□	●	□	●	□	□
PRO BPI	Patient		□	●	□	●	□	□
Instruction (Reinstruction if needed) of use for Amsa	Study assistant		□	(●)	(□)	(●)	(□)	
Amsa assessment recorded twice a day over 7 days	Patient		●	●	●	●	●	
Reporting of AE and safety issues related to Amsa self-assessment	Patient		●	●	●	●	●	
PRO Pain-NAS, EQ-VAS, state fatigue once a day on each day of functional assessment	Patient		●	●	●	●	●	
Usability rating	Patient		●	●	●	●	●	
Brain MRI			□				□	
OCT			□				□	
Clinical global impression of change	Treating neurologist			◊	◊	◊	◊	◊

(Continued)

TABLE 1 (Continued)

Assessment	Rater	Screening	Baseline visit (V) 1	Visit 2	Visit 3	Visit 4	Visit 5	Visit 6
			Month 1	Month 6	Month 12	Month 18	Month 24	Month 27
Most recent relapse incl treatment and course of remission	Treating neurologist		◊	◊	◊	◊	◊	◊
Current medication/Change in medication from baseline/ comorbidities	Treating neurologist		◊	◊	◊	◊	◊	◊
MSFC-3	Treating neurologist		◊	◊	◊	◊	◊	◊

The components of each visit are denoted as (□) annual research grade assessment at study center, (●) remote self-assessment of motor functions at home (Amsa) and (◊) clinical data collected from routine visits.

Assessments and their motor outcomes for this study include:

1. Stance with open and closed eyes and closed feet (20s eyes open, 20s eyes closed): angular sway speed 3D (°/s) separately for phases of stance with open and closed eyes.
2. Stepping in place (40 s): knee amplitude (m) and arrhythmicity (%).
3. Short walk in comfortable speed (Movement toward the system, stopped automatically in a certain distance): Short walk in comfortable speed: comfortable walk speed (m/s) and step width (cm).
4. Short walk in maximum speed (Movement toward the system, stopped automatically in a certain distance): maximum walking speed (m/s).
5. Line walk (Movement toward the system, stopped automatically in a certain distance): mean trunk roll deflection (°).
6. Standing up and sitting down from a chair: up time (s) and down time (s).

Performing the whole set of assessments, including in-between system operation, positioning, instructions and conduction takes at maximum 10 min. If particular assessments are deemed too risky for an individual participant by the investigator, the participant may be instructed to record only a subset of the assessments.

On each day of home-based assessment of motor function, participants are asked to answer three simple questions as potential determinants for day-to-day fluctuations: (1) about the severity of pain on a 0–10 numerical analog scale pain (painNAS), (2) about the current health status on a 0–100 visual analog scale (EQ-VAS) (38) and (3) about the current state of fatigue using a 0–10 numerical analog scale devised for that purpose. To cover aspects of patient safety, participants are reminded to report on any incidents occurring during Amsa assessment within the user interface. At the end of each week of home-based assessment, the participant is asked to fill out a questionnaire on usability of the measurement device, the System Usability Scale (SUS) Plus (39–41), translated and modified for the purpose of this project. The SUS was developed to evaluate a wide variety of products and services with a 10-item scale using five response options from "strongly agree" to "strongly disagree" to explore aspects of usability. Furthermore, participants can make suggestions how usability might be improved.

2.3.2. Patient-reported outcomes

PROs listed below were applied in validated translations—except for PGIC, for which own translation was used—and completed directly in eCRF via individualized links.

2.3.2.1. The patient global impression of change

The Patients' Global Impression of Change (PGIC) scale was first developed in context of patients' perception of changes after intervention (i.e., "feeling better" or "feeling worse"). It is a 7-point verbal scale, with the options "very much improved," "much improved," "minimally improved," "no change," "minimally worsened," "much worsened," and "very much worsened." The PGIC is commonly used in clinical trials for treatments of pain, but it has also been applied as a generic measure applicable to a wide variety of conditions and treatments. Worsening of any grade is considered clinically meaningful (42).

2.3.2.2. The multiple sclerosis walking scale-12

The Multiple Sclerosis Walking Scale-12 (MSWS-12) is a patient-rated measure assessing the extent to which a person's ability to walk is affected by MS., i.e., it is conceived to capture the impairment level. It has been developed from patients' experience and has undergone psychometric validation and translations (43). The 12 items are rated on a five-point scale (1, "not limited" to 5, "extremely"). Total scores are calculated as sum score (range 12–60) and transformed to a scale of 0–100 to aid interpretation. Higher scores reflect greater impact of MS on walking ability. An increase of >8-point in 0–100 MSWS-12 score is considered clinically meaningful (44).

2.3.2.3. Fatigue scale for motor and cognitive functions

The fatigue scale for motor and cognitive functions (FSMC) is a patient questionnaire to assess MS-related cognitive and motor fatigue (45, 46). A Likert-type 5-point item rating (ranging from 1 "does not apply at all" to 5 "applies completely") produces a sum score between 20 (no fatigue at all) and 100 (most severe fatigue). Two subscales (cognitive and physical fatigue) can be derived from the FSMC. Items included in the cognitive subscale are 1-4-7-8-11-13-15-17-18-20 and items included in the physical subscale are 2-3-5-6-9-10-12-14-16-19. An increase in FSMC category (sum score: <43: no fatigue; 43–52: mild fatigue; 53–62 moderate fatigue; >63 severe fatigue) is considered clinically meaningful (45).

2.3.2.4. Spasticity using numeric rating scale

The clinical rating of spasticity will be performed using a patient-rated measure of the perceived severity of spasticity, employing a numeric rating scale (47, 48) for several aspects of spasticity, each rated on a scale of 0 to 10. Total rating is the mean of item-level answers, where 0 is no spasticity and 10 is the worst possible spasticity. Appropriate patient training has to be ensured to obtain reliable results. Any increase in 0–10 Numeric rating scale (NRS) for spasticity is considered clinically meaningful (49).

2.3.2.5. Hamburg quality of life questionnaire for multiple sclerosis

The Hamburg Quality of Life Questionnaire for Multiple Sclerosis (HAQUAMS) is a health-related quality of life measure designed for pwMS (50). The HAQUAMS consists of 38 questions, 28 of which address major dimensions of health-related quality of life in MS: Fatigue/thinking (four items), mobility lower limb (five items), mobility upper limb (five items), social function (six items) and mood (eight items). Subscales and total score range from 1 to 5. Higher scores indicate a lower quality of life. Cognitive impairment in MS does not impact psychometric properties. A HAQUAMS total score increase of at least 0.22 is considered clinically meaningful worsening (51).

2.3.2.6. The 9-item patient health questionnaire-9

The 9-item Patient Health Questionnaire-9 (PHQ-9) was devised to screen for depressive disorders in primary care and the setting. It is based on the DSM-IV diagnostic criteria for a major depression episode. The PHQ-9 can be used both as a screening instrument for a depressive episode and can be used to provide information about the severity of a depressive episode. Each question in the scale has four response choices: "not at all," "several days," "more than half the days," and "nearly every day" and classifications of no/possibly relevant depressive disorder are made according to manual (52, 53).

2.3.2.7. Godin leisure-time exercise questionnaire

The Godin leisure-time exercise questionnaire (GLTEQ) is applied here to assess physical activity levels in MS. It contains three core items regarding the frequency of strenuous, moderate, and mild physical activity for bouts of 15 or more minutes during a 7-day period (54). The scores are multiplied by weights and summed into an overall score (i.e., leisure-time physical activity [LTPA] score) that ranges between 0 and 119 metabolic equivalents of task/min of physical activity per week (55).

2.3.2.8. EQ-5D/EQ—visual analog scale

EQ-5D is a generic and widely used measure of health status developed by the EuroQol Group.

Participants are asked to classify and rate their own health according to five dimensions. These dimensions comprise mobility, self-care, usual activities, pain/discomfort and anxiety. Each dimension is divided into five levels, i.e., 1 "no problems," 2 "slight problems," 3 "moderate problems," 4 "severe problems," and 5 "extreme problems." (56). While answers on EQ-5D consider variable timeframes, the single-item EQ-VAS provides a global assessment of perceived health at the time of assessment. It consists of a vertical visual analog scale that takes values between 0 (worst imaginable health) and 100 (best imaginable health) (38).

2.3.2.9. Brief pain inventory

Given the high prevalence and clinical relevance of pain, the Brief Pain Inventory (BPI) was developed as a brief instrument with low respondent burden that can be easily administered by large numbers of patients (57). The BPI measures both the intensity of pain (sensory dimension) and impact of pain with patients' lives (reactive dimension). Pain relief, pain quality, and patient perception of the cause of pain are also addressed (58).

2.3.3. Data acquisition from routine care

Information from routine care is retrieved repeatedly throughout the observation period from treating neurologists. The baseline data set comprises information on diagnosis and comorbidities, most recent relapse including its treatment and clinical outcome and full list of current medication as well as EDSS and MSFC-3, if performed routinely. Follow-up data are requested from any clinical visit throughout the observation period, at least semiannually, and comprise clinician's global ratings of change, information on relapses since last visit in medication or comorbidities, as well as EDSS and MSFC-3.

2.3.4. Data acquisition at annual study visits

2.3.4.1. Study assessment

Time since diagnosis of multiple sclerosis, prior manifestations of disease, current symptoms, prior and current disease modifying therapy, supportive therapy and relapses in past 24 months as well as comorbidities and changes thereof are acquired by the clinical investigator.

Current therapy will be documented at baseline and changes thereof will be reported at each visit. This also extends to rehabilitative interventions.

2.3.4.2. Expanded disability status scale

The expanded disability status scale (EDSS) is used to quantify disability in MS. The scale was first developed by Kurtzke in 1955 and then expanded in 1983. It is usually referred to as a measure which is scaled on 10 steps from 0 (no disability) to 10 (death from MS). Scoring is based on an examination by a neurologist. EDSS steps 1.0 to 3.5 refer to people with MS who are able to walk without any limitation, while EDSS steps 4.0 and higher are defined by decrease in walking capacity. Assessment of EDSS will follow instructions of Neurostatus for functional systems scores and EDSS step (59) by certified raters. In our study, the 3 m-CDP is defined as a 1.0 step increase from baseline EDSS when baseline EDSS was 0.0 to 5.0 and 0.5 step increase from baseline when baseline EDSS was 5.5 to 6.5, rated at 24 months with change confirmed at month 27.

2.3.4.3. Multiple sclerosis functional composite (MSFC-3 and MSFC-4)

The MSFC was developed by a special Task Force on Clinical Outcomes Assessment as a clinically applicable standardized, quantitative assessment instrument for use in MS trials (35). The MSFC-3 measures three clinical dimensions: leg function/ambulation using the Timed 25-foot Walk test; arm/hand function using the 9 Hole Peg Test (9HPT); and cognitive function using the Paced Auditory Serial Addition Test (PASAT-3 version). Because the PASAT is not popular among patients and given the relevance of visual dysfunction in MS, an expert group (60), convened by the National MS Society,

recommended two adaptations to the MSFC: (1) inclusion of the Sloan Low Contrast Letter Acuity test (60) (MSFC-4) and (2) use of the oral version of the Symbol Digit Modalities Test (SDMT) instead of the PASAT-3. In our study, the MSFC-4, will be administered on occasion of the annual visit at study site by a trained rater. In addition, the MSFC-3 will be collected from routine clinical visits semiannually. Both versions will use SDMT for the cognitive component.

The MSFC will be performed and analyzed in accordance with the respective testing manual issued by.

the National Multiple Sclerosis Society. Cut-offs for clinically meaningful change in MSFC and component Z-scores have been defined as >20% worsening (61).[1]

2.3.4.4. The 6-min walk

The 6-min walk (6 MW) is applied here to measure of walking endurance/ walking capacity in pwMS (62). The test is characterized by good practicability, reproducibility and reliability in MS. Furthermore, ecological validity is supported by strong correlation to patient report of ambulation and physical fatigue (63). A $\geq$ 20 m decrease in distance covered in the 6-min walking test at comfortable speed is usually considered clinically meaningful (64).

2.3.4.5. Supervised operator-based assessment of motor function (Motognosis Labs PASS-MS)

Our group developed a clinically applicable assessment protocol (PASS-MS) for usage with the Motognosis Labs system (Motognosis GmbH, Berlin, Germany). Motognosis Labs functions similar to Amsa in terms of technology. It differs *in camera* version used (Microsoft Kinect v2 for Motognosis Labs vs. Azure Kinect for Motognosis Amsa) and test set-up, as Motognosis Labs uses a camera plugged in to a laptop and participants are guided through assessments by a trained operator according to standard instructions.

PASS-MS consists of 10 short motor tasks performed in front of the RGB-D camera and parameters for the description of performance are generated by custom scripts. In operator-based application, this system proved acceptable to patients and was easily applied. Previous validation showed accuracy of derived parameters against gold standard multi-camera motion capture (33) and sufficient reliability and validity to measure balance and gait function in MS (65, 66).

Assessment of PASS-MS includes:

1. Stance with open and closed eyes and closed feet (20s eyes open, 20s eyes closed).
2. Dual Task Stance with open and closed eyes and closed feet.
3. Stepping on place (40s).
4. Short walk in comfortable speed.
5. Short walk in maximum speed.
6. Line walk.
7. Standing up and sitting down from a chair.
8. Pronator drift test.
9. Finger-to-nose-test.
10. Finger tapping.

2.3.4.6. Magnetic resonance imaging

In this study a standardized MR protocol was performed consisting of: a 3D-T1-weighted sequence (MPRAGE), a 3D T2-SPACE, a 3D fluid attenuated inversion recovery (FLAIR), a Diffusion Weighted Imaging sequence (DWI) and a resting state functional MRI (rsfMRI). To define progression, we use operational cut-offs for brain volume loss known to increase with age. Mean BVL per year amounts to by 0.15, 0.30, 0.46, and 0.61% of baseline brain volume at ages 45, 55, 65, and 75 years, respectively (67). The corresponding age-dependent 95th percentiles of BVL per year were 0.52%, 0.77%, 1.05%, and 1.45%. Pathological BVL can be assumed if an individual BVL per year exceeds these thresholds for a given age (67).

2.3.4.7. Optical coherence tomography

Optical coherence tomography (OCT) is a suitable high-resolution imaging method for the assessment of retinal integrity with good reproducibility. Peripapillary retinal nerve fiber layer thickness and macular volume are the most reported indicators to measure retinal atrophy on OCT. It has been shown that pwMS with a pRNFL thickness of less than or equal to 87 µm (88 µm) measured with Spectralis (Cirrus) OCT devices had double the risk of disability worsening in the follow-up (68).

which led us to consider this measure as a component of the inclusion criteria. With respect to progression of structural abnormalities of the retina, an absolute thinning of pRNFL of more than 1.25 µm at 24 months against baseline is considered clinically meaningful. This threshold has been established previously as the upper limit to define stability in multiple sclerosis (69).

2.3.5. Visit schedule

See Table 1.

2.4. Pre-processing of data

All study data will undergo plausibility checks including description of missings prior to further analysis. Definitions of progression events by EDSS or alternative definitions for secondary outcomes are applied as provided in section 2.3.

Data from technical recordings (Amsa, Motognosis Labs, MRI, and OCT) are continuously monitored by trained users to check usability and plausibility according to standard operating procedures for quality control (QC). Specifically, for Amsa and PASS-MS, presentations of all assessments are systematically inspected and evaluated for quality concerns following the QC pipeline developed by Röhling et al. (70).

For RGB-D camera based motion capture, both Amsa and PASS-MS, a list of task-specific kinematic parameters is generated according to custom scripts by the provider. Kinematic parameters include for example gait speed for the short walking tasks. Primary analysis will consider only one parameter per test condition, i.e., seven parameters.

2.5. Data management

Data flow is shown in Figure 1. Study data are stored in an study-specific Electronic Data Capture platform (REDCap) (71). The platform

1 http://main.nationalmssociety.org/docs/HOM/MSFC_Manual_and_Forms.pdf

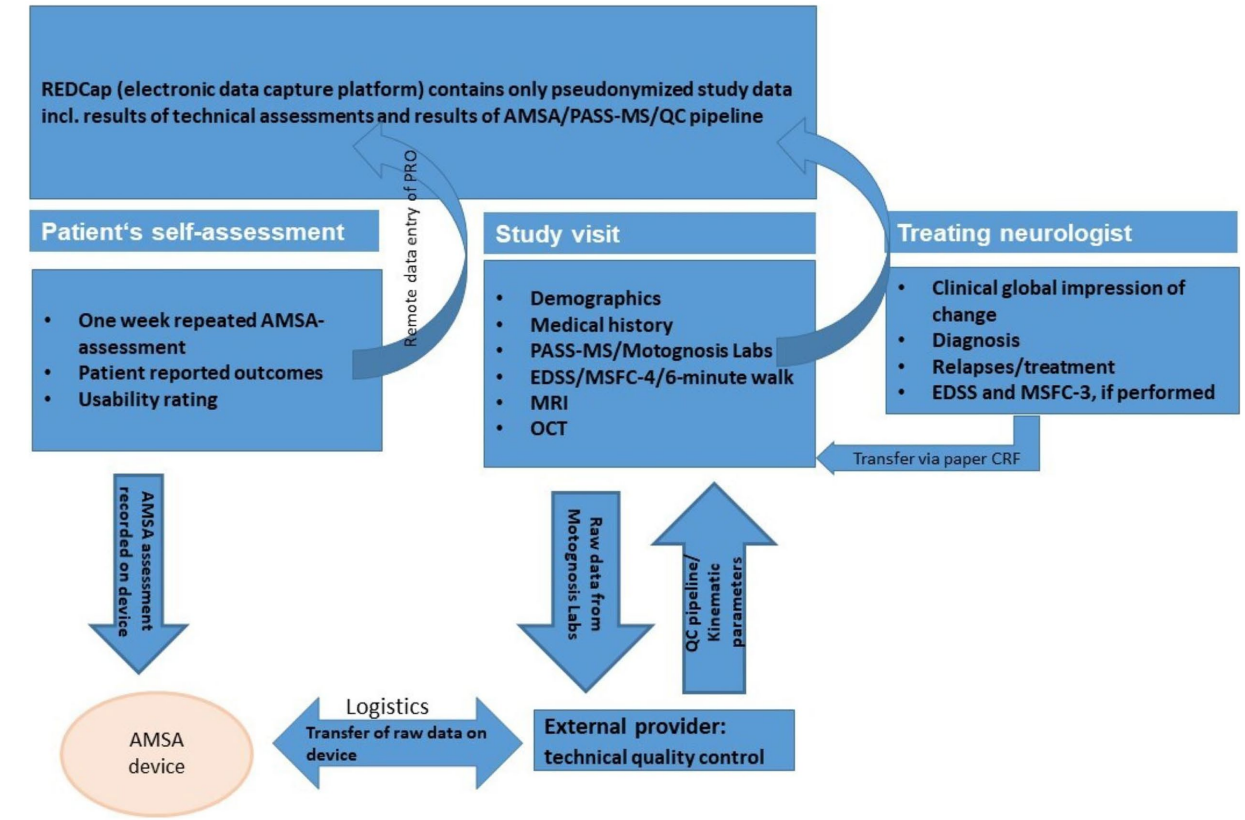

FIGURE 1
Data flow.

also enables remote data entry of PRO by patients themselves via personalized links. The study team provides the links to each participant at the appropriate timepoints throughout the observation period.

For the technical assessments performed in this study (Amsa, PASS-MS/Motognosis Labs, MRI, OCT), test results (e.g., gait speed from PASS-MS, number of T2 lesions on MRI, pRNFL thickness in OCT) are only transferred into REDCap system after pre-processing as described in section 2.4 along with results of QC.

All pseudonymized raw data are digitally stored in separate archives on local platforms.

With regard to data imports from home-based repeated Amsa assessments, raw data and metadata are saved on and retrieved with the device after each 1-week assessment period by the provider. The provider, after checking for technical issues and completeness, transfers results of daily self-ratings and pseudonymized metadata and raw data from Amsa recordings to the study site. Data are provided for QC application as well as kinematic parameters for analysis and archiving.

Data from routine care are collected from treating neurologists using structured paper templates.

2.6. Status of the study

Approval of the institutional review board (Charité—Universitätsmedizin Berlin) was obtained on 21 October 2021 (EA1/293/21). The study is active with first patient first visit in June 2022.

2.7. Statistical analysis plan

Based on the study question, the primary hypothesis is to assess the accuracy of detecting disease progression by the repeated short motor assessments at 24 months, compared to progression defined by EDSS at 24 months and confirmed at 27 months.

The sample size is justified via the expected precision of the estimate of the area under the receiver operating characteristic curve (AUC) provided in terms of the 95% confidence interval. We hypothesize that the parameters derived from repeated short motor assessment at home can reliably identify disease progression compared to detection of progression according to EDSS.

If the AUC is 0.9, and the sample size is 150, from which 10% are diagnosed with a progression according to EDSS at 24 months, then the width of the 95% confidence interval will be 0.103. In case of a lower AUC, e.g., 0.8, the 95% confidence interval would be of width 0.138. These calculations were performed using nQuery version 8.7.0.0, procedure AOC6-1. Given these calculations, the expected precision of the estimated quantity seems sufficient to evaluate the exploratory research hypothesis of this study.

Given the baseline definition, the primary endpoint is analyzed as AUC of detection of disease progression according to the repeated short motor assessment at home compared to detection of disease progression according to the EDSS score at 24 months, confirmed at 27 months. The AUC is calculated alongside with the 95% confidence interval. Event of progression at 24 months detected by parameters from repeated short motor assessment at home is defined as

observed reliable change in pre-defined direction of worsening in one or more of the parameters derived from this assessment. Threshold for reliable change will be defined based on analysis of baseline data. Secondary endpoint analyses are planned for MSWS-12, HAQUAMS, PGIC, CGI, MSFC, and 6 MW. Respective receiver operating characteristic curves and their AUC will be calculated based on published evidence on minimally important difference for MSFC, 6 MW, MSWS-12, and HAQUAMS while any transition in the direction of worsening will be considered an important change on PGIC and CGI.

Subgroup analysis are planned for stratification by age > 55 years vs. younger and EDSS < 3.5 vs. higher. Further exploratory subgroup analysis may be conducted for all endpoints, if there exist relevant subgroups, using standard statistical methods such as parametric or non-parametric location tests and regression methods.

3. Discussion

This study evaluates the concept of remote multipoint assessment of motor performance to improve definitions of disease progression in MS over current definitions of 3 m-CDP. Being among the first and larger studies to evaluate quantitative motor assessments longitudinally (28, 72–76), it is also the first study to apply RGB-D technology for the remote assessment of motor functions in MS (77). The prospective design and multimodal examination protocol ensures that changes defined by remote assessment can be compared with state-of-the-art clinical and imaging endpoints in MS.

Primary analysis will use 3 m-CDP defined by EDSS as the main comparator, which is most commonly used as an endpoint of disability accumulation in MS clinical trials to date. Still, more general concerns have been raised with respect to disability confirmation by EDSS (78). For example, 3 m-CDP may overestimate the accumulation of disability in the longer term and, thus, longer confirmation periods should be preferred (79) which would extend observation times. We here adhere to an observation period of 24 months as the minimum among previous studies that used CDP as their main endpoint. Within this timeframe, reasonable proportions of progression events can be expected according to previous reports. Nonetheless, proportions were not much higher than 10% in earlier disease stages (80–82). Targeting this group for our study has the risk that progression observed is too subtle to yield numbers that could answer the primary research question. Therefore, the inclusion criteria were set to increase the likelihood of disability progression while at the same time maintaining generalizability for early MS.

The technical approach applied in this study is novel in two aspects: first, assessments of motor function are recorded by patients themselves in their home setting, and second, this approach enables frequent (multi-point) assessment. Both aspects hold potential to overcome the limitations of conventional rater-based assessments in single and infrequent clinical visits. Previous evidence suggests that different features of MS may vary considerably within the same subject, including self-ratings of health status (83). For fatigue, over one-third of the variability can be attributed to moment-dependent fluctuations, 8.2% to day-to-day fluctuations, while 56.6% can be attributed to individual differences (84) and many pwMS report increased fatigue in the afternoon and evening (85). Day-to-day variability has also been shown for maximum walking distance that would equal changes of up to 1.5 EDSS points (86). We therefore expect to observe day-to-day variability of motor performance throughout each week of remote assessment and consider this in definitions of change at follow-up. Further, our study protocol combines repeated self-recording of motor functions with a daily self-report of health status, pain and state fatigue. This will allow us to study possible correlates.

For a quantitative assessment of motor functions in MS, this study follows the technical approach of a task-based assessment. Clinical relevance of instrumentally assessed gait quality has been shown in early-stage multiple sclerosis (87). However, their ecological validity may be limited, depending on task and setting (88).

Shema-Shiratzky et al. found that dual-task walking in the lab better represents walking ability in everyday life, whereas usual walking in the lab is more likely to represent best performance in everyday life (89).

We therefore included additional performance-based and patient-reported outcomes of walking function for contextualization. Another novelty of our study is the integration of data acquired semiannually in the course of routine clinical care by treating neurologists. Analysis will use these, specifically their global ratings of change, as one of the alternative secondary definitions of change. This intends to explore the validity and generalizability of our findings for the setting, in which approved treatments or digital motor applications will ultimately be applied.

We aimed to address potential drawbacks of remote task-based assessment in study design and analysis plan. First, variability in task performance can be expected to be higher in unsupervised settings. We aim to mitigate this point by control of device set-up by a trained operator, standardized instructions and by technical design. Second, we apply a standardized quality control pipeline on recordings to identify relevant protocol deviations. Roehling et al. showed the feasibility but also the necessity for a *post hoc* quality control using this method of instrumented motion analysis (70). In this study, we extend this QC pipeline exploring its practicality to Amsa measurements. Furthermore, participants' adherence is surely a concern in this long-term observation. A recent 8-week RCT study investigated participants' short term adherence in using digital tools in multiple sclerosis. The average overall adherence for all three measurement tools (1. MS patient-reported outcome tool accessible via a smartphone app, 2. Floodlight open, a app-based assessment of hand and gait function, and 3. Fitbit, a smart watch for passive monitoring of sleep duration and quality) was 81% in the intervention group (90). Midaglia et al. analyzed the practicability of remote active testing and passive monitoring using digital tools in pwMS and showed 70% (16.68/24 weeks) adherence to active testing and 79% (18.89/24 weeks) to passive monitoring (74). Rates of attrition in application of remote assessment have not yet been reported over longer time-frames. In order to sustain adherence in our 24 months-study, participants will receive a reminder link about 4 weeks before the upcoming measurement and the Amsa device will be delivered by the study team at the appropriate time.

Our aim is to evaluate subtle changes in motor signs to identify chronic progression in MS independent of relapse by remote task-based assessment. This new approach will be related to the EDSS as well as imaging surrogates (OCT, MRI). Reliable

remote assessment of disability would seamlessly fit in the landscape of digital health solutions that are highly important in situations where specialized care is scarce or episodically unavailable, such as in recent pandemic conditions. If utility can be shown for this home-based setting, such assessment may serve as a valuable source of information in patient care. An appropriate re-definition of progression events may substantially reduce total observation times and rater involvement in clinical trials that aim to establish clinical stability or clinical progression in MS as their outcome of interest.

Ethics statement

The study was approved by the Institutional Review Board (Ethikkommission Charité Universitätsmedizin Berlin, EA1/293/21). Participants are enrolled only after written informed consent. The study was registered at Deutsches Register für Klinische Studien (DRKS00027042). Dissemination includes this submission of the study protocol for peer-reviewed publication and discussion of interim and final results at conferences as well as prospective publication in peer-reviewed journals.

Author contributions

E-MD: Conceptualization, Data curation, Investigation, Methodology, Project administration, Supervision, Writing – original draft, Writing – review & editing. HR: Conceptualization, Data curation, Software, Writing – review & editing. DZ: Conceptualization, Formal Analysis, Writing – review & editing. LH: Conceptualization, Formal Analysis, Writing – review & editing. FP: Supervision, Writing – review & editing. TS-H: Conceptualization, Data curation, Funding acquisition, Investigation, Methodology, Project administration, Supervision, Writing – original draft, Writing – review & editing.

Funding

The author(s) declare financial support was received for the research, authorship, and/or publication of this article. This study was funded by research grant celgene/bms. We received financial support from the Open Access Publication Fund of Charité – Universitätsmedizin Berlin and the German Research Foundation (DFG).

Acknowledgments

The study was performed in collaboration with the Bernstein Center for Neuroimaging (BCAN) at Charité—Universitätsmedizin Berlin. We further acknowledge institutional support by NeuroScience Clinical Research Center (NCRC), funded by the Deutsche Forschungsgemeinschaft (DFG, German Research Foundation) under Germany's Excellence Strategy—EXC-2049-390688087 and Charité-BIH Clinical Study Center.

Conflict of interest

HR was a paid employee of Motognosis GmbH until March 2023.

The remaining authors declare that the research was conducted in the absence of any commercial or financial relationships that could be construed as a potential conflict of interest.

Publisher's note

References

1. Kappos L, Wolinsky JS, Giovannoni G, Arnold DL, Wang Q, Bernasconi C, et al. Contribution of relapse-independent progression vs relapse-associated worsening to overall confirmed disability accumulation in typical relapsing multiple sclerosis in a pooled analysis of 2 randomized clinical trials. *JAMA Neurol.* (2020) 77:1132–40. doi: 10.1001/jamaneurol.2020.1568

2. D'Amico E, Haase R, Ziemssen T. Review: patient-reported outcomes in multiple sclerosis care. *Mult Scler Relat Disord.* (2019) 33:61–6. doi: 10.1016/j.msard.2019.05.019

3. van Munster CE, Uitdehaag BM. Outcome measures in clinical trials for multiple sclerosis. *CNS Drugs.* (2017) 31:217–36. doi: 10.1007/s40263-017-0412-5

4. McAdams M, Stankiewicz JM, Weiner HL, Chitnis T. Review of phase III clinical trials outcomes in patients with secondary progressive multiple sclerosis. *Mult Scler Relat Disord.* (2021) 54:103086. doi: 10.1016/j.msard.2021.103086

5. Kurtzke JF. Rating neurologic impairment in multiple sclerosis: an expanded disability status scale (EDSS). *Neurology.* (1983) 33:1444–52. doi: 10.1212/WNL.33.11.1444

6. Gehr S, Kaiser T, Kreutz R, Ludwig WD, Paul F. Suggestions for improving the design of clinical trials in multiple sclerosis-results of a systematic analysis of completed phase III trials. *EPMA J.* (2019) 10:425–36. doi: 10.1007/s13167-019-00192-z

7. Montalban X, Hauser SL, Kappos L, Arnold DL, Bar-Or A, Comi G, et al. Ocrelizumab versus placebo in primary progressive multiple sclerosis. *N Engl J Med.* (2017) 376:209–20. doi: 10.1056/NEJMoa1606468

8. Kappos L, Bar-Or A, Cree BAC, Fox RJ, Giovannoni G, Gold R, et al. Siponimod versus placebo in secondary progressive multiple sclerosis (EXPAND): a double-blind, randomised, phase 3 study. *Lancet.* (2018) 391:1263–73. doi: 10.1016/S0140-6736(18)30475-6

9. Kalincik T, Cutter G, Spelman T, Jokubaitis V, Havrdova E, Horakova D, et al. Defining reliable disability outcomes in multiple sclerosis. *Brain.* (2015) 138:3287–98. doi: 10.1093/brain/awv258

10. Dandu SR, Engelhard MM, Qureshi A, Gong J, Lach JC, Brandt-Pearce M, et al. Understanding the physiological significance of four inertial gait features in multiple sclerosis. *IEEE J Biomed Health Inform.* (2018) 22:40–6. doi: 10.1109/JBHI.2017.2773629

11. Shanahan CJ, Boonstra FMC, Cofré Lizama LE, Strik M, Moffat BA, Khan F, et al. Technologies for Advanced Gait and Balance Assessments in people with multiple sclerosis. *Front Neurol.* (2017) 8:708. doi: 10.3389/fneur.2017.00708

12. Goldman MD, Motl RW, Rudick RA. Possible clinical outcome measures for clinical trials in patients with multiple sclerosis. *Ther Adv Neurol Disord.* (2010) 3:229–39. doi: 10.1177/1756285610374117

13. Kasser SL, Goldstein A, Wood PK, Sibold J. Symptom variability, affect and physical activity in ambulatory persons with multiple sclerosis: understanding patterns and time-bound relationships. *Disabil Health J.* (2017) 10:207–13. doi: 10.1016/j.dhjo.2016.10.006

14. Grobe-Einsler M, Taheri Amin A, Faber J, Schaprian T, Jacobi H, Schmitz-Hübsch T, et al. Development of SARA(home), a new video-based tool for the assessment of Ataxia at home. *Mov Disord.* (2021) 36:1242–6. doi: 10.1002/mds.28478

15. Shah VV, McNames J, Mancini M, Carlson-Kuhta P, Spain RI, Nutt JG, et al. Laboratory versus daily life gait characteristics in patients with multiple sclerosis, Parkinson's disease, and matched controls. *J Neuroeng Rehabil.* (2020) 17:159. doi: 10.1186/s12984-020-00781-4

16. Havrdová E, Arnold DL, Bar-Or A, Comi G, Hartung HP, Kappos L, et al. No evidence of disease activity (NEDA) analysis by epochs in patients with relapsing

multiple sclerosis treated with ocrelizumab vs interferon beta-1a. *Mult Scler J Exp Transl Clin*. (2018) 4:205521731876064. doi: 10.1177/2055217318760642

17. Cohen JA, Coles AJ, Arnold DL, Confavreux C, Fox EJ, Hartung HP, et al. Alemtuzumab versus interferon beta 1a as first-line treatment for patients with relapsing-remitting multiple sclerosis: a randomised controlled phase 3 trial. *Lancet*. (2012) 380:1819–28. doi: 10.1016/S0140-6736(12)61769-3

18. Kappos L, de Stefano N, Freedman MS, Cree BAC, Radue EW, Sprenger T, et al. Inclusion of brain volume loss in a revised measure of 'no evidence of disease activity' (NEDA-4) in relapsing-remitting multiple sclerosis. *Mult Scler*. (2016) 22:1297–305. doi: 10.1177/1352458515616701

19. Mayssam EN, Eid C, Khoury SJ, Hannoun S. "no evidence of disease activity": is it an aspirational therapeutic goal in multiple sclerosis? *Mult Scler Relat Disord*. (2020) 40:101935. doi: 10.1016/j.msard.2020.101935

20. Bovis F, Signori A, Carmisciano L, Maietta I, Steinerman JR, Li T, et al. Expanded disability status scale progression assessment heterogeneity in multiple sclerosis according to geographical areas. *Ann Neurol*. (2018) 84:621–5. doi: 10.1002/ana.25323

21. Hobart J, Lamping D, Fitzpatrick R, Riazi A, Thompson A. The multiple sclerosis impact scale (MSIS-29): a new patient-based outcome measure. *Brain*. (2001) 124:962–73. doi: 10.1093/brain/124.5.962

22. Alexander S, Peryer G, Gray E, Barkhof F, Chataway J. Wearable technologies to measure clinical outcomes in multiple sclerosis: a scoping review. *Mult Scler J*. (2020) 27:1643–56. doi: 10.1177/1352458520946005

23. Zhai Y, Nasseri N, Pöttgen J, Gezhelbash E, Heesen C, Stellmann JP. Smartphone Accelerometry: a smart and reliable measurement of real-life physical activity in multiple sclerosis and healthy individuals. *Front Neurol*. (2020) 11:688. doi: 10.3389/fneur.2020.00688

24. Frechette ML, Meyer BM, Tulipani LJ, Gurchiek RD, McGinnis RS, Sosnoff JJ. Next steps in wearable technology and community ambulation in multiple sclerosis. *Curr Neurol Neurosci Rep*. (2019) 19:80. doi: 10.1007/s11910-019-0997-9

25. Block VA, Pitsch E, Tahir P, Cree BAC, Allen DD, Gelfand JM. Remote physical activity monitoring in neurological disease: a systematic review. *PLoS One*. (2016) 11:e0154335. doi: 10.1371/journal.pone.0154335

26. Midaglia L, Mulero P, Montalban X, Graves J, Hauser SL, Julian L, et al. Correction: adherence and satisfaction of smartphone- and smartwatch-based remote active testing and passive monitoring in people with multiple sclerosis: nonrandomized interventional feasibility study. *J Med Internet Res*. (2019) 21:e16287. doi: 10.2196/16287

27. Spain RI, St. George RJ, Salarian A, Mancini M, Wagner JM, Horak FB, et al. Body-worn motion sensors detect balance and gait deficits in people with multiple sclerosis who have normal walking speed. *Gait Posture*. (2012) 35:573–8. doi: 10.1016/j.gaitpost.2011.11.026

28. Block VJ, Lizée A, Crabtree-Hartman E, Bevan CJ, Graves JS, Bove R, et al. Continuous daily assessment of multiple sclerosis disability using remote step count monitoring. *J Neurol*. (2017) 264:316–26. doi: 10.1007/s00415-016-8334-6

29. Yetisen AK, Martinez-Hurtado JL, da Cruz Vasconcellos F, Simsekler MCE, Akram MS, Lowe CR. The regulation of mobile medical applications. *Lab Chip*. (2014) 14:833–40. doi: 10.1039/c3lc51235e

30. Yetisen AK, Martinez-Hurtado JL, Ünal B, Khademhosseini A, Butt H. Wearables in medicine. *Adv Mater*. (2018) 30:1706910. doi: 10.1002/adma.201706910

31. Galna B, Barry G, Jackson D, Mhiripiri D, Olivier P, Rochester L. Accuracy of the Microsoft Kinect sensor for measuring movement in people with Parkinson's disease. *Gait Posture*. (2014) 39:1062–8. doi: 10.1016/j.gaitpost.2014.01.008

32. Müller B, Ilg W, Giese MA, Ludolph N. Validation of enhanced kinect sensor based motion capturing for gait assessment. *PLoS One*. (2017) 12:e0175813. doi: 10.1371/journal.pone.0175813

33. Otte K, Kayser B, Mansow-Model S, Verrel J, Paul F, Brandt AU, et al. Accuracy and reliability of the Kinect version 2 for clinical measurement of motor function. *PLoS One*. (2016) 11:e0166532. doi: 10.1371/journal.pone.0166532

34. Otte K, Ellermeyer T, Vater TS, Voigt M, Kroneberg D, Rasche L, et al. Instrumental assessment of stepping in place captures clinically relevant motor symptoms of Parkinson's disease. *Sensors*. (2020) 20:5465. doi: 10.3390/s20195465

35. Cutter GR, Baier ML, Rudick RA, Cookfair DL, Fischer JS, Petkau J, et al. Development of a multiple sclerosis functional composite as a clinical trial outcome measure. *Brain*. (1999) 122:871–82. doi: 10.1093/brain/122.5.871

36. Busner J, Targum SD. The clinical global impressions scale: applying a research tool in clinical practice. *Psychiatry*. (2007) 4:28–37.

37. Thompson AJ, Banwell BL, Barkhof F, Carroll WM, Coetzee T, Comi G, et al. Diagnosis of multiple sclerosis: 2017 revisions of the McDonald criteria. *Lancet Neurol*. (2018) 17:162–73. doi: 10.1016/S1474-4422(17)30470-2

38. Feng Y, Parkin D, Devlin NJ. Assessing the performance of the EQ-VAS in the NHS PROMs programme. *Qual Life Res*. (2014) 23:977–89. doi: 10.1007/s11136-013-0537-z

39. Borsci S, Federici S, Lauriola M. On the dimensionality of the system usability scale: a test of alternative measurement models. *Cogn Process*. (2009) 10:193–7. doi: 10.1007/s10339-009-0268-9

40. Mol M, van Schaik A, Dozeman E, Ruwaard J, Vis C, Ebert DD, et al. Dimensionality of the system usability scale among professionals using internet-based interventions for depression: a confirmatory factor analysis. *BMC Psychiatry*. (2020) 20:218. doi: 10.1186/s12888-020-02627-8

41. Lewis JR. The system usability scale: past, present, and future. *Int J Hum–Comput Interact*. (2018) 34:577–90. doi: 10.1080/10447318.2018.1455307

42. Perrot S, Lanteri-Minet M. Patients' global impression of change in the management of peripheral neuropathic pain: clinical relevance and correlations in daily practice. *Eur J Pain*. (2019) 23:1117–28. doi: 10.1002/ejp.1378

43. Hawton A, Green C, Telford CJ, Wright DE, Zajicek JP. The use of multiple sclerosis condition-specific measures to inform health policy decision-making: mapping from the MSWS-12 to the EQ-5D. *Mult Scler*. (2012) 18:853–61. doi: 10.1177/1352458511429319

44. Goldman MD, Ward MD, Motl RW, Jones DE, Pula JH, Cadavid D. Identification and validation of clinically meaningful benchmarks in the 12-item multiple sclerosis walking scale. *Mult Scler*. (2017) 23:1405–14. doi: 10.1177/1352458516680749

45. Penner IK, Raselli C, Stöcklin M, Opwis K, Kappos L, Calabrese P. The fatigue scale for motor and cognitive functions (FSMC): validation of a new instrument to assess multiple sclerosis-related fatigue. *Mult Scler*. (2009) 15:1509–17. doi: 10.1177/1352458509348519

46. Krupp LB, NG LR, Muir-Nash J, Steinberg AD. The fatigue severity scale. Application to patients with multiple sclerosis and systemic lupus erythematosus. *Arch Neurol*. (1989) 46:1121–3. doi: 10.1001/archneur.1989.00520460115022

47. Bohannon RW, Smith MB. Interrater reliability of a modified Ashworth scale of muscle spasticity. *Phys Ther*. (1987) 67:206–7. doi: 10.1093/ptj/67.2.206

48. Naghdi S, Nakhostin Ansari N, Azarnia S, Kazemnejad A. Interrater reliability of the modified modified Ashworth scale (MMAS) for patients with wrist flexor muscle spasticity. *Physiother Theory Pract*. (2008) 24:372–9. doi: 10.1080/09593980802278959

49. Farrar JT, Troxel AB, Stott C, Duncombe P, Jensen MP. Validity, reliability, and clinical importance of change in a 0-10 numeric rating scale measure of spasticity: a post hoc analysis of a randomized, double-blind, placebo-controlled trial. *Clin Ther*. (2008) 30:974–85. doi: 10.1016/j.clinthera.2008.05.011

50. Gold SM, Heesen C, Schulz H, Guder U, Mönch A, Gbadamosi J, et al. Disease specific quality of life instruments in multiple sclerosis: validation of the Hamburg quality of life questionnaire in multiple sclerosis (HAQUAMS). *Mult Scler J*. (2001) 7:119–30. doi: 10.1177/135245850100700208

51. Gold SM, Schulz H, Stein H, Solf K, Schulz KH, Heesen C. Responsiveness of patient-based and external rating scales in multiple sclerosis: head-to-head comparison in three clinical settings. *J Neurol Sci*. (2010) 290:1–2. doi: 10.1016/j.jns.2009.10.020

52. Urtasun M, Daray FM, Teti GL, Coppolillo F, Herlax G, Saba G, et al. Validation and calibration of the patient health questionnaire (PHQ-9) in Argentina. *BMC Psychiatry*. (2019) 19:291. doi: 10.1186/s12888-019-2262-9

53. Loewe B, Zipfel S, Herzog W. *PHQ-D: Gesundheitsfragebogen für Patienten; Manual Komplettversion und Kurzform*. Medizinische Universitaetsklinik Heidelberg: Pfizer GmbH (2002).

54. Nigg CR, Fuchs R, Gerber M, Jekauc D, Koch T, Krell-Roesch J, et al. Assessing physical activity through questionnaires – a consensus of best practices and future directions. *Psychol Sport Exerc*. (2020) 50:101715. doi: 10.1016/j.psychsport.2020.101715

55. Motl RW, Bollaert RE, Sandroff BM. Validation of the Godin leisure-time exercise questionnaire classification coding system using accelerometry in multiple sclerosis. *Rehabil Psychol*. (2018) 63:77–82. doi: 10.1037/rep0000162

56. Rabin R, de Charro F. EQ-5D: a measure of health status from the EuroQol group. *Ann Med*. (2001) 33:337–43. doi: 10.3109/07853890109002087

57. Radbruch L, Loick G, Kiencke P, Lindena G, Sabatowski R, Grond S, et al. Validation of the German version of the brief pain inventory. *J Pain Symptom Manag*. (1999) 18:180–7. doi: 10.1016/S0885-3924(99)00064-0

58. Cleeland CS, Ryan KM. Pain assessment: global use of the brief pain inventory. *Ann Acad Med Singap*. (1994) 23:129–38.

59. D'Souza M, Yaldizli Ö, John R, Vogt DR, Papadopoulou A, Lucassen E, et al. Neurostatus e-scoring improves consistency of expanded disability status scale assessments: a proof of concept study. *Mult Scler*. (2017) 23:597–603. doi: 10.1177/1352458516657439

60. Ontaneda D, LaRocca N, Coetzee T, Rudick RA. Revisiting the multiple sclerosis functional composite: proceedings from the National Multiple Sclerosis Society (NMSS) task force on clinical disability measures. *Mult Scler*. (2012) 18:1074–80. doi: 10.1177/1352458512451512

61. Hobart J, Blight AR, Goodman A, Lynn F, Putzki N. Timed 25-foot walk: direct evidence that improving 20% or greater is clinically meaningful in MS. *Neurology*. (2013) 80:1509–17. doi: 10.1212/WNL.0b013e31828cf7f3

62. Cederberg KLJ, Sikes EM, Bartolucci AA, Motl RW. Walking endurance in multiple sclerosis: Meta-analysis of six-minute walk test performance. *Gait Posture*. (2019) 73:147–53. doi: 10.1016/j.gaitpost.2019.07.125

63. Goldman MD, Marrie RA, Cohen JA. Evaluation of the six-minute walk in multiple sclerosis subjects and healthy controls. *Mult Scler*. (2008) 14:383–90. doi: 10.1177/1352458507082607

64. Baert I, Freeman J, Smedal T, Dalgas U, Romberg A, Kalron A, et al. Responsiveness and clinically meaningful improvement, according to disability level, of five walking measures after rehabilitation in multiple sclerosis: a European multicenter study. *Neurorehabil Neural Repair*. (2014) 28:621–31. doi: 10.1177/1545968314521010

65. Behrens JR, Mertens S, Krüger T, Grobelny A, Otte K, Mansow-Model S, et al. Validity of visual perceptive computing for static posturography in patients with multiple sclerosis. *Mult Scler*. (2016) 22:1596–606. doi: 10.1177/1352458515625807

66. Grobelny A, Behrens JR, Mertens S, Otte K, Mansow-Model S, Krüger T, et al. Maximum walking speed in multiple sclerosis assessed with visual perceptive computing. *PLoS One*. (2017) 12:e0189281. doi: 10.1371/journal.pone.0189281

67. Opfer R, Ostwaldt AC, Sormani MP, Gocke C, Walker-Egger C, Manogaran P, et al. Estimates of age-dependent cutoffs for pathological brain volume loss using SIENA/FSL-a longitudinal brain volumetry study in healthy adults. *Neurobiol Aging*. (2018) 65:1–6. doi: 10.1016/j.neurobiolaging.2017.12.024

68. Martinez-Lapiscina EH, Arnow S, Wilson JA, Saidha S, Preiningerova JL, Oberwahrenbrock T, et al. Retinal thickness measured with optical coherence tomography and risk of disability worsening in multiple sclerosis: a cohort study. *Lancet Neurol*. (2016) 15:574–84. doi: 10.1016/S1474-4422(16)00068-5

69. Pisa M, Guerrieri S, di Maggio G, Medaglini S, Moiola L, Martinelli V, et al. No evidence of disease activity is associated with reduced rate of axonal retinal atrophy in MS. *Neurology*. (2017) 89:2469–75. doi: 10.1212/WNL.0000000000004736

70. Röhling HM, Althoff P, Arsenova R, Drebinger D, Gigengack N, Chorschew A, et al. Proposal for post hoc quality control in instrumented motion analysis using Markerless motion capture: development and usability study. *JMIR Hum Factors*. (2022) 9:e26825. doi: 10.2196/26825

71. Harris PA, Taylor R, Thielke R, Payne J, Gonzalez N, Conde JG. Research electronic data capture (REDCap)--a metadata-driven methodology and workflow process for providing translational research informatics support. *J Biomed Inform*. (2009) 42:377–81. doi: 10.1016/j.jbi.2008.08.010

72. Woelfle T, Pless S, Reyes O, Wiencierz A, Feinstein A, Calabrese P, et al. Reliability and acceptance of dreaMS, a software application for people with multiple sclerosis: a feasibility study. *J Neurol*. (2023) 270:262–71. doi: 10.1007/s00415-022-11306-5

73. Mazzà C, Alcock L, Aminian K, Becker C, Bertuletti S, Bonci T, et al. Technical validation of real-world monitoring of gait: a multicentric observational study. *BMJ Open*. (2021) 11:e050785. doi: 10.1136/bmjopen-2021-050785

74. Midaglia L, Mulero P, Montalban X, Graves J, Hauser SL, Julian L, et al. Adherence and satisfaction of smartphone- and smartwatch-based remote active testing and passive monitoring in people with multiple sclerosis: nonrandomized interventional feasibility study. *J Med Internet Res*. (2019) 21:e14863. doi: 10.2196/14863

75. Creagh AP, Simillion C, Bourke AK, Scotland A, Lipsmeier F, Bernasconi C, et al. Smartphone- and smartwatch-based remote characterisation of ambulation in multiple sclerosis during the two-minute walk test. *IEEE J Biomed Health Inform*. (2021) 25:838–49. doi: 10.1109/JBHI.2020.2998187

76. Montalban X, Graves J, Midaglia L, Mulero P, Julian L, Baker M, et al. A smartphone sensor-based digital outcome assessment of multiple sclerosis. *Mult Scler*. (2022) 28:654–64. doi: 10.1177/13524585211028561

77. van der Walt A, Butzkueven H, Shin RK, Midaglia L, Capezzuto L, Lindemann M, et al. Developing a digital solution for remote assessment in multiple sclerosis: from concept to software as a medical device. *Brain Sci*. (2021) 11:1247. doi: 10.3390/brainsci11091247

78. Kalincik T, Sormani MP, Tur C. Has the time come to revisit our standard measures of disability progression in multiple sclerosis? *Neurology*. (2021) 96:12–3. doi: 10.1212/WNL.0000000000011120

79. Healy BC, Glanz BI, Swallow E, Signorovitch J, Hagan K, Silva D, et al. Confirmed disability progression provides limited predictive information regarding future disease progression in multiple sclerosis. *Mult Scler J Exp Transl Clin*. (2021) 7:205521732199907. doi: 10.1177/2055217321999070

80. Cohen JA, Comi G, Selmaj KW, Bar-Or A, Arnold DL, Steinman L, et al. Safety and efficacy of ozanimod versus interferon beta-1a in relapsing multiple sclerosis (RADIANCE): a multicentre, randomised, 24-month, phase 3 trial. *Lancet Neurol*. (2019) 18:1021–33. doi: 10.1016/S1474-4422(19)30238-8

81. Hauser SL, Bar-Or A, Comi G, Giovannoni G, Hartung HP, Hemmer B, et al. Ocrelizumab versus interferon Beta-1a in relapsing multiple sclerosis. *N Engl J Med*. (2017) 376:221–34. doi: 10.1056/NEJMoa1601277

82. Hauser SL, Bar-Or A, Cohen JA, Comi G, Correale J, Coyle PK, et al. Ofatumumab versus Teriflunomide in Multiple Sclerosis. *N Engl J Med*. (2020) 383:546–57. doi: 10.1056/NEJMoa1917246

83. Blome C, Carlton J, Heesen C, Janssen MF, Lloyd A, Otten M, et al. How to measure fluctuating impairments in people with MS: development of an ambulatory assessment version of the EQ-5D-5L in an exploratory study. *Qual Life Res*. (2021) 30:2081–96. doi: 10.1007/s11136-021-02802-8

84. Powell DJH, Liossi C, Schlotz W, Moss-Morris R. Tracking daily fatigue fluctuations in multiple sclerosis: ecological momentary assessment provides unique insights. *J Behav Med*. (2017) 40:772–83. doi: 10.1007/s10865-017-9840-4

85. Feys P, Gijbels D, Romberg A, Santoyo C, Gebara B, de Noordhout BM, et al. Effect of time of day on walking capacity and self-reported fatigue in persons with multiple sclerosis: a multi-center trial. *Mult Scler*. (2012) 18:351–7. doi: 10.1177/1352458511419881

86. Albrecht H, Wötzel C, Erasmus LP, Kleinpeter M, König N, Pöllmann W. Day-to-day variability of maximum walking distance in MS patients can mislead to relevant changes in the expanded disability status scale (EDSS): average walking speed is a more constant parameter. *Mult Scler*. (2001) 7:105–9. doi: 10.1177/135245850100700206

87. Carpinella I, Gervasoni E, Anastasi D, di Giovanni R, Tacchino A, Brichetto G, et al. Instrumentally assessed gait quality is more relevant than gait endurance and velocity to explain patient-reported walking ability in early-stage multiple sclerosis. *Eur J Neurol*. (2021) 28:2259–68. doi: 10.1111/ene.14866

88. Maetzler W, Rochester L, Bhidayasiri R, Espay AJ, Sánchez-Ferro A, van Uem JMT. Modernizing daily function assessment in Parkinson's disease using capacity, perception, and performance measures. *Mov Disord*. (2021) 36:76–82. doi: 10.1002/mds.28377

89. Shema-Shiratzky S, Hillel I, Mirelman A, Regev K, Hsieh KL, Karni A, et al. A wearable sensor identifies alterations in community ambulation in multiple sclerosis: contributors to real-world gait quality and physical activity. *J Neurol*. (2020) 267:1912–21. doi: 10.1007/s00415-020-09759-7

90. Katrine W, Ritzel SB, Caroline K, Marie L, Olsgaard BS, Lasse S. Potentials and barriers of using digital tools for collecting daily measurements in multiple sclerosis research. *Digit Health*. (2021) 7:205520762110555. doi: 10.1177/20552076211055552

Glossary

AUC	Area under the receiver operating characteristic curve
BVL	Brain volume loss
BPI	Brief pain inventory
CDP	Confirmed disability progression
CGI	Clinical global impression of change
DMTs	Disease modifying therapies
EDSS	Expanded disability status scale
FSMC	Fatigue scale for motor and cognitive functions
GLTEQ	Godin leisure-time exercise questionnaire
HAQUAMS	Hamburg quality of life questionnaire for multiple sclerosis
MRI	Magnetic resonance imaging
MS	Multiple sclerosis
MSFC	Multiple sclerosis functional composite
MSWS-12	The multiple sclerosis walking scale-12
NAS	Numerical analog scale
NEDA	No evidence of disease activity
NRS	Numeric rating scale
OCT	Optical coherence tomography
PASAT	Paced auditory serial addition test
PGIC	Patients' global impression of change
PHQ-9	Patient health questionnaire-9
pRNFL	Peripapillary retinal nerve fiber layer
PRO	Patient reported outcome
pwMS	People with multiple sclerosis
QC	Quality control
RCTs	Randomized controlled trials
REDCap	Research electronic data capture
RGB-D	RGB-D camera that provides both depth (D) and color (RGB) data
RRMS	Relapsing–remitting multiple sclerosis
SDMT	Symbol digit modalities test
SUS-Plus	System usability scale plus
V	Visit
VAS	Visual analog scale
VPC	Visual perceptive computing
3 m-CDP	3-month confirmed disease progression
6 MW	6-min walk

frontiers | Frontiers in Immunology

TYPE Original Research
PUBLISHED 16 November 2023
DOI 10.3389/fimmu.2023.1280020

OPEN ACCESS

EDITED BY
Shougang Guo,
Shandong Provincial Hospital, China

REVIEWED BY
Faiez Al Nimer,
Karolinska Institutet (KI), Sweden
Christian Moritz,
Centre Hospitalier Universitaire (CHU) de Saint-Étienne, France

*CORRESPONDENCE
Xiangjun Chen
xiangjchen@fudan.edu.cn
Haifeng Li
drlhf@163.com
Hongyu Zhou
924339836@qq.com

RECEIVED 19 August 2023
ACCEPTED 27 October 2023
PUBLISHED 16 November 2023

CITATION
Zhang X, Hao H, Jin T, Qiu W, Yang H, Xue Q, Yin J, Shi Z, Yu H, Ji X, Sun X, Zeng Q, Liu X, Wang J, Li H, He X, Yang J, Li Y, Liu S, Lau AY, Gao F, Hu S, Chu S, Ding D, Zhou H, Li H and Chen X (2023) Cerebrospinal fluid oligoclonal bands in Chinese patients with multiple sclerosis: the prevalence and its association with clinical features.
Front. Immunol. 14:1280020.
doi: 10.3389/fimmu.2023.1280020

Cerebrospinal fluid oligoclonal bands in Chinese patients with multiple sclerosis: the prevalence and its association with clinical features

Xiang Zhang[1], Hongjun Hao[2], Tao Jin[3], Wei Qiu[4], Huan Yang[5], Qun Xue[6], Jian Yin[7], Ziyan Shi[8], Hai Yu[1], Xiaopei Ji[6], Xiaobo Sun[4], Qiuming Zeng[5], Xiaoni Liu[1], Jingguo Wang[1], Huining Li[9], Xiaoyan He[10], Jing Yang[11], Yarong Li[1], Shuangshuang Liu[12], Alexander Y. Lau[13], Feng Gao[2], Shimin Hu[12,14], Shuguang Chu[15], Ding Ding[1], Hongyu Zhou[8]*, Haifeng Li[12]* and Xiangjun Chen[1]*

[1]Department of Neurology, Huashan Hospital, Fudan University and Institute of Neurology, Fudan University, National Center for Neurological Disorders, Shanghai, China, [2]Department of Neurology, Peking University First Hospital, Beijing, China, [3]Department of Neurology and Neuroscience Center, The First Hospital of Jilin University, Changchun, China, [4]Department of Neurology, The Third Affiliated Hospital of Sun Yat-sen University, Guangzhou, China, [5]Department of Neurology, Xiangya Hospital, Central South University, Changsha, China, [6]Department of Neurology, The First Affiliated Hospital of Soochow University, Suzhou, China, [7]Department of Neurology, Beijing Hospital, Beijing, China, [8]Department of Neurology, West China Hospital, Sichuan University, Chengdu, China, [9]Department of Neurology, Tianjin Neurological Institute, Tianjin Medical University General Hospital, Tianjin, China, [10]Department of Neurology, The Xinjiang Uygur Autonomous Region People's Hospital, Urumqi, China, [11]Department of Neurology, The First Affiliated Hospital of Zhengzhou University, Zhengzhou, China, [12]Department of Neurology, Xuanwu Hospital, Capital Medical University, Beijing, China, [13]Department of Medicine and Therapeutics, Prince of Wales Hospital, The Chinese University of Hong Kong, Hong Kong, Hong Kong SAR, China, [14]Department of Clinical Epidemiology and Evidence-Based Medicine, Xuanwu Hospital Capital Medical University, Beijing, China, [15]Department of Radiology, Shanghai East Hospital, Tongji University School of Medicine, Shanghai, China

Background: Cerebrospinal fluid oligoclonal band (CSF-OCB) is an established biomarker in diagnosing multiple sclerosis (MS), however, there are no nationwide data on CSF-OCB prevalence and its diagnostic performance in Chinese MS patients, especially in the virtue of common standard operation procedure (SOP).

Methods: With a consensus SOP and the same isoelectric focusing system, we conducted a nationwide multi-center study on OCB status in consecutively, and recruited 483 MS patients and 880 non-MS patients, including neuro-inflammatory diseases (NID, n = 595) and non-inflammatory neurological diseases (NIND, n=285). Using a standardized case report form (CRF) to collect the clinical, radiological, immunological, and CSF data, we explored the association of CSF-OCB positivity with patient characters and the diagnostic performance of CSF-OCB in Chinese MS patients. Prospective source data collection, and retrospective data acquisition and statistical data analysis were used.

Findings: 369 (76.4%) MS patients were OCB-positive, while 109 NID patients (18.3%) and 6 NIND patients (2.1%) were OCB-positive, respectively. Time from symptom onset to diagnosis was significantly shorter in OCB-positive than that in OCB-negative MS patients (13.2 vs 23.7 months, P=0.020). The prevalence of CSF-OCB in Chinese MS patients was significantly higher in high-latitude regions (41°-50°N)(P=0.016), and at high altitudes (>1000m)(P=0.025). The diagnostic performance of CSF-OCB differentiating MS from non-MS patients yielded a sensitivity of 76%, a specificity of 87%.

Interpretation: The nationwide prevalence of CSF-OCB was 76.4% in Chinese MS patients, and demonstrated a good diagnostic performance in differentiating MS from other CNS diseases. The CSF-OCB prevalence showed a correlation with high latitude and altitude in Chinese MS patients.

KEYWORDS

oligoclonal bands, cerebrospinal fluid, multiple sclerosis, prevalence, diagnostic performance, China

Introduction

Multiple sclerosis (MS) is a typical chronic inflammatory demyelinating disease of the central nervous system (CNS) (1). The clinical manifestations of MS are diverse, and the core diagnostic points are neurological deficits disseminated in time and space. The diagnosis of MS is challenging, and it should be prudent to differentiate it from other diseases with similar clinical manifestations (2, 3), especially in other inflammatory demyelinating diseases, such as neuromyelitis optica spectrum disorders (NMOSD), and myelin oligodendrocyte glycoprotein antibody-associated disease (MOGAD). Therefore, MS-related biomarkers have become the focus of ongoing research. Although in recent years many diagnostic biomarkers have been reported to be related to MS, few of them have clinical applicability and reliability (4, 5). The presence of immunoglobulin G (IgG) oligoclonal band (OCB) in cerebrospinal fluid (CSF) indicates intrathecal synthesis of immunoglobulin in response to chronic inflammation in CNS (6, 7). CSF-OCB was found in MS patients in the 1960s (8). Since then, it was confirmed as an established biomarker in diagnosing MS and is widely used in the diagnosis of MS globally (9–14).

In the 2017 McDonald diagnostic criteria of MS, OCB is included and can be used as a substitution for dissemination in time (15), which promotes the early diagnosis of MS in patients with the clinically isolated syndrome (CIS) (13, 16, 17). However, the expert panel emphasized that this criteria should be used prudently in Asian patients (15), because of the higher prevalence of non-MS demyelinating diseases in Asia and some of these patients also have CSF-OCB but with short segmental spinal lesions and atypical cerebral lesions. Due to the more important role of CSF-OCB in the diagnosis of MS, Chinese scholars recognized the lack of nationwide data on CSF-OCB in Chinese MS patients might lead to under or over-diagnosis of MS. CSF-OCB was reported in over 85% of MS patients in Europe and the United States (14, 18, 19). However, the prevalence of CSF-OCB in Chinese MS patients was reported as about 30~70% by several single centers (17, 20–23), and was lower than that reported in Western countries. In China, MS was defined as a rare disease (24) with an estimated prevalence of 1~5 per 100,000 (25). Nevertheless, due to the large population in China, the total number of MS patients in China is still large. Till now there are no nationwide data on CSF-OCB positivity and its diagnostic performance in Chinese MS patients.

Using different testing methods of CSF-OCB in different regional studies was previously presumed as the difference in reported OCB positivity in Chinese MS patients and the difference from that reported in Western countries. China is a vast country, hence there might be differences in regional CSF-OCB prevalence due to differences in latitude and altitude. There are also different backgrounds in culture and conventions in different regions of China. Therefore, experts in 12 regional referring MS centers in mainland of China formed the Multiple Sclerosis Collaborative Research Group in 2019 and started the project "CNS-OCB, China National Study for Oligo-Clonal Band"in 2020. We first developed a consensus standard operation procedure (SOP) with an isoelectric focusing system and validated the inter-laboratory agreement (26). With this SOP and the same isoelectric focusing system, we conducted a nationwide multi-center study on OCB status in consecutively, and recruited 483 MS patients and 880 non-MS patients. Using a standardized case report form (CRF) to collect the clinical, radiological, immunological, and CSF data, we explored the association of CSF-OCB positivity with patient characters and the diagnostic performance of CSF-OCB in Chinese MS patients.

Methods

Patients

All patients included in this study were diagnosed with MS or non-MS diseases in the recruiting centers from May 2020 to May 2022 (ChiCTR2000040363). This study was approved by the Ethics Committee of Shanghai Huashan Hospital and all other participating centers. The study was conducted according to the principles of the Declaration of Helsinki. All patients have signed the informed consent and agreed with sample collection and data publication. Prospective source data collection, and retrospective data acquisition and statistical data analysis were used. The data was collected at all centers with a structured database issued by a cooperation project ("CNS-OCB, China National Study for Oligo-Clonal Band") from 2019, and acquired from the database of each center according to the inclusion and exclusion criteria.

In this study, the 2010 McDonald criteria (27) was required to be used for MS diagnosis, and a total of 525 MS patients were consecutively recruited and met the below inclusive criteria: (1) Chinese origin; (2) 14 to 65 years old; (3) two experienced neurologists in each center confirmed the diagnosis of MS independently from the collected CRF in reference to the original medical record when needed; (4) data on demography, CSF test, MRI examination, disease duration, numbers of relapse, annualized relapse rate (ARR), Expanded Disability Status Scale (EDSS), concomitant autoantibodies of or clinical diagnosis of other autoimmune diseases were available. 42 cases were excluded for the following reasons: 9 cases due to concurrent malignant tumors, 27 cases due to meeting the 2017 McDonald criteria but not the 2010 McDonald criteria, and 6 repeated-entry cases from different regional referring neurology centers. The remaining 483 patients were analyzed (Figure 1). The concomitant connective tissue disease (CTD) or autoimmune thyroid disease (AITD) was diagnosed according to relevant diagnostic criteria by consulting rheumatologists or endocrinologists. The number of attacks during the entire disease duration and the EDSS were recorded at the time of CSF collection.

CSF data of 880 consecutively recruited patients with the final diagnosis of other diseases in the 12 centers were collected during the same period, and used as the control group in the evaluation of the diagnostic performance of CSF-OCB in MS. All included patients were: (1) Chinese origin; (2) age of 14 to 65 years; (3) no MS history and two experienced neurologists excluded the diagnosis of MS when differential diagnosis presented; (4) data on demography and CSF-OCB were available. The 880 patients with non-MS diseases were divided into 2 categories: (1) neuro-inflammatory diseases (NID, n=595), including NMOSD (280 cases), MOGAD (45 cases), acute disseminated encephalomyelitis (ADEM) (15 cases), Guillain-Barré syndrome (127 cases) and autoimmune encephalitis (128 cases); (2)non-inflammatory neurological diseases (NIND, n=285), including primary headaches (56 cases), idiopathic epilepsy (20 cases), cerebrovascular diseases (79 cases), dementia (17 cases), motor neuron disease (23 cases), parkinsonism (6 cases), multiple system atrophy (6 cases), spinal vascular disease (7 cases), central nervous system involvement related to acute leukemia (10 cases), somatization disorder (7 cases), metabolic neuropathy (34 cases), hereditary neuropathy (14 cases), normal pressure hydrocephalus (4 cases) and peripheral vertigo (2 cases).

Evaluation of the blood-CSF barrier and intrathecal IgG synthesis

The concentrations of IgG and albumin in serum and CSF were determined by the turbidimetric scattering method. The BCB permeability was assessed using CSF/serum albumin quotient:

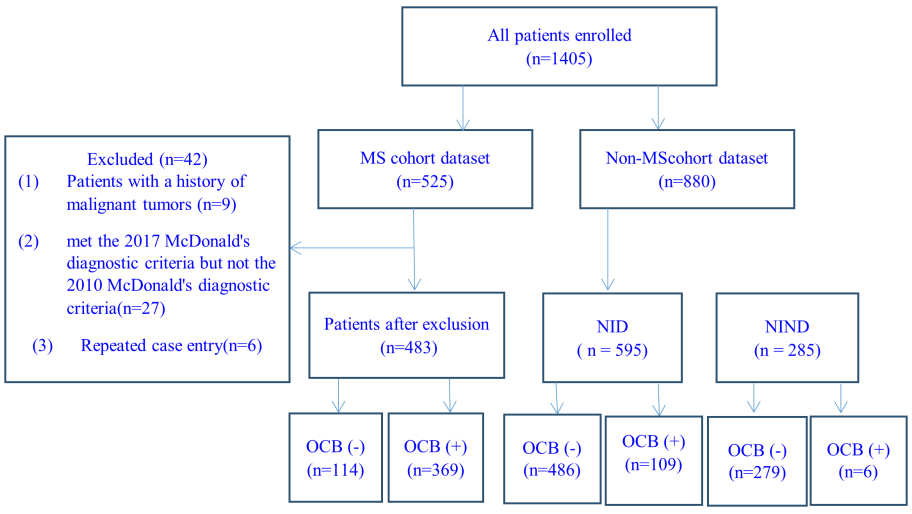

FIGURE 1
Case-screening flowchart. MS, multiple sclerosis; NID, neuro-inflammatory diseases; NIND: neurological non-inflammatory diseases.

Q_{Alb} = CSF-Alb [mg/l]/serum-Alb [g/l]. Increased BCB permeability is defined as Q_{Alb}>4+ (age/15). The IgG index, calculated as (CSF-IgG/serum-IgG)/(CSF-Alb/serum-Alb), is a measure of intrathecal IgG synthesis. An IgG index below 0.7 is considered normal. Tourtellotte IgG synthesis rate (IgG-SR), calculated as [(CSF IgG- serum IgG/369)- (CSF albumin- serum albumin/230) ×(serum IgG/serum albumin)]× 0.43 × 5, is an approach to determine intrathecal IgG synthesis with adjusting of BCB permeability. An IgG-SR below 3.3 mg/24 hours is considered normal (28, 29).

OCB detection

According to the Isoelectric Focusing Electrophoresis (IEF) SOP for the detection of CSF-OCB (26, 30), the detection was performed with Sebia HYDRASYS 2 Isofocusing system PN1211 (France) according to the manufacturer's instructions for the evaluation of IgG OCB. Briefly, CSF and serum samples were run in parallel at a concentration of 10-20 mg/L. After electrophoresis, the gel was incubated with peroxidase-labeled anti-IgG antibodies, and the bands were displayed using TTF1/2 chromogenic agents. Two inspectors independently interpreted the electrophoresis results according to the key points of interpretation, including the presence, number, and patterns of bands in the serum and CSF.

The electrophoresis results were classified into 5 main OCB types. Type I: no bands in both serum and CSF; Type II: ≥ 2 bands in CSF and no band in serum; Type III: additional bands in CSF despite of bands in serum; Type IV: identical bands in both serum and CSF; Type V: twin bands with regular and periodic spacing in both serum and CSF. CSF-OCB positivity was defined as either type II or III bands (29).

Statistical analysis

Patient characters were presented as numbers (percentages), mean ± standard deviation (SD), or median (interquartile range, IQR). Pearson $\chi 2$ test and Fisher's exact test, as well as Student's T test or Mann-Whitney U test, were used for comparison between OCB-positive and OCB-negative groups.

The diagnostic performance of OCB positivity was evaluated as (15):

Accuracy: [(TP+TN)/(TP+TN+FP+FN)]

Sensitivity: [TP/(TP+FN)]

Specificity: [TN/(TN+FP)]

Positive Predictive Value (PPV): [TP/(TP+FP)]

Negative Predictive Value (NPV): [TN/(TN+FN)]

The likelihood ratio for positive test result (PLR): sensitivity/(1-specificity)

The likelihood ratio for negative test result (NLR): (1-sensitivity)/specificity

True positive (TP) was defined as MS according to McDonald 2010 criteria and positive OCB, true negative (TN) was defined as non-MS and negative OCB, false positive (FP) was defined as non-MS but positive OCB, and false negative (FN) was defined as MS but negative OCB.

A two-tailed $p < 0.05$ was considered statistically significant. All statistical analysis was performed using SPSS 26.0 software (IBM SPSS Statistics for Windows, Version 26.0. Armonk, NY: IBM Corp).

Results

General characteristics of patients with MS or other CNS diseases

The general characteristics of patients with MS were shown in Table 1. The mean age of 483 MS patients was 33.63 ± 10.58 years old. Females accounted for 63.2% of overall patients (female/male=2:1). 369 (76.4%) MS patients were OCB-positive (344 with type II, and 25 with type III), and 114 (23.6%) MS patients were OCB-negative (112 with type I, and 2 with type IV) (Table 1).

880 non-MS patients included 595 NID patients and 285 NIND patients. The mean age was 42.10 ± 16.71 years in NID patients and 45.53 ± 18.21 years in NIND patients. The female/male ratio was 1.2:1 in NID patients and 0.8:1 in NIND patients. 109 NID patients (18.3%) were OCB-positive (102 with type II, and 7 with type III), and 6 NIND patients (2.1%) were OCB-positive (5 with type II, and 1 with type III).

The patients with MS had higher prevalence of CSF-OCB than those with non-MS (76.4% vs 13.1%, P<0.001). In comparison with the NIND, NID patients had more percentage of positive CSF-OCB (18.3% vs 2.1%, P<0.001), but had less percentage of positive CSF-OCB when compared with MS (18.3% vs 76.4%, P<0.001).

Diagnostic performance of CSF-OCB for differentiating MS from other CNS diseases

The diagnostic performance of CSF-OCB differentiating MS from non-MS patients yielded an accuracy of 83%, a sensitivity of 76%, a specificity of 87%, a PPV of 76%, a NPV of 87%, a PLR of 5.85, and a NLR of 0.27. The diagnostic performance in differentiating MS from NID patients showed 79%, 76%, 82%, 77%, 81%, 4.17, and 0.29, respectively. The diagnostic performance in differentiating MS from NIND patients showed 84%, 76%, 98%, 98%, 71%, 36.29, and 0.24, respectively (Table 2).

Moreover, considering that in most clinical cases, it is mainly CNS inflammatory demyelinating diseases (CIDD) that needs to be carefully distinguished from MS, we extracted data on the OCB status of the patients with CIDD (including NMOSD, MOGAD, ADEM) and compared it with MS patients, the diagnostic performance in differentiating MS from CIDD patients showed an accuracy of 77%, a sensitivity of 76%, a specificity of 79%, a PPV of 86%, a NPV of 66%, a PLR of 3.64, and a NLR of 0.30 (Table 2).

10.3389/fimmu.2023.1280020

TABLE 1 The clinical characteristics of MS patients with different CSF-OCB.

Item	Overall	CSF-OCB		p value
		Negative	Positive	
Age (years), mean ± SD	33.63 ± 10.58	34.95 ± 11.55	33.23 ± 10.24	0.129
Age ≤ 50, n (%)	443	100 (87.7)	343 (93.0)	0.076
> 50, n (%)	40	14(12.3)	26(7.0)	
Sex, n (%)				
Male	178	48 (42.1)	130 (35.2)	0.184
Female	305	66 (57.9)	239 (64.8)	
With a history of other autoimmune disease				
No	452	99(86.8)	353(95.7)	0.001
Yes	31	15(13.2)	16(4.3)	
Time from symptom onset to diagnosis, months (P_{25}, P_{75})	14.80 (2.13, 44.87)	23.70 (5.05, 50.73)	13.20 (1.58, 42.77)	0.020
Disease duration, n (%)				
≤1 year	218	47 (41.2)	171 (46.3)	0.499
1-5 years	173	46 (40.4)	127 (34.4)	
>5 years	92	21 (18.4)	71 (19.2)	
The number of attacks, mean #	2.45 ± 2.01	2.43 ± 2.15	2.48 ± 1.47	0.824
1-2 attacks	316	75 (65.8)	241(65.8)	0.784
3-5 attacks	144	33 (28.9)	111(30.3)	
>5 attacks	20	6 (5.3)	14 (3.8)	
ARR (P_{25}, P_{75})	0.66 (0.31, 1.29)	0.66 (0.31, 1.00)	0.65 (0.30, 1.33)	0.907
EDSS, mean ± SD # #	2.54 ± 1.76	2.58 ± 1.79	2.42 ± 1.67	0.382
EDSS < 3, n (%)	309	70 (61.9)	239 (67.0)	0.224
3 ≤ EDSS ≤ 6, n (%)	140	40 (35.4)	100 (28.0)	
EDSS > 6, n (%)	21	3 (2.7)	18 (5.0)	

#Data missing in 3 patients; ##Data missing in 13 patients.
CSF, cerebrospinal fluid; OCB, oligoclonal bands; CTD, connective tissue disease; AITD, autoimmune thyroid disease; ARR, annualized relapse rate; EDSS, Expanded Disability Status Scale.

Association between clinical characteristics and CSF-OCB positivity

The included MS patients were from 25 provinces and 4 cities (Beijing, Shanghai, Guangzhou, and Chongqing) (Figure 2). Based on the characteristics of the geographical condition and human geography in China, they were divided into 7 regions, including Northeast (Heilongjiang, Jilin, and Liaoning), North (Beijing, Tianjin, Shanxi, Hebei, and Inner Mongolia), East (Shanghai, Jiangsu, Zhejiang, Anhui, Jiangxi, Shandong and Fujian), Central (Henan, Hunan, and Hubei), South (Guangdong and Guangxi), Southwest (Chongqing, Sichuan, Guizhou, and Yunnan), and Northwest (Shanxi, Gansu, Qinghai, Ningxia, and Xinjiang). The prevalence of CSF-OCB was around 60% in MS patients originating in the East and South regions and more than 80% in the other regions. The provinces and cities were also classified into low latitude (20°-30°N), middle latitude (31°-40°N), and high latitude (41°-50°N) regions (Figure 2). The prevalence of CSF-OCB in MS patients in these regions was 68.1% (81/119), 77.0% (217/282), and 86.6% (71/82), significantly higher in high-latitude regions (P=0.016) (Table 3). They were also classified into low-altitude (<500m) and high-altitude (>1000m) regions (Figure 2). The prevalence of CSF-OCB in MS patients at high altitudes (82.63%, 138/167) was significantly higher than those at low altitudes (73.1%, 231/316) (P=0.025) (Table 3).

As shown in Table 1, there were no differences about age and gender between OCB positive and negative patients (P=0.129, P=0.184). Time from symptom onset to diagnosis was significantly shorter in OCB-positive patients than that in OCB-negative patients (13.2 months vs. 23.7 months, P=0.020). There were fewer patients with concomitant autoimmune diseases in the OCB-positive patients (4.3%, 16/369) than in the OCB-negative patients (13.2%, 15/114) (P=0.001). No significant differences were observed among OCB status and disease duration, the number of attacks, ARR and EDSS (P=0.499, P=0.824, P=0.907, P=0.382) (Table 1).

10.3389/fimmu.2023.1280020

TABLE 2 Diagnostic value of CSF-OCB between MS and non-MS.

	Total, n	CSF-OCB		Accuracy (95% CI)	Sensitivity (95% CI)	Specificity (95% CI)	PPV (95% CI)	NPV (95% CI)	PLR (95% CI)	NLR (95% CI)
		Negative, n	Positive, n							
MS vs non-MS										
MS	483	114	369	0.83 (0.81, 0.85)	0.76 (0.72, 0.80)	0.87 (0.85, 0.89)	0.76 (0.72, 0.80)	0.87 (0.85, 0.89)	5.85 (4.90, 6.98)	0.27 (0.23, 0.32)
Non-MS	880	765	115							
MS vs NID										
MS	483	114	369	0.79 (0.77, 0.82	0.76 (0.72, 0.80)	0.82 (0.78, 0.85)	0.77 (0.73, 0.81)	0.81 (0.78, 0.84)	4.17 (3.49, 4.98)	0.29 (0.25, 0.34)
NID	595	486	109							
MS vs CIDD										
MS	483	114	369	0.77 (0.74, 0,80)	0.76 (0.72, 0.80)	0.79 (0.74, 0,84)	0.86 (0.83, 0.90)	0.66 (0.61, 0.71)	3.64 (2.78, 4.49)	0.30 (0.25, 0.35)
CIDD	276	218	58							
MS vs NIND										
MS	483	114	369	0.84 (0.82, 0.87)	0.76 (0.72, 0.80)	0.98 (0.95, 0.99)	0.98 (0.97, 0.99)	0.71 (0.66, 0.75)	36.29 (16.42, 80.22)	0.24 (0.21, 0.28)
NIND	285	279	6							

CNS, the central nervous system; MS, multiple sclerosis; non-MS, CNS disease other than MS; NID, CNS inflammatory diseases; CIDD, CNS inflammatory demyelinating diseases; NIND, CNS non-inflammatory diseases; PPV, Positive predictive value; NPV, Negative predictive value; PLR, Likelihood ratio for positive test results; NLR, Likelihood ratio for negative test results.

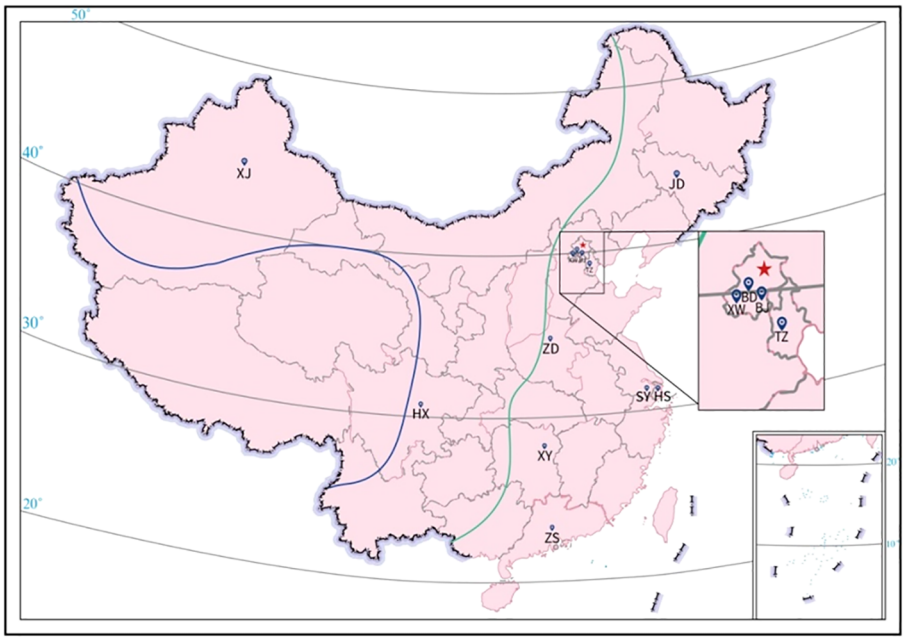

FIGURE 2
Geographical distribution of participating neurology centers. BD, Peking University First Hospital; BJ, Beijing Hospital; HS, Huashan Hospital affiliated to Fudan University; HX, West China Hospital of Sichuan University; JD, The First Hospital of Jilin University; SY, The First Affiliated Hospital of Soochow University; TZ; Tianjin Medical University General Hospital; XJ, People's Hospital of Xinjiang Uygur Autonomous Region; XW, Xuanwu Hospital, Capital Medical University; XY, Xiangya Hospital of Central South University; ZD, The First Affiliated Hospital of Zhengzhou University; ZS, The Third Affiliated Hospital of Sun Yat-sen University. All patients were recruited from the 12 neurology centers in China and originated from 25 provinces and Beijing, Shanghai, Guangzhou, Chongqing (except Tibet, Hainan, Hong Kong, Macau, and Taiwan) spanning 20° and 50° North Latitude (20°-50°N). The altitude of China decreases from west to east and is commonly divided into 3 subregions: < 500m (east of green line), 1000-2000m (between green and blue line), and >4000m (southwest of blue line).

TABLE 3 Geographical distribution of CSF-OCB positivity.

Geographical regions	Overall, n	CSF-OCB, n (%)		*p* value
		Negative	Positive	
Latitude				
Low (20° – 30°N)	119	38 (31.9)	81 (68.1)	0.016
Medium (31° – 40°N)	282	65 (23.0)	217 (77.0)	
High (41° – 50°N)	82	11 (13.4)	71 (86.6)	
Altitude				
Low (< 500 m)	316	85 (26.9)	231(73.1)	0.025
High (> 1000 m)	167	29 (17.4)	138 (82.6)	

The association between CSF-OCB and MRI features

The attacks of MS affect various parts of the CNS, in this study T2 weighted MRI lesions in different locations of CNS were compared between OCB-positive and negative patients. More OCB-positive patients have periventricular lesions than OCB-negative patients (93.6% vs 86.5%, P= 0.017) (Table 4).

The association between CSF-OCB and CSF parameters

The mean level of CSF protein was lower in OCB-positive patients than that in OCB-negative patients (340.00 mg/L vs 370.00 mg/L, P<0.001). Less OCB-positive MS patients had elevated Q_{Alb} in comparison with OCB-negative MS patients (16.0%, 37/231 vs 29.3%, 22/75, P=0.011). The proportions of MS patients with increased IgG index and abnormal IgG-SR were greater in OCB-positive patients than those in OCB-negative patients (69.8%, 215/308 vs 33.7%, 32/95, P<0.001; 69.3%, 212/306 vs 38.5%, 37/96, P<0.001, respectively).

Discussion

In our study, the enrolled MS patients originated from 25 provinces and 4 cities, covering most regions in mainland of China, which depicted a representative nationwide portrait of Chinese MS patients, and provided insight into the clinical and diagnostic value of CSF-OCB in Chinese MS patients. As we know, this is the first report about nationwide data on CSF-OCB positivity and its diagnostic performance in Chinese MS patients, especially in the virtue of common SOP.

We adopted the 2010 McDonald Criteria because it did not need the information of CSF-OCB, and had fairly good sensitivity for diagnosing MS in CIS patients (27). Moreover, the prevalence of CSF-OCB is easily compared with earlier researchers. Importantly, this would avoid bias from the incorporation of OCB in diagnostic studies because the 2017 McDonald criteria and other diagnostic criteria all incorporate OCB as supporting conditions (15).

OCB suggests intrathecally synthesized immunoglobulin in response to B cell activation as a result of CNS inflammation (12). It is not only detected in MS but also in other neurological disease (19). Several previous reports had shown that CSF-OCB had a high specificity for diagnosing MS. In these articles, MS was often compared to healthy individuals or patients with non-neurological inflammatory diseases (12, 30–32). However, A meta-analysis had shown that when patients with neurological inflammatory diseases were used as the control group, the specificity of CSF-OCB for diagnosing MS would reduce from 94% to 61% (32). These suggested that the differences in the control group used in research could greatly affect the evaluation of the specificity of CSF-OCB in diagnosing MS, and was one of the reasons for the significant differences about specificity reported in various studies. In clinical practice, the differential diagnosis between MS and neurological inflammatory diseases is crucial. In this study, 18.3% of patients in the NID were CSF-OCB positive, which is significantly higher than those in the NIND. Therefore, we included NID and NIND patients as the controls, and found that when NIND was used as the control, the specificity of CSF-OCB for diagnosing MS could reach 98%, while when NID was used as the control, the specificity dropped to 77%.

In clinical practice, it is crucial for MS to be distinguished from CIDD. The significant difference in OCB prevalence between MS and CIDD (76.4% vs 21.0%) shown in this study (diagnostic spectivity 79%) suggests that negative CSF-OCB could be a “red flag” for the diagnosis of MS. When some patients with central demyelinating disease have clinical and/or imaging manifestations that are very similar to MS, and may even be diagnosed as MS according to MS diagnostic criteria at a certain time point, their negative OCB results need to be constantly reminded to doctors during long-term follow-up to pay attention to whether changes in the patient’s clinical and imaging manifestations that were inconsistent with MS, so as to timely revise the diagnosis. Moreover, the time from the onset of disease to clinical diagnosis in our cohort was almost one-year earlier in OCB-positive patients than that in OCB-negative patients, supporting that OCB detection also facilitates early MS diagnosis for Chinese patients with MS.

In previous studies, Zheng et al. reported that the OCB positive rate was 62.5% in Zhejiang, a province of East China (17). Lu et al. have revealed that the OCB positive rate was 59.8% in Guangdong

10.3389/fimmu.2023.1280020

TABLE 4 The CSF-OCB and MRI lesions of MS patients.

Lesion distribution	Overall, n	CSF-OCB, n (%)		*p* value
		Negative	Positive	
Optic nerve				
No	435	104 (95.4)	331 (93.0)	0.365
Yes	30	5 (4.6)	25 (7.0)	
Cortical/Juxtacortical				
No	112	29 (26.1)	83 (23.3)	0.545
Yes	355	82 (73.9)	273 (76.7)	
Periventricular				
No	38	15 (13.5)	23 (6.4)	0.017
Yes	431	96 (86.5)	335 (93.6)	
Brain stem				
No	226	55 (49.5)	171 (47.8)	0.742
Yes	243	56 (50.4)	187 (52.2)	
Cerebellum				
No	355	84 (75.7)	271 (75.7)	0.996
Yes	114	27 (24.3)	87 (24.3)	
Cervical spinal cord				
No	170	45 (42.5)	125 (36.1)	0.239
Yes	282	61 (57.5)	221 (63.9)	
Thoracic spinal cord				
No	259	62 (59.0)	197 (57.9)	0.841
Yes	186	43 (41.0)	143 (42.1)	
Lumbar spinal cord				
No	408	92 (96.8)	316 (96.3)	0.816
Yes	15	3 (3.2)	12 (3.7)	

Province and Hong Kong SAR, two regions belonging to South China (20). In the survey of MS patients in north China, GU et al. and Chen et al. reported that the positive rates of OCB were 69.3% and 72.7% respectively (33, 34). According to China's seven commonly used geographical divisions, China's territory can be divided into North, South, Central, East, Northeast, Northwest, and Southwest. These 7 regions have obvious differences in topography, climate, vegetation types, production modes, habits, customs, and culture. In this study, the overall OCB positivity was 76.4% in Chinese patients with MS, and was about 60% in East and South China which was consistent with the results reported by Zheng et al. and Lu et al (17, 20), and was about 90% in North China, slightly higher than the results reported by GU et al. and Chen et al (33, 34). Thus, the inconsistencies of the previous reports were well explained in the analysis considering the geographical distribution difference of MS patients as the dominant factor.

Our results also showed that the geographical distribution of high OCB prevalence demonstrated a high-latitude feature. Lechner-Scott et al. have prospectively collected and analyzed CSF-OCB data from MSBase, a large international, multi-center database, and found that the frequency of OCB increased with latitude (35). In Lechner-Scott's paper, the OCB positive rate was 85~100% in the regions located North of 40°N, which is similar to the latitudes in our study. The OCB positive rate was 50~90% in the 30°~40°N regions, and again, this is similar to the latitudes in this study. As to the regions in 20° ~30°N, the OCB positive was 35% and 59%, which is lower than the same latitude in our investigation. In another report on the positive OCB and/or increased IgG index and latitude from Japan (36), CSF-OCB prevalence of MS in the northern region(42°-45°N) was higher than that in the southern region (33°-35°N), the average positive rate of the OCB and/or increased IgG index was 58.7%, and was similar to that reported in this study in the eastern coastal region of China (61.5%), which geographical characteristics are similar to those of Japan on the whole. Latitudinally the OCB prevalence in China was comparable to Europe and the United States (18, 35, 37), especially in high-latitudinal regions.

As to the altitude, only a few papers have revealed the relationship between MS morbidity and altitude (38, 39), but no publications had reported the relationship between CSF-OCB positivity and altitude. As shown in Table 3, we noticed that the OCB prevalence of patients observed in this study showed a trend related to altitude, that was, the OCB prevalence of patients in high-altitude areas was higher than that in low-altitude areas. As we know, this is the first report about the relationship between CSF-OCB prevalence and altitude.

People living in high-latitude and high-altitude areas of China, as a whole, tend to have a diet dominated by rice and pasta, with less consumption of vegetables, fruits, and fish, and have lower levels of vitamin D (40, 41). They also have specific human leukocyte antigen (HLA) enabling them to better adapt to high-altitude and high-latitude environments (42, 43).It has been confirmed that the risk of MS was associated with various geographic, environmental, ethnic, and lifestyle factors, especially genetic susceptibility(HLA), diet customs and vitamin D levels, which might promote the occurrence of MS by the influence on the status or function of immune cells, and logically the state of OCB produced by plasma cells in CNS (36, 44–48). However, the relationship between these factors and the productivity of OCB in China still lacks strong validation, and further research is needed to verify.

There were many studies on the correlation between OCB positivity and long-term MS activity and prognosis, but the results were controversial (49). Some studies reported that OCB positivity correlated with disease activity, such as ARR, and EDSS (50, 51), but in some other studies, the opposite conclusion was reported (20, 52). In this study, no significant differences were observed among OCB status and EDSS, ARR, disease course, and the number of relapses. Because this study was only a cross-sectional observation study, the correlation between OCB positivity and long-term MS activity and prognosis in Chinese people needs further study.

Both MRI and CSF-OCB are key indicators in the diagnostic criteria of MS (15). In this study, the lesion locations of MS were summarized as optical nerve, cortical/juxtacortical, periventricular, brain stem, cerebellum, cervical spinal cord, thoracic spinal cord, and lumbar spinal cord. Zhao et al. reported that in comparison with the OCB-negative MS patients, the OCB-positive group had a higher proportion of cerebellar lesions (53); Huttner et al. Suggested that MRI lesions and OCB status were independent of each other (54). However, we found that patients with positive OCB had more periventricular lesions than patients with negative OCB, while there was no significant difference in the proportion of patients with other lesions.

The BCB is an important physiological natural barrier of the CNS and peripheral environment, which can prevent the entry of various proteins and chemicals, including immunoglobulin. The presence of OCB in CSF indicates the existence of chronic persistent inflammation in CNS, suggesting the production of immunoglobulin in CNS, rather than that caused by the peripheral immunoglobulin entering CNS (55). In this study, BCB disruption was only observed in a small proportion (~20%) of MS patients in which most of the patients were OCB negative, and was negatively correlated to OCB positivity, as with previous studies (12, 56, 57).

IgG index and IgG-SR are important parameters of CSF analysis about CNS immune response. Like OCB, they are also designed to evaluate the presence of immunoglobulin synthesis and inflammatory processes in CNS and are widely used in the clinical diagnosis of MS (10, 29). Several studies have reported that an IgG index>0.7 was closely correlated with OCB positivity and was a prognostic marker of early disease activity (58, 59).In agreement with these reports, this study also showed that the proportions of MS patients with increased IgG index and abnormal IgG-SR were greater in OCB-positive patients than those in OCB-negative patients (28, 58–60).

The strength of this study is based on the following: 1. The sample size is large and the SOP adopted in CSF-OCB testing was previously validated. 2. The twelve regional referring MS centers cover the difference in latitude and altitude and represent the typical culture and convention in China. 3. Accurate diagnosis of MS and non-MS demyelinating diseases was guaranteed with the same CRF and we aimed to evaluate the diagnostic performance of CSF-OCB in MS patients, the possibility of misclassification of MS and non-MS demyelinating diseases was tiny based on the consensus from regional and nationwide experts on doubtful patients. 4. Using the 2010 Mcdonald criteria, which is based only with clinical and radiological data, avoiding the inclusion bias by using MS patients diagnosed with criteria that adopt the role of CSF-OCB.

There were some limitations in this study: 1. Only cross-sectional EDSS was collected, and the relapse risk was analyzed with retrospective data. 2. Long-term changes in CSF-OCB status in MS patients and non-MS demyelinating disease patients were not addressed. 3. The association between CSF-OCB status and some radiological features of MS could not be analyzed due to the cross-sectional design and only some retrospective data were acquired by reviewing the case records. Nevertheless, these are not the main focus of this study. We are collecting relevant data in a prospective cohort among all participating centers.

In conclusion, this study reported, for the first time, that the nationwide prevalence of CSF-OCB was 76.4% and conducive to early diagnosis in Chinese patients with MS, and demonstrated a good performance in differentiating MS from other CNS diseases, suggesting that CSF-OCB is a valuable clinical indicator for the diagnosis of MS in Chinese patients. In addition, the CSF-OCB prevalence showed a correlation with high latitude and altitude, reflecting the characteristics of regional distribution of OCB prevalence in Chinese patients with MS.

Data availability statement

The original contributions presented in the study are included in the article/supplementary material. Further inquiries can be directed to the corresponding authors.

Ethics statement

The studies involving humans were approved by the Ethics Committee of Shanghai Huashan Hospital. The studies were

conducted in accordance with the local legislation and institutional requirements. The participants provided their written informed consent to participate in this study.

Author contributions

XZ: Conceptualization, Data curation, Formal Analysis, Investigation, Methodology, Software, Visualization, Writing – original draft, Writing – review & editing. HH: Conceptualization, Data curation, Investigation, Methodology, Writing – original draft. TJ: Data curation, Investigation, Methodology, Writing – review & editing. WQ: Conceptualization, Data curation, Investigation, Methodology, Writing – review & editing. HuY: Conceptualization, Data curation, Investigation, Methodology, Writing – review & editing. QX: Conceptualization, Data curation, Investigation, Methodology, Writing – review & editing. JYi: Conceptualization, Data curation, Investigation, Writing – review & editing. ZS: Data curation, Investigation, Methodology, Writing – review & editing. HaY: Conceptualization, Data curation, Investigation, Writing – review & editing. XJ: Data curation, Investigation, Writing – review & editing. XS: Data curation, Investigation, Methodology, Writing – review & editing. QZ: Data curation, Investigation, Methodology, Writing – review & editing. XL: Data curation, Investigation, Methodology, Writing – original draft. JW: Writing – review & editing, Data curation, Investigation, Methodology. HuL: Data curation, Investigation, Software, Writing – review & editing. XH: Data curation, Investigation, Software, Writing – review & editing. JYa: Data curation, Investigation, Software, Writing – review & editing. YL: Data curation, Methodology, Writing – review & editing. SL: Data curation, Investigation, Methodology, Software, Writing – review & editing. AL: Conceptualization, Data curation, Investigation, Methodology, Writing – review & editing. FG: Conceptualization, Data curation, Investigation, Writing – review & editing. SH: Data curation, Methodology, Software, Writing – review & editing. SC: Conceptualization, Investigation, Methodology, Writing – review & editing. DD: Conceptualization, Investigation, Methodology, Software, Writing – review & editing. HZ: Conceptualization, Data curation, Investigation, Supervision, Visualization, Writing – review & editing. HaL: Conceptualization, Data curation, Investigation, Supervision, Visualization, Writing – review & editing. XC: Conceptualization, Data curation, Funding acquisition, Investigation, Methodology, Resources, Supervision, Validation, Visualization, Writing – review & editing.

Funding

The author(s) declare financial support was received for the research, authorship, and/or publication of this article. This study was supported by the Clinical Research Plan of SHDC (No. SHDC2020CR2027B), 2020 Medical Service and Support Capacity Improvement Project: Construction of the Cohort-Based Multidisciplinary Accurate Diagnosis and Treatment Platform for Neurological Autoimmune and Infectious Diseases, and Shanghai Municipal Science and Technology Major Project (No. 2017SHZDZX01) and State Key Laboratory of Genetic Engineering, Human Phenome Institute, Zhangjiang Fudan International Innovation Center, Fudan University.

Acknowledgments

Special appreciation for recently deceased professor Xianhao Xu who is the key advocate for our “CNS-OCB” project. Thank professors Chuanzhen Lu and Xueqiang Hu for their support for the project. In addition, appreciation is extended to the “CNS-OCB” consortium member: Yan Xu (Department of Neurology, Peking Union Medical College, Peking Union Medical College Hospital, Chinese Academy of Medical Sciences, Beijing, China.); Bitao Bu (Department of Neurology, Tongji Hospital, Tongji Medical College, Huazhong University of Science and Technology, Wuhan, China.); Qi Cheng (Ruijin Hospital, Shanghai Jiaotong University School of Medicine, Shanghai,China.); Huifang Huang (Department of Neurology, The First Affiliated Hospital of Soochow University, Suzhou, China.); Lanjun Li (Department of Neurology, the First Affiliated Hospital of Zhengzhou University, Zhengzhou, China.); Zhiguo Li (Department of Neurology, Tianjin Neurological Institute, Tianjin Medical University General Hospital, Tianjin, China.); Caiyun Liu (Department of Neurology and Neuroscience Center, The First Hospital of Jilin University, Changchun, China.); Tingting Lu (Department of Neurology, The Third Affiliated Hospital of Sun Yat-sen University, Guangzhou, China); Hong Wang (Department of Neurology, Beijing Hospital, Beijing, China.); Thank Zhang Yu from Biogen Medical Affairs (China) for the manuscript editing.

Conflict of interest

The authors declare that the research was conducted in the absence of any commercial or financial relationships that could be construed as a potential conflict of interest.

Publisher’s note

References

1. Perdaens O, van Pesch V. Molecular mechanisms of immunosenescene and inflammaging: relevance to the immunopathogenesis and treatment of multiple sclerosis. *Front Neurol* (2021) 12:811518. doi: 10.3389/fneur.2021.811518

2. Haralur Y, Mechtler LL. Neuroimaging of multiple sclerosis mimics. *Neurol Clin* (2020) 38(1):149–70. doi: 10.1016/j.ncl.2019.09.002

3. Wildner P, Stasiolek M, Matysiak M. Differential diagnosis of multiple sclerosis and other inflammatory CNS diseases. *Mult Scler Relat Disord* (2020) 37:101452. doi: 10.1016/j.msard.2019.101452

4. Kaisey M, Lashgari G, Fert-Bober J, Ontaneda D, Solomon AJ, Sicotte NL. An update on diagnostic laboratory biomarkers for multiple sclerosis. *Curr Neurol Neurosci Rep* (2022) 22(10):675–88. doi: 10.1007/s11910-022-01227-1

5. Saadeh RS, Ramos PA, Algeciras-Schimnich A, Flanagan EP, Pittock SJ, Willrich MA. An update on laboratory-based diagnostic biomarkers for multiple sclerosis and beyond. *Clin Chem* (2022) 68(9):1134–50. doi: 10.1093/clinchem/hvac061

6. Antel J, Bar-Or A. Roles of immunoglobulins and B cells in multiple sclerosis: from pathogenesis to treatment. *J Neuroimmunol* (2006) 180(1-2):3–8. doi: 10.1016/j.jneuroim.2006.06.032

7. Wootla B, Denic A, Keegan BM, Winters JL, Astapenko D, Warrington AE, et al. Evidence for the role of B cells and immunoglobulins in the pathogenesis of multiple sclerosis. *Neurol Res Int* (2011) 2011:780712. doi: 10.1155/2011/780712

8. Holmoy T. The discovery of oligoclonal bands: a 50-year anniversary. *Eur Neurol* (2009) 62(5):311–5. doi: 10.1159/000235944

9. Gastaldi M, Zardini and D. Franciotta E. An update on the use of cerebrospinal fluid analysis as a diagnostic tool in multiple sclerosis. *Expert Rev Mol Diagn* (2017) 17 (1):31–46. doi: 10.1080/14737159.2017.1262260

10. Lo Sasso B, Agnello L, Bivona G, Bellia C, Ciaccio M. Cerebrospinal fluid analysis in multiple sclerosis diagnosis: an update. *Medicina (Kaunas)* (2019) 55(6):245. doi: 10.3390/medicina55060245

11. Cabrera CM. Oligoclonal bands: An immunological and clinical approach. *Adv Clin Chem* (2022) 109:129–63. doi: 10.1016/bs.acc.2022.03.004

12. Link H, Huang YM. Oligoclonal bands in multiple sclerosis cerebrospinal fluid: an update on methodology and clinical usefulness. *J Neuroimmunol* (2006) 180(1-2):17–28. doi: 10.1016/j.jneuroim.2006.07.006

13. Arrambide G, Tintore M, Espejo C, Auger C, Castillo M, Río J, et al. The value of oligoclonal bands in the multiple sclerosis diagnostic criteria. *Brain* (2018) 141 (4):1075–84. doi: 10.1093/brain/awy006

14. Alvarez-Cermeno JC, Villar LM. Multiple sclerosis: Oligoclonal bands–a useful tool to avoid MS misdiagnosis. *Nat Rev Neurol* (2013) 9(6):303–4. doi: 10.1038/nrneurol.2013.74

15. Thompson AJ, Banwell BL, Barkhof F, Carroll WM, Coetzee T, Comi G. Diagnosis of multiple sclerosis: 2017 revisions of the McDonald criteria. *Lancet Neurol* (2018) 17(2):162–73. doi: 10.1016/S1474-4422(17)30470-2

16. van der Vuurst de Vries RM, Mescheriakova JY, Wong YYM, Runia TF, Jafari N, Samijn JP. Application of the 2017 revised McDonald criteria for multiple sclerosis to patients with a typical clinically isolated syndrome. *JAMA Neurol* (2018) 75(11):1392–8. doi: 10.1001/jamaneurol.2018.2160

17. Zheng Y, Shen CH, Wang S, Yang F, Cai MT, Fang W, et al. Application of the 2017 McDonald criteria in a Chinese population with clinically isolated syndrome. *Ther Adv Neurol Disord* (2020) 13:1756286419898083. doi: 10.1177/1756286419898083

18. Dobson R, Ramagopalan S, Davis A, Giovannoni G. Cerebrospinal fluid oligoclonal bands in multiple sclerosis and clinically isolated syndromes: a meta-analysis of prevalence, prognosis and effect of latitude. *J Neurol Neurosurg Psychiatry* (2013) 84(8):909–14. doi: 10.1136/jnnp-2012-304695

19. Carta S, Ferraro D, Ferrari S, Briani C, Mariotto S. Oligoclonal bands: clinical utility and interpretation cues. *Crit Rev Clin Lab Sci* (2022) 59(6):391–404. doi: 10.1080/10408363.2022.2039591

20. Lu T, Zhao L, Sun X, Au C, Huang Y, Yang Y. Comparison of multiple sclerosis patients with and without oligoclonal IgG bands in South China. *J Clin Neurosci* (2019) 66:51–5. doi: 10.1016/j.jocn.2019.05.025

21. Li B, Dong H, Zhang J, Song X, Guo L. Cerebrospinal fluid IgG profiles and oligoclonal bands in Chinese patients with multiple sclerosis. *Acta Neurol Scand* (2007) 115(5):319–24. doi: 10.1111/j.1600-0404.2006.00753.x

22. Ming F, Jian Q. Clinical significance of CSF-restricted OCB in neurological diseases. *Chin J Clin Neurosci* (2004) 12(4):365–8. doi: 10.3969/j.issn.1008-0678.2004.04.009

23. Yan W, Hongjun H, Feng G. Application of CSF oligoclonal bands in multiple sclerosis and neuromyelitis optica. *Chin J Pract Nervous Dis* (2013) 16(2):29–30. doi: 10.1097/WCO.0000000000000699

24. Lu Y, Gao Q, Ren X, Li J, Yang D, Zhang Z, et al. Incidence and prevalence of 121 rare diseases in China: Current status and challenges: 2022 revision. *Intractable Rare Dis Res* (2022) 11(3):96–104. doi: 10.5582/irdr.2022.01093

25. Jia D, Zhang Y, Yang C. The incidence and prevalence, diagnosis, and treatment of multiple sclerosis in China: a narrative review. *Neurol Sci* (2022) 43(8):4695–700. doi: 10.1007/s10072-022-06126-4

26. Liu XN, Chen XJ, Sun XB, Qiu W, Peng LS, Li HF, et al. [Establishment and consistency verification of the standard operation procedure for laboratory detection of immunoglobulin G oligoclonal bands in cerebrospinal fluid]. *Zhonghua Yi Xue Za Zhi* (2021) 101(31):2465–70. doi: 10.3760/cma.j.cn112137-20201127-03210

27. Polman CH, Reingold SC, Banwell B, Clanet M, Cohen JA, Filippi M, et al. Diagnostic criteria for multiple sclerosis: 2010 revisions to the McDonald criteria. *Ann Neurol* (2011) 69(2):292–302. doi: 10.1002/ana.22366

28. Caroscio JT, Kochwa S, Sacks H, Cohen JA, Yahr MD. Quantitative CSF IgG measurements in multiple sclerosis and other neurologic diseases. *update Arch Neurol* (1983) 40(7):409–13. doi: 10.1001/archneur.1983.04050070039007

29. Gastaldi M, Zardini E, Leante R, Ruggieri M, Costa G, Cocco E, et al. Cerebrospinal fluid analysis and the determination of oligoclonal bands. *Neurol Sci* (2017) 38(Suppl 2):217–24. doi: 10.1007/s10072-017-3034-2

30. Freedman MS, Thompson EJ, Deisenhammer F, Giovannoni G, Grimsley G, Keir G, et al. Recommended standard of cerebrospinal fluid analysis in the diagnosis of multiple sclerosis: a consensus statement. *Arch Neurol* (2005) 62(6):865–70. doi: 10.1001/archneur.62.6.865

31. Villar LM, Masjuan J, Sádaba MC, González-Porqué P, Plaza J, Bootello A, et al. Early differential diagnosis of multiple sclerosis using a new oligoclonal band test. *Arch Neurol* (2005) 62(4):574–7. doi: 10.1001/archneur.62.4.574

32. Petzold A. Intrathecal oligoclonal IgG synthesis in multiple sclerosis. *J Neuroimmunol* (2013) 262(1-2):1–10. doi: 10.1016/j.jneuroim.2013.06.014

33. Kelin C, Xue Z, Guoge L, Xixiong K, Guojun Z. Clinical significance of CSF-OCB and intrathecal IgG synthesis related indicators in multiple sclerosis. *Int J Lab Med* (2018) 39(23):2873–2875,2888. doi: 10.3969/j.issn.1673-4130.2018.23.007

34. Yuyu GU, Zhou J, Wang D, Liu J, Wang L, Chen K, et al. An analysis of 4514 electrophoresis samples of cerebrospinal fluid oligoclonal bands in a hospital. *Labeled Immunoassays Clin Med* (2021) 28(10):1681–8. doi: 10.11748/bjmy.issn.1006-1703.2021.10.012

35. Lechner-Scott J, Spencer B, de Malmanche T, Attia J, Fitzgerald M, Trojano M, et al. The frequency of CSF oligoclonal banding in multiple sclerosis increases with latitude. *Mult Scler* (2012) 18(7):974–82. doi: 10.1177/1352458511431729

36. Nakamura Y, Matsushita T, Sato S, Niino M, Fukazawa T, Yoshimura S, et al. Latitude and HLA-DRB1*04:05 independently influence disease severity in Japanese multiple sclerosis: a cross-sectional study. *J Neuroinflamm* (2016) 13(1):239. doi: 10.1186/s12974-016-0695-3

37. Peña-Sánchez M, Lestayo Lestayo O Z, Farril L, Valido Luna L, Betancourt Loza M, González-Garcia S, Hernández-Díaz ZM, et al. CSF oligoclonal band frequency in a Cuban cohort of patients with multiple sclerosis. comparison with Latin American countries and association with latitude. *Mult Scler Relat Disord* (2020) 45:102412. doi: 10.1016/j.msard.2020.102412

38. Tian DC, Zhang C, Yuan M, Yang X, Gu H, Li Z, et al. Incidence of multiple sclerosis in China: A nationwide hospital-based study. *Lancet Reg Health West Pac* (2020) 1:100010. doi: 10.1016/j.lanwpc.2020.100010

39. Lauer K. Environmental associations with the risk of multiple sclerosis: the contribution of ecological studies. *Acta Neurol Scand Suppl* (1995) 161(Suppl 161):77–88. doi: 10.1111/j.1600-0404.1995.tb05861.x

40. Li L, Li K, Li J, Luo Y, Cheng Y, Jian M, et al. Ethnic, geographic, and seasonal differences of vitamin D status among adults in south-west China. *J Clin Lab Anal* (2020) 34(12):e23532. doi: 10.1002/jcla.23532

41. Mata-Greenwood E, Westenburg HCA, Zamudio S, Illsley NP, Zhang L. Decreased vitamin D levels and altered placental vitamin D gene expression at high altitude: role of genetic ancestry. *Int J Mol Sci* (2023) 24(4). doi: 10.3390/ijms24043389

42. Wang B, Zhang YB, Zhang F, Lin H, Wang X, Wan N, et al. On the origin of Tibetans and their genetic basis in adapting high-altitude environments. *PloS One* (2011) 6(2):e17002. doi: 10.1371/journal.pone.0017002

43. Zhang YB, Li X, Zhang F, Wang DM, Yu J. A preliminary study of copy number variation in Tibetans. *PloS One* (2012) 7(7):e41768. doi: 10.1371/journal.pone.0041768

44. Guglielmetti M, Al-Qahtani WH, Ferraris C, Grosso G, Fiorini S, Tavazzi E, et al. Adherence to mediterranean diet is associated with multiple sclerosis severity. *Nutrients* (2023) 15(18). doi: 10.3390/nu15184009

45. Lehman PC, Ghimire S, Price JD, Ramer-Tait AE, Mangalam AK. Diet-microbiome-immune interplay in multiple sclerosis: Understanding the impact of phytoestrogen metabolizing gut bacteria. *Eur J Immunol* (2023) 53(11):e2250236. doi: 10.1002/eji.202250236

46. Jacobs BM, Tank P, Bestwick JP, Noyce AJ, Marshall CR, Mathur R, et al. Modifiable risk factors for multiple sclerosis have consistent directions of effect across diverse ethnic backgrounds: a nested case-control study in an English population-based cohort. *J Neurol* (2023). doi: 10.1007/s00415-023-11971-0

47. Amato MP, Derfuss T, Hemmer B, Liblau R, Montalban X, Soelberg Sørensen P, et al. Environmental modifiable risk factors for multiple sclerosis: Report from the 2016 ECTRIMS focused workshop. *Mult Scler* (2018) 24(5):590–603. doi: 10.1177/1352458516686847

48. Olsson T, Barcellos LF, Alfredsson L. Interactions between genetic, lifestyle and environmental risk factors for multiple sclerosis. *Nat Rev Neurol* (2017) 13(1):25–36. doi: 10.1038/nrneurol.2016.187

49. Magliozzi R, Cross AH. Can CSF biomarkers predict future MS disease activity and severity? *Mult Scler* (2020) 26(5):582–90. doi: 10.1177/1352458519871818

50. Ben Noon G, Vigiser I, Shiner T, Kolb H, Karni A, Regev K. Reinforcing the evidence of oligoclonal bands as a prognostic factor in patients with Multiple sclerosis. *Mult Scler Relat Disord* (2021) 56:103220. doi: 10.1016/j.msard.2021.103220

51. Rojas JI, Tizio S, Patrucco L, Cristiano E. Oligoclonal bands in multiple sclerosis patients: worse prognosis? *Neurol Res* (2012) 34(9):889–92. doi: 10.1179/1743132812Y.0000000088

52. Frau J, Villar LM, Sardu C, Secci MA, Schirru L, Ferraro D, et al. Intrathecal oligoclonal bands synthesis in multiple sclerosis: is it always a prognostic factor? *J Neurol* (2018) 265(2):424–30. doi: 10.1007/s00415-017-8716-4

53. Zhao L, Abrigo J, Chen Q, Au C, Ng A, Fan P, et al. Advanced MRI features in relapsing multiple sclerosis patients with and without CSF oligoclonal IgG bands. *Sci Rep* (2020) 10(1):13703. doi: 10.1038/s41598-020-70693-9

54. Huttner HB, Schellinger PD, Struffert T, Richter G, Engelhorn T, Bassemir T, et al. MRI criteria in MS patients with negative and positive oligoclonal bands: equal fulfillment of Barkhof's criteria but different lesion patterns. *J Neurol* (2009) 256 (7):1121–5. doi: 10.1007/s00415-009-5081-y

55. Meinl E, Krumbholz M, Derfuss T, Junker A, Hohlfeld R. Compartmentalization of inflammation in the CNS: a major mechanism driving progressive multiple sclerosis. *J Neurol Sci* (2008) 274(1-2):42–4. doi: 10.1016/j.jns.2008.06.032

56. Akaishi T, Takahashi T, Nakashima I. Oligoclonal bands and periventricular lesions in multiple sclerosis will not increase blood-brain barrier permeability. *J Neurol Sci* (2018) 387:129–33. doi: 10.1016/j.jns.2018.02.020

57. Deisenhammer F, Zetterberg H, Fitzner B, Zettl UK. The cerebrospinal fluid in multiple sclerosis. *Front Immunol* (2019) 10:726. doi: 10.3389/fimmu.2019.00726

58. Zheng Y, Cai MT, Yang F, Zhou JP, Fang W, Shen CH, et al. IgG index revisited: diagnostic utility and prognostic value in multiple sclerosis. *Front Immunol* (2020) 11:1799. doi: 10.3389/fimmu.2020.01799

59. Simonsen CS, Flemmen HØ, Lauritzen T, Berg-Hansen P, Moen SM, Celius EG. The diagnostic value of IgG index versus oligoclonal bands in cerebrospinal fluid of patients with multiple sclerosis. *Mult Scler J Exp Transl Clin* (2020) 6 (1):2055217319901291. doi: 10.1177/2055217319901291

60. Belimezi M, Kalliaropoulos A, Mentis AA, Chrousos GP. Diagnostic significance of IgG and albumin indices versus oligoclonal band types in demyelinating disorders. *J Clin Pathol* (2021) 76(3):166–71. doi: 10.1136/jclinpath-2021-207766

10.3389/fimmu.2023.1280020

APPENDIX 1 The information regarding MRI collected in CRF.

MRI with and without intravenous gadolinium-based contrast agent administration	
Lesion distribution:	
Optic nerve: Yes/No	Contrast-enhancing lesions: Yes/No
Cortical/Juxtacortical: Yes/No	Contrast-enhancing lesions: Yes/No
Periventricular: Yes/No	Contrast-enhancing lesions: Yes/No
Brain stem: Yes/No	Contrast-enhancing lesions: Yes/No
Cerebellum: Yes/No	Contrast-enhancing lesions: Yes/No
Cervical spinal cord: Yes/No	Contrast-enhancing lesions: Yes/No
Thoracic spinal cord: Yes/No	Contrast-enhancing lesions: Yes/No
Lumbar spinal cord: Yes/No	Contrast-enhancing lesions: Yes/No
Are the radiological McDonald criteria fulfilled:	
• Dissemination in time: Yes/No	
• Dissemination in space: Yes/No	

Standardized imaging protocol: ①At least 1·5T; 3T if available; ②Core sequences: axial T2-weighted, and T1-weighted with and without gadolinium;T2-weighted fluid-attenuated inversion recovery.

frontiers | Frontiers in Neurology

TYPE Original Research
PUBLISHED 24 November 2023
DOI 10.3389/fneur.2023.1295904

OPEN ACCESS

EDITED BY
Cong-Cong Wang,
Shandong Provincial Qianfoshan Hospital, China

REVIEWED BY
Chunfu Zheng,
University of Calgary, Canada
Zhan-hui Feng,
Affiliated Hospital of Guizhou Medical University, China

*CORRESPONDENCE
Xuhua Yin
yinxuhua1116@163.com
Ya Chen
chenya8706@163.com

†These authors have contributed equally to this work

RECEIVED 17 September 2023
ACCEPTED 09 November 2023
PUBLISHED 24 November 2023

CITATION
Mi F, Wang Y, Chai W, Chen Y and Yin X (2023) Application value of plasma Neurofilament light combined with magnetic resonance imaging to comprehensively evaluate multiple sclerosis activity and status.
Front. Neurol. 14:1295904.
doi: 10.3389/fneur.2023.1295904

Application value of plasma Neurofilament light combined with magnetic resonance imaging to comprehensively evaluate multiple sclerosis activity and status

Feiyue Mi[1†], Yingchun Wang[1†], Wenqiang Chai[2], Ya Chen[3*] and Xuhua Yin[1*]

[1]Department of Neurology, Affiliated Hospital of Inner Mongolia Medical University, Hohhot, Inner Mongolia Autonomous Region, China, [2]General Hospital of Inner Mongolia Autonomous Region of the Chinese People's Armed Police Force, Hohhot, Inner Mongolia Autonomous Region, China, [3]Department of Neurology, Affiliated Hospital of Zunyi Medical University, Zunyi, Guizhou province, China

Objective: Compare the levels of plasma neurofilament light (NfL) in patients with multiple sclerosis (MS) at acute and remission stages and healthy individuals to explore the role of plasma NfL in monitoring the activity and severity of the disease and predicting disease prognosis.

Methods: Information on healthy individuals and patients with MS who visited the outpatient and inpatient departments of Inner Mongolia Medical University Affiliated Hospital from October 2020 to August 2022 was collected. EDSS assessment and plain scan+enhanced magnetic resonance imaging (MRI). Plasma Nfl levels were measured using Simoa. Moreover, the relationship between the level of Nlf and the disease status of patients with MS was analyzed.

Results: Through the self-comparison of the plasma NfL levels of MS patients in the acute and remission stages, it was noted that the levels in the acute stage are higher than those in the remission stage ($p < 0.001$). Among the plasma NfL levels of healthy individuals and MS patients in the acute and remission stages, there were statistically significant differences ($p < 0.001$). Furthermore, the plasma NfL level did not correlate with age or course of disease ($p = 0.614$ and $p = 0.058$), whereas it correlated with EDSS score, the number of MRI T2 subtentorial and spinal cord lesions, and the number of MRI enhanced lesions ($r = 0.789$, $p < 0.001$; r = 0.846, $p < 0.001$; $r = 0431$, $p = 0.005$, respectively).

Conclusion: Combining the level of plasma NfL with clinical and MRI estimations will be instrumental in monitoring condition changes and optimizing treatments. The level of plasma NfL is related to the activity and severity of MS, and it is expected to become a new biomarker for assessing the activity and disease status of MS.

KEYWORDS

multiple sclerosis, Neurofilament light, magnetic resonance imaging, activity, biomarkers

1 Introduction

Multiple sclerosis (MS) is a chronic degenerative autoimmune disease of the central nervous system (CNS), with inflammation, demyelination, and axis cylinder loss occurring in the early stage (1). Differential involvements of motor, sensory, visual, and autonomic nervous systems can cause a series of symptoms and signs, such as limb weakness, sensory abnormalities, impaired vision, and dystaxia (2), which are the main etiologies of disability among young people globally, placing a significant burden on the social economy (3). The Global Burden of Disease (GBD) research team of the Institute of Health Metrics and Evaluation of the University of Washington discovered that there were approximately 2.3 million MS cases globally, with an increase of 10.4% in morbidity since 1990. Between 1990 and 2016, the prevalence rates in Chinese Mainland and Taiwan rose by 45.6 and 49.5%, respectively. Approximately three-quarters of the global MS patients are women (4). In 2018, China marked MS as a rare disease. In 2020, MS incidence rates in China were released for the first time: 0.235/100,000 per year, 0.055/100,000 in children, and 0.288/100,000 in adults. The geographical distribution of MS shows an east–west altitude gradient. Residents in high latitude and altitude areas tend to develop MS. The incidence rate in Inner Mongolia is more than 0.4/100,000, ranking first in China (5).

MS has multiple temporal and spatial clinical features. At present, the 2017 McDonald criteria is recommended, and the diagnosis mainly depends on clinical manifestations, cerebrospinal fluid and MRI (6). The abovementioned indicators are also applied in prognostic evaluation. However, assessing the prognoses of patients with MS only based on clinical and imaging evidence is hysteretic. Therefore, clinicians need new highly specific and sensitive biomarkers that can monitor disease activity and severity and indicate a prognosis to comprehensively understand MS, implement precise and personalized management of patients with feasible methods as much as possible, improve prognosis, raise patients' quality of life, and lighten the economic burden on patients.

Neurofilament (NF) is a specific component of the cytoskeleton, primarily maintaining the elasticity and integrity of nerve fibers and ensuring their functions. NF includes Neurofilament light (NfL), Neurofilament medium (NfM), Neurofilament heavy (NfH), α-endonuclease, and type-III peripherin. When CNS axons are injured, the NF released into the cerebrospinal fluid indicates axonal injury and neuronal death (7). Under normal physiological conditions, low concentrations of NfL are released from axons into the cerebrospinal fluid and enter the bloodstream through the blood–brain barrier (BBB) at low concentrations. The release of NfL gradually increases with age (8). If affect neuronal axonal damage, the release process will be accelerated, which is the basis for using NfL as a marker for axonal damage (9, 10). Williams et al. (11) found a strong correlation between NfL and disease activity. As an ongoing quantitative measurement of axonal injury, the increase in NfL may be conducive to the prognosis of neurological diseases (12).

When the CNS axonal injury occurs, NfL is first released into the cerebrospinal fluid, and a small portion enters the peripheral blood through the BBB. The content of NfL in the peripheral blood is 40 times lower than that in the cerebrospinal fluid. In the past, NfL detection was mainly based on cerebrospinal fluid measurement using the ELISA method. However, the traditional ELISA method usually fails to detect it. The advanced detection method, Simoa, has a sensitivity 1000 times higher than traditional ELISA, making it possible to plasma NfL. Moreover, NfL sampling in the peripheral blood is easy and convenient to store, allowing for testing (13). It has become a trend of replacing cerebrospinal fluid NfL with plasma NfL.

Relapsing remitting multiple sclerosis (RRMS) is a recurrent process. Nerve fiber damage and axonal loss are the main mechanisms causing neurological disability. Therefore, simple and direct multimode methods are required to monitor disease changes and perform follow-up. NfL may play a specific role in monitoring the activity, severity, treatment efficacy, and prognosis of MS as a marker of axonal injury.

2 Experimental materials and methods

2.1 Research subjects

This study included 42 patients with MS who visited the outpatient and inpatient departments of Inner Mongolia Medical University Affiliated Hospital from October 2020 to August 2022, including 25 patients in the acute stage and 17 patients in the remission stage. All patients with MS met the 2017 edition of the McDonald's criteria and were classified as relapsing–remitting. As healthy controls, 26 healthy individuals were included, aged from 20 to 60 years. All enrolled patients signed an informed consent form, and all research procedures were approved by the Ethics Committee (Inner Mongolia Medical University Affiliated Hospital, NO. WZ2023056).

The enrolled 25 acute patients were treated with steroid pulse or intravenous immunoglobulin therapy and improved. After discharge, 20 patients were followed up within 6 months. The patients without new clinical symptoms or enhanced MRI lesions were classified as in the remission stage and underwent plasma NfL testing. Those who recurred or had enhanced lesions were excluded. For the present study, the acute stage was regarded as the current event with pathological changes in the CNS acute inflammatory demyelination. It was found according to the subjective description of patients or objective examination and lasted more than 24 h and less than 1 month. The remission stage was regarded as no recurrence within 6 months before sampling, no progression in EDSS assessment, and no new lesions found on MRI scans. Five cases dropped out of the study: one who went to study abroad, two who changed their residences, and two who were lost due to the Covid-19 pandemic (Figure 1).

2.1.1 Inclusion criteria

1. The seizure type and clinical symptoms of MS complied with the revised McDonald criteria in 2017. After a detailed inquiry of medical history, physical examination, and head MRI examination, the patient was diagnosed with MS;
2. Aged 18–60 years;
3. No recurrence within 6 months before sampling, no progression in EDSS assessment, and no new lesions on MRI scans;
4. Those who were able to complete survey scales and MRI;
5. The patient and their family agreed to participate in this study and signed an informed consent form.

2.1.2 Exclusion criteria

1. Those with clear liver and kidney function damage, hypertension, diabetes, and heart disease;
2. Combined with fever, elevated hemogram, and other infectious symptoms;
3. Concomitant cerebrovascular disease and tumor;
4. Concomitant peripheral neuropathy, motor neuron disease, and Parkinson's disease;
5. Concomitant diseases that affect information collection, such as dementia and mental illness, and those who were not interested in participating in this study.

2.2 Experimental methods

MS patients were required to complete their basic information, including age, gender, body mass index (BMI), and course of disease, and plasma NfL testing were carried out. Patients who were followed up within 6 months to 1 year also underwent the abovementioned examinations. Healthy individuals improved their basic information and underwent the plasma NfL testing.

2.2.1 EDSS evaluation and imaging examination

On the day of blood collection, two professional neurologists conducted EDSS evaluations on all patients with MS, and scores were given. The scoring criteria were strictly followed to decline errors. All MS patients underwent a plain scan and enhanced 3.0 T MRI on the head, cervical, and thoracic spinal cord. With the assistance of professional neurologists and imaging neurologists, the presence and the number of enhanced lesions were checked, as well as the number of T2 subtentorial and spinal cord lesions (Figure 2).

2.2.2 Plasma NfL detection

During blood collection, 5 mL of fasting peripheral blood was extracted from all participants using EDTA tubes. The blood was centrifuged at 1000 rpm for 10 min, and then the upper layer was extracted. The plasma sample was transferred to a 96-well plate, shaking magnetic beads for at least 30 s. The machine was turned on to preheat and entered the NfL detection program. The Simoa platform was used for batch or individual testing. Finally, a report of the results was generated and exported in PDF format for subsequent analysis (Figure 3).

2.3 Statistical methods

All data were analyzed using SPSS26.0. Normally distributed measurement data were described as mean ± standard deviation. A T-test was used for two groups, and analysis of variance was used for multiple groups. The measurement data of non-normal distribution were represented by median and interquartile intervals, and non-parametric tests were used: K-W test or Wilcoxon test. The enumeration data were expressed as composition ratio, and the X^2 test was used for comparison between groups. Spearman correlation analysis was used. The significance level was $\alpha = 0.05$, with $p < 0.05$ considered as statistically significant (Figure 4).

3 Results

3.1 Basic information

This study screened and incorporated 42 patients with RRMS, aged between 20 and 60 years, with an average age of 40 years. As controls, 26 healthy individuals were included. The basic information on patients with MS and healthy individuals is shown in Table 1. There was no statistically significant difference in age, sex, and BMI between the two groups ($p > 0.05$). The results were comparable.

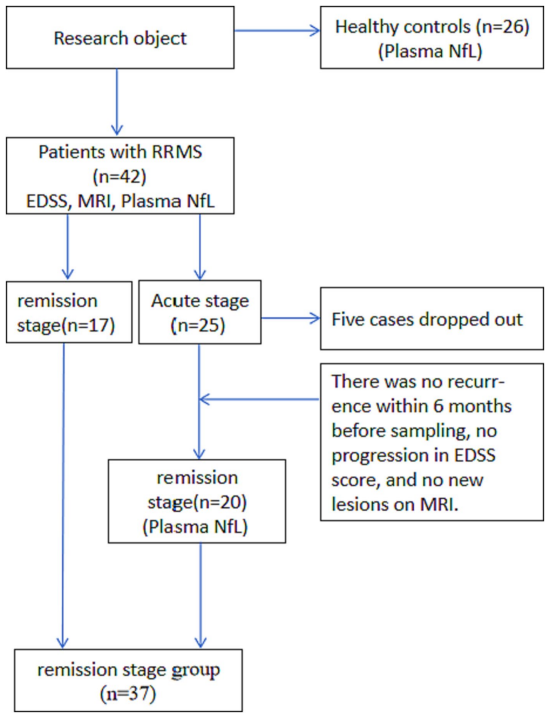

FIGURE 1
Flowchart.

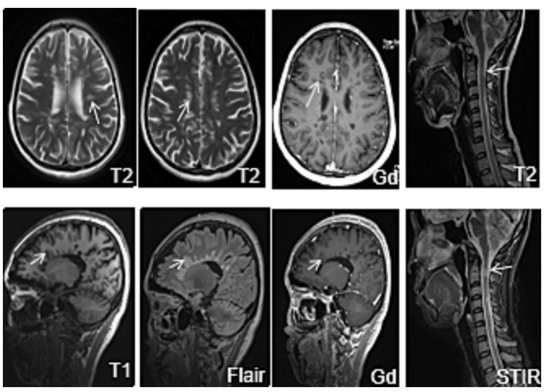

FIGURE 2
Lesions on MRI.

10.3389/fneur.2023.1295904

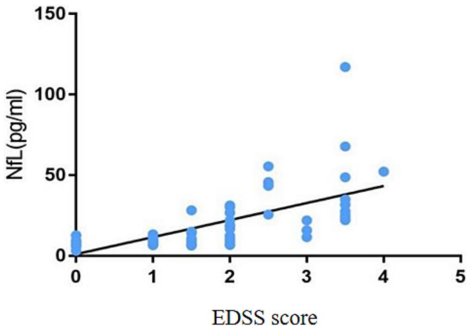

FIGURE 3
Correlation between EDSS score and the plasma NfL level.

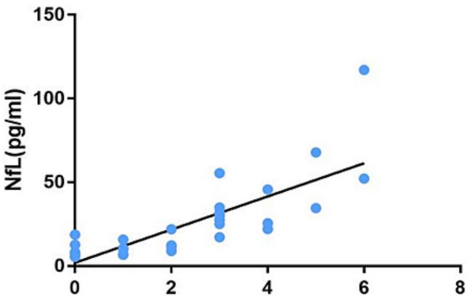

FIGURE 4
Correlation between the number of infratentorial and spinal cord lesions on MRI and the plasma NfL level.

TABLE 1 Basic information of patients with MS and healthy individuals.

	MS	CG	T/χ^2	*P*
Sample size	42	26		
Age (year, x ± S)	40.12 ± 12.45	40.81 ± 12.92	−0.219	0.828
Sex (male/female)	12/30	7/19	0.022	0.883
BMI (kg/m^2, x ± S)	23.99 ± 3.68	23.94 ± 2.62	0.058	0.954

Statistical description and analysis were conducted on the course of the disease, EDSS score, number of infratentorial and spinal cord lesions on MRI, and number of enhanced MRI lesions of the two groups. The results are shown in Table 2. Between the two groups, there was no statistically significant difference in the course of disease ($p = 0.523$), whereas the EDSS score and number of enhanced lesions on MRI had statistical significance ($p < 0.001$) and the number of MRI T2 infratentorial and spinal cord lesions also had statistical significance ($p = 0.037$).

3.2 Plasma NfL comparison between MS patients in acute and remission stages and healthy individuals

To further analyze plasma NfL levels of different stages of MS and healthy individuals, the study subjects were divided into three groups

TABLE 2 Comparison of clinical data of patients with MS.

Indicator	Acute stage ($n = 25$)	Remission stage ($n = 37$)	*Z*	*P*
Course of disease (month)	46.0 (17.5, 101.5)	57.0 (26.5, 87.5)	−0.639	0.523
EDSS score	2.5 (2.0, 3.5)	1.0 (0, 1.5)	−5.137	<0.001
Number of MRI T2 infratentorial and spinal cord lesions	3.0 (1.0, 4.0)	0.5 (0, 1.8)	−2.081	0.037
Number of MRI-enhanced lesions	1.0 (1.0, 2.0)	0 (0, 0)	−7.142	<0.001

TABLE 3 Comparison of plasma NfL levels between MS acute and remission stages and healthy individuals.

	NfL(pg/ml)	*H*	*P*
Acute stage($n = 25$)	21.96 (10.8933.12)[a,b]		
Remission stage ($n = 37$)	9.43 (7.4515.81)[c]	23.856	<0.001
Healthy individuals group($n = 26$)	7.90 (3.83,10.63)		

[a]indicates a significant difference between the acute stage and the remission stage; [b]denotes a significant difference between the acute stage and the healthy individual group; [c]represents a significant difference between the remission stage and the healthy individual group.

for intergroup comparison. The differences in plasma NfL levels were statistically significant (Table 3).

3.3 Plasma NfL comparison between MS patients in acute and remission stages

A self-control study was conducted on the changes in the plasma NfL levels of the acute and remission stages of 20 MS patients who were followed up and re-examined after treatment in the acute stage. The results are shown in Table 4. There was statistical significance in plasma NfL levels between the acute and remission stages of patients with MS ($p < 0.001$).

3.4 Correlation analysis of NfL in MS patients

This study analyzed the correlations between the plasma NfL level and age, course of disease, EDSS score, number of infratentorial and spinal cord lesions on MRI T2, and MRI-enhanced lesions. The results are shown in Table 5. The plasma NfL level is not correlated with age and course of disease ($p = 0.614$ and $p = 0.058$). However, it had correlations with EDSS score, the number of infratentorial and spinal cord lesions on MRI T2, and the number of MRI enhanced lesions ($r = 0.789$, $p < 0.001$; $r = 0.846$, $p < 0.001$; $r = 0431$, $p = 0.005$, respectively).

4 Discussion

MS is a complex heterogeneous disease with unpredictable course and prognosis. In the past few decades, the clinical application of biomarkers in neurodegenerative diseases has gradually increased.

TABLE 4 Comparison of plasma NfL levels between acute and remission stages in patients with MS.

	NfL(pg/ml)	*Z*	*P*
Acute stage ($n = 20$)	23.54 (13.1734.12)	−3.696	<0.001
Remission stage ($n = 20$)	12.05 (8.6818.33)		

TABLE 5 Correlation analysis of NfL in patients with MS.

	NfL level	
Indicator	*r*	*p*
Age	−0.065	0.614
Course of disease	−0.243	0.058
EDSS score	0.789	<0.001
Number of MRI T2 infratentorial and spinal cord lesions	0.846	<0.001
Number of enhanced lesions	0.495	0.005

Scholars have disclosed that plasma NfL is a promising indicator for axonal injury.

Research on NfL began with cerebrospinal fluid specimens. NfL in the cerebrospinal fluid possesses potential prognostic value in clinical isolation syndrome (CIS) and RRMS and can be a disease activity biomarker (14). Gaetani et al. collected cerebrospinal fluid samples from 32 patients with MS within 30 days after the first demyelination event and followed them up for 3.8 ± 2.5 years. The cerebrospinal fluid NfL was measured using ELISA. In the first demyelination event, patients with subsequent disease activities had higher baseline cerebrospinal fluid NfL values than clinically and radiologically stable patients (15). Scholars outside China have recognized a high correlation between blood and the cerebrospinal fluid NfL level, indicating that blood sampling can replace cerebrospinal fluid collection. Repeated measurement of NfL in the peripheral blood to detect axonal damage may become a new approach for monitoring MS (16). This experiment compared the NfL levels of 20 patients with MS. It was found that the NfL levels of patients in the acute stage were significantly higher than those of patients in the remission stage, with significant differences. The plasma NfL levels in both the acute and remission stages of MS were higher than those in healthy individuals, implying a significant increase in NfL during the acute stage of the disease, further demonstrating that NfL, as a marker of neuronal axonal injury, is always associated with inflammatory activity in MS, and has important significance in monitoring disease activity.

In addition to inflammatory activity, another related aspect of MS pathology is the occurrence of neurodegeneration and progressive disability, which can also be objectively measured using NfL. Research has confirmed that patients with progressive MS have higher NfL levels than age and sex-matched recurrent patients (17). Generally, in contrast with RRMS, patients with progressive MS are more severe, with more functional lesions in the neurological system. A study incorporated 41 patients with CIS, 34 patients with MS, 73 patients with neuromyelitis optica spectrum disease as the patients groups; 40 lumbar puncture patients diagnosed with neurosis and migraine as the normal control groups. The clinical and neuroimaging features of the MS group and cerebrospinal fluid samples from the two groups were collected. An enzyme-linked immunosorbent assay was used to measure the NfL level in the cerebrospinal fluid of patients in each group. The NfL levels in the CSF of CIS, MS, and neuromyelitis optica spectrum disease groups were correlated with EDSS score and MRI gadolinium enhancement. The results manifest that the NfL level in the cerebrospinal fluid is conducive to assessing the severity and possible progression of demyelinating diseases (18). In MS patients, there is a correlation between the plasma NfL level and EDSS score, and the EDSS score is strongly correlated with multiple MRI volume parameters (19). Pauwels et al. conducted a prospective cohort study of 115 MS patients and 30 controls, and disease deterioration was defined as an increase in at least one of three measures (EDSS score, timed 25-foot walk, and 9-hole peg test). They found a significant correlation between the plasma NfL level and disability deterioration (20). Scholars from outside of China have detected the NfL levels of MS patients and conducted long-term follow-ups. Patients with high baseline NfL levels have a significantly high risk of developing EDSS.

The results in this study illustrate a positive correlation between the EDSS score and the plasma NfL level, meaning that the higher the EDSS score, the higher the plasma NfL level, possibly due to two aspects. First, there is persistent chronic inflammation in the CNS of patients with MS. Although active lesions or disability progression was not found in most patients through MRI scans and EDSS scores, this chronic injury can cause continuous axonal damage and release NfL into the cerebrospinal fluid and blood. Second, in the later stage of the disease, the compensatory repair effect of patients diminishes, and the axonal regeneration ability weakens. Therefore, the NfL content in the cerebrospinal fluid and blood of MS is significantly high. It suggests that NfL can be used to some extent for assessing MS severity and is an essential indicator of disability progression in patients.

The diagnosis of MS recurrence primarily relies on MRI gadolinium enhancement and clinical recurrence. Some patients do not have typical clinical manifestations of recurrence, and some patients only present discomfort or limb numbness, making it difficult to determine whether there is a recurrence. Moreover, even false seizures exist in some patients. Enhanced MRI is an objective indicator. However, there still may be omissions due to limitations. The role of NfL in monitoring disease activity and severity is extensively recognized. Some reports have shown a strong correlation between the NfL level and the number of active lesions on MRI. The disease activity caused by active inflammation (new T2 and gadolinium-enhanced lesions) is a critical factor in the elevation of NfL. A prospective cohort study included 58 Canadian and Italian MS patients. In this study, patients with active MS were followed up every 3 months or less for 1 year, including clinical evaluation, MRI scanning, and serum extraction. Quantitative analysis was performed using the Simoa platform. NfL with a high baseline was associated with future recurrence, MRI lesions, compound recurrence-related deterioration, and progression independent of recurrent activity (21). After the acute recurrence of MS, NfL is damaged and released into the cerebrospinal fluid and peripheral blood, consistent with MRI recurrence. In a 2018 prospective study involving 259 patients with MS, it was found that for each enhancement lesion in MS patients, the NfL level increased by 17.8%, and for each new or enlarged T2 high signal lesion, the sNfL level increased by 4.9%. However, it was not correlated with the volume of T2 lesions (22). In this study, the number of MRI-enhanced lesions in patients in the acute stage was higher than that in patients in the remission stage, representing that enhanced lesions are essential for seizure determination. The number of MRI-enhanced lesions was positively correlated with the plasma NfL level. The more MRI-enhanced lesions, the higher the plasma NfL level, indicating that enhanced lesions reflect the activity of inflammation and are related to the severity of axonal injuries. Therefore, an increase in the NfL level may imply the recurrence of the disease.

Recent studies have proven that an increase in NfL during the clinical stage of MS may be an ideal prognostic biomarker for predicting disease progression and guiding treatment decisions. As visual evoked potential (VEP) is increasingly used as a quantitative parameter for myelin sheath in clinical trials, scholars evaluate the correlation between VEP latency and retinal neurodegeneration and prognostic potential in RRMS using optical coherence tomography (OCT). P100 latency can indicate disease prognosis and is correlated with NfL at the baseline (23). NfL levels increase 6 years before the clinical onset of MS, representing that MS may have a prodromal stage that lasts for several years, during which axonal damage has already occurred. Therefore, the main pathogenesis of MS may not be inflammation but neurodegeneration. It can lead to irreversible neurological deficits. This transformation is a key factor in long-term prognosis (24). With the approval of efficient disease modifying therapies (DMTs), some of these drugs have verified effects on neurodegeneration. Therefore, there is an urgent need for reliable biomarkers to identify this transitional stage early and actively intervene in high-risk progressive patients.

MRI is irreplaceable in diagnosing MS, monitoring clinical medication, and evaluating suspected recurrence or disability deterioration (25). MRI is the gold standard for diagnosing patients with MS and the most powerful clinical tool (26). The 2021 European Neurology Annual Conference brought many advancements in iconography. The conference expounded that in patients with MS, massive T2 lesions of large volume, the occurrence of gadolinium-enhanced lesions and spinal cord lesions, whole brain atrophy, and gray matter atrophy were observed, all of which predicted poor prognosis (26). To analyze which lesion sites on MRI were most closely associated with the cerebrospinal fluid NfL level, Adams et al. performed a lumbar puncture, collected the cerebrospinal fluid from 139 patients with MS, and followed 25 of them. The cerebrospinal fluid NfL and MRI relationship was evaluated based on the location and number of lesions. Spearman rank correlation was used to assess the correlations between the cerebrospinal fluid NfL and MRI lesion location, as well as baseline and 1-year follow-up lesion count. The results suggest that the correlations between the baseline cerebrospinal fluid NfL and lesion location and subsequent lesion are general, while the correlation between baseline MRI and the cerebrospinal fluid NfL is strong: periventricular, juxtacortical, infratentorial, and spinal cord injuries (27). It can be seen that there is a weak positive correlation between the cerebrospinal fluid NfL and typical periventricular lesions of MS, a moderate positive correlation between juxtacortical lesions and the cerebrospinal fluid NfL, and a strong positive correlation between the cerebrospinal fluid NfL and infratentorial and spinal cord lesions. This study found in clinical work that MS patients with MRI infratentorial and spinal cord lesions usually had poor prognoses. Therefore, the MRI examination of the head, cervical, and thoracic spinal cord was performed on patients with MS, and the number of T2 lesions was counted. According to rank correlation analysis, there is a correlation between the plasma NfL level and the number of MRI T2 infratentorial and spinal cord lesions. In the 2020 EMotion Forum, experts affirmed the role of plasma NfL in diagnosing MS and its potential for evaluating prognosis (28). This study shows a positive correlation between the number of MRI infratentorial and spinal cord lesions and the plasma NfL level, demonstrating that poor prognosis may exist in MS patients with infratentorial and spinal cord injuries. This study suggests that elevated NfL may be one of the indicators for poor prognosis in patients with infratentorial and spinal cord lesions. However, long-term follow-up is required for further verification.

Significant breakthroughs have been achieved in MS treatment in the past 25 years. As more and more DMT drugs enter the Chinese market, the main problems faced by doctors are deciding who should receive treatment, for how long treatment should be given, and whether to choose high-efficient or low to medium-efficient DMT drugs. These decisions are usually based on treatment tolerance and reasonable expectations for long-term efficacy (29). The plasma NfL level can indicate prognosis and help, to some extent, clinical doctors make optimal choices.

MS is a rare disease in China. The sample size of this study is relatively small. Only patients with MS from the Inner Mongolia Autonomous Region were selected, possibly leading to selection bias. Increasing the sample size and expanding the selection range is necessary in future studies. The present study only followed some patients for 6 months to 1 year. Due to time constraints, long-term follow-up was not conducted. So far, there has been increasing research on liquid-phase biomarkers of MS. Existing studies have demonstrated NfL's sensitivity to disease activity and status assessment as a biological counterpart for CNS axonal injury, manifesting its potential applicability in MS. Therefore, in the future, whether NfL can be used as a routine examination for MS in clinical diagnosis and treatment still needs to be verified through large-scale longitudinal cohort studies of different populations, more standardized detection methods, time point, and critical value, and the combination with MRI, thus assisting clinic-customized medical practices of MS.

Data availability statement

The raw data supporting the conclusions of this article will be made available by the authors, without undue reservation.

Ethics statement

The studies involving humans were approved by the Inner Mongolia Medical University Affiliated Hospital, no. WZ2023056. The studies were conducted in accordance with the local legislation and institutional requirements. The participants provided their written informed consent to participate in this study.

Author contributions

FM: Conceptualization, Methodology, Writing – original draft. YW: Data curation, Writing – review & editing. WC: Writing – review & editing. YC: Writing – review & editing. XY: Writing – review & editing.

Funding

The author(s) declare that no financial support was received for the research, authorship, and/or publication of this article.

Conflict of interest

The authors declare that the research was conducted in the absence of any commercial or financial relationships that could be construed as a potential conflict of interest.

Publisher's note

References

1. Perrot R, Berges R, Bocquet A, Eyer J. Review of the multiple aspects of neurofilament functions, and their possible contribution to neurodegeneration. *Mol Neurobiol*. (2008) 38:27–65. doi: 10.1007/s12035-008-8033-0

2. Petzold A. The 2022 lady estelle wolfson lectureship on neurofilaments. *Neurochem*. (2022) 163:179–219. doi: 10.1111/jnc.15682

3. Stenager E. A global perspective on the burden of multiple sclerosis. *Lancet Neurol*. (2019) 18:227–8. doi: 10.1016/S1474-4422(18)30498-8

4. Wallin MT, Culpepper WJ, Nichols E, Bhutta ZA, Gebrehiwot TT, Hay SI, et al. Global, regional, andnational burden of multiple sclerosis 1990–2016: a systematic analysis for theGlobal burden of disease study 2016. *Lancet Neurol*. (2019) 18:269–85. doi: 10.1016/S1474-4422(18)30443-5

5. Tian DC, Zhang C, Yuan M, Yang X, Gu H, Li Z, et al. Incidence of multiple sclerosis in China: a nationwide hospital-based study. *Lancet Reg Health West Pac*. (2020) 1:100010. doi: 10.1016/j.lanwpc.2020.100010

6. Gunnarsson M, Malmeström C, Axelsson M, Sundström P, Dahle C, Vrethem M, et al. Axonal damage in relapsing multiple sclerosis is markedly reduced by natalizumab. *Ann Neurol*. (2011) 69:83–9. doi: 10.1002/ana.22247

7. Humayun S, Gohar M, Volkening K, Moisse K, Leystra-Lantz C, Mepham J, et al. The complement factor C5a receptor is upregulated in NFL−/− mouse motor neurons. *Neuroimmunol*. (2009) 210:52–62. doi: 10.1016/j.jneuroim.2009.01.028

8. Schreiber S, Spotorno N, Schreiber F, Acosta-Cabronero J, Kaufmann J, Machts J, et al. Significance of CSF NfL and tau in ALS. *J Neurol*. (2018) 265:2633–45. doi: 10.1007/s00415-018-9043-0

9. Sugimoto K, Han Y, Song Y, Gao Y. Correlational analysis of ALS progression and serum NfL measured by Simoa assay in Chinese patients. *Front Neurol*. (2020) 11:579094. doi: 10.3389/fneur.2020.579094

10. Sun Q, Zhao X, Li S, Yang F, Wang H, Cui F, et al. CSF Neurofilament light chain elevation predicts ALS severity and progression. *Front Neurol*. (2020) 11:919. doi: 10.3389/fneur.2020.00919

11. Miller RG, Mitchell JD, Moore DH. Riluzole for amyotrophic lateral sclerosis (ALS)/motor neuron disease (MND). *Cochrane Database Syst Rev*. (2001) 4:CD001447. doi: 10.1002/14651858.CD001447

12. Benatar M, Zhang L, Wang L, Granit V, Statland J, Barohn R, et al. CReATe consortium. Validation of serum neurofilaments as prognostic and potential pharmacodynamic biomarkers for ALS. *Neurology*. (2020) 95:e59–69. doi: 10.1212/WNL.0000000000009559

13. Morris JK, Honea RA, Vidoni ED, Swerdlow RH, Burns JM. Is Alzheimer's disease a systemic disease? *Biochim Biophys Acta*. (2014) 1842:1340–9. doi: 10.1016/j.bbadis.2014.04.012

14. Parker K, Rhee Y. Alzheimer's disease warning signs: gender and education influence modifiable risk factors-a pilot survey study. *J Am Coll Nutr*. (2021) 40:583–8. doi: 10.1080/07315724.2020.1812451

15. Jeong W, Joo JH, Kim H, Kim YK, Park EC, Jang SI. Association between the use of hypnotics and the risk of Alzheimer's disease. *J Alzheimers Dis*. (2021) 81:1381–9. doi: 10.3233/JAD-201319

16. López-Riquelme N, Alom-Poveda J, Viciano-Morote N, Llinares-Ibor I, Tormo-Díaz C. Apolipoprotein E ε4 allele and malondialdehyde level are independent risk factors for Alzheimer's disease. *SAGE Open Med*. (2016) 4:205031211562673. doi: 10.1177/2050312115626731

17. Park JE, Gunasekaran TI, Cho YH, Choi SM, Song MK, Cho SH, et al. Diagnostic blood biomarkers in Alzheimer's disease. *Biomedicines*. (2022) 10:169. doi: 10.3390/biomedicines10010169

18. Giacomucci G, Mazzeo S, Bagnoli S, Ingannato A, Leccese D, Berti V, et al. Plasma neurofilament light chain as a biomarker of Alzheimer's disease in subjective cognitive decline and mild cognitive impairment. *J Neurol*. (2022) 269:4270–80. doi: 10.1007/s00415-022-11055-5

19. Preische O, Schultz SA, Apel A, Kuhle J, Kaeser SA, Barro C, et al. Serum neurofilament dynamics predicts neurodegeneration and clinical progression in presymptomatic Alzheimers disease. *Nat Med*. (2019) 25:277–83. doi: 10.1038/s41591-018-0304-3

20. Mielke MM, Syrjanen JA, Blennow K, Zetterberg H, Vemuri P, Skoog I, et al. Plasma and CSF neurofilament light: relation to longitudinal neuroimaging and cognitive measures. *Neurology*. (2019) 93:e252–60. doi: 10.1212/WNL.0000000000007767

21. Fortea J, Carmona-Iragui M, Benejam B, Fernández S, Videla L, Barroeta I, et al. Plasma and CSF biomarkers for the diagnosis of Alzheimers disease in adults with down syndrome: a cross-sectional study. *Lancet Neurol*. (2018) 17:860–9. doi: 10.1016/S1474-4422(18)30285-0

22. Barro C, Benkert P, Disanto G, Tsagkas C, Amann M, Naegelin Y, et al. Serum neurofilament as a predictor of disease worsening and brain and spinal cord atrophy in multiple sclerosis. *Brain*. (2018) 141:2382–91. doi: 10.1093/brain/awy154

23. Kern D, Khalil M, Pirpamer L, Buchmann A, Hofer E, Dal-Bianco P, et al. Serum NfL in Alzheimer dementia: results of the prospective dementia registry Austria. *Medicina (Kaunas)*. 58:433. doi: 10.3390/medicina58030433

24. Silva-Spínola A, Lima M, Leitão MJ, Durães J, Tábuas-Pereira M, Almeida MR, et al. Serum neurofilament light chain as a surrogate of cognitive decline in sporadic and familial frontotemporal dementia. *Eur J Neurol*. (2022) 29:36–46. doi: 10.1111/ene.15058

25. Tomassini V, Sinclair A, Sawlani V, Overell J, Pearson OR, Hall J, et al. Diagnosis and management of multiple sclerosis: MRI in clinical practice. *J Neurol*. (2020) 267:2917–25. doi: 10.1007/s00415-020-09930-0

26. Enziger Ch. Imaging methods to predict and monitor individual disease course. Session: SYMP 12 towards personalizes multiple sclerosis care. EAN Virtual Congress (2021) 19–22.

27. Niu LD, Xu W, Li JQ, Tan TC, Cao XP, Yu J, et al. Genome-wide association study of cerebrospinal fluid neurofilament light levelsin non-demented elders. *Ann Transl Med*. (2019) 7:657. doi: 10.21037/atm.2019.10.66

28. Liu S, Huang Z, Zhang L, Pan J, Lei Q, Meng Y, et al. Plasma Neurofilament light chain may be a biomarker for the inverse association between cancers and neurodegenerative diseases. *Front Aging Neurosci*. (2020) 12:10. doi: 10.3389/fnagi.2020.00010

29. Marques TM, van Rumund A, Oeckl P, Kuiperij HB, Esselink RAJ, Bloem BR, et al. Serum NFL discriminates Parkinson disease from atypical parkinsonisms. *Neurology*. (2019) 92:e1479–86. doi: 10.1212/WNL.0000000000007179

frontiers | Frontiers in Immunology

TYPE Original Research
PUBLISHED 13 December 2023
DOI 10.3389/fimmu.2023.1234869

OPEN ACCESS

EDITED BY
Jinzhou Feng,
First Affiliated Hospital of Chongqing Medical University, China

REVIEWED BY
Simona Rolla,
University of Turin, Italy
Vincent Van Pesch,
Université Catholique de Louvain, Belgium

*CORRESPONDENCE
Antonella Conte
antonella.conte@uniroma1.it

†These authors share first authorship

‡These authors share senior authorship

RECEIVED 05 June 2023
ACCEPTED 06 November 2023
PUBLISHED 13 December 2023

CITATION
Arisi I, Malimpensa L, Manzini V, Brandi R, Gosetti di Sturmeck T, D'Amelio C, Crisafulli S, Ferrazzano G, Belvisi D, Malerba F, Florio R, Pascale E, Soreq H, Salvetti M, Cattaneo A, D'Onofrio M and Conte A (2023) Cladribine and ocrelizumab induce differential miRNA profiles in peripheral blood mononucleated cells from relapsing–remitting multiple sclerosis patients.
Front. Immunol. 14:1234869.
doi: 10.3389/fimmu.2023.1234869

Cladribine and ocrelizumab induce differential miRNA profiles in peripheral blood mononucleated cells from relapsing–remitting multiple sclerosis patients

Ivan Arisi[1,2†], Leonardo Malimpensa[3†], Valeria Manzini[1], Rossella Brandi[1], Tommaso Gosetti di Sturmeck[1], Chiara D'Amelio[1], Sebastiano Crisafulli[4], Gina Ferrazzano[5], Daniele Belvisi[3,5], Francesca Malerba[1], Rita Florio[1], Esterina Pascale[6], Hermona Soreq[7], Marco Salvetti[3,8], Antonino Cattaneo[1,9], Mara D'Onofrio[1‡] and Antonella Conte[3,5*‡]

[1]European Brain Research Institute (EBRI) Rita Levi-Montalcini, Rome, Italy, [2]Institute of Translational Pharmacology, National Research Council, Rome, Italy, [3]Istituto di Ricovero e Cura a Carattere Scientifico (IRCCS) Istituto Neurologico Mediterraneo Neuromed, Pozzilli, Italy, [4]Neuroimmunology and Neuromuscular Diseases Unit, Fondazione Istituto di Ricovero e Cura a Carattere Scientifico (IRCCS) Istituto Neurologico Carlo Besta, Milan, Italy, [5]Department of Human Neurosciences, Sapienza University of Rome, Rome, Italy, [6]Department of Medical-Surgical Sciences and of Biotechnologies, "Sapienza" University of Rome, Rome, Italy, [7]The Edmond and Lily Safra Center of Brain Science and The Life Sciences Institute, The Hebrew University of Jerusalem, Jerusalem, Israel, [8]Centre for Experimental Neurological Therapies (CENTERS), Department of Neurosciences, Mental Health and Sensory Organs, Sapienza University of Rome, Rome, Italy, [9]Bio@SNS Laboratory of Biology, Scuola Normale Superiore, Pisa, Italy

Background and objectives: Multiple sclerosis (MS) is a chronic, progressive neurological disease characterized by early-stage neuroinflammation, neurodegeneration, and demyelination that involves a spectrum of heterogeneous clinical manifestations in terms of disease course and response to therapy. Even though several disease-modifying therapies (DMTs) are available to prevent MS-related brain damage—acting on the peripheral immune system with an indirect effect on MS lesions—individualizing therapy according to disease characteristics and prognostic factors is still an unmet need. Given that deregulated miRNAs have been proposed as diagnostic tools in neurodegenerative/neuroinflammatory diseases such as MS, we aimed to explore miRNA profiles as potential classifiers of the relapsing–remitting MS (RRMS) patients' prospects to gain a more effective DMT choice and achieve a preferential drug response.

Methods: A total of 25 adult patients with RRMS were enrolled in a cohort study, according to the latest McDonald criteria before (pre-cladribine, pre-CLA; pre-ocrelizumab, pre-OCRE, time T0) and after high-efficacy DMTs, time T1, 6 months post-CLA (n = 10, 7 F and 3 M, age 39.0 ± 7.5) or post-OCRE (n = 15, 10 F and 5 M, age 40.5 ± 10.4) treatment. A total of 15 age- and sex-matched

healthy control subjects (9 F and 6 M, age 36.3 ± 3.0) were also selected. By using Agilent microarrays, we analyzed miRNA profiles from peripheral blood mononuclear cells (PBMC). miRNA–target networks were obtained by miRTargetLink, and Pearson's correlation served to estimate the association between miRNAs and outcome clinical features.

Results: First, the miRNA profiles of pre-CLA or pre-OCRE RRMS patients compared to healthy controls identified modulated miRNA patterns (40 and seven miRNAs, respectively). A direct comparison of the two pre-treatment groups at T0 and T1 revealed more pro-inflammatory patterns in the pre-CLA miRNA profiles. Moreover, both DMTs emerged as being capable of reverting some dysregulated miRNAs toward a protective phenotype. Both drug-dependent miRNA profiles and specific miRNAs, such as miR-199a-3p, miR-29b-3p, and miR-151a-3p, emerged as potentially involved in these drug-induced mechanisms. This enabled the selection of miRNAs correlated to clinical features and the related miRNA–mRNA network.

Discussion: These data support the hypothesis of specific deregulated miRNAs as putative biomarkers in RRMS patients' stratification and DMT drug response.

KEYWORDS

multiple sclerosis, cladribine, ocrelizumab, DMT, biomarker, miRNA, PBMC

Introduction

Multiple sclerosis (MS) is a chronic and progressive autoimmune demyelinating disease that affects the central nervous system (CNS). MS is characterized by a heterogeneous disease course and response to therapy (1–3). It is classified into three main phenotypes depending on the clinical disease course: relapsing–remitting (RRMS), displaying relapses and remission phases, and primary progressive MS characterized by gradual disability progression without acute relapses. Lastly, about 85% of patients initially diagnosed with RRMS shift toward a progressive stage called secondary progressive MS (SPMS) (4). People affected by MS accumulate progressive disability due to chronic inflammation and neurodegeneration which develop early in the disease process and are major drivers of progressive disability. It is generally felt that existing classifications of MS clinical course need improvements as they do not reflect the clinical and biological heterogeneity of the disease (5, 6).

Many disease-modifying therapies (DMTs) are now available to prevent the MS-related CNS damage (7, 8). Based on their efficacy, DMTs are identified as moderately (interferon-β dimethyl fumarate, etc.) and highly effective (ocrelizumab, OCRE; cladribine, CLA; etc.). Two high-efficacy DMTs were selected for the current study: CLA and OCRE. CLA is a synthetic purine analogue that induces apoptosis of B and T lymphocytes by the accumulation of intracellular chloro-deoxyadenosine triphosphate. In addition, it mediates immunomodulation in different immune cell populations. CLA tablets are administered in two short courses 1 year apart and reduce rapidly peripheral lymphocyte levels in patients with MS. Nadir is usually reached at week 9, and after that the lymphocyte counts gradually increase but remain lower than at baseline. OCRE (7, 9) is a humanized anti-CD20 monoclonal antibody which is administered intravenously every 6 months. It depletes CD20+ B cells in the blood to negligible levels after 14 days with a median time to B cell repletion of 72 weeks. Repopulation in CLA-treated patients is faster, with 91% of patients having at least 3% of B lymphocyte in the blood after 24 weeks compared to OCRE-treated patients (with 2% of patients having at least 3% of B lymphocyte after 23 weeks) (10–12). OCRE and CLA may act through mechanisms of action that, although different, could be both more "upstream" in the pathogenetic cascade with respect to others (e.g., they have a preponderant action on B cells, which may harbor an EBV infection which may have an etiologic relevance).

There is a high interindividual heterogeneity in the response patterns to DMTs. Identifying biological markers predictive of treatment response might allow the recognition of non-responders *versus* responders to drugs (13), enhancing the individualization of this therapeutic approach, respecting the individual patient's needs, and optimizing healthcare costs. In this context, different miRNAs have been proposed as potential biomarkers of treatment response in neurodegenerative/neuroinflammatory diseases, such as MS (14–16). miRNAs are small non-coding RNAs that regulate gene expression at the post-transcriptional level, affecting several cellular processes,

Abbreviations: DMT, disease-modifying therapy; DE, differentially expressed; CLA, cladribine; OCRE, ocrelizumab; RRMS, relapsing–remitting multiple sclerosis; EDSS, expanded disability status scale; FI, Frailty Index; PBMC, peripheral blood mononuclear cells.

including inflammation, neurodegeneration, and remyelination by regulating different cellular processes (14). A large part of miRNAs are primate-specific, requiring human rather than murine studies (15). Many miRNAs are dysregulated in MS (16, 17). Specifically, studies have suggested that miRNAs are central in the functioning of T lymphocyte subtypes in MS and that their dysregulation may lead to a variation in the subtype balance (17, 18). Moreover, miRNAs play a regulatory role in maintaining proper B cell selection and activation (19).

Nowadays, the selection of specific DMTs is based on either the patient's related factors such as disease-specific prognostic factors, comorbidities, risk tolerance, and pregnancy planning or drug-specific features such as efficacy and safety profile, route of administration, and treatment costs (20). Such criteria still need to be refined. The current study aimed to explore the use of miRNA profiles to improve patients' stratification and potentially aid in treatment selection and efficacy.

Here we first compared two high-efficacy DMTs' (CLA and OCRE) miRNA profiling in PBMCs from patients with RRMS. Initially, we compared the RRMS patients' miRNA levels to those of a healthy population as control (CTRs). Remarkable differences were highlighted in the miRNA profiles between the two subgroups previously selected for either treatment. The characterization of miRNA profiles before and after treatment, their correlation to clinical features (Frailty Index, FI; Expanded Disability Status Scale, EDSS) and the constitution of a specific miRNA–mRNA-related network allowed us to underpin differences in miRNA profiles under CLA or OCRE treatment and unveil specific miRNAs as potential biomarkers.

Methods

Patients' selection and clinical evaluation for enrollment

A total of 25 adult patients with RRMS according to the latest McDonald revised criteria at the time of diagnosis (21) and followed at the Center for Multiple Sclerosis (Department of Human Neurosciences, Policlinico Umberto I—Sapienza University of Rome) were enrolled in a cohort study between 2021 and 2022. Furthermore, 15 healthy control subjects (age- and sex-matched) were selected. Furthermore, 10 RRMS patients received the first cycle of CLA tablets (1.75 mg/kg dose given in two treatment weeks of 5 days separated by 1 month), and 15 received the first course of OCRE (two 300-mg infusions at 2 weeks apart). DMTs have been chosen as clinically indicated (22). The patients were clinically tested before treatment initiation (pre-CLA/pre-OCRE – time 0 = T0) and 6 months after treatment (time 1 = T1). Sex, age at disease onset, FI, urinary symptoms, and EDSS were collected after the neurologist's evaluation (Table 1). FI was calculated as the proportion of patient's deficits based on a list of 42 binary items (23). To protect sensitive data, anonymous codes were assigned to each participant and preserved for the study duration. All subjects gave written informed consent to participate in the study. The research was conducted following the Helsinki Declaration and approved by the Ethics of Sapienza University—Policlinico Umberto I (Rif. 6361, protocol number 0635/2021). To minimize potential bias factors, all clinical data were collected in the same clinical center following the same guidelines.

Blood sample and PBMC collection

The patients' peripheral blood was collected by venipuncture at T0 and T1 for miRNAs' profiling and other laboratory tests. The blood samples for both patients and healthy subjects were collected in Vacutainer tubes containing EDTA. Then, 15 ml of phosphate-buffered saline (PBS; without Ca^{2+}, Mg^{2+}) was added to 10 ml of each samples' blood; after mixing, the diluted blood samples were carefully layered onto 7.5 ml of Ficoll for 30 min of centrifugation (18–20°C) at 1,800 rpm. The tubes exhibited four different layers containing plasma, lymphocytes, and monocytes, Ficoll, granulocytes, and erythrocytes, respectively, from top to bottom. The lymphocytes/monocytes layer was accurately collected in clean tubes; the cells were then pelleted (1,400 rpm for 10 min at 18–20°C) and washed with PBS. The dry pellet was finally stored at -80°C.

RNA extraction and quality control

RNA extraction was performed according to the miRNeasy Tissue/Cells Advanced Mini Kit (QIAGEN©) instructions: the cells were suspended in 500 µL of RTL buffer + β mercaptoethanol, incubated at 37°C for 10 min, and homogenized. The samples were passed through two different spin columns: the gDNA Eliminator spin column to remove all DNA and the Rneasy spin column to select RNA molecules. The miRNeasy Tissue/Cells Advanced Kits enabled efficient RNA enrichment down to approximately 18 nucleotides in size. All RNA samples were again stored at -80°C. RNA purity and concentration quality control included the evaluation of absorbance at 260 nm by NanoDrop ND-1000 (Labtech International, Ringmer, UK). To assess the RNA integrity, samples were tested in the Agilent 2100 Bioanalyzer (Agilent Technologies, Santa Clara, CA, USA) *via* the Eukaryote Total RNA 6000 Nano kit (Agilent Technologies, Santa Clara, CA, USA) and the Small RNA kit (Agilent Technologies, Santa Clara, CA, USA). The bioanalyzer assessed each sample's RNA integrity number (RIN). Samples displaying an under-threshold RIN value <8.0 were excluded.

miRNA profiles

miRNA profiles were performed according to the standard "Agilent miRNA Microarray System, miRNA Complete Labelling, and Hyb Kit" protocol (Agilent Technologies, Version 3.1.1, 2015). After a phosphatase treatment and a denaturation process *via* DMSO, 100 ng of RNA, extracted from each sample, was labeled with 3-pCp cyanine. The samples were then dried through a vacuum concentrator, and a 45-µl hybridization solution was added to each one. Then, the samples were

10.3389/fimmu.2023.1234869

TABLE 1 Demographic and clinical features in enrolled relapsing–remitting multiple sclerosis patients treated with cladribine (CLA) or ocrelizumab (OCRE).

Age	Sex	Disease duration at T1 (years)	EDSS T0	EDSS T1	FI T0	FI T1	Previous therapy	New lesions T0	GD+ enhancing lesions T0	Number of relapses in the last 12 months
A) CLA-treated patients										
36	F	1	1.5	1.5	0.10	0.10	Naïve	1	0	1
37	F	1	0	0	0.12	0.12	Naive	1	0	1
56	F	1	2	2	0.10	0.10	Naive	1	1	1
45	M	2	1.5	1.5	0.02	0.07	Naive	1	0	1
30	M	2	0	0	0.02	0.02	Naive	1	1	1
38	M	2	4	4	0.19	0.19	Naive	1	1	1
31	F	3	1	1	0.17	0.17	Switched	1	1	1
36	F	9	1.5	1.5	0.05	0.05	Switched	1	1	1
38	F	14	2	2.5	0.19	0.19	Switched	0	0	1
43	F	21	1	1	0.12	0.12	Switched	1	1	1
B) OCRE-treated patients										
36	F	1	1	1	0.02	0.02	Naïve	1	0	1
23	M	1	2	1	0.05	0.05	Naive	1	0	1
56	M	2	2	2	0.26	0.26	Naive	1	1	1
36	F	3	2.5	2.5	0.24	0.24	Naive	1	1	1
41	M	15	2.5	1.5	0.07	0.07	Naive	1	0	1
52	M	2	5.5	1.5	0.19	0.19	Switched	0	0	1
32	F	3	1.5	1	0.07	0.07	Switched	1	1	1
37	F	3	1.5	1.5	0.05	0.05	Switched	1	1	1
44	F	3	1	1	0.07	0.07	Switched	1	0	1
28	F	6	1.5	1.5	0.12	0.12	Switched	1	1	1
43	F	15	2	1.5	0.12	0.12	Switched	0	0	1
44	F	18	5.5	6	0.19	0.19	Switched	1	0	1
60	M	26	7	7	0.14	0.14	Switched	1	0	1
46	F	27	2	2	0.07	0.07	Switched	1	0	1
30	F	7	2	2	0.05	0.05	Switched	1	0	1

hybridized to the Agilent Human miRNA Microarrays chip 8x60K (Agilent PN G4870-60530, grid ID = 070156) containing 2,549 human miRNAs. The glasses were incubated in the Agilent Hybridization Oven at 55°C, 10 RPM, for 20 h, washed according to the protocol, and scanned using the Agilent DNA Microarray Scanner (G2539C).

Statistical analysis

miRNAs' profiling was assessed by using Agilent Platform (Agilent Technologies, Milan, Italy). The samples were processed according to Agilent's standard experimental procedure. Data analysis was performed using R-Bioconductor (Seattle, WA, USA). The samples were $\log_2$-transformed and normalized by the median alignment method; differentially expressed (DE) miRNAs were selected by the R-limma tool with threshold false discovery rate <0.05 and linear |fold change| >1.5 (24). Possible confounding factors such as sex (M/F) and previous therapy (yes/no) were included in limma linear models as covariates. Only miRNAs with expression values >0.0 in every sample were included in the analysis. Pearson's correlation coefficient was used to estimate the association between miRNA profiles and clinical measures. Interaction miRNA–target networks were obtained using miRTargetLink 2.0, selecting only validated connections and miRNAs with >4 targets, and further processed through using

Cytoscape. Clinical information was compared using either Mann–Whitney or Fisher's exact test according to data type.

The manuscript preparation followed the STROBE cohort reporting guidelines (25).

Data availability statement

Anonymized data not published within this article will be made available upon request from any qualified investigator. Access to anonymized individual patient's data, including raw datasets, analysis-ready datasets, statistical analysis plans, clinical data, and dataset specifications, may be provided upon request of any qualified investigator. miRNAs' complete raw and processed data are freely available from the Gene Expression Omnibus database with accession number GSE230064.

Results

Multiple sclerosis miRNAs' profiling

A total of 25 adult patients with RRMS were enrolled in a cohort study according to the latest McDonald criteria (21) before (pre-CLA; pre-OCRE, time T0) and after high-efficacy DMTs, time T1, 6 months post-CLA (n = 10, 7 F and 3 M, age 39.0 ± 7.5) and post-OCRE (n = 15, 10 F and 5 M, age 40.5 ± 10.4) treatments. The demographic and clinical features of the CLA- or OCRE-treated RRMS patients are reported in Table 1 and the statistical comparisons in Supplementary Table S5.

A total of fifteen healthy control subjects who were age- and sex-matched (9 F and 6 M, age 36.3 ± 3.0) were selected. All 25 RRMS patients had completed follow-up 6 months after specific treatment. miRNAs' profiling was performed by microarray analysis on PBMCs from whole blood. To identify specific modulated miRNAs, the following comparisons were analyzed: pre-CLA vs. CTRs, pre-OCRE vs. CTRs, pre-CLA vs. pre-OCRE, CLA post-treatment (T1) vs. pre-CLA (T0), and OCRE post-treatment (T1) vs. pre-OCRE (T0).

Comparison between pre-treatment patients and controls

We identified a final list of 200 miRNAs expressed in every sample. The patients' miRNA profiling preceding CLA (pre-CLA) and OCRE treatment (pre-OCRE), compared to CTRs, was analyzed and reported in Figures 1A, B. A total of 40 miRNAs resulted to be deregulated, of which 17 were upregulated (among which were miR-181b-5p, miR-186-5p, miR-486-5p, and miR-29b-3p) and 23 were downregulated (including miR-151a-3p, miR-151a-5p, miR-23b-3p, miR-27b-3p, and miR-199a-3p) when comparing pre-CLA-treated patients to CTRs (Figure 1B). Conversely, seven miRNAs were downregulated (miR-155-5p, miR-199a-5p, miR-26a-5p, miR-30b-5p, miR-30c-5p, miR-30e-5p, and miR-374-5p) in the pre-OCRE vs. CTRs comparison (Figure 1A). These results highlight how the RRMS patients displayed deregulated miRNA profiles compared to healthy controls.

MS patients' stratification and response to specific DMTs (CLA or OCRE) according to the miRNA profiles

The miRNA profiles were compared between the two groups of patients before (pre-CLA T0 vs. pre-OCRE T0) and 6 months after treatment (CLA T1 vs. OCRE T1) to explore differences between baseline and treatment-specific response. The volcano plot resulting from the pre-CLA vs. the pre-OCRE miRNAs' comparison exhibited (Figure 2B) 28 DE miRNAs: 22 upregulated miRNAs (out of which the most upregulated were miR-1260a, miR-1260b, miR-186-5p, miR-6085, miR-142-3p, miR-29b-3p, miR-29c-3p, and miR-155-5p) and six downregulated ones (miR-638, miR-130a-3p, miR-151a-5p, miR-126-3p, miR-151a-3p, and miR-199a-3p) (15 + 13 in the Venn diagram, Figure 2A), whose main functions are described in Supplementary Table S1, according to the cited literature.

The Venn diagram shows the DE miRNAs shared between patients preceding CLA (pre-CLA) or OCRE (pre-OCRE) treatment (Figure 2A) and between the same subjects analyzed 6 months post-treatment: (CLA T1 vs. OCRE T1) (Supplementary Figure S1). The $\log_2$ median expression values of the DE miRNAs in the pre-CLA vs. the pre-OCRE comparison are shown in Figure 2C. Furthermore, the data indicated 25 DE miRNAs in the CLA T1 vs. OCRE T1 comparison, with five downregulated and 20 upregulated (Supplementary Figure S1).

Literature annotation is reported in Supplementary Table S2. The differential miRNAs' profiling underlined a higher expression of inflammation-related miRNAs in patients selected for CLA treatment (pre-CLA) compared to patients selected for OCRE treatment (pre-OCRE). These dysregulated miRNAs are known to be involved in inflammatory and immune pathways (Supplementary Table S1), including miR-155-5p, which is highly pro-inflammatory, and the upregulated miR-186-5p, over-expressed in MS while downregulated in other neurodegenerative diseases and aging.

The multidimensional scaling plot of miRNA profiles in Figure 3B displayed how most of the patients had similar miRNA responses to CLA treatment, as suggested by the largely parallel direction of the T0 to T1 trajectories, while the response to OCRE (Supplementary Figure S2) was more heterogeneous. To unveil the impact of the selected DMT on the enrolled RRMS patients, we compared the miRNA profiles 6 months after CLA or OCRE treatment to the pre-treatment levels. A total of 22 miRNAs resulted to be modulated by CLA (Figures 3A, B) (14 upregulated: miR-151a-3p, miR-151a-5p, miR-130a-3p, miR-126-3p, miR-151b, miR-326, miR-584-5p, miR-1991a-3p, miR-199a-5p, miR-23b-3p, miR-221-3p, miR-27b-3p, miR-486-5p, and miR-148b-3p and eight downregulated: miR-150-5p, miR-197-5p, miR-29c-3p, miR-4299, miR-4443, miR-4505, miR-4507, and miR-8069), while only one was modulated by OCRE treatment

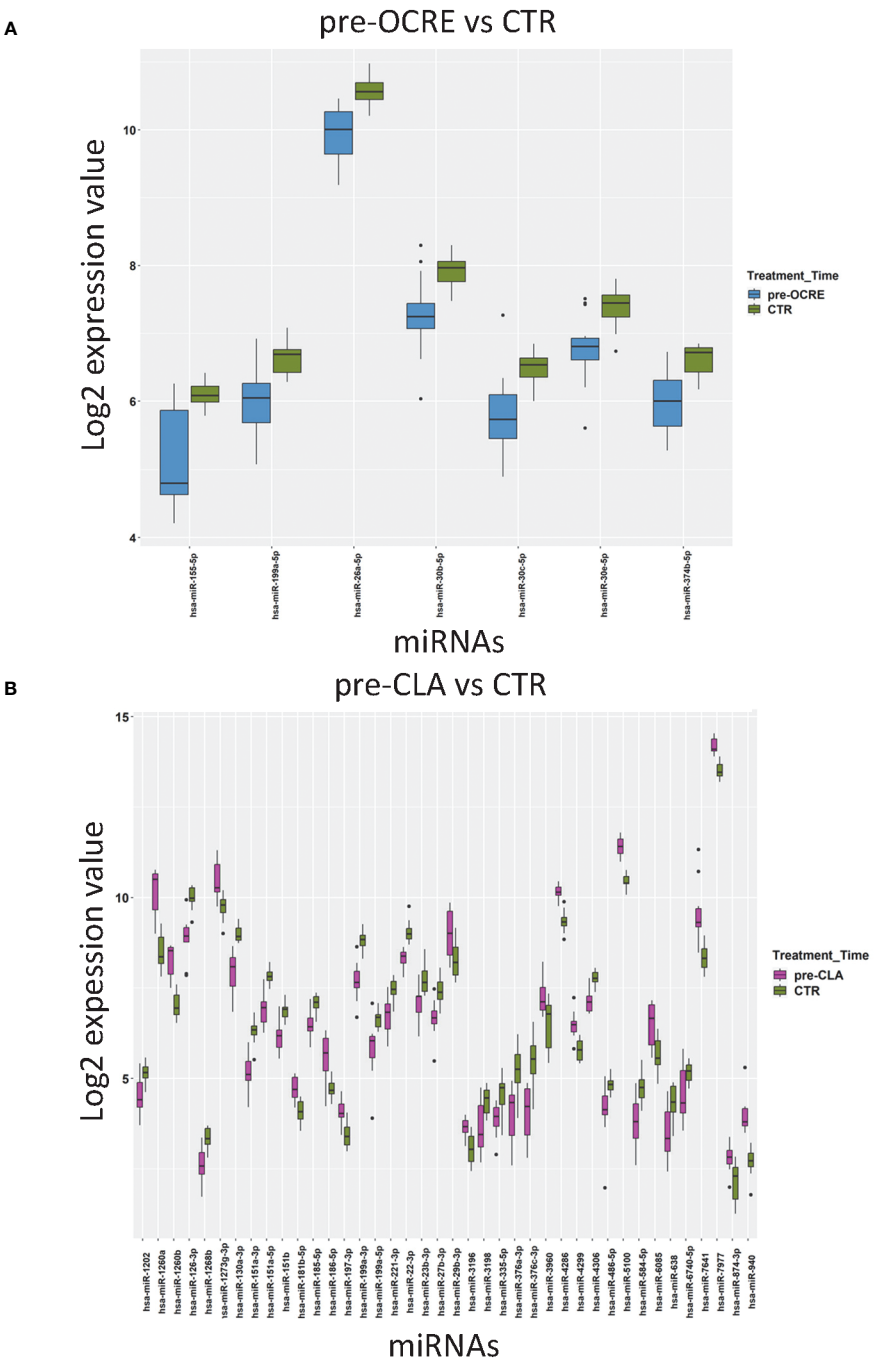

FIGURE 1
Relapsing–remitting multiple sclerosis patients, clinically selected for cladribine (CLA) or ocrelizumab (OCRE) treatment, display different miRNA profiles. **(A)** Pre-OCRE (n = 15) vs. CTRs (n = 15) comparison. **(B)** Pre-CLA (n = 10) vs. CTRs (n = 15) comparison. Log_2 median normalized values of differentially expressed miRNAs were selected using the following thresholds: R limma test false discovery rate <0.05 + linear |fold change| >1.5. The boxes correspond to median ± interquartile range, and the black dots are outliers.

(Supplementary Figure S2). Concerning the differential CLA profiling, most DE miRNAs were involved in MS, as described in the literature mentioned in Supplementary Table S3. Specifically, some of the DE responding miRNAs (miR-199a-3p, miR-199a-5p, miR-29b-3p, and miR-23b-3p), whose levels were modulated by the CLA treatment, are known to be dysregulated and of clinical interest in MS. In comparison, the OCRE treatment modulated only miR-3653-3p (Supplementary Figure S2), which resulted to be downregulated and is known to be involved in carcinogenesis and glioma progression and other carcinoma diffusions.

Associations between clinical measures and DE miRNAs

The Pearson's analysis between DE miRNAs and clinical data in the pre- and post-CLA treatment groups showed miRNAs which

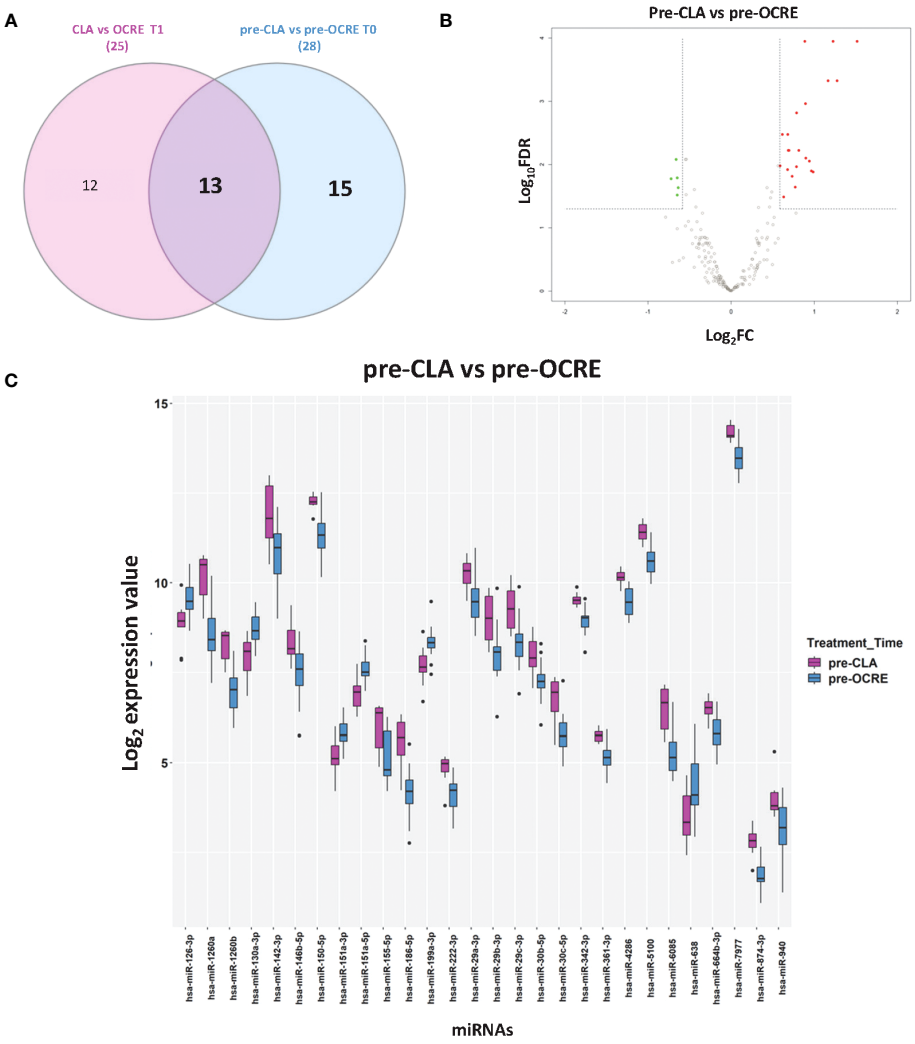

FIGURE 2
Direct comparison of pre-cladribine (CLA) and pre-ocrelizumab (OCRE) miRNA profiles. **(A)** Venn diagram for the differentially expressed (DE) miRNAs between groups of patients preceding either CLA (pre-CLA) or OCRE (pre-OCRE) treatment or CLA at T1 vs. OCRE at T1. **(B)** Volcano plot of the pre-CLA (n = 10) vs. the pre-OCRE (n = 15) miRNAs. DE miRNAs (green: downregulated; red: upregulated) are shown. **(C)** Levels of DE miRNAs in pre-CLA vs. pre-OCRE. Log2 median normalized values of DE miRNAs are shown; miRNAs were selected using R limma test false discovery rate <0.05 + linear |fold change| >1.5 thresholds. The boxes correspond to median ± interquartile range, and the black dots are outliers.

were significantly correlated to the FI (miR-186-5p), disease duration (miR-23b-3p and miR-27b-3p), or urinary symptoms (miR-186-5p, miR-29b-3p, miR-151a-5p, miR-199a-3p, and miR-151-3p), as reported in Figures 4A–C. Other analyses are reported in Supplementary Figures S3–S5. We then compared the dysregulated miRNAs associated with MS, according to the human miRNA Disease Database and the miR2 Disease Database (26), to the clinical features. A total of 10 miRNAs were selected for further analysis (miR-126-3p, miR-186-5p, miR-29b-3p, miR-23b-3p, miR-27b-3p, miR-199a-3p, miR-199a-5p, miR-151a-3p, miR-151a-5p, and miR-584-5p). Eight out of 10 were significantly upregulated in the CLA T1 vs. pre-CLA comparison while downregulated in the pre-CLA vs. CTRs comparison (Figure 4A). The miRNAs also presented a few opposite clinical correlation profiles when comparing pre-CLA to post-CLA treatment. In particular, specific miRNAs shifted from being directly correlated to a significant inverse correlation to urinary symptoms (Figures 4B, C).

miRNA target network

We analyzed the mRNA–miRNA network to assess the effect of the 10 selected miRNAs whose expression levels were reverted by the specific DMT (CLA) and were also correlated to clinical features (Figure 5). The network comprises 335 validated edges between the nine miRNAs (miR-126-3p, miR-186-5p, miR-29b-3p, miR-23b-3p, miR-27b-3p, miR-199a-3p, miR-199a-5p, miR-151a-3p, and miR-151a-5p, with miR-584-5p excluded as presenting no strong interactions to targets) and mRNA targets. Out of the 335 validated

FIGURE 3
The impact of cladribine (CLA) treatment on miRNA profiles. **(A)** Volcano plot of the CLA T1 (n = 10) vs. pre-CLA (n = 10) miRNAs. **(B)** Multidimensional scaling of CLA samples based on the miRNA profiles. Each arrow corresponds to a different patient treated with CLA and connects the miRNA profile at T0 (light purple dot) to the profile at T1 (dark purple dot). **(C)** Levels of differentially expressed (DE) miRNAs in CLA T1 vs. pre-CLA. Log2 median normalized values of DE miRNA are shown. The CLA T1 samples correspond to subjects with relapsing–remitting multiple sclerosis, whose miRNA levels were analyzed 6 months after CLA treatment initiation. miRNAs were selected using R limma test false discovery rate <0.05 + linear |fold change| >1.5 thresholds. The boxes correspond to median ± interquartile range, and the black dots are outliers.

edges, 272 were single connections, 26 genes are targets shared by two miRNAs, MET and SIRT1 are targets shared by three miRNAs (miR-199a-3p, miR-27b-3p, and miR-23b-3p as well as miR-126-3p, miR-199a-5p, and miR-23b-3p, respectively), and lastly VEGF-α is a predicted target for 5 miRNAs (miR-29b-3p, miR-126-3p, miR-186-5p and 199a-3p and miR-199a-5p). To better outline the cellular functions involved in the produced network (Figure 5), a pathway enrichment analysis was generated (Figure 6). Most of the specific genes in the network are involved in pathways including processes concerning interleukins 4 and 13 signaling, PIK3T/AKT second messengers, collagen, extra-nuclear estrogen signaling and signaling by PDGF, inflammation, angiogenesis, and blood–brain barrier integrity; others appeared to present a neuroprotective role as shown in the pathway dendrogram (Figure 6).

Discussion

The present cohort study investigated miRNA profiles in PBMCs collected from RRMS patients before and after treatment with CLA or OCRE. Since miRNAs are increasingly considered as biomarkers in multiple neurodegenerative/neuroinflammatory diseases, we first compared the miRNA profiles of patients who were clinically selected for either CLA or OCRE treatment to healthy controls (pre-CLA vs. CTRs or pre-OCRE vs. CTRs). The analysis identified some dysregulated miRNAs possibly involved in MS pathogenesis and specifically characterized each group. Among the 40 DE miRNAs (pre-CLA vs. CTRs), several are notably involved in inflammatory and immune pathways, such as miR-23b-3p (27), the downregulated miR-151-5p (28, 29) and miR-151-

10.3389/fimmu.2023.1234869

A

	CLA T1 vs CTRs	pre-CLA vs CTRs	CLA T1 vs pre-CLA	pre-CLA vs pre-OCRE
miRNAs	Log_2FC	Log_2FC	Log_2FC	Log_2FC
miR-186-5p	0.63	0.83	-0.20	1.42
miR-29b-3p	0.18	0.74	-0.56	0.96
miR-23b-3p	0.04	-0.64	0.64	-0.50
miR-27b-3p	-0.16	-0.76	0.60	-0.42
miR-199a-5p	-0.06	-0.83	0.77	-0.19
miR-151a-5p	-0.22	-0.90	0.63	-0.70
miR-584-5p	-0.05	-0.96	0.90	-0.54
miR-199a-3p	-0.38	-1.14	0.66	-0.64
miR-126-3p	-0.33	-1.16	0.81	-0.69
miR-151a-3p	-0.43	-1.19	0.75	-0.68

B

	pre-CLA			CLA T1			
miRNAs	urinary symptoms	FI T0	FI T1	Disease Duration	urinary symptoms	FI T0	FI T1
miR-186-5p	-	0.824	0.828	-	0.761	0.697	0.718
miR-29b-3p	-	-	-	-	0.905	-	-
miR-23b-3p	0.744	-	-	0.885	-	-	-
miR-27b-3p	-	-	-	0.762	-	-	-
miR-199a-5p	-	-	-	-	-	-	-
miR-151a-5p	0.707	-	-	-	-0.752	-	-
miR-584-5p	0.664	-	-	-	-	-	-
miR-199a-3p	-	-	-	-	-0.714	-	-
miR-126-3p	-	-	-	-	-0.569	-0.630	-0.607
miR-151a-3p	-	-	-	-	-0.748	-0.675	-0.677

C

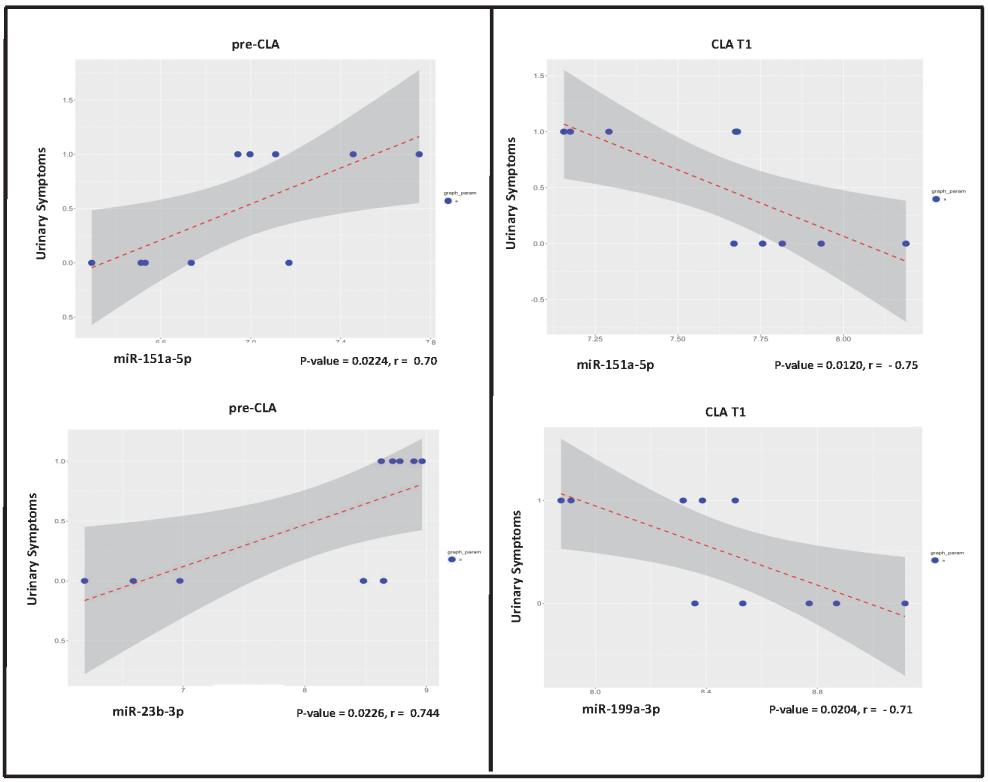

FIGURE 4
Pearson correlations between miRNA levels and clinical data. **(A)** Pearson's correlation index between differentially expressed miRNAs (cladribine (CLA) T1 vs. pre-CLA) and selected statistically significant clinical variables. T1 = 6 months after the treatment's first administration/infusion. Analyzed clinical variables: urinary symptoms (yes/no, binary); EDSS score (integer discrete); FI score; disease duration in months. **(B)** Table of significant correlations. **(C)** Scatter plot of expression levels vs. clinical variable for selected correlations with miRNA in the pre-CLA and CLA T1 groups; the regression line is drawn.

3p (26), miR-27b (30), and miR-29b, contributing to the regulation of Th1 and Th17 differentiation (31). In line with part of the current literature (32), we found a downregulation of miR-126-3p which, however, has also been reported as increased in RRMS patients (33). Furthermore, miR-126-3p, expressed in the CNS endothelium, displays a possible contribution to the regulation of leukocyte adhesion to human brain endothelium (34), a critical step in triggering the blood–brain barrier's (BBB) damage process. Thus, we suggest that these miRNAs may influence the inflammatory process and play a role in the MS patients' BBB disruption.

The pre-OCRE miRNAs' profiling (*vs* CTRs) is characterized by a significant downregulation of miR-155-5p (Figure 1), known as *inflamma-miR*, which influences myeloid cell polarization, leading to a pro-inflammatory phenotype (35). miR-155-5p also disrupts the BBB *via* key junctional proteins under inflammatory conditions. It drives demyelination processes by contributing to microglial activation, the polarization of astrocytes, and the downregulation of CD47 protein and affecting crucial transcription factors.

miR-155-5p has been reported as downregulated exclusively in SPMS patients (36). Since OCRE is used in patients with highly

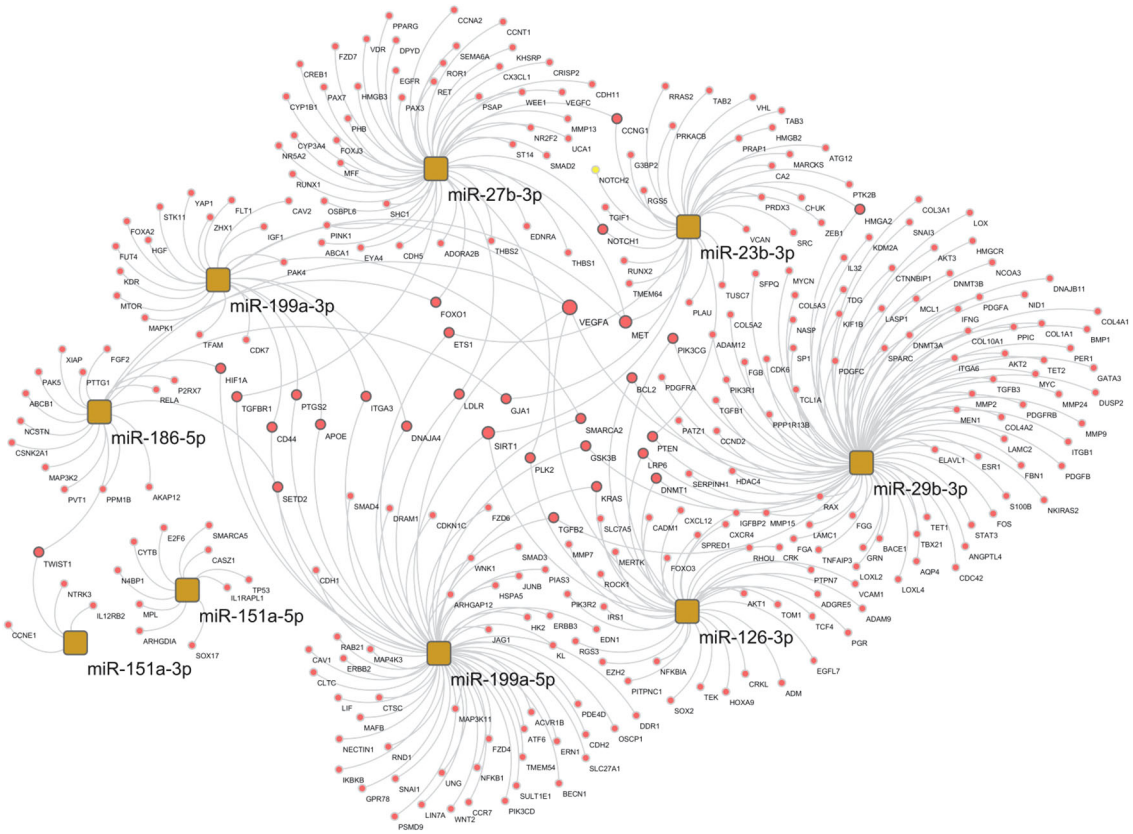

FIGURE 5
Selected miRNA–target network in the cladribine (CLA) T1 vs. pre-CLA T0 comparison. miRNA–target network of selected miRNAs in the CLA T1 vs. pre-CLA T0 comparison obtained by the miRTargetLink 2.0 tool, selecting only validated mRNA targets and miRNAs with >4 targets, and further processed through Cytoscape.

active MS and due to the current lack of prognostic factors for long-term disability (i.e., at a higher risk for neurodegenerative mechanisms), our data regarding the downregulation of miR-155-5p in OCRE groups propose miRNA profiles as possible prognostic factors in the disease progression.

The only DE miRNA, shared by both pre-CLA and pre-OCRE populations when compared with CTRs, is the downregulated miR-199a-5p, which negatively correlates with EDSS in MS (18). Together with other miRNAs, miR-199a-5p may participate in the control of the balance between innate and adaptive immunity, avoid chronic inflammation, and prevent neuroinflammation. The imbalance between pro- and anti-inflammatory processes may modify the immune activities at the glia level, leading to neuronal damage and altering BBB's integrity (37).

In addition to analyzing differences in the pre-treatment profiles, we directly compared the two miRNA profiles (pre-CLA vs. pre-OCRE). This comparison confirmed that the modulated miRNAs were involved in inflammatory and immune pathways (Supplementary Table S1), including relevant upregulated genes such as miR-155-5p and miR-186-5p, which are downregulated in elderly people and those with a neurodegenerative disease (26, 38). The upregulation of miR-30c, previously implicated in MS (39) and characterized in response to pharmacological treatments (19, 40), together with the downregulation of miR-199a in the MS relapsing phase is correlated with more frequent Th17 cell differentiation and the severity of the disease (41). These data suggest a more inflammatory profiling of the patients selected for CLA compared to the pre-OCRE ones, supporting the possible use of miRNAs for a personalized DMT choice.

When we compared the expression profiles in samples obtained during the two treatment courses, we found that CLA produced a higher impact on DE miRNAs than OCRE, i.e., CLA modulated a higher number of miRNAs (22 vs. one miRNA), mainly involving immune and inflammatory targets. This is also suggested by the clinical trajectories (from T0 to T1) in multidimensional scaling plots: CLA trajectories (Figure 3) are largely parallel, with T0 and T1 sets clearly separated, while under OCRE treatment (Supplementary S2) the T0 and T1 sets are widely overlapping. The homogeneous response in the multidimensional scaling plot of CLA patients compared to the heterogeneous one of OCRE patients can be related to the different mechanism of action of the DMTs or to the different kinetic of cell depletion and reconstitution. It may also reflect an immunomodulatory effect of CLA on the immune system. However, further studies of miRNA profiles in different lymphocyte subsets should be performed.

Anyway, no statistically significant differences were found between the two groups regarding EDSS, duration of disease, number of relapses, presence of new lesions, or presence of

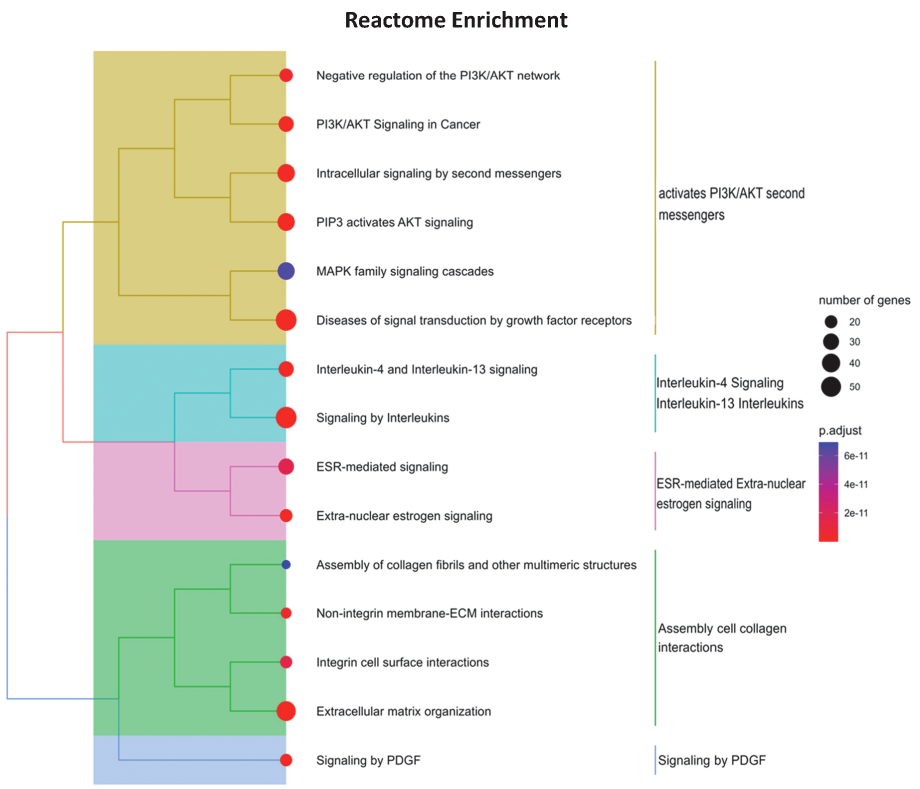

FIGURE 6
Pathway enrichment analysis of miRNA gene targets. The dendrogram is a hierarchical clustering of enriched Reactome pathways, using the gene lists overlap as distance metric. The pathways are further clustered into broader functional categories. The dot size is proportional to the gene list size, while the dot color corresponds to the false discovery rate adjusted *p*-value of enriched terms. The analyzed gene list was selected by the mirTargetLink predictor, using only strong validated targets. The plot was obtained by the clusterProfiler R package.

gadolinium-enhancing lesions on magnetic resonance imaging (MRI) at T0 and the number of relapses in the last 6 months (Supplementary Table S5). A wider number of patients and a longer follow-up might be necessary to identify clinical changes.

Notably, miR-3653-3p is involved in carcinogenesis and glioma progression and other carcinoma diffusions. Correspondingly, the OCRE effect may be related to its direct long-term depletion of memory B cells (42) or through the T cell activity blockade (43). Furthermore, most CLA-treated patients maintained B cell levels of at least 1% of total lymphocyte count and recovered to at least 10–20 circulating CD19 B cells/μL at 24 weeks after treatment, contrasting with prolonged B cell depletion detected after OCRE (11). Importantly, nevertheless, both DMTs successfully reverted some dysregulated miRNA profiles toward a protective phenotype. Our analysis exhibited baseline DE values of specific miRNAs (miR-199a-3p, miR-199a-5p, miR-29b-3p, and miR-23b-3p) whose expression is reversed by CLA. As discussed above, miR-199a-3p and 199-5p upregulation, together with the dysregulation of miR-23b-3p, miR-151a-5p, and miR-151a-3p, are directed toward an anti-inflammatory and neuroprotective phenotype. Pearson's correlations allowed the identification of miRNAs that better correlate to some clinical features, such as urinary symptoms, FI, or EDSS. Additionally, it has been estimated that 80%–90% of patients living with MS suffer from some form of lower urinary tract symptoms over the course of the disease, representing an important challenge for both patients and caregivers (44). Correspondingly, some miRNAs present opposite clinical correlation profiles when comparing the pre-CLA and post-CLA treatments. Thus, both miR-23b-3p and miR-199a-3p, which correlated to urinary symptoms, have been reported as downregulated in MS inflammatory lesions, which was compatible to our findings in the pre-CLA profiling, and were then reverted by the CLA treatment. Interestingly, specific miRNAs whose levels correlated to urinary symptoms shifted from direct to a significantly inverse correlation (Figures 4A, B). It would be interesting to monitor these clinical features over time to reveal whether these correlations, which shift from direct to inverse, correspond to symptom improvement and better prognosis.

To better outline the different pathways involved in the mRNAs–miRNA–target network (Figure 5), a pathway enrichment analysis was generated (Figure 6) and revealed potential mechanisms linking neuroinflammation and neurodegeneration to CLA treatment. Briefly, interleukins 4 and 13 signaling, PIK3T/AKT second messengers, collagen, extra-nuclear estrogen signaling, and signaling by PDGF emerged as functionally involved in CLA-modulated miRNA pathways. Both the closely related interleukin (IL)-13, T cell-derived cytokine, and Il-4 routes play powerful anti-inflammatory roles in MS (45). Concerning the extracellular matrix (ECM) members in MS, such as collagen, we propose that these miRNAs control the inflammatory response and treatment induces repair since the

crosstalk between the ECM and immune responses (IL-4 and Il-13) is known to modulate lesions for recovery or worsening (46). Furthermore, the link with estrogen nuclear signaling in MS might mediate anti-inflammatory cytokine production and Treg cell expansion (47).

We also evinced that platelet-derived growth factor (PDGF) signaling is involved in the network modulated by miR-29b-3p (which is downregulated by the CLA treatment). PDGF plays a substantial role in long-term potentiation (LTP) and brain reserve in MS patients, as this molecule is associated with more pronounced LTP in RRMS patients and with the compensation of new brain lesions in RRMS (48). The brain plasticity reserve, in the form of LTP, is crucial to contrast clinical deterioration in MS. Enhancing PDGF signaling might represent a valuable treatment option to slow disease progression by maintaining brain reserve and reducing neuronal damage (49).

The tightly connected genes in the abovementioned network (Figure 5) further include the vascular endothelial growth factor alpha (VEGF-α), known to be involved in inflammation, angiogenesis (50), and BBB integrity with a crucial role in MS development and progression. VEGF-α plays a major role in the development of neurodegenerative diseases through inflammation, first acting as a pro-inflammatory initiator but later leading to lower responsivity of angiogenic molecules. On one hand, significant correlations were reported between VEGF-α levels and BBB disruption in MS plaques. On the other hand, decreased levels of VEGF-α have been reported in MS patients' CSF (51, 52). Other network genes include Sirtuin1 (SIRT1) and hepatocyte growth factor receptor (MET). SIRT1 was found to be elevated in MS brain lesions and in cells from both acute and chronic active MS lesions (53). However, altered SIRT1 expression and activity have also been linked to inflammatory diseases. MET activation is involved in angiogenesis, wound healing, cell scattering, proliferation, and cancer invasion (54) and might exert neuroprotective and immunomodulatory effects in the experimental allergic encephalomyelitis model (EAE) of MS.

Between the miRNAs reverted by the CLA treatment, we discussed relevant candidates including miR-199a, miR-151a-5p, and miR-29b-3p. miR-199a, which is downregulated in the pre-CLA vs. the CTRs and upregulated by CLA, is involved in Treg differentiation (41). miR-151a-5p, the most widely modulated miRNA by CLA treatment, is not yet characterized in MS pathophysiology and needs to be further explored, and miR-29b-3p, the only downregulated miRNA after CLA treatment, is strongly connected to the PDGF pathway as discussed above.

In conclusion, we identified drug-dependent changes in miRNA profiles and identified potential candidate miRNAs that we propose to be involved in the corresponding pharmacological mechanisms.

The strength of this study is the identification of DE miRNAs as potential biomarkers in RRMS patients' stratification and of CLA or OCRE drug response. The limitations of the study include the limited number of participants, duration of the follow-up, and the fact that not all patients are naïve to DMTs. Thus, further studies on a wider population and independent cohorts monitored for longer time periods are needed. Moreover, small RNA-Seq analysis could extend our findings, allowing the identification of other short non-coding RNAs potentially involved in MS pathogenesis, monitoring, and therapeutic response.

Data availability statement

The datasets presented in this study can be found in online repositories. The names of the repository/repositories and accession number(s) can be found below: https://www.ncbi.nlm.nih.gov/geo/, GSE230064.

Ethics statement

The studies involving humans were approved by Ethics of Sapienza University – Policlinico Umberto I. The studies were conducted in accordance with the local legislation and institutional requirements. The participants provided their written informed consent to participate in this study.

Author contributions

IA: including medical writing, study concept or design, analysis or data interpretation, and statistical analysis. LM: including medical writing, major role in data acquisition, study concept or design, and analysis or data interpretation. VM and RB: major role in data acquisition, RNA extraction and qualitative analysis, and microarray analysis. TS: major role in data acquisition and RNA extraction and microarray analysis. CD'A: major role in the acquisition of data, RNA extraction and qualitative analysis, and microarray analysis. SC and GF: major role in data acquisition and critical reading of the manuscript. DB: including medical writing and analysis or interpretation of data. FM and RF: analysis or interpretation of data and revision of the manuscript. EP: including medical writing and major role in data acquisition. HS: analysis or data interpretation and revision of the manuscript. MS: including medical writing and analysis or data interpretation. ACa: analysis or data interpretation. MD'O: including medical writing, study concept or design, and analysis or data interpretation. ACo: including medical writing for content and major role in data acquisition, study concept or design, and analysis or data interpretation. All authors contributed to the article and approved the submitted version.

Funding

This research was funded by Fondo Ordinario Enti (FOE D.M 865/2019) in the framework of a collaboration agreement between the Italian National Research Council and EBRI, by Regione Lazio, Public Notice "LIFE 2020", BioproSM, Gruppi di Ricerca n. A0375-2020- 36677, and by the Ministry of University and Research (MUR), National Recovery and Resilience Plan (NRRP), project

MNESYS (PE0000006)—a multiscale integrated approach to the study of the nervous system in health and disease (DN. 1553 11.10.2022). ACo is recipient of funding from the Italian Ministry of Health "Progetto di Ricerca Corrente 2023".

Acknowledgments

The authors thank Simona Caporilli and Stefano Gabriele, Agilent Technologies, for their technical assistance in the microarray analysis.

Conflict of interest

SC received travel grants from Merck and Novartis. ACo received consulting research funding from Novartis, Roche, Biogen, Merck Serono, and Almirall. MS received research support and has received fees as speaker from Sanofi, Biogen, Roche, Novartis, Bayer Schering, and Merck Serono.

The remaining authors declare that the research was conducted in the absence of any commercial or financial relationships that could be construed as a potential conflict of interest.

Publisher's note

All claims expressed in this article are solely those of the authors and do not necessarily represent those of their affiliated organizations, or those of the publisher, the editors and the reviewers. Any product that may be evaluated in this article, or claim that may be made by its manufacturer, is not guaranteed or endorsed by the publisher.

Supplementary material

The Supplementary Material for this article can be found online at: https://www.frontiersin.org/articles/10.3389/fimmu.2023.1234869/full#supplementary-material

References

1. Filippi M, Preziosa P, Meani A, Ciccarelli O, Mesaros S, Rovira A, et al. Prediction of a multiple sclerosis diagnosis in patients with clinically isolated syndrome using the 2016 MAGNIMS and 2010 McDonald criteria: a retrospective study. *Lancet Neurol* (2018) 17:133–42. doi: 10.1016/S1474-4422(17)30469-6

2. Katz Sand I. Classification, diagnosis, and differential diagnosis of multiple sclerosis. *Curr Opin Neurol* (2015) 28:193–205. doi: 10.1097/WCO.0000000000000206

3. Frischer JM, Bramow S, Dal-Bianco A, Lucchinetti CF, Rauschka H, Schmidbauer M, et al. The relation between inflammation and neurodegeneration in multiple sclerosis brains. *Brain* (2009) 132:1175–89. doi: 10.1093/brain/awp070

4. Perrone V, Veronesi C, Giacomini E, Citraro R, Dell'Orco S, Lena F, et al. The epidemiology, treatment patterns and economic burden of different phenotypes of multiple sclerosis in Italy: relapsing-remitting multiple sclerosis and secondary progressive multiple sclerosis. *CLEP* (2022) 14:1327–37. doi: 10.2147/CLEP.S376005

5. Pitt D, Lo CH, Gauthier SA, Hickman RA, Longbrake E, Airas LM, et al. Toward precision phenotyping of multiple sclerosis. *Neurol Neuroimmunol Neuroinflamm* (2022) 9:e200025. doi: 10.1212/NXI.0000000000200025

6. Kuhlmann T, Moccia M, Coetzee T, Cohen JA, Correale J, Graves J, et al. Multiple sclerosis progression: time for a new mechanism-driven framework. *Lancet Neurol* (2023) 22:78–88. doi: 10.1016/S1474-4422(22)00289-7

7. Giovannoni G, Soelberg Sorensen P, Cook S, Rammohan K, Rieckmann P, Comi G, et al. Safety and efficacy of cladribine tablets in patients with relapsing–remitting multiple sclerosis: Results from the randomized extension trial of the CLARITY study. *Mult Scler* (2018) 24:1594–604. doi: 10.1177/1352458517727603

8. Comi G, Radaelli M, Soelberg Sørensen P. Evolving concepts in the treatment of relapsing multiple sclerosis. *Lancet* (2017) 389:1347–56. doi: 10.1016/S0140-6736(16)32388-1

9. Hauser SL, Bar-Or A, Comi G, Giovannoni G, Hartung H-P, Hemmer B, et al. Ocrelizumab versus interferon beta-1a in relapsing multiple sclerosis. *N Engl J Med* (2017) 376:221–34. doi: 10.1056/NEJMoa1601277

10. Lamb YN. Ocrelizumab: a review in multiple sclerosis. *Drugs* (2022) 82:323–34. doi: 10.1007/s40265-022-01672-9

11. Baker D, MacDougall A, Kang AS, Schmierer K, Giovannoni G, Dobson R. CD19 B cell repopulation after ocrelizumab, alemtuzumab and cladribine: Implications for SARS-CoV-2 vaccinations in multiple sclerosis. *Multiple Sclerosis Related Disord* (2022) 57:103448. doi: 10.1016/j.msard.2021.103448

12. Deeks ED. Cladribine tablets: a review in relapsing MS. *CNS Drugs* (2018) 32:785–96. doi: 10.1007/s40263-018-0562-0

13. Furlan R. Definition of non-responders: biological markers. *Neurol Sci* (2008) 29:214–5. doi: 10.1007/s10072-008-0940-3

14. Mohr A, Mott J. Overview of microRNA biology. *Semin Liver Dis* (2015) 35:003–11. doi: 10.1055/s-0034-1397344

15. Barbash S, Shifman S, Soreq H. Global coevolution of human microRNAs and their target genes. *Mol Biol Evol* (2014) 31:1237–47. doi: 10.1093/molbev/msu090

16. Otaegui D, Baranzini SE, Armañanzas R, Calvo B, Muñoz-Culla M, Khankhanian P, et al. Differential micro RNA expression in PBMC from multiple sclerosis patients. *PloS One* (2009) 4:e6309. doi: 10.1371/journal.pone.0006309

17. Piket E, Zheleznyakova GY, Kular L, Jagodic M. Small non-coding RNAs as important players, biomarkers and therapeutic targets in multiple sclerosis: a comprehensive overview. *J Autoimmun* (2019) 101:17–25. doi: 10.1016/j.jaut.2019.04.002

18. Regev K, Healy BC, Paul A, Diaz-Cruz C, Mazzola MA, Raheja R, et al. Identification of MS-specific serum miRNAs in an international multicenter study. *Neurol Neuroimmunol Neuroinflamm* (2018) 5:e491. doi: 10.1212/NXI.0000000000000491

19. Sievers C, Meira M, Hoffmann F, Fontoura P, Kappos L, Lindberg RLP. Altered microRNA expression in B lymphocytes in multiple sclerosis. *Clin Immunol* (2012) 144:70–9. doi: 10.1016/j.clim.2012.04.002

20. Rotstein D, Montalban X. Reaching an evidence-based prognosis for personalized treatment of multiple sclerosis. *Nat Rev Neurol* (2019) 15:287–300. doi: 10.1038/s41582-019-0170-8

21. Thompson AJ, Banwell BL, Barkhof F, Carroll WM, Coetzee T, Comi G, et al. Diagnosis of multiple sclerosis: 2017 revisions of the McDonald criteria. *Lancet Neurol* (2018) 17:162–73. doi: 10.1016/S1474-4422(17)30470-2

22. Montalban X, Gold R, Thompson AJ, Otero-Romero S, Amato MP, Chandraratna D, et al. ECTRIMS/EAN Guideline on the pharmacological treatment of people with multiple sclerosis. *Multiple Sclerosis J* (2018) 24(2):96-120. doi: 10.1177/1352458517751049

23. Belvisi D, Canevelli M, Marfia GA, Ferraro E, Centonze D, Salvetti M, et al. Response to "Frailty in multiple sclerosis: A closer look at the deficit accumulation framework." *Mult Scler* (2022) 28:1001–2. doi: 10.1177/13524585211068150

24. Rao Y, Lee Y, Jarjoura D, Ruppert AS, Liu C, Hsu JC, et al. A comparison of normalization techniques for microRNA microarray data. *Stat Appl Genet Mol Biol* (2008) 7(1)22. doi: 10.2202/1544-6115.1287

25. Von Elm E, Altman DG, Egger M, Pocock SJ, Gøtzsche PC, Vandenbroucke JP. The Strengthening the Reporting of Observational Studies in Epidemiology (STROBE) Statement: Guidelines for reporting observational studies. *Int J Surg* (2014) 12:1495–9. doi: 10.1016/j.ijsu.2014.07.013

26. Keller A, Leidinger P, Steinmeyer F, Stähler C, Franke A, Hemmrich-Stanisak G, et al. Comprehensive analysis of microRNA profiles in multiple sclerosis including next-generation sequencing. *Mult Scler* (2014) 20:295–303. doi: 10.1177/1352458513496343

27. Teuber-Hanselmann S, Meinl E, Junker A. MicroRNAs in gray and white matter multiple sclerosis lesions: impact on pathophysiology. *J Pathol* (2020) 250:496–509. doi: 10.1002/path.5399

28. Zhang Y, Gao T, Li X, Wen C-C, Yan X-T, Peng C, et al. Circ_0005075 targeting miR-151a-3p promotes neuropathic pain in CCI rats via inducing NOTCH2 expression. *Gene* (2021) 767:145079. doi: 10.1016/j.gene.2020.145079

29. Dobrowolny G, Martone J, Lepore E, Casola I, Petrucci A, Inghilleri M, et al. A longitudinal study defined circulating microRNAs as reliable biomarkers for disease prognosis and progression in ALS human patients. *Cell Death Discov* (2021) 7:4. doi: 10.1038/s41420-020-00397-6

30. Guerau-de-Arellano M, Alder H, Ozer HG, Lovett-Racke A, Racke MK. miRNA profiling for biomarker discovery in multiple sclerosis: From microarray to deep sequencing. *J Neuroimmunol* (2012) 248:32–9. doi: 10.1016/j.jneuroim.2011.10.006

31. Karimi L, Eskandari N, Shaygannejad V, Zare N, Andalib A, Khanahmad H, et al. Comparison of Expression Levels of miR-29b-3p and miR-326 in T Helper-1 and T Helper-17 Cells Isolated from Responsive and Non-responsive Relapsing-remitting Multiple Sclerosis Patients Treated with Interferon-beta. *IJAAI* (2020) 19(4):416-425. doi: 10.18502/ijaai.v19i4.4116

32. Mancuso R, Agostini S, Hernis A, Caputo D, Galimberti D, Scarpini E, et al. Alterations of the miR-126-3p/POU2AF1/spi-B axis and JCPyV reactivation in multiple sclerosis patients receiving natalizumab. *Front Neurol* (2022) 13:819911. doi: 10.3389/fneur.2022.819911

33. Cox MB, Cairns MJ, Gandhi KS, Carroll AP, Moscovis S, Stewart GJ, et al. MicroRNAs miR-17 and miR-20a Inhibit T Cell Activation Genes and Are Under-Expressed in MS Whole Blood. *PloS One* (2010) 5:e12132. doi: 10.1371/journal.pone.0012132

34. Cerutti C, Edwards LJ, De Vries HE, Sharrack B, Male DK, Romero IA. MiR-126 and miR-126* regulate shear-resistant firm leukocyte adhesion to human brain endothelium. *Sci Rep* (2017) 7:45284. doi: 10.1038/srep45284

35. Maciak K, Dziedzic A, Miller E, Saluk-Bijak J. miR-155 as an important regulator of multiple sclerosis pathogenesis. *A Review. IJMS* (2021) 22:4332. doi: 10.3390/ijms22094332

36. Sanders KA, Benton MC, Lea RA, Maltby VE, Agland S, Griffin N, et al. Next-generation sequencing reveals broad down-regulation of microRNAs in secondary progressive multiple sclerosis CD4+ T cells. *Clin Epigenet* (2016) 8:87. doi: 10.1186/s13148-016-0253-y

37. Zorbaz T, Madrer N, Soreq H. Cholinergic blockade of neuroinflammation: from tissue to RNA regulators. *Neuronal Signal* (2022) 6:NS20210035. doi: 10.1042/NS20210035

38. Angerstein C, Hecker M, Paap BK, Koczan D, Thamilarasan M, Thiesen H-J, et al. Integration of microRNA databases to study microRNAs associated with multiple sclerosis. *Mol Neurobiol* (2012) 45:520–35. doi: 10.1007/s12035-012-8270-0

39. Kumar M, Li G. Emerging role of microRNA-30c in neurological disorders. *IJMS* (2022) 24:37. doi: 10.3390/ijms24010037

40. Waschbisch A, Atiya M, Linker RA, Potapov S, Schwab S, Derfuss T. Glatiramer acetate treatment normalizes deregulated microRNA expression in relapsing remitting multiple sclerosis. *PloS One* (2011) 6:e24604. doi: 10.1371/journal.pone.0024604

41. Ghadiri N, Emamnia N, Ganjalikhani-Hakemi M, Ghaedi K, Etemadifar M, Salehi M, et al. Analysis of the expression of mir-34a, mir-199a, mir-30c and mir-19a in peripheral blood CD4+T lymphocytes of relapsing-remitting multiple sclerosis patients. *Gene* (2018) 659:109–17. doi: 10.1016/j.gene.2018.03.035

42. Baker D, Pryce G, James LK, Schmierer K, Giovannoni G. Failed B cell survival factor trials support the importance of memory B cells in multiple sclerosis. *Eur J Neurol* (2020) 27:221–8. doi: 10.1111/ene.14105

43. Jelcic I, Al Nimer F, Wang J, Lentsch V, Planas R, Jelcic I, et al. Memory B cells activate brain-homing, autoreactive CD4+ T cells in multiple sclerosis. *Cell* (2018) 175:85–100.e23. doi: 10.1016/j.cell.2018.08.011

44. Zhang E, Tian X, Li R, Chen C, Li M, Ma L, et al. Dalfampridine in the treatment of multiple sclerosis: a meta-analysis of randomised controlled trials. *Orphanet J Rare Dis* (2021) 16:87. doi: 10.1186/s13023-021-01694-8

45. Morawiec N, Techmański T, Tracz K, Kluska A, Arendarczyk M, Baran M, et al. The comparative analysis of selected interleukins and proinflammatory factors in CSF among *de novo* diagnosed patients with RRMS. *Clin Neurol Neurosurg* (2023) 225:107522. doi: 10.1016/j.clineuro.2022.107522

46. Ghorbani S, Yong VW. The extracellular matrix as modifier of neuroinflammation and remyelination in multiple sclerosis. *Brain* (2021) 144:1958–73. doi: 10.1093/brain/awab059

47. Maglione A, Rolla S, Mercanti SFD, Cutrupi S, Clerico M. The adaptive immune system in multiple sclerosis: an estrogen-mediated point of view. *Cells* (2019) 8:1280. doi: 10.3390/cells8101280

48. Mori F, Rossi S, Piccinin S, Motta C, Mango D, Kusayanagi H, et al. Synaptic plasticity and PDGF signaling defects underlie clinical progression in multiple sclerosis. *J Neurosci* (2013) 33:19112–9. doi: 10.1523/JNEUROSCI.2536-13.2013

49. Stampanoni Bassi M, Iezzi E, Marfia GA, Simonelli I, Musella A, Mandolesi G, et al. Platelet-derived growth factor predicts prolonged relapse-free period in multiple sclerosis. *J Neuroinflamm* (2018) 15:108. doi: 10.1186/s12974-018-1150-4

50. Harati R, Hammad S, Tlili A, Mahfood M, Mabondzo A, Hamoudi R. miR-27a-3p regulates expression of intercellular junctions at the brain endothelium and controls the endothelial barrier permeability. *PloS One* (2022) 17:e0262152. doi: 10.1371/journal.pone.0262152

51. Chapouly C, Tadesse Argaw A, Horng S, Castro K, Zhang J, Asp L, et al. Astrocytic TYMP and VEGFA drive blood–brain barrier opening in inflammatory central nervous system lesions. *Brain* (2015) 138:1548–67. doi: 10.1093/brain/awv077

52. Kouchaki E, Shahreza BO, Faraji S, Nikoueinejad H, Sehat M. The association between vascular endothelial growth factor-related factors and severity of multiple sclerosis. (2016) 15(3):204-11.

53. Zhang W, Xiao D, Li X, Zhang Y, Rasouli J, Casella G, et al. SIRT1 inactivation switches reactive astrocytes to an antiinflammatory phenotype in CNS autoimmunity. *J Clin Invest* (2022) 132:e151803. doi: 10.1172/JCI151803

54. Trusolino L, Bertotti A, Comoglio PM. MET signalling: principles and functions in development, organ regeneration and cancer. *Nat Rev Mol Cell Biol* (2010) 11:834–48. doi: 10.1038/nrm3012

frontiers | Frontiers in Immunology

TYPE Original Research
PUBLISHED 08 January 2024
DOI 10.3389/fimmu.2023.1293100

OPEN ACCESS

EDITED BY
Jinzhou Feng,
First Affiliated Hospital of Chongqing Medical University, China

REVIEWED BY
Chun-sheng Yang,
Tianjin Medical University General Hospital, China
Yi Nan Zhao,
China Medical University, China

*CORRESPONDENCE
Jingli Shan
364855712@qq.com
Shengjun Wang
junwang9999@sina.com

RECEIVED 12 September 2023
ACCEPTED 18 December 2023
PUBLISHED 08 January 2024

CITATION
Wang L, Xia R, Li X, Shan J and Wang S (2024) Systemic inflammation response index is a useful indicator in distinguishing MOGAD from AQP4-IgG-positive NMOSD. *Front. Immunol.* 14:1293100. doi: 10.3389/fimmu.2023.1293100

Systemic inflammation response index is a useful indicator in distinguishing MOGAD from AQP4-IgG-positive NMOSD

Lei Wang, Ruihong Xia, Xiangliang Li, Jingli Shan* and Shengjun Wang*

Department of Neurology, Qilu Hospital, Cheeloo College of Medicine, Shandong University, Jinan, Shandong, China

Objective: To identify reliable immune-inflammation indicators for distinguishing myelin oligodendrocyte glycoprotein antibody-associated disease (MOGAD) from anti–aquaporin-4 immunoglobulin G (AQP4-IgG)-positive neuromyelitis optica spectrum disorders (NMOSD). To assess these indicators' predictive significance in MOGAD recurrence.

Methods: This study included 25 MOGAD patients, 60 AQP4-IgG-positive NMOSD patients, and 60 healthy controls (HCs). Age and gender were matched among these three groups. Participant clinical and imaging findings, expanded disability status scale (EDSS) scores, cerebrospinal fluid (CSF) information, and blood cell counts were documented. Subsequently, immune-inflammation indicators were calculated and compared among the MOGAD, AQP4-IgG-positive NMOSD, and HC groups. Furthermore, we employed ROC curve analysis to assess the predictive performance of each indicator and binary logistic regression analysis to assess potential risk factors.

Results: In MOGAD patients, systemic inflammation response index (SIRI), CSF white cell count (WCC), and CSF immunoglobulin A (IgA) levels were significantly higher than in AQP4-IgG-positive NMOSD patients ($p = 0.038$, $p = 0.039$, $p = 0.021$, respectively). The ROC curves showed that SIRI had a sensitivity of 0.68 and a specificity of 0.7 for distinguishing MOGAD from AQP4-IgG-positive NMOSD, with an AUC of 0.692 (95% CI: 0.567-0.818, $p = 0.0054$). Additionally, compared to HCs, both MOGAD and AQP4-IgG-positive NMOSD patients had higher neutrophils, neutrophil-to-lymphocyte ratio (NLR), SIRI, and systemic immune-inflammation index (SII). Eight (32%) of the 25 MOGAD patients had recurrence within 12 months. We found that the monocyte-to-lymphocyte ratio (MLR, AUC = 0.805, 95% CI = 0.616–0.994, cut-off value = 0.200, sensitivity = 0.750, specificity = 0.882) was an effective predictor of MOGAD recurrence. Binary logistic regression analysis showed that MLR below 0.200 at first admission was the only risk factor for recurrence ($p = 0.005$, odds ratio =22.5, 95% CI: 2.552–198.376).

Conclusion: Elevated SIRI aids in distinguishing MOGAD from AQP4-IgG-positive NMOSD; lower MLR levels may be linked to the risk of MOGAD recurrence.

KEYWORDS

myelin oligodendrocyte glycoprotein antibody-associated disease (MOGAD), neuromyelitis optica spectrum disorders (NMOSD), systemic inflammation response index (SIRI), monocyte-to-lymphocyte ratio (MLR), cerebrospinal fluid (CSF)

1 Introduction

Myelin oligodendrocyte glycoprotein antibody-associated disease (MOGAD) can occur in individuals across all age groups, with an incidence rate of 1.6-3.4 per million and a prevalence of 20 per million (1, 2). The application of cell-based assays (CBA) has clarified MOGAD diagnoses for patients who were previously categorized as anti–aquaporin-4 immunoglobulin G (AQP4-IgG)-negative neuromyelitis optica spectrum disorders (NMOSD) (3). These patients often present with optic neuritis, longitudinally extensive transverse myelitis, or related conditions. Despite its rarity, research on MOGAD remains in its nascent stages. The clinical and radiological features of both MOGAD and AQP4-IgG-positive NMOSD exhibit some overlap, creating challenges for early diagnosis. A UK study with a median follow-up of 15.5 months found that 27% of MOGAD patients experienced recurrence, and 47% suffered lasting neurological deficits (4). Thus, it is crucial to identify indicators that can early distinguish MOGAD from AQP4-IgG-positive NMOSD and predict recurrence in MOGAD.

Systemic inflammation response index (SIRI), a marker of systemic inflammation calculated as the product of monocyte and neutrophil-to-lymphocyte ratio (NLR), has demonstrated its predictive power in various conditions like ischemic stroke, aneurysmal subarachnoid hemorrhage, glioma, and rheumatoid arthritis (5–8). However, its role in predicting MOGAD has not been explored.

Previous investigations have emphasized monocytes as significant contributors in demyelination (9–11). In AQP4-IgG-positive NMOSD mice, promoting neutrophil apoptosis showed potential for reducing brain damage (12). Early-stage inhibition of peripheral blood platelet elevation was linked to halting disease progression (13). Furthermore, AQP4-IgG-positive NMOSD patients exhibited significantly elevated neutrophils, NLR, platelet-to-lymphocyte ratio (PLR), and platelet × NLR (systemic immune-inflammation index, SII) compared to both multiple sclerosis (MS) patients and healthy individuals (14). Additionally, the monocyte-to-lymphocyte ratio (MLR) was effective in predicting NMOSD recurrence (14). Moreover, the expression of MOG protein is generally limited to the nervous system (15), unlike AQP4, which is widely distributed throughout the human body (16). This implies differences in CSF white cell count (WCC) and immunoglobulin between MOGAD and AQP4-IgG-positive NMOSD. Building upon these findings, we propose that these immune-inflammatory indicators could potentially assist in the early differentiation of MOGAD from AQP4-IgG-positive NMOSD and recurrence prediction of MOGAD.

2 Method

2.1 Study population

This study included 25 patients diagnosed with MOGAD and 60 patients with age- and sex-matched AQP4-IgG-positive NMOSD at Qilu Hospital, Cheeloo College of Medicine, Shandong University, from January 2018 to August 2022. Inclusion criteria were as follows: (1) Serum MOG antibody positivity detected through CBA and meeting the 2023 International MOGAD Panel proposed criteria (17); (2) AQP4-IgG-positive NMOSD diagnosis according to the 2015 International Panel for NMO Diagnosis (IPND) criteria (18); (3) All MOGAD and AQP4-IgG-positive NMOSD patients admitted to our hospital within 2 weeks of symptom onset; (4) No symptoms of systemic infection (like respiratory, urinary, skin, or soft tissue infections) or recent corticosteroid/immunosuppressive therapy within 14 days before blood collection; (5) Comprehensive clinical evaluations and laboratory assessments (including anti-double-stranded DNA antibodies, anti-SS-A and anti-SS-B antibodies, etc.) revealed no coexistence with hematological disorders or other autoimmune diseases; (6) Ages 14 and older. Exclusion criteria included: (1) Loss of follow-up, which referred to patients no longer returning for outpatient visits and couldn't be reached by phone; (2) Inability to comply with neurologist-prescribed ongoing treatment. We also included 60 healthy individuals matched for gender and age with MOGAD patients as a control group; all were recruited from the Health Examination Center of Qilu Hospital, Shandong University.

2.2 Data collection

Upon admission, fasting blood samples were collected to evaluate neutrophils, monocytes, lymphocytes, and platelets. And then, calculations were calculated for NLR, MLR, PLR, SIRI, and SII. In addition to this, we gathered data on CSF, including WCC, proteins, and the levels of immunoglobulins A (IgA), G (IgG), and M (IgM). Neurologists determined Extended Disability Status Scale (EDSS) scores in MOGAD and AQP4-IgG-positive NMOSD patients to assess disability. For each MOGAD patient, we conducted follow-ups at three and twelve months after their discharge to assess recurrence. Clinical recurrence refers to the emergence of new neurological deficits more than one month after the initial attack (17).

2.3 MOG-IgG and AQP4-IgG assay

MOG-IgG and AQP4-IgG were detected by means of commercial CBA (Euroimmun, Lübeck, Germany) according to the manufacturer's recommendations. CBA using HEK-293 cells stably transfected with human full-length MOG and human AQP4, and then MOG-IgG and AQP4-IgG were detected using anti-human IgG (Fc) secondary antibodies and subsequently visualized by microscopy.

2.4 Data analysis

Statistical analysis utilized SPSS 26.0 and GraphPad Prism 8.0. The normality of continuous variables was determined using the Shapiro-Wilk test. For non-normally distributed continuous data, we presented the results as the median with the interquartile range (IQR). Comparisons between two-group variables were conducted by the Mann–Whitney U test, and the Kruskal-Wallis H test was used in three-group comparisons, with *post hoc* tests conducted using the Bonferroni method. We used the Chi-square test for categorical variables and conducted *post hoc* Chi-square tests for multiple comparisons. Receiver operating characteristic (ROC) curves evaluated the predictive ability of each index. The optimal cut-off value was calculated using the Youden test. Binary logistic regression analysis was used to determine risk factors.

3 Results

3.1 Baseline characteristics

The analysis included 25 MOGAD patients with a median age of 27 (15, 35), of whom 40% were female. The median EDSS score before treatment was 3.0 (2.0, 4.5) (Table 1). The major symptoms were cerebral monofocal or polyfocal deficits, accounting for 44% (n = 11). In addition, cerebral cortical encephalitis, often with seizures, was detected in 28% of cases (n = 7). Brainstem deficits were found in 6 cases (24%). Optic neuritis (ON) occurred in 4 cases, making up 16% of all cases. Acute disseminated encephalomyelitis was observed in 3 cases (12%), and cerebellar deficits were presented in 2 cases (8%). Among 60 AQP4-IgG-positive NMOSD patients, the most common was acute transverse myelitis, found in 35 cases (58.3%), followed by cerebral syndrome in 15 cases (25.0%). Additionally, area postrema syndrome occurred in 18 cases (30%), while ON was present in 13 cases (21.7%). Diencephalic syndrome was observed in 4 cases (6.7%). Within 12 months after discharge, 32% (n = 8) of MOGAD patients experienced recurrence, with a median time to recurrence of 3 (2, 9.75) months and a median EDSS score of 3.5 (2.0, 4.5) at recurrence. The most common recurrent symptoms were cerebral monofocal or polyfocal deficits, seen in 5 cases (62.5%). ON and brainstem deficits each occurred in 2 cases (25%), while myelitis was observed in 1 case (12.5%).

3.2 Differences in immune-inflammation indicators among three groups

In comparison to AQP4-IgG-positive NMOSD, MOGAD exhibited greater levels of SIRI, CSF WCC, and CSF IgA. (Table 1). SIRI was identified as a risk factor in the univariate analysis (Table 2). After excluding collinearity factors and after adjusting for other factors, multivariate analysis showed that SIRI was an independent factor to distinguish MOGAD from NMOSD (Table 2). It exhibited a high sensitivity and specificity at the cut-off value, and its elevated positive predictive value (PPV), positive likelihood ratio (PLR+), and diagnostic odds ratio (dOR) also indicated its diagnostic value (cut-off value = 1.565, sensitivity =0.68, specificity =0.70, PPV = 0.49, PLR+ =2.27, dOR = 5.04) (Table 3, Figure 1A). The ROC curve analysis indicated that CSF WCC had the highest specificity, PPV, PLR+, and dOR at the cut-off value (cut-off value = 17.5, specificity = 0.818, PPV = 0.58, PLR+ = 3.36, dOR = 7.00) (Table 3, Figure 1A). However, the univariate analysis showed that CSF WCC were not a risk factor (Table 2). We then analyzed the association between SIRI and other indicators in MOGAD patients and NMOSD patients, respectively. Spearman's correlation analysis showed that SIRI was positively correlated with CSF WCC in MOGAD patients ($p = 0.002$, $r = 0.667$) and negatively correlated with CSF proteins and CSF IgG levels in NMOSD patients ($p = 0.025$, $rs = -0.331$; $p = 0.011$, $rs = -0.379$). When compared to HC, both MOGAD and AQP4-IgG-positive NMOSD presented significantly elevated neutrophils, NLR, SIRI, and SII (Table 1, Figure 2). ROC curve analysis indicated that all four of these indicators had excellent diagnostic performance for separating MOGAD from HC (Figure 1B).

3.3 Factors predicting recurrence in patients with MOGAD

In the exploration of recurrent factors in MOGAD patients, we compared admission indicators between the 8 recurrent patients and the remaining 17 (Table 4). ROC curve analysis of the admission test results indicated MLR (AUC=0.805, 95%

10.3389/fimmu.2023.1293100

TABLE 1 Comparison of immune-inflammation indicators among the three groups.

Variables	MOGAD (n=25)	NMOSD (n=60)	HC (n=60)	P1	P2	P3
Age, median, (IQR)	27 (15,35)	25 (19,35)	28 (17,35)	>0.999	>0.999	>0.999
Female (n%)	10 (40)	30 (50)	25 (42)	0.400	0.887	0.360
Relapse (n%)	8 (32)	15 (25)	–	0.508	–	–
EDSS, median, (IQR)	3.0 (2.0,4.5)	3.5 (3.0,6.0)	–	0.393	–	–
NEU, median, (IQR), 10^9/L	6.53 (5.19,11.65)	5.47 (4.02,7.63)	3.12 (2.57,4.04)	0.155	**<0.001**	**<0.001**
LYM, median, (IQR), 10^9/L	1.85 (1.00,2.50)	1.87 (1.27,2.38)	1.98 (1.49,2.47)	>0.999	>0.999	0.826
MON, median, (IQR), 10^9/L	0.41 (0.35,0.63)	0.44 (0.28,0.62)	0.40 (0.31,0.49)	>0.999	0.356	0.772
PLT, median, (IQR), 10^9/L	283 (240,304)	258 (223,302)	250 (202,293)	0.500	0.067	0.718
NLR, median, (IQR)	3.66 (2.40,8.58)	2.93 (1.72,5.50)	1.66 (1.14,2.48)	0.454	**<0.001**	**<0.001**
MLR, median, (IQR)	0.27 (0.18,0.39)	0.20 (0.16,0.30)	0.18 (0.14,0.30)	0.259	0.057	>0.999
SIRI, median, (IQR), 10^9/L	1.74 (1.04,4.40)	1.07 (0.69,1.89)	0.61 (0.39,1.04)	**0.038**	**<0.001**	**<0.001**
PLR, median, (IQR)	138.29 (109.48,273.79)	138.59 (92.56,215.87)	115.32 (103.92,143.73)	>0.999	0.051	0.172
SII, median, (IQR), 10^9/L	1054.62 (601.58,2493.39)	702.72 (449.21,1512.26)	381.74 (272.88,577.00)	0.225	**<0.001**	**<0.001**
Imaging profile						
Cerebrum (without cortex) (n%)	13 (52)	16 (27)	–	**0.025**	–	–
Cerebral cortex (n%)	8 (32)	0	–	**<0.001**	–	–
Optic nerve (n%)	4 (16)	13 (22)	–	0.552	–	–
Diencephalon (n%)	2 (8)	4 (7)	–	>0.999	–	–
Pons (n%)	6 (24)	6 (10)	–	0.168	–	–
Medulla (n%)	1 (4)	19 (32)	–	**0.006**	–	–
Cerebellum (n%)	3 (12)	1 (2)	–	0.074	–	–
Cervical spinal cord (n%)	3 (12)	30 (50)	–	**0.001**	–	–
Thoracic spinal cord (n%)	1 (4)	21 (35)	–	**0.003**	–	–
Lumbar spinal cord (n%)	0	1	–	>0.999	–	–
CSF profile						
Proteins, median, (IQR), g/L	0.40 (0.28,0.52)	0.30 (0.23,0.46)	–	0.056	–	–
WCC, median, (IQR), 10^6/L	20.5 (1.5,72.8)	4.0 (0.2,11.0)	–	**0.039**	–	–
IgG, median, (IQR), mg/L	35.50 (28.40,47.20)	31.85 (20.50,46.65)	–	0.156	–	–
IgA, median, (IQR), mg/L	5.06 (3.73,6.41)	2.58 (1.79,6.16)	–	**0.021**	–	–
IgM, median, (IQR), mg/L	0.62 (0.37,1.56)	0.45 (0.20,0.85)	–	0.070	–	–
Treatment						
Steroid hormone (n%)	17 (68)	44 (73)	–	0.619	–	–
Steroid hormone + IVIG (n%)	6 (24)	9 (15)	–	0.321	–	–
Steroid hormone + MMF (n%)	0	3 (5)	–	0.552	–	–
Steroid hormone + IVIG + MMF (n%)	2 (8)	1 (2)	–	0.206	–	–
Steroid hormone + IVIG + CYP (n%)	0	2 (3)	–	>0.999	–	–
Inebilizumab (n%)	0	1 (2)	–	>0.999	–	–

NEU, neutrophil; LYM, lymphocyte; MON, monocyte; PLT, platelet; NLR, neutrophil to lymphocyte ratio; MLR, monocyte to lymphocyte ratio; PLR, platelet to lymphocyte ratio; SIRI, systemic inflammation response index, monocyte × NLR; SII, systemic immune inflammation index, platelet × NLR; EDSS, Expanded Disability Status Scale; CSF, cerebrospinal fluid; WCC, white cell counts; IgG, immunoglobulin G; IgA, immunoglobulin A; IgM, immunoglobulin M; IVIG, intravenous immunoglobulin; MMF, mycophenolate mofetil; CYP, cyclophosphamide;
P1, Comparative findings between MOGAD and AQP4-IgG-positive NMOSD. P2, Comparative outcomes between MOGAD and HC. P3, Comparative analysis between AQP4-IgG-positive NMOSD and HC; bold, p<0.05.

10.3389/fimmu.2023.1293100

TABLE 2 Indicators for distinguishing MOGAD from AQP4-IgG-positive NMOSD .

Variables	Univariate analysis			Multivariate analysis		
	OR	95% CI	P value	OR	95% CI	P value
NEU, 10^9/L	1.206	1.048-1.389	**0.009**			
LYM, 10^9/L	0.919	0.547-1.542	0.748			
MON, 10^9/L	2.146	0.275-16.717	0.466			
PLT, 10^9/L	1.006	0.998-1.014	0.152	1.000	0.992–1.009	0.937
NLR	1.059	0.987-1.135	0.111			
MLR	8.134	0.376-175.938	0.181			
SIRI, 10^9/L	1.320	1.021-1.705	**0.034**	1.316	1.009–1.716	**0.043**
PLR	1.001	0.998-1.004	0.597			
SII, 10^9/L	1.000	1.000-1.000	0.116			
CSF proteins, g/L	1.015	0.512-2.014	0.965			
CSF WCC, 10^6/L	1.005	0.997-1.012	0.222			
CSF IgG, mg/L	1.002	0.995-1.009	0.574			
CSF IgA, mg/L	1.029	0.977-1.085	0.282			
CSF IgM, mg/L	1.023	0.924-1.133	0.658			

NEU, neutrophil; LYM, lymphocyte; MON, monocyte; PLT, platelet; NLR, neutrophil to lymphocyte ratio; MLR, monocyte to lymphocyte ratio; PLR, platelet to lymphocyte ratio; SIRI, systemic inflammation response index, monocyte × NLR; SII, systemic immune inflammation index, platelet × NLR; CSF, cerebrospinal fluid; WCC, white cell counts; IgG, immunoglobulin G; IgA, immunoglobulin A; IgM, immunoglobulin M; OR, odds ratio. bold, p<0.05.

CI=0.616–0.994, cut-off value=0.200, sensitivity=0.750, specificity=0.882) was the only predictor for recurrence (Figure 1C). The other indicators were not statistically significant. In binary logistic regression analysis, MLR levels below 0.200 (odds ratio =22.5, 95% CI: 2.552–198.376, p = 0.005) were independently associated with recurrence. The PPV, negative predictive value (NPV), PLR+, negative likelihood ratio (NLR-), and dOR were 0.75, 0.88, 6.36, 0.28, and 22.71, respectively.

TABLE 3 The ROC curve's capacity to discriminate between MOGAD and AQP4-IgG-positive NMOSD.

Variables	AUC	95% CI	P value	Cut-off value	Sensitivity	Specificity	PPV	NPV	PLR+	NLR-	dOR
NEU, 10^9/L	0.658	0.528-0.788	**0.022**	11.240	0.360	0.933	0.69	0.78	5.37	0.69	7.78
LYM, 10^9/L	0.503	0.364-0.642	0.965								
MON, 10^9/L	0.613	0.482-0.745	0.101								
PLT, 10^9/L	0.599	0.472-0.725	0.154								
NLR	0.613	0.482-0.745	0.101								
MLR	0.624	0.494-0.755	0.072								
SIRI, 10^9/L	0.692	0.567-0.818	**0.005**	1.565	0.680	0.700	0.49	0.85	2.27	0.45	5.04
PLR	0.554	0.424-0.685	0.432								
SII, 10^9/L	0.623	0.497-0.750	0.074								
CSF proteins, g/L	0.644	0.511-0.776	0.057								
CSF WCC, 10^6/L	0.667	0.499-0.834	**0.041**	17.500	0.611	0.818	0.58	0.86	3.36	0.48	7.00
CSF IgG, mg/L	0.609	0.471-0.747	0.157								
CSF IgA, mg/L	0.679	0.546-0.811	**0.021**	3.945	0.762	0.659	0.38	0.91	2.23	0.36	6.19
CSF IgM, mg/L	0.639	0.494-0.784	0.072								

NEU, neutrophil; LYM, lymphocyte; MON, monocyte; PLT, platelet; NLR, neutrophil to lymphocyte ratio; MLR, monocyte to lymphocyte ratio; PLR, platelet to lymphocyte ratio; SIRI, systemic inflammation response index, monocyte × NLR; SII, systemic immune inflammation index, platelet × NLR; CSF, cerebrospinal fluid; WCC, white cell counts; IgG, immunoglobulin G; IgA, immunoglobulin A; IgM, immunoglobulin M; AUC, area under the curve; PPV, positive predictive value; NPV, negative predictive value; PLR+, positive likelihood ratio; NLR-, negative likelihood ratio; dOR, diagnostic odds ratio. bold, p<0.05.

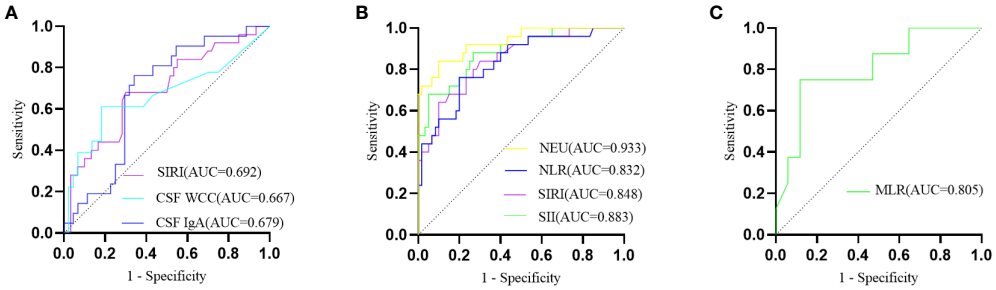

FIGURE 1
(A) The ROC curve depicting the discriminative prowess of SIRI, CSF WCC, and CSF IgA in differentially diagnosing between MOGAD and AQP4-IgG-positive NMOSD; **(B)** The ROC curve analysis delineating MOGAD from HC; **(C)** The ROC curve illustrating the predictive potential of MLR for MOGAD recurrence.

4 Discussion

Our findings show that MOGAD and AQP4-IgG-positive NMOSD are different illnesses, as evidenced by imaging, blood, and CSF data. MOGAD primarily affected the cerebrum and cerebral cortex, while the medulla, cervical spinal cord, and thoracic spinal cord were more likely to be observed in AQP4-IgG-positive NMOSD. Significant differences were also observed in SIRI, CSF WCC, and CSF IgA levels between MOGAD and AQP4-IgG-positive NMOSD.

SIRI is a useful indicator for predicting the prognosis of a number of inflammatory diseases. According to Topkan et al., a low SIRI score is associated with prolonged progression-free survival and overall survival in patients with glioblastoma multiforme of the brain (19). Yun et al. found that SIRI is an independent risk factor for poor outcomes in patients with aneurysmal subarachnoid hemorrhage (8). Zhang et al. discovered that SIRI is closely linked to stroke mortality and severity, as well as the risk of sepsis. The worse the stroke prognosis, the higher the SIRI value (5). In our study, we found that the MOGAD group had greater SIRI levels than the AQP4-IgG-positive NMOSD and HC groups. We identified a key SIRI threshold of 1.565 for distinguishing MOGAD from AQP4-IgG-positive NMOSD. Although clinical evidence on SIRI in demyelinating diseases is limited, further

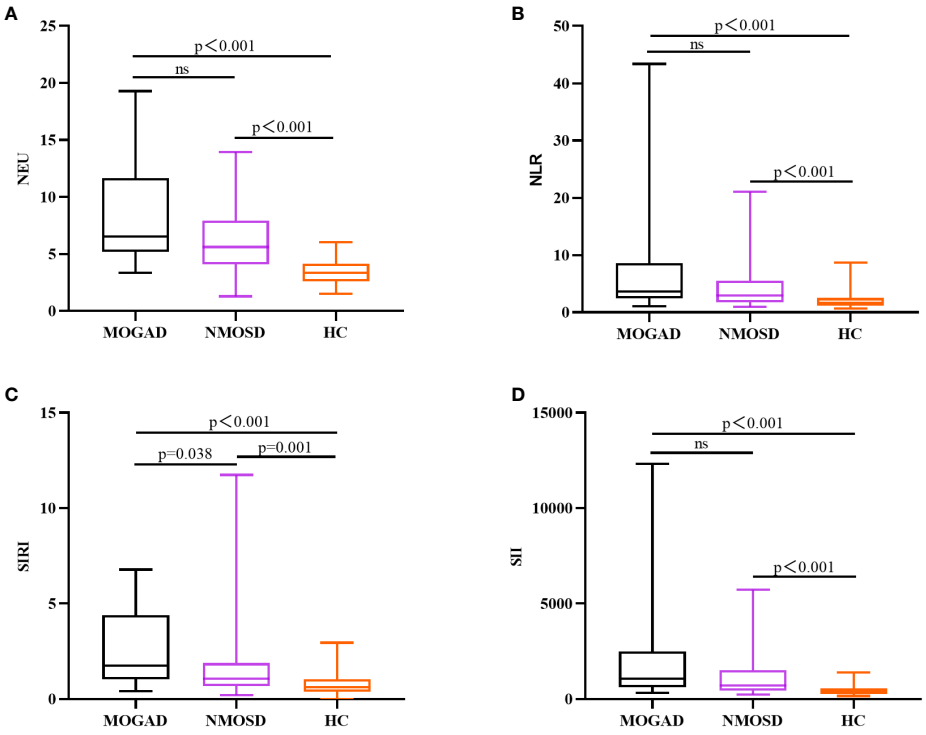

FIGURE 2
Box plots (with a median line at the center, a box representing the interquartile range, and whiskers extending from maximum to minimum) are used to elucidate the distributions of NEU **(A)**, NLR **(B)**, SIRI **(C)**, and SII **(D)** among MOGAD, AQP4-IgG-positive NMOSD, and HC.

10.3389/fimmu.2023.1293100

TABLE 4 Comparison of indicators of MOGAD patients with and without recurrence.

Variables	Recurrence (n=8)	Without recurrence (n=17)	P
Age, median, (IQR)	25(16.5,33.8)	27(14.5,38.5)	0.711
Female (n%)	3(37.5)	7(41.2)	1.000
EDSS, median, (IQR)	3.5(2.3,4.5)	3.0(1.5,4.3)	0.315
NEU, median, (IQR), 10^9/L	7.70(5.43,12.46)	6.53(5.01,11.48)	0.628
LYM, median, (IQR), 10^9/L	2.49(1.09,3.20)	1.75(1.00,2.30)	0.124
MON, median, (IQR), 10^9/L	0.42(0.24,0.59)	0.41(0.35,0.65)	0.628
PLT, median, (IQR), 10^9/L	268(226,310)	283(244,304)	0.842
NLR, median, (IQR)	2.71(1.92,12.91)	4.15(2.76,8.58)	0.406
MLR, median, (IQR)	0.18(0.14,0.26)	0.29(0.24,0.44)	**0.013**
SIRI, median, (IQR), 10^9/L	1.35(0.95,3.75)	2.27(1.33,4.62)	0.215
PLR, median, (IQR)	107.74 (88.02,246.13)	166.67 (124.67,273.79)	0.124
SII, median, (IQR), 10^9/L	731.90 (478.84,3054.98)	1475.97 (698.95,2493.39)	0.374
Imaging profile			
Cerebrum (without cortex) (n%)	4(50)	10(59)	>0.999
Cerebral cortex(n%)	2(25)	5(29)	>0.999
Optic nerve(n%)	2(25)	2(12)	0.570
Diencephalon(n%)	2(25)	0	0.093
Pons(n%)	2(25)	4(24)	>0.999
Medulla(n%)	0	1(6)	>0.999
Cerebellum(n%)	0	2(12)	>0.999
Cervical spinal cord(n%)	0	3(18)	0.527
Thoracic spinal cord(n%)	0	1(6)	>0.999
CSF profile			
Proteins, median, (IQR), g/L	0.44(0.26,0.61)	0.39(0.28,0.42)	0.731
WCC, median, (IQR), 10^6/L	6(0,28)	38(2,110)	0.246
IgG, median, (IQR), mg/L	40.50 (28.90,47.70)	35.40 (26.45,59.70)	0.913
IgA, median, (IQR), mg/L	5.20(4.18,5.85)	5.05(3.07,11.80)	0.743
IgM, median, (IQR), mg/L	1.02(0.43,1.18)	0.55(0.26,2.96)	0.799
Treatment			
Steroid hormone(n%)	7(87.5)	10(58.8)	0.205
Steroid hormone + IVIG (n%)	1(12.5)	5(29.4)	0.624
Steroid hormone + IVIG + MMF(n%)	0	2(11.8)	>0.999

NEU: neutrophil; LYM: lymphocyte; MON: monocyte; PLT: platelet; NLR: neutrophil to lymphocyte ratio; MLR: monocyte to lymphocyte ratio; PLR: platelet to lymphocyte ratio; SIRI: systemic inflammation response index, monocyte × NLR; SII: systemic immune inflammation index, platelet × NLR; CSF: cerebrospinal fluid; WCC: white cell counts; IgG: immunoglobulin G; IgA: immunoglobulin A; IgM: immunoglobulin M; IVIG: intravenous immunoglobulin; MMF: mycophenolate mofetil. bold, p<0.05.

investigation is recommended for its potential clinical utility in MOGAD.

SIRI reflects complex interactions among neutrophils, monocytes, and lymphocytes. It's worth mentioning that SIRI integrates monocytes, whereas SII incorporates platelets. Our study demonstrated that MOGAD patients had higher platelets and SII levels compared to AQP4-IgG-positive NMOSD patients, though without statistical significance. This implies that monocytes could contribute to the distinct SIRI disparity between MOGAD and AQP4-IgG-positive NMOSD. In experimental autoimmune encephalomyelitis (EAE), monocytes played a decisive role in disease onset and demyelination (9–11). Monocytes infiltrating the central nervous system (CNS), particularly Ly6ChiCCR2+ inflammatory monocytes, promoted EAE progression by crossing the blood-brain barrier in a CCR2-dependent manner (9, 20). Once inside the CNS, these cells released inflammatory mediators that accelerated disease development (20–22). Cost-effective and easily obtainable from blood samples, SIRI emerges as a novel inflammatory indicator for distinguishing MOGAD from AQP4-IgG-positive NMOSD.

MOGAD had considerably greater CSF WCC and CSF IgA levels than AQP4-IgG-positive NMOSD. Liu et al. found that C3 levels in the blood plasma were positively correlated with CSF WCC (23). In the MOGAD group, C3 consumption was lower, while CSF WCC were higher (23). This indirectly supports the earlier idea that the majority of MOG-IgG detected in the CSF is synthesized intrathecally by plasmablasts inside the CSF, whereas most of the AQP4-IgG in the CSF originated from extrathecal sources and passively entered the CSF through the blood-brain barrier (24).

MLR emerges as a predictor of MOGAD recurrence, implying that MOGAD patients with low MLR may require intensified treatment strategies. Previous research has shown that high MLR is correlated with poor prognosis in stroke patients and increased susceptibility to recurrence in AQP4-IgG-positive NMOSD patients (14, 25), in contrast to our findings of an association between lower MLR and MOGAD recurrence. These discrepancies potentially arise from functional disparities between neutrophils, monocytes, and lymphocytes across distinct diseases. Increasing evidence points to the detrimental role of neutrophils in CNS inflammation (26–29). Neutrophils have been detected in active lesions of both AQP4-IgG-induced NMO animal models and early-stage NMOSD patients (26, 30). Furthermore, damaged neutrophils in MOGAD

and AQP4-IgG-positive NMOSD had distinct mechanisms of demise (28). Although neutrophils may have differences in the pathological aspects of these two diseases, no difference was found in the blood examinations of our patients.

Several limitations of our study deserve acknowledgment. Firstly, as a single-center investigation with only Han Chinese participants, it may introduce selection bias. The small sample size is another constraint of our study, which could limit our capacity to establish the potential significance of particular indicators. Additionally, the 12-month follow-up period might not fully capture disease dynamics in this demyelinating disorder. Future research should explore larger samples with a longer follow-up duration for more comprehensive insights. With more and more antibodies identified, some of the AQP4-IgG-negative NMOSD may be rectified as a new entity; hence, only AQP4-IgG-positive NMOSD patients were included in our study.

5 Conclusion

Our research found that increased SIRI may serve as indicators for distinguishing MOGAD from AQP4-IgG-positive NMOSD. Decreased MLR levels may be associated with the probability of MOGAD recurrence.

Data availability statement

The raw data supporting the conclusions of this article will be made available by the authors, without undue reservation.

Ethics statement

The studies involving humans were approved by The ethics committee of the Qilu Hospital of Shandong University (KLL2021-283). The studies were conducted in accordance with the local legislation and institutional requirements. Written informed consent for participation was not required from the participants or the participants' legal guardians/next of kin in accordance with the national legislation and institutional requirements.

Author contributions

LW: Conceptualization, Formal Analysis, Investigation, Methodology, Software, Visualization, Writing – original draft, Writing – review & editing. RX: Data curation, Formal Analysis, Software, Writing – review & editing. XL: Data curation, Formal Analysis, Software, Writing – review & editing. JS: Conceptualization, Formal Analysis, Project administration, Supervision, Validation, Writing – review & editing. SW: Conceptualization, Formal Analysis, Methodology, Project administration, Supervision, Validation, Writing – review & editing.

Funding

The author(s) declare that no financial support was received for the research, authorship, and/or publication of this article.

Acknowledgments

We are grateful to Professor Yuan Zhang (Laboratory of Clinical Epidemiology, Qilu Hospital, Cheeloo College of Medicine, Shandong University) for the instructions in statistics for this study.

Conflict of interest

The authors declare that the research was conducted in the absence of any commercial or financial relationships that could be construed as a potential conflict of interest.

Publisher's note

References

1. de Mol CL, Wong YYM, van Pelt ED, Wokke BHA, Siepman TAM, Neuteboom RF, et al. The clinical spectrum and incidence of anti-MOG-associated acquired demyelinating syndromes in children and adults. *Multiple Sclerosis J* (2020) 26 (7):806–14. doi: 10.1177/1352458519845112

2. O'Connell K, Hamilton-Shield A, Woodhall M, Messina S, Mariano R, Waters P, et al. Prevalence and incidence of neuromyelitis optica spectrum disorder, aquaporin-4 antibody-positive NMOSD and MOG antibody-positive disease in Oxfordshire, UK. *J Neurol Neurosurg Psychiatry* (2020) 91(10):1126–8. doi: 10.1136/jnnp-2020-323158

3. Reindl M, Waters P. Myelin oligodendrocyte glycoprotein antibodies in neurological disease. *Nat Rev Neurology* (2019) 15(2):89–102. doi: 10.1038/s41582-018-0112-x

4. Jurynczyk M, Messina S, Woodhall MR, Raza N, Everett R, Roca-Fernandez A, et al. Clinical presentation and prognosis in MOG-antibody disease: a UK study. *Brain* (2017) 140(12):3128–38. doi: 10.1093/brain/awx276

5. Zhang Y, Xing Z, Zhou K, Jiang S. The predictive role of systemic inflammation response index (SIRI) in the prognosis of stroke patients. *Clin Interv Aging* (2021) 16:1997–2007. doi: 10.2147/CIA.S339221

6. Xu Y, He H, Zang Y, Yu Z, Hu H, Cui J, et al. Systemic inflammation response index (SIRI) as a novel biomarker in patients with rheumatoid arthritis: a multi-center retrospective study. *Clin Rheumatol* (2022) 41(7):1989–2000. doi: 10.1007/s10067-022-06122-1

7. He Q, Li L, Ren Q. The prognostic value of preoperative systemic inflammatory response index (SIRI) in patients with high-grade glioma and the establishment of a nomogram. *Front Oncol* (2021) 11:671811. doi: 10.3389/fonc.2021.671811

8. Yun S, Yi HJ, Lee DH, Sung JH. Systemic inflammation response index and systemic immune-inflammation index for predicting the prognosis of patients with aneurysmal subarachnoid hemorrhage. *J Stroke Cerebrovascular Dis* (2021) 30 (8):105861. doi: 10.1016/j.jstrokecerebrovasdis.2021.105861

9. Ajami B, Bennett JL, Krieger C, McNagny KM, Rossi FMV. Infiltrating monocytes trigger EAE progression, but do not contribute to the resident microglia pool. *Nat Neurosci* (2011) 14(9):1142–9. doi: 10.1038/nn.2887

10. Huitinga I, van Rooijen N, de Groot CJ, Uitdehaag BM, Dijkstra CD. Suppression of experimental allergic encephalomyelitis in Lewis rats after elimination of macrophages. *J Exp Med* (1990) 172(4):1025–33. doi: 10.1084/jem.172.4.1025

11. Yamasaki R, Lu H, Butovsky O, Ohno N, Rietsch AM, Cialic R, et al. Differential roles of microglia and monocytes in the inflamed central nervous system. *J Exp Med* (2014) 211(8):1533–49. doi: 10.1084/jem.20132477

12. Gong Y, Zhang Y-l, Wang Z, Song H-h, Liu Y-c, Lv A-w, et al. Tanshinone IIA alleviates brain damage in a mouse model of neuromyelitis optica spectrum disorder by inducing neutrophil apoptosis. *J Neuroinflammation* (2020) 1:17. doi: 10.1186/s12974-020-01874-6

13. Carnero Contentti E, López PA, Criniti J, Pettinicchi JP, Cristiano E, Patrucco L, et al. Platelet-to-lymphocyte ratio differs between MS and NMOSD at disease onset and predict disability. *Multiple Sclerosis Related Disord* (2022) 58:103507. doi: 10.1016/j.msard.2022.103507

14. Fang X, Sun S, Yang T, Liu X. Predictive role of blood-based indicators in neuromyelitis optica spectrum disorders. *Front Neurosci* (2023) 17:1097490. doi: 10.3389/fnins.2023.1097490

15. Peschl P, Bradl M, Höftberger R, Berger T, Reindl M. Myelin oligodendrocyte glycoprotein: deciphering a target in inflammatory demyelinating diseases. *Front Immunol* (2017) 8:529. doi: 10.3389/fimmu.2017.00529

16. Mobasheri A, Marples D, Young I, Floyd R, Moskaluk C, Frigeri A. Distribution of the AQP4 water channel in normal human tissues: protein and tissue microarrays reveal expression in several new anatomical locations, including the prostate gland and seminal vesicles. *Channels (Austin Tex)* (2007) 1(1):29–38. doi: 10.4161/chan.3735

17. Banwell B, Bennett JL, Marignier R, Kim HJ, Brilot F, Flanagan EP, et al. Diagnosis of myelin oligodendrocyte glycoprotein antibody-associated disease: International MOGAD Panel proposed criteria. *Lancet neurology* (2023) 22(3):268–82. doi: 10.1016/S1474-4422(22)00431-8

18. Wingerchuk DM, Banwell B, Bennett JL, Cabre P, Carroll W, Chitnis T, et al. International consensus diagnostic criteria for neuromyelitis optica spectrum disorders. *Neurology* (2015) ;85(2):177–89. doi: 10.1212/WNL.0000000000001729

19. Topkan E, Kucuk A, Ozdemir Y, Mertsoylu H, Besen AA, Sezen D, et al. Systemic inflammation response index predicts survival outcomes in glioblastoma multiforme patients treated with standard stupp protocol. *J Immunol Res* (2020) 2020:8628540. doi: 10.1155/2020/8628540

20. Mildner A, Mack M, Schmidt H, Brück W, Djukic M, Zabel MD, et al. CCR2+Ly-6Chi monocytes are crucial for the effector phase of autoimmunity in the central nervous system. *Brain* (2009) 132(9):2487–500. doi: 10.1093/brain/awp144

21. Locatelli G, Theodorou D, Kendirli A, Jordão MJC, Staszewski O, Phulphagar K, et al. Mononuclear phagocytes locally specify and adapt their phenotype in a multiple sclerosis model. *Nat Neurosci* (2018) 21(9):1196–208. doi: 10.1038/s41593-018-0212-3

22. Mrdjen D, Pavlovic A, Hartmann FJ, Schreiner B, Utz SG, Leung BP, et al. High-dimensional single-cell mapping of central nervous system immune cells reveals distinct myeloid subsets in health, aging, and disease. *Immunity* (2018) 48(2):380–395.e6. doi: 10.1016/j.immuni.2018.01.011

23. Lin L, Wu Y, Hang H, Lu J, Ding Y. Plasma complement 3 and complement 4 are promising biomarkers for distinguishing NMOSD from MOGAD and are associated with the blood-brain-barrier disruption in NMOSD. *Front Immunol* (2022) 13:853891. doi: 10.3389/fimmu.2022.853891

24. Akaishi T, Takahashi T, Misu T, Kaneko K, Takai Y, Nishiyama S, et al. Difference in the source of anti-AQP4-igG and anti-MOG-igG antibodies in CSF in patients with neuromyelitis optica spectrum disorder. *Neurology* (2021) 97(1):e1–e12. doi: 10.1212/WNL.0000000000012175

25. Wang CJ, Pang CY, Huan Y, Cheng YF, Wang H, Deng BB, et al. Monocyte-to-lymphocyte ratio affects prognosis in LAA-type stroke patients. *Heliyon* (2022) 8(10): e10948. doi: 10.1016/j.heliyon.2022.e10948

26. Iwamoto S, Itokazu T, Sasaki A, Kataoka H, Tanaka S, Hirata T, et al. RGMa signal in macrophages induces neutrophil-related astrocytopathy in NMO. *Ann Neurol* (2022) 91(4):532–47. doi: 10.1002/ana.26327

27. Murata H, Kinoshita M, Yasumizu Y, Motooka D, Beppu S, Shiraishi N, et al. Cell-free DNA derived from neutrophils triggers type 1 interferon signature in neuromyelitis optica spectrum disorder. *Neurol - Neuroimmunology Neuroinflammation* (2022) 9(3):e1149. doi: 10.1212/NXI.0000000000001149

28. Schroeder-Castagno M, Del R-SA, Wilhelm A, Romero-Suarez S, Schindler P, Alvarez-Gonzalez C, et al. Impaired response of blood neutrophils to cell-death stimulus differentiates AQP4-IgG-seropositive NMOSD from MOGAD. *J Neuroinflammation* (2022) 19(1):239. doi: 10.1186/s12974-022-02600-0

29. Winkler A, Wrzos C, Haberl M, Weil M-T, Gao M, Möbius W, et al. Blood-brain barrier resealing in neuromyelitis optica occurs independently of astrocyte regeneration. *J Clin Invest* (2021) 5:131. doi: 10.1172/JCI141694

30. Misu T, Höftberger R, Fujihara K, Wimmer I, Takai Y, Nishiyama S, et al. Presence of six different lesion types suggests diverse mechanisms of tissue injury in neuromyelitis optica. *Acta neuropathologica* (2013) 125(6):815–27. doi: 10.1007/s00401-013-1116-7

frontiers | Frontiers in Neurology

TYPE Original Research
PUBLISHED 26 January 2024
DOI 10.3389/fneur.2024.1308498

OPEN ACCESS

EDITED BY
Cong-Cong Wang,
Shandong Provincial Qianfoshan Hospital, China

REVIEWED BY
Ruth Schneider,
St. Josef Hospital, Germany
Tingjun Chen,
Mayo Clinic, United States
Yuanqi Zhao,
Guangzhou University of Chinese Medicine, China

*CORRESPONDENCE
Claudia Chien
✉ claudia.chien@charite.de

†These authors have contributed equally to this work and share first authorship

RECEIVED 06 October 2023
ACCEPTED 02 January 2024
PUBLISHED 26 January 2024

CITATION
Asseyer S, Zmira O, Busse L, Pflantzer B, Schindler P, Schmitz-Hübsch T, Paul F and Chien C (2024) Regional spinal cord volumes and pain profiles in AQP4-IgG + NMOSD and MOGAD.
Front. Neurol. 15:1308498.
doi: 10.3389/fneur.2024.1308498

Regional spinal cord volumes and pain profiles in AQP4-IgG + NMOSD and MOGAD

Susanna Asseyer[1,2,3†], Ofir Zmira[1,2,4,5†], Laura Busse[1], Barak Pflantzer[4,5], Patrick Schindler[1,2,3], Tanja Schmitz-Hübsch[1,2,3], Friedemann Paul[1,2,3] and Claudia Chien[1,2,6*]

[1]Charité–Universitätsmedizin Berlin, corporate member of Freie Universität Berlin-Universität zu Berlin and Max Delbrück Center for Molecular Medicine in the Helmholtz Association, Experimental and Clinical Research Center, Humboldt, Germany, [2]Charité–Universitätsmedizin Berlin, corporate member of Freie Universität Berlin-Universität zu Berlin, Neuroscience Clinical Research Center, Humboldt, Germany, [3]Department of Neurology, Charité–Universitätsmedizin Berlin, corporate member of Freie Universität Berlin and Humboldt-Universität zu Berlin, Berlin, Germany, [4]Department of Neurology, Sheba Medical Center, Ramat Gan, Tel Hashomer, Israel, [5]Department of Neurology and Neurosurgery, Sackler Faculty of Medicine, Tel Aviv University, Tel Aviv, Israel, [6]Department for Psychiatry and Psychotherapy, Charité–Universitätsmedizin Berlin, corporate member of Freie Universität Berlin, Humboldt-Universität zu Berlin, Berlin, Germany

Objective: Aquaporin-4-antibody-seropositive (AQP4-IgG+) Neuromyelitis Optica Spectrum Disorder (NMOSD) and Myelin Oligodendrocyte Glycoprotein Antibody-Associated Disorder (MOGAD) are relapsing neuroinflammatory diseases, frequently leading to chronic pain. In both diseases, the spinal cord (SC) is often affected by myelitis attacks. We hypothesized that regional SC volumes differ between AQP4-IgG + NMOSD and MOGAD and that pain intensity is associated with lower SC volumes. To evaluate changes in the SC white matter (WM), gray matter (GM), and pain intensity in patients with recent relapses (myelitis or optic neuritis), we further profiled phenotypes in a case series with longitudinal imaging and clinical data.

Methods: Cross-sectional data from 36 participants were analyzed in this retrospective study, including 20 AQP4-IgG + NMOSD and 16 MOGAD patients. Pain assessment was performed in all patients by the Brief Pain Inventory and painDETECT questionnaires. Segmentation of SC WM, GM, cervical cord volumes (combined volume of WM + GM) was performed at the C2/C3 cervical level. WM% and GM% were calculated using the cervical cord volume as a whole per patient. The presence of pain, pain severity, and clinical disability was evaluated and tested for associations with SC segmentations. Additionally, longitudinal data were deeply profiled in a case series of four patients with attacks between two MRI visits within one year.

Results: In AQP4-IgG + NMOSD, cervical cord volume was associated with mean pain severity within 24 h ($\beta = -0.62$, $p = 0.009$) and with daily life pain interference ($\beta = -0.56$, $p = 0.010$). Cross-sectional analysis showed no statistically significant SC volume differences between AQP4-IgG + NMOSD and MOGAD. However, in AQP4-IgG + NMOSD, SC WM% tended to be lower with increasing time from the last attack ($\beta = -0.41$, $p = 0.096$). This tendency was not observed in MOGAD. Our case series including two AQP4-IgG + NMOSD patients revealed SC GM% increased by roughly 2% with either a myelitis or optic neuritis attack between visits. Meanwhile, GM% decreased by 1–2% in two MOGAD patients with a myelitis attack between MRI visits.

Conclusion: In AQP4-IgG + NMOSD, lower cervical cord volume was associated with increased pain. Furthermore, cord GM changes were detected between MRI visits in patients with disease-related attacks in both groups. Regional SC MRI measures are pertinent for monitoring disease-related cord pathology in AQP4-IgG + NMOSD and MOGAD.

KEYWORDS

AQP4-IgG, MOG-IgG, NMOSD, MOGAD, spinal cord, pain, MRI

1 Introduction

Neuromyelitis optica spectrum disorders (NMOSD) are severe and relapsing inflammatory diseases of the central nervous system (CNS). Attacks occur mainly in the spinal cord (SC) and optic nerves and lead to persistent damage; however, diencephalon and cerebral attacks are also well described (1, 2). Pathogenic serum IgG antibodies against aquaporin-4 (AQP4-IgG) can be detected in ~70% of NMOSD patients (3).

Myelin oligodendrocyte glycoprotein (MOG) antibody-associated disorder (MOGAD) is a different disease entity that also affects the CNS with symptoms of optic neuritis, myelitis, and/or encephalomyelitis (4).

MOGAD and AQP4-IgG-seropositive (AQP4-IgG+) NMOSD have distinct pathogenesis. While AQP4-IgG + NMOSD causes complement activation resulting in astrocytic death, pathological specimens from MOGAD are more similar to demyelination in MS, with T-cells and macrophages found around blood vessels and with relative preservation of oligodendrocytes (5, 6).

Spinal cord affection by myelitis, in the form of longitudinally extensive transverse myelitis (LETM) or shorter lesions, occurs in both diseases (5). Chronic LETM/myelon lesions can cause SC atrophy and have been found to be significantly more prevalent in AQP4-IgG + NMOSD than in MOGAD (7). Meanwhile, multiple locations (≥2) of SC and SC gray matter (GM) hyperintense lesions (H-sign) are presented more often in MOGAD patients (8). AQP4-IgG + NMOSD patients have been shown to have reduced GM cord volumes localized to lesion regions, whereas MOGAD patients had reduced GM cord volumes only when lesions were not resolved (9).

Clinically, patients with LETM typically present with paresis, sensory deficits, bowel, and bladder disturbances, and intense neuropathic pain (10–13). However, myelitis is only one of many triggers causing pain in NMOSD and MOGAD. Pain syndromes in NMOSD and MOGAD comprise headache, neuropathic pain, and musculoskeletal pain, including spasticity, painful tonic spasms, and back pain (14). Especially, in AQP4-IgG + NMOSD, pain is frequently chronic over the disease course and is one of the most disabling symptoms in over 80% of the patients (13, 15). Chronic pain is less prevalent in MOGAD (14), which may be linked to better recovery of acute lesions. Currently, it is unclear if non-myelitis attacks affect the SC or if myelitis attacks affect other CNS regions (16, 17), and also if subclinical affection relates to the pain experienced by patients.

This study aims to investigate the relationship between cervical SC volumes as well as white matter (WM) percentages and pain intensity in AQP4-IgG+NMOSD and MOGAD.

We hypothesized that different SC regional measures, in particular, WM percentages, between MOGAD and AQP4-IgG + NMOSD, will be observed.

We further aimed to profile in detail, SC magnetic resonance imaging (MRI), pain, and clinical data collected from subjects with relapses in between two consecutive visits as a case series in the two disease groups.

2 Methods

2.1 Participants

Cross-sectional data from 51 participants from an ongoing observational study in NMOSD and MOGAD (Experimental and Clinical Research Center, Charite—Universitätsmedizin Berlin) were screened for inclusion. Inclusion criteria were a minimum age of 18 years and seropositivity for antibodies against AQP4 in a fixed cell-based assay or MOG in a live cell-based assay at any time during the disease, along with the availability of SC MRI. Patients who were seronegative for AQP4-IgG and MOG-IgG or did not receive SC MRI were excluded. A total of 39 patients fulfilled the inclusion criteria. Twenty-three patients had a diagnosis of AQP4-IgG + NMOSD according to the international consensus diagnostic criteria for NMOSD 2015 (18). Due to MRI quality issues (motion artifacts), four AQP4-IgG + NMOSD participants were removed from the cohort. Fifteen subjects had a diagnosis of MOGAD according to the new MOGAD criteria (4). One subject with low-positive MOG-IgG titer (AQP4-IgG negative) and recurrent ON did not fulfill the MOGAD criteria by Banwell et al. but was included in the study as part of the MOGAD group. In our cross-sectional analysis, 20 AQP4-IgG + NMOSD and 16 MOGAD patients with previous disease-related attacks were included. Previous attacks consisted of myelitis, optic neuritis, brainstem attacks, and cerebral syndrome. Disease duration was calculated from the first clinical symptom to the MRI visit date.

Longitudinal data were available from four patients with additional attacks between two MRI visits, performed within one year. Phenotypes were described in detail to evaluate changes in the SC GM and WM percentages and pain in subjects with recent relapses, outside the acute stage. For this study, the "baseline" visit of each patient refers to the date when the first SC MRI was available.

2.2 Standard protocol approvals, registrations, and patient consent

The study was approved by the local ethics committee (EA1/131/09) and was conducted in accordance with the Declaration of Helsinki in its currently applicable version and specific German laws. All participants provided written informed consent.

2.3 Pain and disability assessment

A central characteristic of pain is that pain is identified from the first-person perspective. This is reflected in the current definition of pain by the International Association for the Study of Pain (IASP) as a sensory and emotional experience, giving epistemic authority to the person who qualifies their experience as pain.[1]

The Brief Pain Inventory (BPI) and the painDETECT Questionnaire (PDQ) were used to assess pain in general (BPI) and neuropathic pain (PDQ) (19–21). The BPI assesses the presence of pain, other than everyday kinds of pain such as minor headaches. It does not provide information on the type or origin of pain. It rates the average pain intensity experienced in the last 24 h as a mean of four subscales with an assessment of worst, least, average, and current by using numeric scales from 0 ("no pain") to 10 ("pain as bad as you can imagine"). Furthermore, the BPI assesses seven domains of pain-related interference with daily life, including general activity, mood, walking ability, working ability, relations with other people, sleep, and enjoyment of life by using numeric scales from 0 to 10. A pain interference score is built as a mean of the seven subscales. Higher scores indicate worse health. The BPI reflects the current burden of pain on a person's life.

The PDQ is designed to differentiate between nociceptive and neuropathic pain. PDQ scores ranging from 0 to 12 indicate nociceptive pain, scores from 13 to 18 indicate possible neuropathic pain, and scores from 19 to 35 indicate definite neuropathic pain. The PDQ allows for rating of average pain intensity in the last 4 weeks prior to the clinical visit by using a single numeric scale of 0–10.

Clinical disability was evaluated using the expanded disability status scale (EDSS) (22, 23), and we included sensory and pyramidal functional system scores as separate indicators for possible SC-related disability. The timed 25-foot walk (T25FW) and 9-hole peg tests (9HPT) performance scores (22, 24) were calculated by averaging the results from each repeat run. For T25FW, both forward and return runs were averaged, while for 9HPT, all runs—two per hand—were summed together and averaged.

2.4 MRI acquisition

Magnetic resonance imaging scans were performed on two 3-Tesla (Siemens MAGNETOM Trio Tim and Prisma, Erlangen, Germany) scanner models. The Trio MRI (Scanner 1) protocol included (1) a T1-weighted 3D magnetization prepared rapid gradient echo (MPRAGE) cerebral MRI [1 mm isotropic resolution, repetition time (TR) = 1,900 ms, time to echo (TE) = 3.03 ms], including the upper cervical cord; (2) a 2D-sagittal T2-weighted SC sequence (slice thickness = 2 mm, TR = 3,500 ms, TE = 101 ms, in-plane resolution = 0.91 mm × 0.91 mm) at the cervicothoracic and lumbar levels of the SC; and (3) a 2D phase-sensitive inversion recovery (PSIR) sequence (slice thickness = 5 mm, TR = 930 ms, TE = 3.22 ms, TI = 400 ms, in-plane resolution = 0.78mm × 0.78 mm) at the cervical C2-C3 intervertebral space level. The Prisma MRI (Scanner 2) protocol included (1) a T1-weighted 3D MPRAGE cerebral MRI (0.8 mm isotropic resolution, TR = 2,500 ms, TE = 2.22 ms, TI = 1,000 ms), including the upper cervical cord; (2) a 2D-sagittal short T1 inversion recovery (STIR) SC sequence (slice thickness = 3 mm, TR = 3,700 ms, TE = 36 ms, TI = 220 ms, in-plane resolution = 0.81 mm × 0.81 mm) at the cervicothoracic and lumbar levels; and (3) a 2D PSIR sequence with same parameters as with the Trio. No patients were imaged in the acute disease/myelitis phase or were treated with steroids less than 2 months prior to MRI scanning.

2.5 Spinal cord lesion analysis

SC T2-hyperintense lesion location and length (measured as vertebral segments spanned, where half segments were rounded up to the next full length) were analyzed using SC MRIs as detailed in Chien et al. (7), using 2D T2-weighted or 2D STIR SC scans. All images were reviewed and evaluated by CC (who had 8 years of experience in SC MRI reading and research). Of note, each level of cord lesion was only counted once.

2.6 Spinal cord gray matter and white matter segmentation

The PSIR sequence has been previously shown to allow for robust segmentation of SC GM using both semi-and fully automated algorithms (25). Thus, for the evaluation of regional SC measures, PSIR sequences at the C2/C3 intervertebral level were collected. Fifty PSIR scans from AQP4-IgG + NMOSD, MOGAD, multiple sclerosis patients, and healthy participants were converted to NIFTI format, and WM and GM were manually segmented in the phase-sensitive image, with reference to the magnitude image when lesions in the cord occurred in the image slice using ITK-SNAP[2] (26). These WM and GM binary masks were used to train ($n = 35$ for training, $n = 15$ for validation) a deep learning, convolutional neural network (CNN) algorithm to automatically segment the phase-sensitive images of the PSIR scans with default training hyperparameters (27) to create a final model for use in our cohort PSIR scans. Segmented WM and GM and cervical cord (WM + GM) masks were then extracted for their volumes using fslstats,[3] and WM and GM volumes were converted to percentages by dividing by the cervical cord volume and multiplying by 100. In this study, "cervical cord

1 https://www.iasp-pain.org/

2 www.itksnap.org

3 https://fsl.fmrib.ox.ac.uk/fsl/fslwiki/Fslutils

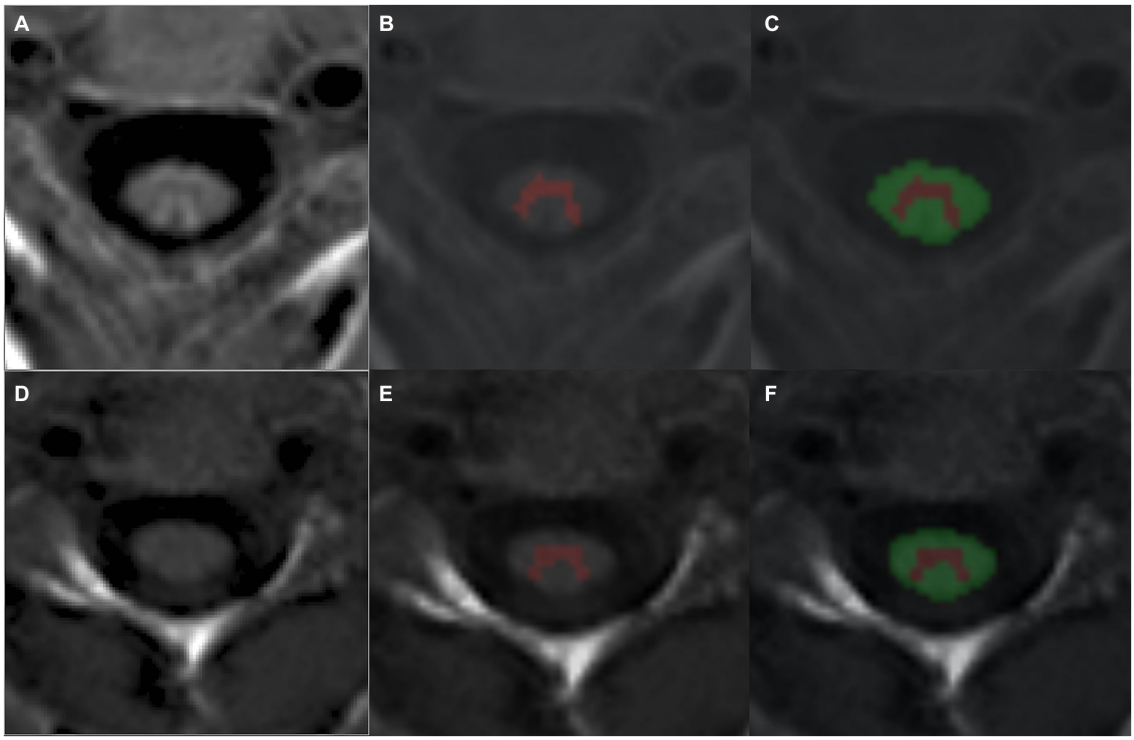

FIGURE 1
Representative segmentations of PSIR phase scans from an **(A–C)** AQP4-IgG + NMOSD and **(D–F)** a MOGAD patient using a trained CNN to automatically detect cervical cord GM **(B,E)** and WM **(C,F)**. AQP4-IgG + NMOSD, Aquaporin-4 antibody seropositive neuromyelitis optica spectrum disorders; WM, White matter; GM, Gray matter; MOGAD, Myelin oligodendrocyte associated disease.

volume" is defined as the combined WM and GM volume extracted from the PSIR scans. As mentioned above, four patients from the AQP4-IgG + NMOSD sub-group were removed from the cohort due to MRI quality issues (motion artifacts and/or poor image quality causing erroneous segmentation). Figure 1 shows representative automatic segmentations of PSIR scans from AQP4-IgG + NMOSD (Figures 1A–C) and MOGAD (Figures 1D–F) patients.

2.7 Mean upper cervical cord area analysis

All mean upper cervical cord area (MUCCA) (28) measurements were performed on 3D cerebral MPRAGE scans and blinded to patient antibody serostatus, as detailed in Chien et al. (29). Briefly, five consecutive slices, using the C2-C3 intervertebral space as a middle landmark, were segmented using JIM software (Version 7.0, http://www.xinapse.com/) and then averaged to obtain one mean cross-sectional area for each subject using an in-house python script. MUCCA was calculated in this cohort as a representative (gold-standard) total SC atrophy measure, as shown previously to be robust in AQP4-IgG + NMOSD patients (15).

2.8 Statistical analysis

Demographic values were compared between AQP4-IgG + NMOSD and MOGAD patients using appropriate parametric and non-parametric statistical tests as described in Table 1. Chi-squared tests were used to compare SC lesion load between patient groups. Multivariable linear regression models were applied to test associations of SC WM% and cervical cord volumes with clinical disability and pain measures, controlling for age, sex, and disease duration in each group. We chose to only perform all multivariable linear regression analyses using only the cervical cord volume and SC WM% metrics, since the SC GM% is relative to the WM%.

Cervical cord volume extracted from PSIR scans was compared with MUCCA (gold standard) using a Pearson's correlation test as an evaluation for the robustness of the automated SC segmentation in this cohort. Pearson's correlation test was used to analyze the association between GM and WM volumes, as well as GM% and WM% with cervical cord volume in both patient groups.

Comparison within and between group SC WM%, GM%, and cervical cord volume were performed using Welch two-sample *t*-tests and effect sizes were evaluated using Cohen's *d*, which were also applied to compare these SC metrics in patients with and without pain.

Multivariable linear regression modeling in each patient group to investigate associations between time since the last clinical attack with SC WM% and cervical cord volumes included age and sex as covariates.

In all tests, a value of p of <0.05 was considered statistically significant. All data were analyzed and graphs were created using R.[4] The longitudinal case series data were presented without statistical analysis due to the small sample size ($n = 4$).

4 https://www.r-project.org/

TABLE 1 Demographics of the study cohort.

	AQP4-IgG+ NMOSD ($n = 20$)	MOGAD ($n = 16$)	Test statistics
Age (years), Mean ± SD	49.5 ± 14.4	45.3 ± 16.9	$\chi^2 = 36$, $p = 0.33$
F:M, *n* (%)	19:1 (95:5)	11:5 (69:31)	$\chi^2 = 4.41$, $\mathbf{p = 0.04}$
Disease duration (years), mean (range)	9.12 (1–28.9)	9.97 (0.2–42.6)	$t = -0.26$, $p = 0.79$
Number of subjects with a history of clinical myelitis, *n* (%)	17 (85%)	8 (50%)	$\chi^2 = 5.13$, $p = 0.023$[b]
Number of myelitis attacks, median (range)	1 (0–4)	0.5 (0–3)	$\chi^2 = 6.51$, $p = 0.16$
Time since last attack (years), mean (range)	6.56 (1–16.61)	5.08 (0.15–39.6)	$t = -0.6$, $p = 0.56$
Time since last myelitis attack (years), mean (range)	7.41 (1–15.98)	5.09 (1.46–12.77)	$t = 0.814$, $p = 0.43$
MUCCA (mm^2), mean ± SD	68.54 ± 6.81	71.52 ± 9.69	$t = -1.04$, $p = 0.307$
Cervical cord volume (mL), mean ± SD	0.41 ± 0.04	0.44 ± 0.05	$t = -1.83$, $p = 0.076$
Cord WM percent (%), mean ± SD	80.70 ± 2.21	81.04 ± 1.77	$t = -0.50$, $p = 0.618$
Cord GM percent (%), mean ± SD	19.19 ± 2.17	18.88 ± 1.76	$t = 0.47$, $p = 0.644$
EDSS, median (range)	3.5 (0–6.5)	2.5 (0–4)	$\mathbf{t = 2.12, p = 0.04}$
25-foot walk speed (m/s), mean ± SD	1.65 ± 1.06	1.15 ± 0.2	$t = 2.03$, $p = 0.056$
9HPT performance dominant hand (s), mean ± SD	20.97 ± 3.98	22.09 ± 3.73	$t = -0.86$, $p = 0.4$
9HPT performance non-dominant hand (s), mean ± SD	42.92 ± 10.73	44.35 ± 5.09	$t = -5.3$, $p = 0.63$
Number of patients with pain (BPI), *n* (%)	14 (65%)	10 (62.5%)	$\chi^2 = 0.23$, $p = 0.64$
Average pain intensity within 24 h in pain patients (BPI), mean (range)	2.07 (0–6.25)	1.45 (0–5.25)	$t = 0.88$, $p = 0.38$
Number of patients with neuropathic pain, *n* (%)	8 (40%)	2 (12.5%)	n.a.
Average neuropathic pain intensity within 4 weeks (in neuropathic pain patients), mean (range)	5.5 (0–8)	4.33 (0–7)	n.a.

AQP4-IgG + NMOSD, Aquaporin-4 antibody seropositive neuromyelitis optica spectrum disorders; WM, White matter; GM, Gray matter; EDSS, Expanded disability status scale; MOGAD, Myelin oligodendrocyte associated disease; *n*, number; 9HPT, 9-Hole peg test; χ^2, Chi-squared; and *t*, *t*-statistic. Bold text indicates statistical significance.

3 Results

3.1 Cohort demographics

Demographics of AQP4-IgG + NMOSD and MOGAD patients in this cohort are shown in Table 1.

Fourteen subjects with AQP4-IgG + NMOSD and 10 subjects with MOGAD experienced pain, other than everyday kinds of minor pain at the time of assessment. Eight subjects with AQP4-IgG + NMOSD and two subjects with MOGAD fulfilled the criteria for neuropathic pain. Pain courses comprised persistent pain with slight fluctuations ($n = 3$), persistent pain with pain attacks ($n = 4$), and pain attacks without pain between them ($n = 3$). The pain was located on one or several parts of the body, including legs ($n = 10$), trunk ($n = 9$), feet ($n = 4$), hip/bottom ($n = 3$), hands ($n = 2$), arms ($n = 1$), and head ($n = 1$). The pain was described to be electric-like ($n = 9$), tingling ($n = 9$), burning ($n = 6$), associated with mechanical ($n = 8$) and thermal ($n = 8$) allodynia, and/or in an area of numbness ($n = 9$).

Table 2 provides a summary of the SC lesion count and spinal cord levels affected in each patient group.

3.2 Cervical cord volume and WM percentage associations with pain and disability measurements

In AQP4-IgG + NMOSD, the cervical cord volume was associated with mean pain severity within 24 h. The lower the cervical cord volume, the higher the pain intensity (Table 3).

Neither WM% or GM% differed in AQP4-IgG + NMOSD patients with and without pain (WM%: $t = -0.18$, $p = 0.862$, Cohen's $d = -0.09$, GM%: $t = 0.16$, $p = 0.873$, Cohen's $d = 0.08$). In MOGAD, both cervical cord volume and WM% did not differ between patients with and without pain (cervical cord volume: $t = -0.55$, $p = 0.605$, Cohen's $d = -0.37$; WM%: $t = -0.42$, $p = 0.680$, Cohen's $d = -0.21$; GM%: $t = 0.43$, $p = 0.677$, Cohen's $d = 0.21$). There was a difference in cervical cord volumes between AQP4-IgG + NMOSD patients with pain vs. those without ($t = -2.3$, $p = 0.042$, Cohen's $d = -1.2$), where patients with pain had on average lower cervical cord volumes than those without pain.

Figure 2 illustrates the associations found between BPI pain severity and intensity vs. cervical cord volume in AQP4-IgG + NMOSD patients.

No significant associations were found between cervical cord volume and SC WM percentage with pain metrics, EDSS, or the sensory and pyramidal functional systems scores (Table 4).

No associations were found between cervical cord volume or SC WM% and 9HPT test times or T25FW speed (shown in Supplementary Table 1).

3.3 Cervical cord volume in relation to MUCCA and WM, GM volumes, and percentages

To check the segmentation of SC regions using the CNN algorithm, we tested the cervical cord volume against MUCCA, the gold standard in SC atrophy measures (28), in the whole cohort. To

TABLE 2 Patients with T2-hyperintense spinal cord lesions counts and levels of injury.

	AQP4-IgG + NMOSD ($n = 20$)	MOGAD ($n = 16$)	Test statistics
Spinal cord lesions, *n* (%)	10 (50%)	6 (37.5%)	$\chi^2 = 0.56$, $p = 0.45$
Cervical cord lesions (Dens–C7), *n* (%)	6 (30%)	4 (25%)	$\chi^2 = 0.11$, $p = 0.74$
Cervico-thoracic lesions, *n* (%)	2 (10%)	1 (6.25%)	$\chi^2 = 0.16$, $p = 0.69$
Thoracic cord lesions, *n* (%)	2 (10%)	1 (6.25%)	$\chi^2 = 0.16$, $p = 0.69$
History of myelitis, *n* (%)	17 (85%)	8 (50%)	**$\chi^2 = 5.13$, $p = 0.02$**

AQP4-IgG+, Aquaporin-4 antibody seropositive; NMOSD, Neuromyelitis optica spectrum disorders; MOG-IgG+, Myelin oligodendrocyte glycoprotein antibody; χ^2, Chi-square; *n*, Number. Bold text indicates statistical significance.

TABLE 3 SC cervical cord volume and WM percentage associations with pain severity and interference within the previous 24 h of assessment.

Cervical cord volume		
	AQP4-IgG + NMOSD	MOGAD
Mean pain severity within 24 h	**ß = −0.62, p = 0.009**	ß = 0.12, $p = 0.707$
Mean pain interference within 24 h	**ß = −0.56, p = 0.010**	ß = 0.04, $p = 0.896$
SC WM percentage		
	AQP4-IgG+NMOSD	MOGAD
Mean pain severity within 24 h	ß = −0.26, $p = 0.323$	ß = 0, $p = 0.996$
Mean pain interference within 24 h	ß = −0.34, $p = 0.157$	ß = −0.05, $p = 0.871$

AQP4-IgG + NMOSD, Aquaporin-4 antibody seropositive neuromyelitis optica spectrum disorders; MOGAD, Myelin oligodendrocyte antibody associated disease; and WM, White matter. Bold text indicates statistical significance ($p < 0.05$).

evaluate the contributions of GM and WM volumes and percentages from each group at the C2/C3 level to the cervical cord volume, we similarly conducted Pearson's correction tests (Supplementary Figure 1).

The cervical cord volume and MUCCA were strongly associated ($R = 0.51$, $p = 0.0015$). Interestingly, the cord GM volume was highly associated with cervical cord volume in MOGAD, while there was slightly less contribution of the GM volume to the PSIR cervical cord volume in AQP4-IgG + NMOSD patients ($R = 0.69$, $p = 0.0033$ and $R = 0.53$, $p = 0.015$, respectively; Supplementary Figure 1B). Cord WM volume was highly associated with cervical cord volume in both cohorts (AQP4-IgG + NMOSD: $R = 0.98$, $p = 2e{-}13$ and MOGAD: $R = 0.99$, $p = 3.9e{-}12$; Supplementary Figure 1C). Our analysis revealed similar non-significant trends with AQP4-IgG + NMOSD and MOGAD GM% decreasing, with larger cervical cord volumes. The opposite trend was also seen in the WM% vs. cervical cord volume in both disease groups (Supplementary Figures 1D,E).

3.4 Cervical cord volume, GM, and WM percentage comparisons between patient groups

No significant differences in cervical cord volume or WM% were found between AQP4-IgG + NMOSD or MOGAD at the C2/C3 level of the cord ($t = -1.84$, $p = 0.076$, Cohen's $d = -0.626$; $t = -0.503$, $p = 0.618$, Cohen's $d = -0.165$; respectively). There was also no difference found between group SC GM% ($t = 0.47$, $p = 0.644$, Cohen's $d = -0.621$). However, it was observed that both patient groups with a history of myelitis attacks showed a general (but not significant) decrease in both cervical cord volume and SC WM percentage compared to patients without myelitis attacks within each group (Figure 3). As a consequence of GM% being complementary to the WM%, in both groups, there was a slight, non-significant increase in SC GM% in patients with a history of myelitis attacks (data not shown). From Figure 3, it can be seen that 71% (12 of 17) of AQP4-IgG + NMOSD and 88% (7 of 8) of MOGAD patients with a history of myelitis attacks reported current pain. Meanwhile, 47% (8 of 17) of AQP4-IgG + NMOSD and only 13% (1 of 8) of MOGAD patients with previous myelitis reported neuropathic pain. Thus, we did not test associations of neuropathic pain with SC measures further in the MOGAD patients.

3.5 Time since last attack, SC cervical volume, and WM percentage

No associations were found when evaluating cervical cord volume (AQP4-IgG + NMOSD: $\beta = 0.20$, $p = 0.419$; MOGAD: $\beta = -0.23$, $p = 0.438$), and time passed since the last clinical symptom of any type. In AQP4-IgG + NMOSD, we observed some SC WM% decreased over time after an attack ($\beta = -0.41$, $p = 0.096$). In MOGAD, this trend was not observed ($\beta = -0.16$, $p = 0.570$).

3.6 Longitudinal case series of patients with additional attacks between follow-up visits

Out of the 35 patients included in this study, four patients with longitudinal clinical and MRI data were found to have an additional attack between visits. Supplementary Table 2 shows an in-depth qualitative assessment of these patients in relation to their attack history, prevalence of pain, and SC MRI findings.

Subject 1 (AQP4-IgG + NMOSD) experienced an optic neuritis attack 1 month prior to the second SC scan (two optic neuritis attacks in total between visits). This patient showed an increased GM% in the cord of approximately 2% (from 0.079 to 0.091 mL) at follow-up, with an increase in cervical cord volume (from 0.38 to 0.40 mL) and

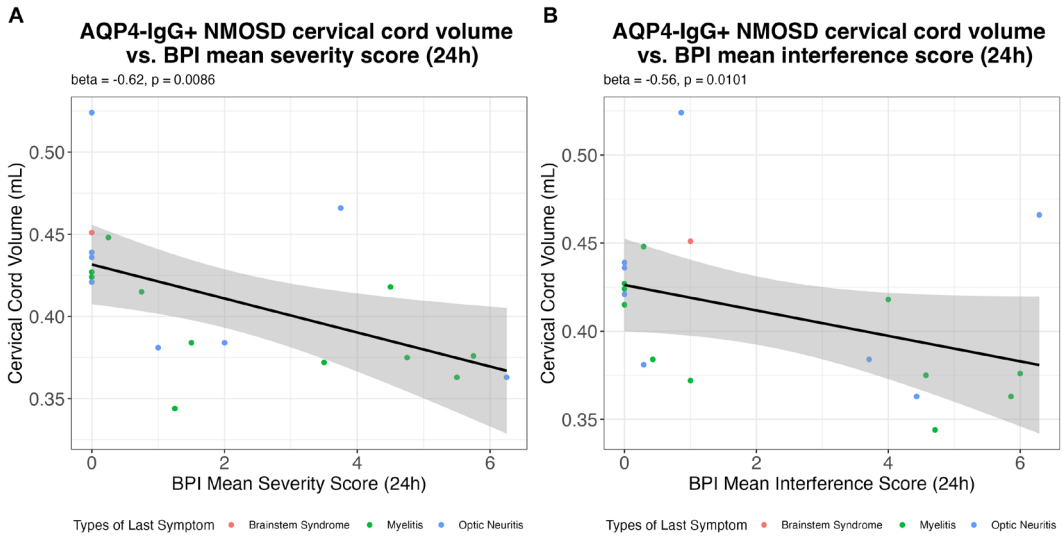

FIGURE 2
The association of the **(A)** BPI mean pain severity score; and **(B)** BPI mean interference score in the previous 24 h with cervical cord volume (mL) in AQP4-IgG + NMOSD. AQP4-IgG + NMOSD, Aquaporin-4 antibody seropositive neuromyelitis optica spectrum disorders; BPI, Brief pain inventory.

TABLE 4 Cervical cord volume and SC WM percentage associations with clinical disability.

Cervical cord volume		
	AQP4-IgG + NMOSD	MOGAD
EDSS	$\beta = 0.14$, $p = 0.516$	$\beta = -0.31$, $p = 0.242$
Sensory EDSS	$\beta = -0.26$, $p = 0.307$	$\beta = -0.41$, $p = 0.149$
Pyramidal EDSS	$\beta = -0.24$, $p = 0.166$	$\beta = -0.30$, $p = 0.296$
SC WM percentage		
	AQP4-IgG+NMOSD	MOGAD
EDSS	$\beta = -0.07$, $p = 0.762$	$\beta = -0.36$, $p = 0.182$
Sensory EDSS	$\beta = -0.01$, $p = 0.973$	$\beta = -0.45$, $p = 0.112$
Pyramidal EDSS	$\beta = -0.23$, $p = 0.191$	$\beta = -0.21$, $p = 0.473$

AQP4-IgG + NMOSD, Aquaporin-4 antibody seropositive neuromyelitis optica spectrum disorders; EDSS, Expanded disability status scale; and MOGAD, Myelin oligodendrocyte associated disease.

relatively stable WM volume (0.302–0.308 mL). Interestingly, although pain intensity was stable in this patient, the pain location expanded from the feet to the legs and additionally to the head/neck during the second visit.

Subject 2 was also diagnosed with AQP4-IgG + NMOSD and experienced a myelitis attack 5 months prior to the follow-up visit. Again, GM% was increased by roughly 3% (from 0.070 to 0.079 mL), but with an associated 3% decrease in WM% (from 0.347 to 0.317 mL) and a decrease in cervical cord volume (from 0.42 to 0.40 mL). In this patient, the neuropathic pain score increased from baseline to follow-up.

Two MOGAD patients (Subjects 3 and 4) had a visit more than 6 months after a myelitis attack. Both subjects showed a GM% decrease of ~1–2% between the two visits, along with a decrease in the cervical cord volume. In both MOGAD patients, pain decreased over time.

4 Discussion

Spinal cord affection is a central issue in AQP4-IgG + NMOSD and MOGAD. Our study highlights regional SC affection in these diseases and its relation to pain intensity:

1 Higher mean pain severity and pain interference with daily-life activities in AQP4-IgG + NMOSD patients were significantly associated with decreased cervical cord volume at the C2-C3 cord level.
2 GM volume at the C2-C3 intervertebral level tended to contribute more to cervical cord volume in MOGAD than in AQP4-IgG + NMOSD patients.
3 WM percentage in AQP4-IgG + NMOSD patients tended to decrease after a myelitis attack (non-significant).
4 Two AQP4-IgG + NMOSD patients with clinical attacks between longitudinal follow-up visits showed an increase in GM% (2–3%), while two MOGAD patients showed a decrease in GM% (1–2%).

4.1 Association of pain intensity and cervical cord volume

Pain is one of the most disabling symptoms of AQP4-IgG + NMOSD patients and has a severe impact on the quality of life (13). Pain syndromes have various origins, comprising among others myelitis-mediated neuropathic pain, ON-related headaches, musculoskeletal pain, and spasticity-related pain (13). The origin of pain is often complex and difficult to determine and it is important to note that pain is always an individual experience, comprising sensory and emotional aspects. Unfortunately, structural pain assessment is frequently lacking in clinical practice and the investigation of associations between pain and structural disease

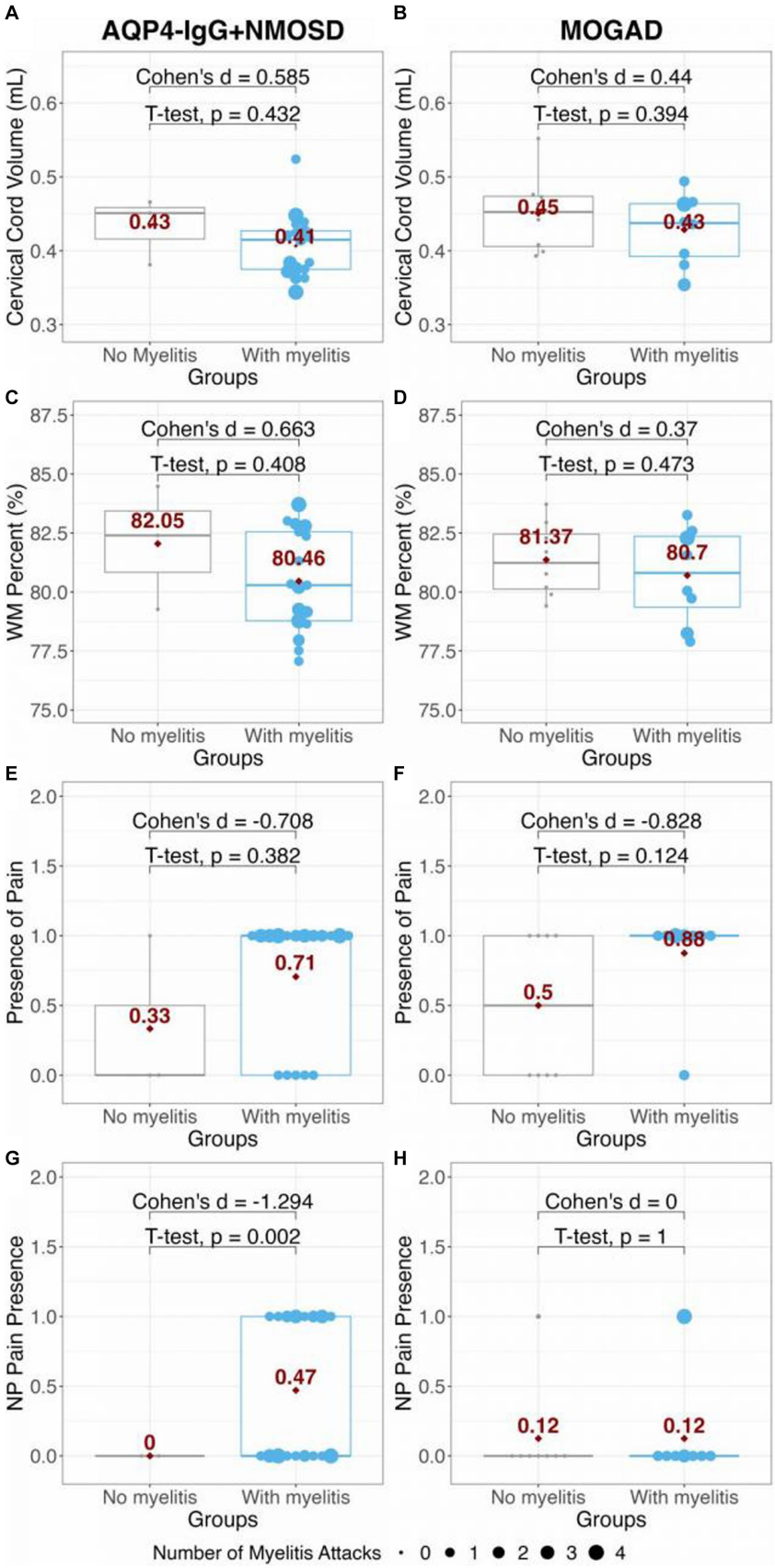

FIGURE 3
Comparison of panels **(A,B)** cervical cord volume; and **(C,D)** WM percent in AQP4-IgG + NMOSD and MOGAD patients. The presence of pain and presence of NP in AQP4-IgG + NMOSD and MOGAD patients are shown in panels **(E–H)**. The red dots and numbers indicate the mean values of each metric per group. AQP4-IgG + NMOSD, Aquaporin-4 antibody seropositive neuromyelitis optica spectrum disorders; MOGAD, Myelin oligodendrocyte associated disease; WM, White matter; and NP, Neuropathic pain.

markers is scarce. In our cohort, the examination of the interrelation between cervical cord volume on the cervical level and measurements of pain revealed a negative association with the mean pain severity and pain interference with daily-life activities in AQP4-IgG + NMOSD patients. These findings add to our previous study, showing an inverse correlation of the thalamic VPN volume with pain intensity in AQP4-IgG + NMOSD (30). An association between lower cervical cord volume and higher pain intensity through both damage of decussating fibers of the spinothalamic tract as previously described in MS (31) and through myelitis-related GM damage is conceivable (32, 33). Further exploration is needed to detect if attack-independent tissue damage (34) may contribute to SC atrophy (16, 17), and thus aggravate pain over time. Moreover, longitudinal pain assessment from disease onset is necessary to analyze pathogenic interrelations between the origin of pain and structural pathology. Consequently, pain assessment is necessary to rate disease-related disability beyond the EDSS (35) and to gain further insights into the disease mechanisms of AQP4-IgG + NMOSD.

No associations occurred between WM percentages and clinical pain measurements in AQP4-IgG + NMOSD patients and between SC cervical volume or WM percentage and clinical pain measurements in MOGAD patients. Our findings are consistent with the literature showing that MOGAD has a lower clinical myelitis incidence with a smaller chronic lesion burden (7) and a lower impact of chronic pain syndromes than AQP4-IgG + NMOSD (14). Larger study samples are needed to detect a potential association between pain and spinal cord affection in MOGAD.

In line with previous studies, overall clinical disability, as measured by EDSS, was higher in AQP4-IgG + NMOSD than in MOGAD patients (7, 9). However, this difference in general disability was not reflected in cross-sectional cervical cord volume and/or WM percentage in the cervical cord measured using PSIR scans. Furthermore, cervical cord volume and SC WM percentages were not associated with the EDSS, 9HPT, and T25FW in either patient group. Although our AQP4-IgG + NMOSD cohort had a higher EDSS at baseline compared to that of the MOGAD cohort, the effect of SC injury may not be well reflected in EDSS scores ≤4 (36).

4.2 Cervical GM and WM profiles in AQP4-IgG + NMOSD and MOGAD

MUCCA has previously been shown to reflect total cord volumes in AQP4-IgG + NMOSD (28). Our findings that the cervical cord volumes are highly correlated with MUCCA in the entire cohort indicate that our method is reliable for evaluation of SC changes in these diseases. When investigating WM and GM regional contributions to the cervical cord volume, we found that in both diseases, GM volume increased with increasing cervical cord volume. However, the AQP4-IgG + NMOSD patient cervical cord volumes were generally lower and this correlation analysis showed less contribution of the GM volume to the cervical cord volume than in MOGAD. The range of SC GM% measured in our entire cohort is similar to the 15–20% GM proportion found in a post-mortem study in healthy donor spines (37). Interestingly, the mean SC GM% of AQP4-IgG+ patients was higher than in MOGAD, although not statistically significant. Assuming that both diseases are associated with a reduced SC volume, these findings could indicate that WM pathology contributes to pain increase in NMOSD. Due to the small sample size, this theory remains speculative and should be investigated in a larger cohort.

4.3 Associations of SC metrics with clinical attacks

Generally, we observed that AQP4-IgG + NMOSD patients had lower cervical cord volumes than MOGAD, both without and with myelitis. When assessing how the last clinical attack(s) influences the SC, we observed that AQP4-IgG + NMOSD patients tended toward cord WM% decrease after any type of disease-related attack. These observations were cross-sectional and did not include MRIs close to an attack. Our observation could indicate continued SC WM degeneration after AQP4-IgG + NMOSD-related attacks (33), although this decrease in WM could be due to an increase in the GM% when the primary lesional site is located purely in the GM (38). SC GM has also been found to be about twice as stiff as SC WM, such that mechanical compression of the WM is much easier, especially in the axial plane (to which our PSIR sequence was oriented) (39). It stands to reason that GM inflammation, edema, or astrogliosis could cause this region to expand and effectively compress the WM in the SC. Thus, it may well be important to evaluate both GM and WM in relation to time since an acute attack for dynamic changes in the SC.

We did not restrict our analysis to only myelitis attacks as it is unclear how non-attack-related regions are affected by either disease. In one study, it has been found that SC and retinal measures are associated with multiple sclerosis, suggesting a whole CNS pathology may occur during the disease course (40). Furthermore, we have previously shown that combinations of attacks are associated with damage outside of the attack location (34). Thus, we included PSIR SC analysis in this study from patients who did not only have a myelitis attack, although myelitis does increase SC atrophy in these patients (7), which was also evident in our current findings.

4.4 Longitudinal case series

In one AQP4-IgG + NMOSD patient, SC GM% increase was evident after an optic neuritis attack with stable WM% and cervical cord volume, as well as stable pain intensity.

Meanwhile, in another AQP4-IgG + NMOSD patient, there was an emergence of neuropathic pain after a myelitis attack five months prior to the follow-up visit. This characteristic is conceivably linked to the SC GM% increase with WM% decrease and myelitis attack.

Since AQP4 is expressed on astrocytes, and AQP4-IgG has been shown to cause a complement-mediated injury of astrocytes and neurons, this injury could lead to astrogliosis and cellular hypertrophy in the GM (41). As a consequence, secondary WM damage could occur nearby (42). Thus, our observation of increased GM% in the SC in two AQP4-IgG + NMOSD patients indicates that systemic inflammatory mechanisms (43) may be at play in this disease, even when an attack occurs elsewhere in the CNS, e.g., in the optic nerves.

In both MOGAD patients, cervical cord volume and GM% were decreased with additional myelitis attacks, however pain was decreased. These observations are in line with a previous study, where GM volume was found to be decreased in MOGAD patients who had

resolved SC lesions compared to MOGAD patients without any lesions/myelitis attacks (9).

4.5 Limitations

The main limitation of our study is that our sample sizes are generally small and differ between AQP4-IgG + NMOSD and MOGAD patients. This limitation did not allow us to evaluate our data with true statistical equivalency and might have concealed significant findings in the trends we observed. Furthermore, the sample size restricted us from performing an extensive sub-analysis of subjects with myelitis as well as with respect to different pain syndromes. Future studies will benefit from including detailed pain information beyond questionnaire-based assessment. Still, we found a negative association between pain intensity and SC cervical cord volume in AQP4-IgG + NMOSD. Of note, our data do not give any information about the origin of pain and the pain duration. We therefore cannot show a causal relationship between the origin of pain and the SC volume.

Another limitation is the cross-sectional and non-acute design of this study, which did not allow for measurements of SC WM/GM changes over time. Furthermore, our longitudinal case series does not allow for definite pathogenic conclusions. However, we were able to detail qualitative and quantitative phenotypes of clinical and imaging metrics from four subjects with clinical attacks within one year. Future studies with MRI scans acute to a disease-related attack, larger sample sizes, and longitudinal follow-ups are required to investigate our hypotheses further.

Furthermore, our study lacks a SC imaging dataset from healthy controls. Our findings that the cervical cord volumes extracted from our PSIR sequence are highly associated with MUCCA, the gold standard in evaluating SC atrophy in NMOSD (28), however indicate that the regional SC metrics we extracted are reliable. Moreover, it has previously been shown that MUCCA is decreased in NMOSD, but not in MOGAD compared to healthy controls (7). Similarly, our study provides indications of generally lower cervical cord volumes in AQP4-IgG + NMOSD patients with and without myelitis compared with MOGAD. Future inclusion of healthy participant PSIR-extracted WM and GM SC volumes would benefit evaluations of attack-related damage to different SC regions in these two rare diseases and the collection of this MRI sequence is warranted.

5 Conclusion

Our study shows that in AQP4-IgG + NMOSD, lower SC volume was associated with increased pain intensity. This finding highlights the relevance of thorough pain workup and MRI monitoring during the disease course. Clinically feasible 2D PSIR MRIs at the C2/C3 intervertebral SC level can be reliably segmented using an automated CNN algorithm, even in a longitudinal setting. Interestingly, our MRI results indicate a different affection of GM volumes relative to SC volume between the two disease entities based both on the cross-sectional data and longitudinal data. Larger studies in both diseases with longitudinal and acute monitoring to evaluate if patients show true atrophy and pain symptom evolution, even without additional myelitis attacks are required.

Data availability statement

The raw data supporting the conclusions of this article will be made available by the authors, without undue reservation.

Ethics statement

The studies involving humans were approved by Charité's Ethics Committee, Charité Universitätsmedizin, Berlin, Germany. The studies were conducted in accordance with the local legislation and institutional requirements. The participants provided their written informed consent to participate in this study.

Author contributions

SA: Conceptualization, Data curation, Investigation, Methodology, Project administration, Validation, Writing – original draft, Writing – review & editing. OZ: Writing – original draft, Writing – review & editing. LB: Formal Analysis, Writing – review & editing. BP: Formal Analysis, Writing – original draft, Writing – review & editing. PS: Data curation, Writing – review & editing. TS-H: Data curation, Writing – review & editing. FP: Conceptualization, Supervision, Writing – review & editing. CC: Conceptualization, Formal Analysis, Methodology, Project administration, Supervision, Validation, Writing – original draft, Writing – review & editing.

Funding

The author(s) declare financial support was received for the research, authorship, and/or publication of this article. Financial support was provided from the Open Access Publication Fund of Charité – Universitätsmedizin Berlin.

Acknowledgments

The authors would like to thank Susan Pikol, and Cynthia Kraut for their excellent technical support as well as Jana Bigall and the administrative office of NeuroCure Clinical Research Center (NCRC), funded by the Deutsche Forschungsgemeinschaft (DFG, German Research Foundation) under Germany's Excellence Strategy—EXC-2049—390688087 and Charité-BIH Clinical Study Center for their administrative support. Study data were collected and managed using REDCap electronic data capture tools hosted at Charité, NeuroCure Clinical Research Center (17, 34), and MRI data were collected at the Berlin Center for Advanced Neuroimaging (BCAN). The authors would also like to sincerely thank Nico Papinutto for giving us the PSIR sequence optimized for upper cervical cord MRI scanning on a Siemens scanner.

Conflict of interest

SA has received speaker honoraria from Alexion, Bayer, and Roche and a research grant from Novartis, unrelated to this publication. TS-H reports research grants form Celgene/bms, speaker honoraria from

Bayer. FP reports research grants and speaker honoraria from Bayer, Teva, Genzyme, Merck, Novartis, and MedImmune and is member of the steering committee of the OCTIMS study (Novartis), all unrelated to this work. CC has received research support from Novartis and Alexion and writing honoraria from the British Society for Immunology, as well as serves as a member of the Standing Committee on Science for the Canadian Institutes of Health Research (CIHR).

The remaining authors declare that the research was conducted in the absence of any commercial or financial relationships that could be construed as a potential conflict of interest.

Publisher's note

All claims expressed in this article are solely those of the authors and do not necessarily represent those of their affiliated organizations, or those of the publisher, the editors and the reviewers. Any product that may be evaluated in this article, or claim that may be made by its manufacturer, is not guaranteed or endorsed by the publisher.

Supplementary material

The Supplementary material for this article can be found online at: https://www.frontiersin.org/articles/10.3389/fneur.2024.1308498/full#supplementary-material

SUPPLEMENTARY FIGURE 1
Association of MUCCA with **(A)** total cord volume. Associations of cervical cord volume with **(B)** cord GM volume, **(C)** cord WM volume, **(D)** cord GM percent, and **(E)** cord WM percent extracted from segmented PSIR images at the C2/C3 level. AQP4-IgG+NMOSD, Aquaporin-4 antibody seropositive neuromyelitis optica spectrum disorders; MOGAD, Myelin oligodendrocyte associated disease; MUCCA, Mean upper cervical cord area.

References

1. Kim HJ, Paul F, Lana-Peixoto MA, Tenembaum S, Asgari N, Palace J, et al. MRI characteristics of neuromyelitis optica spectrum disorder: an international update. *Neurology*. (2015) 84:1165–73. doi: 10.1212/WNL.0000000000001367

2. Carnero Contentti E, Okuda DT, Rojas JI, Chien C, Paul F, Alonso R. MRI to differentiate multiple sclerosis, neuromyelitis optica, and myelin oligodendrocyte glycoprotein antibody disease. *J Neuroimaging*. (2023) 33:688–702. doi: 10.1111/jon.13137

3. Mori M, Kuwabara S, Paul F. Worldwide prevalence of neuromyelitis optica spectrum disorders. *J Neurol Neurosurg Psychiatry*. (2018) 89:555–6. doi: 10.1136/jnnp-2017-317566

4. Banwell B, Bennett JL, Marignier R, Kim HJ, Brilot F, Flanagan EP, et al. Diagnosis of myelin oligodendrocyte glycoprotein antibody-associated disease: international MOGAD panel proposed criteria. *Lancet Neurol*. (2023) 22:268–82. doi: 10.1016/S1474-4422(22)00431-8

5. Mewes D, Kuchling J, Schindler P, Khalil AAA, Jarius S, Paul F, et al. Diagnostik der Neuromyelitis-optica-Spektrum-Erkrankung (NMOSD) und der MOG-Antikörper-assoziierten Erkrankung (MOGAD). *Klin Monatsbl Für Augenh*. (2022) 239:1315–24. doi: 10.1055/a-1918-1824

6. Zamvil SS, Slavin AJ. Does MOG Ig-positive AQP4-seronegative opticospinal inflammatory disease justify a diagnosis of NMO spectrum disorder? *Neurol Neuroimmunol Neuroinflammation*. (2015) 2:e62. doi: 10.1212/NXI.0000000000000062

7. Chien C, Scheel M, Schmitz-Hübsch T, Borisow N, Ruprecht K, Bellmann-Strobl J, et al. Spinal cord lesions and atrophy in NMOSD with AQP4-IgG and MOG-IgG associated autoimmunity. *Mult Scler Houndmills Basingstoke Engl*. (2019) 25:1926–36. doi: 10.1177/1352458518815596

8. Dubey D, Pittock SJ, Krecke KN, Morris PP, Sechi E, Zalewski NL, et al. Clinical, radiologic, and prognostic features of myelitis associated with myelin oligodendrocyte glycoprotein autoantibody. *JAMA Neurol*. (2019) 76:301–9. doi: 10.1001/jamaneurol.2018.4053

9. Mariano R, Messina S, Roca-Fernandez A, Leite MI, Kong Y, Palace JA. Quantitative spinal cord MRI in MOG-antibody disease, neuromyelitis optica and multiple sclerosis. *Brain*. (2021) 144:198–212. doi: 10.1093/brain/awaa347

10. Jurynczyk M, Messina S, Woodhall MR, Raza N, Everett R, Roca-Fernandez A, et al. Clinical presentation and prognosis in MOG-antibody disease: a UK study. *Brain J Neurol*. (2017) 140:3128–38. doi: 10.1093/brain/awx276

11. Pandit L, Asgari N, Apiwattanakul M, Palace J, Paul F, Leite M, et al. Demographic and clinical features of neuromyelitis optica: a review. *Mult Scler Houndmills Basingstoke Engl*. (2015) 21:845–53. doi: 10.1177/1352458515572406

12. Asseyer S, Schmidt F, Chien C, Scheel M, Ruprecht K, Bellmann-Strobl J, et al. Pain in AQP4-IgG-positive and MOG-IgG-positive neuromyelitis optica spectrum disorders. *Mult Scler J Exp Transl Clin*. (2018) 4:2055217318796684. doi: 10.1177/2055217318796684

13. Ayzenberg I, Richter D, Henke E, Asseyer S, Paul F, Trebst C, et al. Pain, depression, and quality of life in Neuromyelitis Optica Spectrum disorder: a cross-sectional study of 166 AQP4 antibody–seropositive patients. *Neurol Neuroimmunol Neuroinflammation*. (2021) 8:e985. doi: 10.1212/NXI.0000000000000985

14. Asseyer S, Cooper G, Paul F. Pain in NMOSD and MOGAD: a systematic literature review of pathophysiology, symptoms, and current treatment strategies. *Front Neurol*. (2020) 11:778. doi: 10.3389/fneur.2020.00778

15. Hümmert MW, Schöppe LM, Bellmann-Strobl J, Siebert N, Paul F, Duchow A, et al. Costs and health-related quality of life in patients with NMO Spectrum disorders and MOG-antibody–associated disease: CHANCENMO study. *Neurology*. (2022) 98:e1184–96. doi: 10.1212/WNL.0000000000200052

16. Ventura RE, Kister I, Chung S, Babb JS, Shepherd TM. Cervical spinal cord atrophy in NMOSD without a history of myelitis or MRI-visible lesions. *Neurol Neuroimmunol Neuroinflammation*. (2016) 3:e224. doi: 10.1212/NXI.0000000000000224

17. Macaron G, Ontaneda D. MOG-related disorders: a new cause of imaging-negative myelitis? *Mult Scler J*. (2020) 26:511–5. doi: 10.1177/1352458519840746

18. Wingerchuk DM, Banwell B, Bennett JL, Cabre P, Carroll W, Chitnis T, et al. International consensus diagnostic criteria for neuromyelitis optica spectrum disorders. *Neurology*. (2015) 85:177–89. doi: 10.1212/WNL.0000000000001729

19. Radbruch L, Loick G, Kiencke P, Lindena G, Sabatowski R, Grond S, et al. Validation of the German version of the brief pain inventory. *J Pain Symptom Manag*. (1999) 18:180–7. doi: 10.1016/s0885-3924(99)00064-0

20. Tan G, Jensen MP, Thornby JI, Shanti BF. Validation of the brief pain inventory for chronic nonmalignant pain. *J Pain*. (2004) 5:133–7. doi: 10.1016/j.jpain.2003.12.005

21. Freynhagen R, Baron R, Gockel U, Tölle TR. painDETECT: a new screening questionnaire to identify neuropathic components in patients with back pain. *Curr Med Res Opin*. (2006) 22:1911–20. doi: 10.1185/030079906X132488

22. Kurtzke JF. Rating neurologic impairment in multiple sclerosis: an expanded disability status scale (EDSS). *Neurology*. (1983) 33:1444–52. doi: 10.1212/wnl.33.11.1444

23. Kappos L, D'Souza M, Lechner-Scott J, Lienert C. On the origin of Neurostatus. *Mult Scler Relat Disord*. (2015) 4:182–5. doi: 10.1016/j.msard.2015.04.001

24. Feys P, Lamers I, Francis G, Benedict R, Phillips G, LaRocca N, et al. Multiple sclerosis outcome assessments consortium. The nine-hole peg test as a manual dexterity performance measure for multiple sclerosis. *Mult Scler Houndmills Basingstoke Engl*. (2017) 23:711–20. doi: 10.1177/1352458517690824

25. Papinutto N, Henry RG. Evaluation of intra-and Interscanner reliability of MRI protocols for spinal cord gray matter and Total cross-sectional area measurements. *J Magn Reson Imaging*. (2019) 49:1078–90. doi: 10.1002/jmri.26269

26. Yushkevich PA, Piven J, Hazlett HC, Smith RG, Ho S, Gee JC, et al. User-guided 3D active contour segmentation of anatomical structures: significantly improved efficiency and reliability. *NeuroImage*. (2006) 31:1116–28. doi: 10.1016/j.neuroimage.2006.01.015

27. Paugam F, Lefeuvre J, Perone CS, Gros C, Reich DS, Sati P, et al. Open-source pipeline for multi-class segmentation of the spinal cord with deep learning. *Magn Reson Imaging*. (2019) 64:21–7. doi: 10.1016/j.mri.2019.04.009

28. Chien C, Brandt AU, Schmidt F, Bellmann-Strobl J, Ruprecht K, Paul F, et al. MRI-based methods for spinal cord atrophy evaluation: a comparison of cervical cord cross-sectional area, cervical cord volume, and full spinal cord volume in patients with Aquaporin-4 antibody seropositive Neuromyelitis Optica Spectrum disorders. *AJNR Am J Neuroradiol*. (2018) 39:1362–8. doi: 10.3174/ajnr.A5665

29. Chien C, Juenger V, Scheel M, Brandt AU, Paul F. Considerations for mean upper cervical cord area implementation in a longitudinal MRI setting: methods, interrater reliability, and MRI quality control. *AJNR Am J Neuroradiol*. (2020) 41:343–50. doi: 10.3174/ajnr.A6394

30. Asseyer S, Kuchling J, Gaetano L, Komnenić D, Siebert N, Chien C, et al. Ventral posterior nucleus volume is associated with neuropathic pain intensity in neuromyelitis optica spectrum disorders. *Mult Scler Relat Disord*. (2020) 46:102579. doi: 10.1016/j.msard.2020.102579

31. Österberg A, Boivie J, Thuomas K-Å. Central pain in multiple sclerosis—prevalence and clinical characteristics. *Eur J Pain*. (2005) 9:531–42. doi: 10.1016/j.ejpain.2004.11.005

32. Finnerup NB, Gyldensted C, Nielsen E, Kristensen AD, Bach FW, Jensen TS. MRI in chronic spinal cord injury patients with and without central pain. *Neurology*. (2003) 61:1569–75. doi: 10.1212/01.WNL.0000096016.29134.FA

33. Hayashida S, Masaki K, Yonekawa T, Suzuki SO, Hiwatashi A, Matsushita T, et al. Early and extensive spinal white matter involvement in neuromyelitis optica. *Brain Pathol Zurich Switz*. (2017) 27:249–65. doi: 10.1111/bpa.12386

34. Chien C, Oertel FC, Siebert N, Zimmermann H, Asseyer S, Kuchling J, et al. Imaging markers of disability in aquaporin-4 immunoglobulin G seropositive neuromyelitis optica: a graph theory study. *Brain Commun*. (2019) 1:fcz026. doi: 10.1093/braincomms/fcz026

35. Levy M, Haycox AR, Becker U, Costantino C, Damonte E, Klingelschmitt G, et al. Quantifying the relationship between disability progression and quality of life in patients treated for NMOSD: insights from the SAkura studies. *Mult Scler Relat Disord*. (2022) 57:103332. doi: 10.1016/j.msard.2021.103332

36. Andelova M, Uher T, Krasensky J, Sobisek L, Kusova E, Srpova B, et al. Additive effect of spinal cord volume, diffuse and focal cord pathology on disability in multiple sclerosis. *Front Neurol*. (2019) 10:820. doi: 10.3389/fneur.2019.00820

37. Henmar S, Simonsen EB, Berg RW. What are the gray and white matter volumes of the human spinal cord? *J Neurophysiol*. (2020) 124:1792–7. doi: 10.1152/jn.00413.2020

38. Cacciaguerra L, Sechi E, Rocca MA, Filippi M, Pittock SJ, Flanagan EP. Neuroimaging features in inflammatory myelopathies: a review. *Front Neurol*. (2022) 13:993645. doi: 10.3389/fneur.2022.993645

39. Koser DE, Moeendarbary E, Hanne J, Kuerten S, Franze K. CNS cell distribution and axon orientation determine local spinal cord mechanical properties. *Biophys J*. (2015) 108:2137–47. doi: 10.1016/j.bpj.2015.03.039

40. Oh J, Sotirchos ES, Saidha S, Whetstone A, Chen M, Newsome SD, et al. Relationships between quantitative spinal cord MRI and retinal layers in multiple sclerosis. *Neurology*. (2015) 84:720–8. doi: 10.1212/WNL.0000000000001257

41. Sofroniew MV. Astrogliosis. *Cold Spring Harb Perspect Biol*. (2015) 7:a020420. doi: 10.1101/cshperspect.a020420

42. Duan T, Smith AJ, Verkman AS. Complement-dependent bystander injury to neurons in AQP4-IgG seropositive neuromyelitis optica. *J Neuroinflammation*. (2018) 15:294. doi: 10.1186/s12974-018-1333-z

43. Wang X, Jiao W, Lin M, Lu C, Liu C, Wang Y, et al. Resolution of inflammation in neuromyelitis optica spectrum disorders. *Mult Scler Relat Disord*. (2019) 27:34–41. doi: 10.1016/j.msard.2018.09.040

frontiers | Frontiers in Immunology

TYPE Original Research
PUBLISHED 05 February 2024
DOI 10.3389/fimmu.2024.1345843

OPEN ACCESS

EDITED BY
Cong-Cong Wang,
Shandong Provincial Qianfoshan Hospital, China

REVIEWED BY
Adil Maarouf,
Assistance Publique Hôpitaux de Marseille, France
Shengjun Wang,
Shandong University, China

*CORRESPONDENCE
Fuqing Zhou
ndyfy02301@ncu.edu.cn

†These authors have contributed equally to this work and share first authorship

RECEIVED 28 November 2023
ACCEPTED 15 January 2024
PUBLISHED 05 February 2024

CITATION
Ma H, Zhu Y, Liang X, Wu L, Wang Y, Li X, Qian L, Cheung GL and Zhou F (2024) In patients with mild disability NMOSD: is the alteration in the cortical morphological or functional network topological properties more significant.
Front. Immunol. 15:1345843.
doi: 10.3389/fimmu.2024.1345843

In patients with mild disability NMOSD: is the alteration in the cortical morphological or functional network topological properties more significant

Haotian Ma[1,2†], Yanyan Zhu[1†], Xiao Liang[1], Lin Wu[1], Yao Wang[1], Xiaoxing Li[1], Long Qian[3], Gerald L. Cheung[4] and Fuqing Zhou[1,5*]

[1]Department of Radiology, The First Affiliated Hospital, Jiangxi Medical College, Nanchang University, Nanchang, China, [2]Queen Mary College, Nanchang University, Nanchang, China, [3]Department of Biomedical Engineering, College of Engineering, Peking University, Beijing, China, [4]Spin Imaging Technology Co., Ltd, Nanjing, China, [5]Neuroimaging Laboratory, Jiangxi Medical Imaging Research Institute, Nanchang, China

Objective: To assess the alteration of individual brain morphological and functional network topological properties and their clinical significance in patients with neuromyelitis optica spectrum disorder (NMOSD).

Materials and methods: Eighteen patients with NMOSD and twenty-two healthy controls (HCs) were included. The clinical assessment of NMOSD patients involved evaluations of disability status, cognitive function, and fatigue impact. For each participant, brain images, including high-resolution T1-weighted images for individual morphological brain networks (MBNs) and resting-state functional MR images for functional brain networks (FBNs) were obtained. Topological properties were calculated and compared for both MBNs and FBNs. Then, partial correlation analysis was performed to investigate the relationships between the altered network properties and clinical variables. Finally, the altered network topological properties were used to classify NMOSD patients from HCs and to analyses time- to-progression of the patients.

Results: The average Expanded Disability Status Scale score of NMOSD patients was 1.05 (range from 0 to 2), indicating mild disability. Compared to HCs, NMOSD patients exhibited a higher normalized characteristic path length (λ) in their MBNs ($P = 0.0118$, FDR corrected) but showed no significant differences in the global properties of FBNs (p: 0.405-0.488). Network-based statistical analysis revealed that MBNs had more significantly altered connections ($P< 0.01$, NBS corrected) than FBNs. Altered nodal properties of MBNs were correlated with disease duration or fatigue scores ($P< 0.05/6$ with Bonferroni correction). Using the altered nodal properties of MBNs, the accuracy of classification of NMOSD patients versus HCs was 96.4%, with a sensitivity of 93.3% and a specificity of 100%. This accuracy was better than that achieved using the altered nodal properties of FBNs. Nodal properties of MBN significantly predicted Expanded Disability Status Scale worsening in patients with NMOSD.

Conclusion: The results indicated that patients with mild disability NMOSD exhibited compensatory increases in local network properties to maintain overall stability. Furthermore, the alterations in the morphological network nodal properties of NMOSD patients not only had better relevance for clinical assessments compared with functional network nodal properties, but also exhibited predictive values of EDSS worsening.

KEYWORDS

brain connectomics, neuromyelitis optica spectrum disorder, individual morphological brain network, functional brain networks, topological properties

Highlights

- Disrupted global topological properties of mildly disabled NMOSD patients were found only in MBNs.
- In NMOSD patients, disrupted nodal properties were found in both MBNs and FBNs.
- Network-based statistical analysis revealed that MBNs had more significantly altered morphological connections than FBNs.
- Compared to FBNs, MBNs showed better correlations with clinical variables, and better classification efficacy.
- Nodal properties of MBN were predictive of Expanded Disability Status Scale worsening in NMOSD.

1 Introduction

Neuromyelitis optica spectrum disorder (NMOSD) is a relatively rare central nervous system autoimmune disease. It is more prevalent in young adults of Asian descent, with a higher incidence among females (1). Clinically, it is characterized by severe optic neuritis (ON) and longitudinally extensive transverse myelitis (LETM). Common lesion sites include the bottom of the fourth ventricle, periependymal gray matter (GM), hypothalamus, walls of the third ventricle, and periventricular regions (1, 2). Patients often experience a prolonged and relapsing course, with the possibility of severe neurological symptoms and even residual neurological impairments (3).

Magnetic resonance imaging (MRI) plays a crucial role in the early identification of NMOSD, guiding aquaporin-4 (AQP4) antibody testing, and aiding in acute-phase treatment decisions. It is also a powerful tool for studying the underlying pathological mechanisms of NMOSD when combined with others novel neuroimaging approaches. For instance, some studies have found that NMOSD patients exhibit increased morphological connectivity in the primary motor modules and motor-sensory related areas of the cerebellum (4), while white matter fiber bundles such as the thalamic radiation, corticospinal tracts, and dorsal and ventral longitudinal fasciculi are damaged (5), leading to decreased local connectivity efficiency (6). However, the alterations in brain structure and function, as well as the mechanisms of plasticity in NMOSD patients, are not fully understood. There are contradictory reports regarding functional connectivity changes, with increased functional connections observed in the default mode network, dorsal attention network, and thalamic network (7), while disease-specific functional connections, such as those in the cerebellar motor modules, show a decrease (4). Additionally, there are conflicting reports of significant functional connectivity increases (8) and decreases in the primary and secondary visual networks (4, 7, 9). Despite local functional connectivity changes, the overall topological properties of the brain tend to remain relatively stable, which is considered a compensatory plasticity mechanism to cope with functional disabilities (10).

The brain is a vast, intricate, and highly efficient operating system composed of billions of neurons. As mentioned earlier, the connectomics, as a tool for studying macroscopic brain white matter structure and functional networks, has been used in NMOSD research (4, 6). However, Pang et al. (11) has demonstrated that the geometry of the brain plays a crucial role in brain function, rather than the connectome eigenmodes. The geometric shape of the brain and its cortical morphological brain networks may provide better insights into the clinical symptoms of NMOSD patients. Indeed, studies on NMOSD patients have found brain cortical atrophy associated with disease progression (12). However, the specific associations between cortical changes and clinical symptoms in NMOSD patients have not been clearly established yet. Individual-based graph cortical morphological brain network analysis is a novel and advanced method that can provide mesoscopic-scale cortical structural information and elucidate its biological significance.

This study hypothesized that cortical geometric changes caused by pathological factors, such as inflammatory lesions, in NMOSD patients can lead to individual cortical morphological brain network (MBN) alterations, which may explain the clinical symptoms of these patients. To explore this hypothesis, this study computed single-subject MBNs based on region similarity methods and applied graph theoretical analysis to investigate the topological properties of constructed networks in NMOSD patients. The

resting-state functional brain network (FBN) was also used as a reference for comparison. Correlation analysis was then employed to observe the relationships between network topological properties and clinical variables. Finally, the altered network matrices of topological properties were used to classify NMOSD patients from healthy controls (HCs) and to predictive of disability progression of the patients.

2 Materials and methods

2.1 Participants

In this study, 21 NMOSD patients and 23 HCs were consecutively recruited at the First Affiliated Hospital of Nanchang University from April 2018 to July 2022. The patients' inclusion criteria were as follows: (1) met the 2015 international consensus diagnostic criteria of NMOSD; (2) were right-handed and were 18–60 years of age; (3) were AQP4 antibody-positive in serology and/or cerebrospinal fluid status; (4) had not taken drugs such as high-dose steroids for at least 2 weeks before MRI scanning. The exclusion criteria were as follows: (1) a history of other neurological or psychiatric diseases; (2) had contraindications for MRI scans and, (3) image artifacts or incomplete clinical information. In this study, all the NMOSD patients had mild disabilities with EDSS scores of no more than 2 (13, 14).

All of the healthy controls (HCs) were screened using the Clinical Diagnostic Interview Nonpatient Version without significant cognitive disorders, head trauma, or MRI contraindications.

The study was approved by the local human research Ethics Committee and the institutional review board.

2.2 Clinical assessment

Each NMOSD patient underwent a comprehensive clinical interview and physical examination, which included the following assessments: (1) the Expanded Disability Status Scale (EDSS) to determine the severity of disability on a scale of 0 to 10. The EDSS has been used to assess the neurological disability of multiple sclerosis, as well as the severity of relapses in patients with NMOSD (14–16), it has validated in NMOSD (16). (2) The Paced Auditory Serial Addition Test (PASAT) to evaluate cognitive function, including auditory information processing speed, flexibility, and calculation ability. (3) The Modified Fatigue Impact Scale (MFIS) to assess the impact of fatigue on daily living.

2.3 MRI protocol

The brain images were acquired on a 3.0 Tesla MRI system (Trio, Siemens Healthcare, Erlangen, Germany) with a standard 8-channel head coil. First, 3-D T1-weighted images were acquired on a magnetization-prepared rapid gradient-echo (MP-RAGE) sequence with the following parameters: repetition time = 1,900 ms, echo time = 2.26 ms, matrix size = 256 × 256, field of view = 240×240 mm, flip angle = 9°, and 176 sagittal slices with thickness = 1.0 mm. Second, resting-state functional MRI (fMRI) were acquired on an echo-planar imaging sequence with the following parameters: repetition time = 2000 ms, echo time = 30 ms, field of view = 200 × 200 mm, flip angle = 90°, 30 axial slices, and interleaved scan with 240 time points. Third, a conventional MRI protocol that included diffusion-weighted imaging (DWI), T2-weighted imaging, and T2-fluid attenuated inversion recovery images was also performed for patient diagnosis and lesion detection. The participants were asked to close their eyes, remain motionless, and avoid systematic thinking and falling asleep during the MRI scan.

2.4 Morphological data preprocessing and lesion volume measurement

After manually checking the apparent artifacts, the 3-D T1-weighted data were preprocessed using the Computational Anatomy Toolbox (CAT12; www.neuro.uni-jena.de/cat/) and run through Statistical Parametric Mapping (SPM12, https://www.fil.ion.ucl.ac.uk/spm/software/spm12/). Each individual T1-weighted image was segmented into GM, white matter, and cerebrospinal fluid. Brain parenchymal fraction (BPF) was defined as the ratio between the brain parenchymal (GM + white matter) volume and the total volume. Then, GM images were normalized into Montreal Neurological Institute (MNI) 152 space using the Diffeomorphic Anatomical Registration Through Exponential Lie Algebra (DARTEL) modulation approach. Finally, GM images were resliced to a 2 mm isotropic voxel size and spatially smoothed using a Gaussian kernel of 6 mm full-width at half maximum (FWHM).

T2WI lesion volumes were automatically obtained using the Lesion Segmentation Tool (LST) (17) and SPM12 software. Then, the lesion masks in patients were used to fill 3D T1-weighted MR images by the Lesion-Filling Tool (LFT), thereby eliminating the impact of these lesions on brain network construction.

2.5 Functional data preprocessing

Resting-state fMRI data were preprocessed using Data Processing & Analysis of Brain Imaging (DPABI, v4.2, http://www.rfmri.org/dpabi) based on SPM12. The standard processing steps (18) included discarding the first 10 time points; slice timing; realignment and correcting (230 remaining time points); coregistering to individual 3-D T1-weighted images; normalization to MNI space; reslicing the functional images ($3 \times 3 \times 3$ mm^3); spatially smoothing with a 6 mm-FWHM Gaussian kernel; detrending and temporal filtering (0.01–0.1 Hz); and nuisance regression (Friston 24-parameter model motion parameters, mean framewise displacement, white matter, cerebrospinal fluid, and global signals).

2.6 Network construction

Morphological and functional networks were constructed according to the previous approach (19). First, the nodes of

network were defined according to the automated anatomical atlas (AAL) template including 90 cortical and subcortical regions (20).

The edges of network were defined as the interregional similarity based on Kullback–Leibler divergence-based similarity (KLS) measurements for morphological networks (19, 21) and based on interregional linear Pearson correlations for functional networks (22).

2.7 Network topological properties analysis

Individual network topological properties were processed using the graph-theoretical network analysis (GRETNA; http://www.nitrc.org/projects/gretna/) toolbox based on 90 × 90 weighted matrices at each sparsity threshold (22). According to previous studies (19, 23), we selected a wide range of sparsity (*S*) thresholds (0.05–0.4) and calculated the area under the curve (AUC) over the *S* thresholds with an interval step of 0.01 for global and nodal topological properties of the MBNs, to avoid potential bias of any arbitrary single threshold selection (21, 24). The global topological properties include the small-worldness (sigma, σ), clustering coefficient (*Cp*) and normalized clustering coefficient (gamma, γ), characteristic path length (*Lp*) and normalized characteristic path length (lambda, λ), network global efficiency (E_{glob}) and local efficiency (E_{loc}). For global measures, low values of *Lp*, λ, and high E_{glob} reflect distributed network integration and the ability for information communication; while high values of *Cp*, γ, and E_{loc} reflect network segregation, i.e., strong ability of information transfer of interconnected regions. The nodal topological properties included nodal degree, nodal betweenness centrality and nodal efficiency, reflect the topological importance of nodes in the network.

2.8 Statistical analysis

The demographic and clinical variables of NMOSD and HC groups were compared using the Statistical Package for the Social Sciences (SPSS) software (version 21.0; IBM Corp., Armonk, New York, USA). Each AUC of the global and nodal topological metrics were compared using nonparametric permutation test (10,000 permutations) for between-group differences (24, 25), and the Benjamini-Hochberg false discovery rate (FDR q value< 0.05) correction was used for multiple comparisons (24).

Internodal connections with between-group differences in nodal characteristics were compared by a network-based statistical approach (24, 25) (NBS; http://www.nitrc.org/projects/nbs/; corrected at $P< 0.01$).

Partial correlation analysis was performed to examine the relationships between the significantly altered global and/or nodal network properties and clinical variables, controlling for age and sex as confounding variables (Bonferroni correction< 0.05; IBM SPSS Statistics V21.0).

We performed mediation analysis using the SPSS online (https://spssau.com/en/index.html) to further elucidate the relationship among morphological metrics, functional network metrics, and clinical characteristics. In the mediation analysis, total effect of *X* on *Y*(*c*) = indirect effect of *X* on *Y* through *M* (*a*×*b*) + direct effect of *X* on *Y*(*c'*), only variables that showed a significant correlation with others were considered as independent (morphological metrics), dependent (clinical characteristics), or mediating (functional network metrics) variables. The significance analysis was based on 10,000 bootstrap realizations, and age, sex as nuisance variables.

We performed SVM (https://www.csie.ntu.edu.tw/~cjlin/libsvm/) to determine the efficacy of detecting individual NMOSD using the altered network matrices of topological properties (26). 70% of the data were used as the training set to train and the remaining as the test set. The accuracy, sensitivity and specificity of SVM models were calculated. The receiver operating characteristic (ROC) curve and the area under the curve (AUC) were used to evaluate the performance of the models.

Finally, one-way Cox Regression was used for feature screening in order to avoid overfitting. Cox proportional hazards model and Kaplan-Meier survival analysis were used to analyses time-to-progression data.

3 Results

3.1 Participant demographic and clinical characteristics

Two patients with NMOSD and one HC were excluded due to excessive head motion, and one patient with NMOSD was excluded due to significant data artifacts. Finally, 18 NMOSD patients and 22 healthy participants were included in the comparative study. In the NMOSD patients, the median disease duration was 13 months (2 to 114 months), the median number of relapses was 1 (1 to 4). Four patients had solely spinal lesions, 12 patients had brain lesions (median:1.252 ml; range: 0.016-8.773 ml), including 10 patients with periventricular white matter involvement, 8 patients with centrum semiovale involvement, 6 patients with brain stem or medulla oblongata involvement, 4 patients with area postrema involvement, 2 patients with cerebellum involvement, 1 patient with diencephalon involvement. Seven patients had both spinal cord and brain lesions. The lesion involved the optic nerve alone in 2 patients, and the lesion involved the optic nerve, spinal cord and brain in only 1 patient. There was no significant difference in BPF between patients and controls ($P = 0.929$) (Table 1).

3.2 Global properties of MBNs and FBNs

Based on the predetermined connection density, both the NMOSD patient group and the HC group showed small-world properties in MBNs and FBNs ($\gamma > 1, \lambda \approx 1, \gamma/\lambda > 1$). There were no significant differences in the global properties of FBNs between NMOSD patients and HCs ($P > 0.05$). In contrast, compared with HCs, NMOSD patients showed a significant decrease in λ of MBNs ($P = 0.0118$, FDR corrected, effect size: 0.354) but not in other global properties of MBNs (Table 2).

TABLE 1 Demographic and clinical characteristics of NMOSD patients and HCs.

Characteristics	NMOSD (n = 18)	HCs (n = 22)	*p*-values
Demographics			
Age at testing (years)	42.110 ± 12.171	44.36±9.052	0.506*
Sex (male/female)	2/16	3/19	0.810#
Handedness (right), %	100	100	1#
Disease-related characteristics			
AQP4-Ab, positive/negative	18/0	n.a.	n.a.
Disease duration (month, median, range)	13 (2-114)	n.a.	n.a.
EDSS scores at baseline	1.056 ± 0.591	0 ± 0	< 0.001
PASAT scores	89.778 ± 14.711	n.a.	n.a.
MFIS scores (median, range)	9 (0-17)	n.a.	n.a.
Mean follow-up time, month (min–max)	39.167 (24-62)	n.a.	n.a.
Follow-up EDSS worsening, n (%)	3 (16.667%)	n.a.	n.a.
MRI-related characteristics			
Lesion volume (ml) (median, range)	1.252 (0.016-8.773)	n.a.	n.a.
Brain parenchymal fraction	0.804 ± 0.024	0.805 ± 0.029	0.929
Framewise displacement (mm)	0.201±0.022	0.188±0.031	0.623*

Data are presented as mean ± standard deviation. # p-value was obtained using the two-tailed chi-squared test; * p-value was obtained by the two-sample two-tailed t-test.
EDSS, Expanded Disability Status Scale; HCs, healthy controls; MFIS, Modified Fatigue Impact Scale; NMOSD, Neuromyelitis optica spectrum disorder; PASAT, Paced Auditory Serial Addition Test.

3.3 Nodal properties of MBNs and FBNs

For node centrality measures of MBNs and FBNs, significant differences are shown in Figure 1 (Supplementary Tables S1, S2) between patients with NMOSD and HCs ($P< 0.05$, FDR corrected). In NMOSD patients, except for the left olfactory cortex, both MBN and FBN showed a decrease in nodal betweenness (Nb), but there was no overlap in other nodal properties that decreased in brain regions. Among the brain regions where nodal properties were increased in NMOSD patients, the MBN exhibited more compensatory increases in brain areas associated with motor, visual, and emotional functions, such as the motor network (MON), visual I network (VisI), frontoparietal network (FPN), and medial frontal network (MFN), than the FBN.

3.4 Alterations in the connection of MBNs and FBNs

Compared with HCs, both MBNs and FBNs in NMOSD patients had increased and decreased network connectivity (P< 0.01, NBS corrected) (Figure 2). For MBNs, significantly increased connections involving 54 nodes and 74 edges, as well as decreased connections involving 23 nodes and 23 edges, were observed in patients compared with HCs. For FBNs, there were fewer significant alterations in the connections in patients compared to MBNs, with significantly increased connections involving 16 nodes and 18 edges and decreased connections involving 16 nodes and 13 edges, respectively, compared with HCs.

3.5 Relationships between global network properties and clinical variables

The relationships between the global network properties of patients with NMOSD and clinical variables were shown in

TABLE 2 Group comparisons of AUC values of global properties of MBNs and FBNs between NMOSD patients and HCs.

	MBNs			FBNs		
	NMOSD	Control	*p* values	NMOSD	Control	*p* values
Lp	0.756 ± 0.024	0.767 ± 0.027	0.1062	0.683 ± 0.028	0.683 ± 0.024	0.488
Cp	0.256 ± 0.027	0.257 ± 0.003	0.3737	0.251 ± 0.014	0.252 ± 0.008	0.446
γ	0.502 ± 0.003	0.494 ± 0.005	0.1824	0.635 ± 0.084	0.631 ± 0.066	0.418
λ	0.417 ± 0.005	0.419 ± 0.026	0.0118*	0.423 ± 0.012	0.423 ± 0.008	0.487
σ	0.481 ± 0.025	0.470 ± 0.026	0.1014	0.596 ± 0.081	0.590 ± 0.067	0.406
E_{glob}	0.224 ± 0.026	0.222 ± 0.003	0.1802	0.243 ± 0.006	0.242 ± 0.006	0.405
E_{loc}	0.301 ± 0.003	0.301 ± 0.004	0.4523	0.316 ± 0.008	0.316 ± 0.005	0.408

Permutation tests were used to determine the differences in the global network properties between groups (see Materials and Methods). Values were the fitted AUC values (mean ± SD) of global network properties in each group. *p< 0.05.
Cp = clustering coefficient; Lp = characteristic path length; Gamma = normalized clustering coefficient; Lambda = normalized characteristic path length; Sigma = small-worldness; Eglob = network global efficiency; Eloc = local efficiency; FBNs, functional brain networks; HCs, healthy controls; MBNs, morphological brain networks. The same abbreviations are used in the other figures and tables; therefore, this note is not repeated.

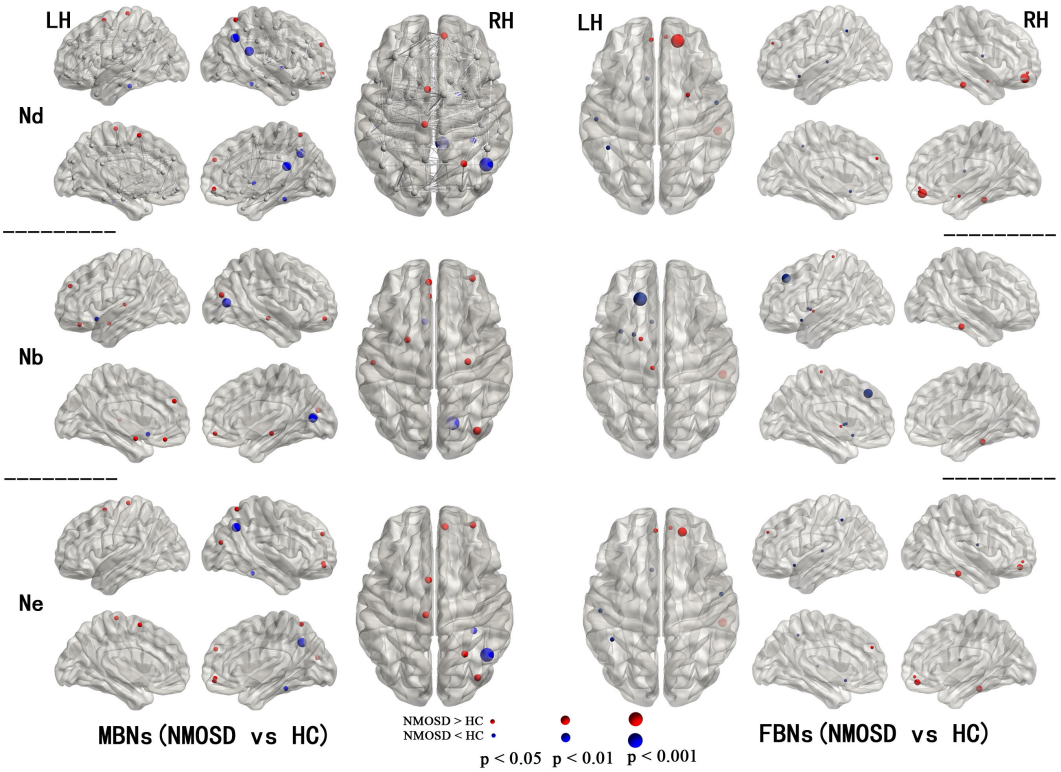

FIGURE 1
Regions with significant alterations in the nodal properties of MBNs and FBNs between NMOSD patients and healthy subjects (*P*< 0.05, FDR corrected). All the brain regions were defined by AAL-90; see Supplementary Tables S1, S2 for the full names of the nodes in the figure.

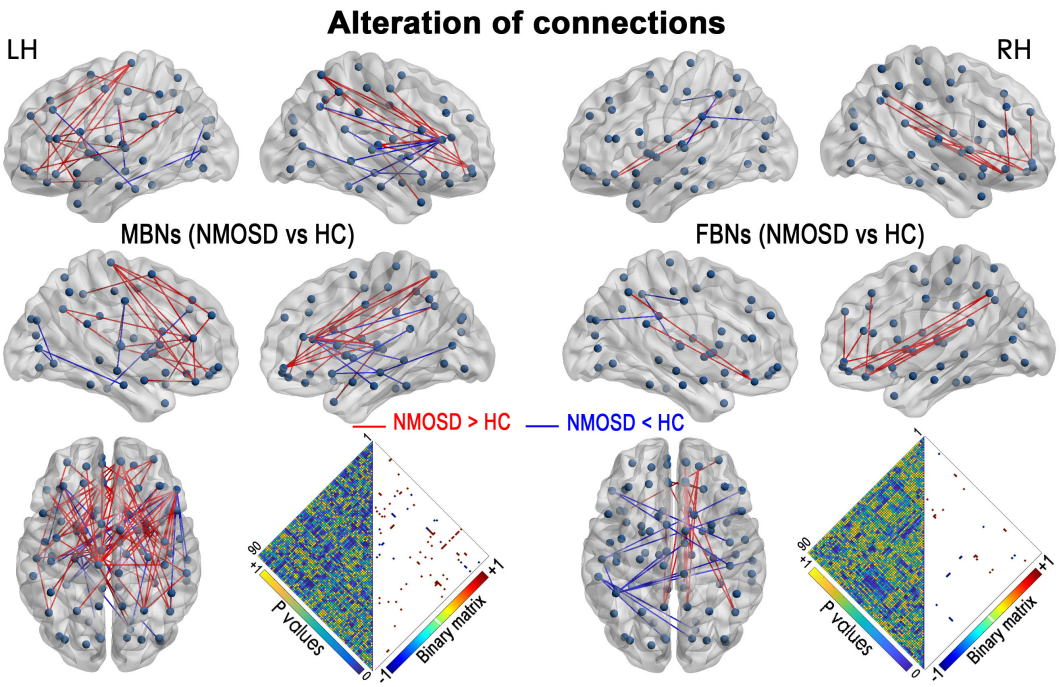

FIGURE 2
NMOSD-related alterations in the network connections in MBNs and FBNs (P< 0.01, NBS corrected). Each node denotes a brain region of AAL-90. Significantly decreased connections in patients with NMOSD compared with HCs are presented in blue, and increased connections are presented in red. Heatmaps show the P values between the nodes and the edges with significant alterations (binary matrix). LH, left hemisphere; RH, right hemisphere.

Figure 3 and Supplementary Tables S3, S4: (1) disease duration was correlated with the gamma (γ) AUC ($P = 0.036$, without correction), the sigma (σ) AUC ($P = 0.049$, without correction) of MBNs; and (2) the lambda (λ) AUC of MBNs was correlated with PASAT scores ($P = 0.049$, without correction). There was no significant correlation between global properties of functional networks and clinical variables.

3.6 Significant relations between nodal properties and clinical variables

Figure 4 showed a correlation between the nodal properties of MBNs or FBNs and clinical variables in patients with NMOSD ($P< 0.05$; see Supplementary Tables S5, S6 for details). After Bonferroni correction, the disease duration was significantly correlated with the Nb AUC of right middle occipital gyrus (MOG) of MBNs ($P = 0.006< 0.05/5$); and the Nb AUC of left olfactory cortex of MBNs was significantly correlated with the MFIS scores ($P = 0.003< 0.05/5$).

3.7 Mediation analysis and single-subject classification

In NMOSD patients, mediation analysis did not find any mediating effect between morphological network topological properties, functional network topological properties, and clinical parameters.

Using the altered nodal properties of MBNs, the accuracy of classifying NMOSD patients versus HCs was 96.4%, with a sensitivity of 93.3% and a specificity of 100%. Using FBNs, the accuracy was 85.7%, with a sensitivity of 73.3% and specificity 100% (Figure 5; Supplementary Table S7). The relevant nodal properties contributing to the SVM classification are shown in Supplementary Table S7. However, when using the altered global properties of MBNs (λ), the discrimination of NMOSD patients from HCs at the single-subject level was insufficient. The accuracy was only 64.3%, with a sensitivity of 53.3% and a specificity of 76.9%.

Kaplan-Meier survival analysis indicated that nodal properties of MBN were predictive of progression in NMOSD patients (Figure 6A). After feature screening by univariate Cox Regression, there were two significant features remaining among the 28 features (Figure 6B), namely Nd AUC of left SMA ($P = 0.022$) and Nd AUC of right pallidum ($P = 0.020$). In a univariable model, Nd AUC of left SMA of MBN (HR=1.56 (95% CI 0.947 to 2.56) p=0.081) and Nd AUC of right pallidum (HR=2.50 (95% CI 0.859 to 7.26) p=0.093) were trend associated with EDSS worsening in patients with NMOSD. Cox proportional hazards model to evaluate their prognostic values. Based on the model, a nomogram was established to predict the time-to-progression (Figure 6C).

4 Discussion

In this study, we first investigated the alterations in MBNs in NMOSD patients and their correlations with clinical variables. (1) The MBNs showed a decrease in lambda that was associated with PASAT scores, indicating a reduced overall efficiency of interregional information integration in NMOSD patients with mild disability. However, the FBNs did not reveal such changes. (2) Compensatory increases in nodal properties, including visual-related networks, MONs, and medial frontal networks (MFNs), contributed to maintaining the stability of global properties in the MBNs of NMOSD patients. (3) Nodal properties of the VisI and the visual association network (VA) were correlated with disease duration, while nodal properties of MFN, FPN, and DMN were correlated with clinical symptom assessment. (4) Nodal properties of MBN were predictive of EDSS worsening in patients with NMOSD, suggesting its additional clinical value as a non-invasive biomarker for mild disability patients with NMOSD. This study provides a new perspective that the properties of local nodes, such as the visual network of MBNs, rather than FBNs, may play a key role in patients with NMOSD.

4.1 Altered global properties of brain networks in NMOSD patients

We found that NMOSD patients exhibited a decrease in the global efficiency of interregional information integration in MBNs, which was significantly correlated with PASAT scores. However, such alterations were not observed in FBNs. NMOSD

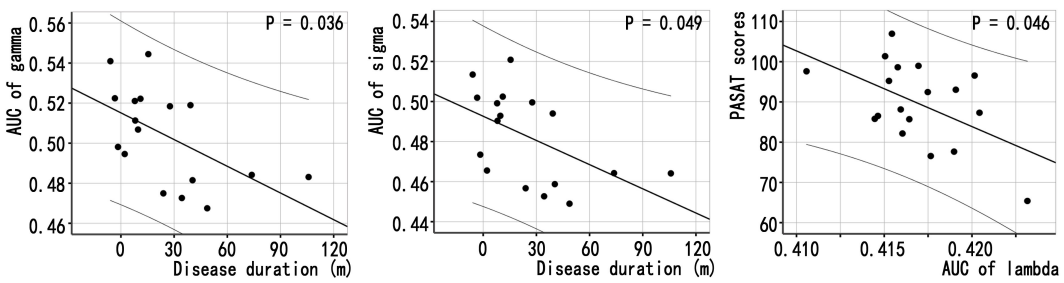

FIGURE 3
Associations between global properties and clinical variables in patients with NMOSD. Scatter plots of global properties of MBNs and clinical variables.

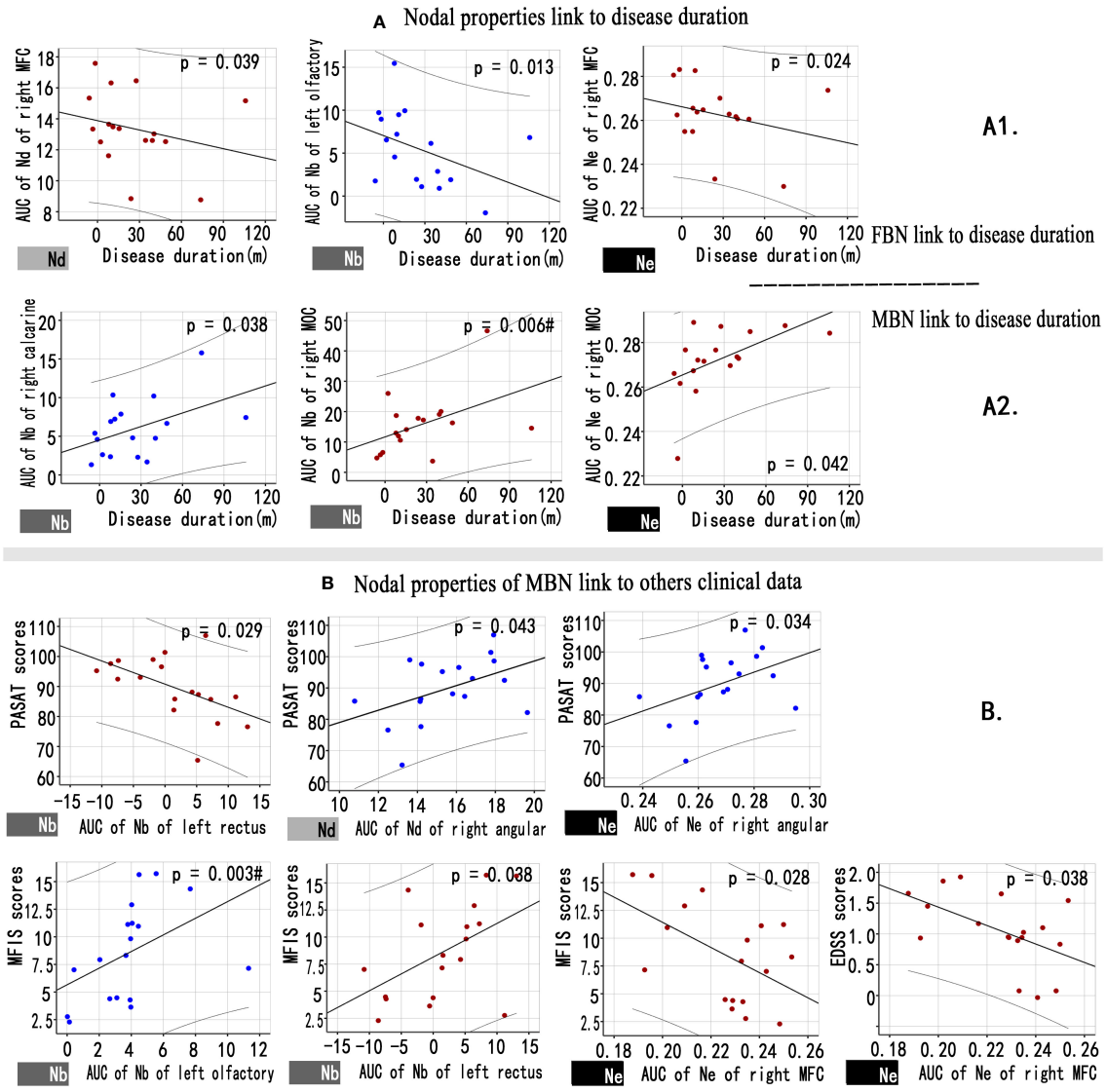

FIGURE 4
Associations between nodal properties and clinical variables in patients with NMOSD. **(A)** Scatter plots of disease duration and the altered FBN (A1), MBN (A2) nodal properties. **(B)** Scatter plots of the altered MBN nodal properties and others clinical variables. Blue points represent attributes that decreased nodal properties in the patient group compared to the control group, while red points represent attributes that increased nodal properties in NMOSD patients. # Bonferroni correction P< 0.05/6. FBN, functional brain network; MBN, morphological brain network; Nd, nodal degree; Nb, nodal betweenness; Ne, nodal efficiency.

patients often experience fatigue, poor sleep quality, and cognitive impairments characterized by decreased processing speed, executive function, and memory, with processing speed decline being particularly prominent (27). Studies on brain white matter structural networks in NMOSD patients have also shown disruptions in white matter fiber connections, which are associated with declines in cognitive functions related to attention, working memory, processing speed, and visuospatial processing (28). The characteristic path length reflects the global feature of a network, and a smaller value indicates faster information transfer within the network. In our study, we observed a mild decrease in lambda in NMOSD patients, which was negatively correlated with the decline in PASAT scores, suggesting that compensatory mechanisms in certain NMOSD patients may help slow the decline in processing speed. This finding may be related to the fact that NMOSD patients in our study had mild disability and mild cognitive impairment.

4.2 Altered nodal properties of brain networks in NMOSD patients

First, nodal property decreases are straightforward, as they are related to inflammatory white matter lesions (5, 29) and network disconnection (28, 30), resulting in corresponding clinical functional impairments (31). The NMOSD patients in our study experienced fatigue, mild disability, and mild cognitive impairment, which are common clinical symptoms of NMOSD (1, 27, 32).

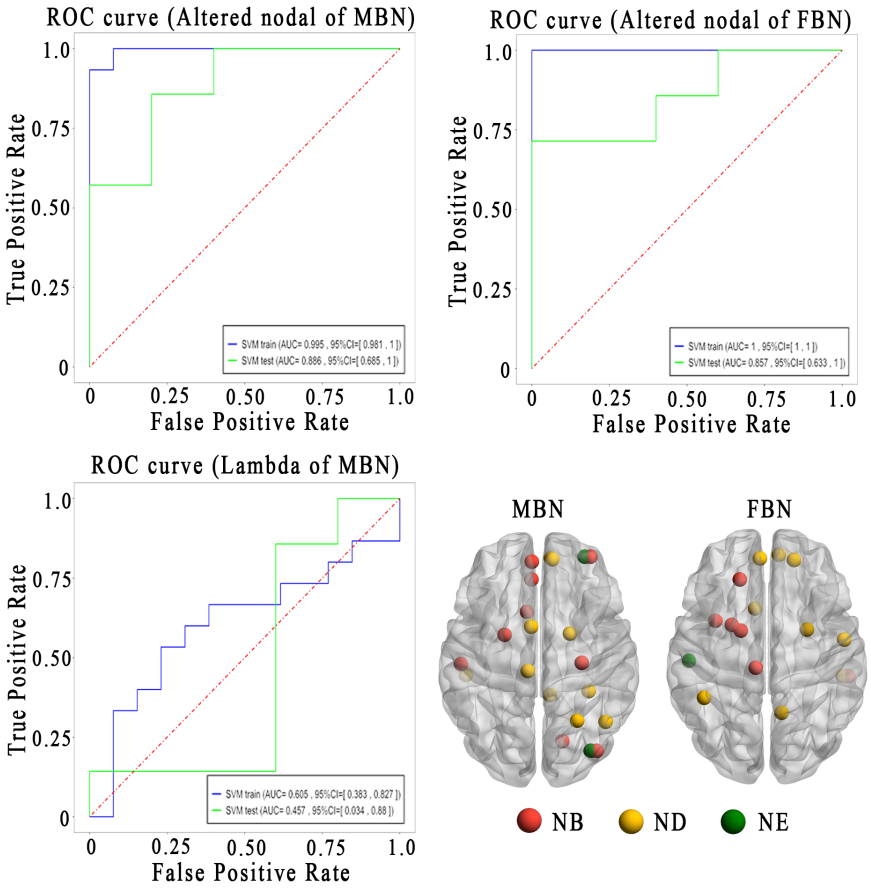

FIGURE 5
Sensitivity and specificity of the altered brain network topological properties in differentiating the patients with NMOSD from HCs. Lower left is the altered brain regions for the classification analysis. AUC, area under the curve; FBN, functional brain network; MBN, morphological brain network; ROC, receiver operating characteristic curves; Nb, nodal betweenness; Nd, nodal degree; Ne, nodal efficiency.

However, the global network properties of patients remained relatively stable, which is related to the observed local increases. In our study, the areas with increased nodal properties were mainly found in the following regions: (1) the MFN. This network is highly implicated in the modulation of internal emotional stimuli and automatic emotional responses. Nodes right medial superior frontal cortex (AAL24) and left rectus gyrus (AAL27) of MFN were correlated with cognitive (PASAT) and fatigue (MFIS) assessments. With the exacerbation of symptoms, NMOSD patients showed increased degree and betweenness centrality, indicating the presence of pseudoadaptive compensation. Similar findings have also been reported in studies of multiple sclerosis (33); (2) the MON and VA. These regions are related to motor and visual functions. Node right middle occipital gyrus (AAL52) of the VA and disease duration were correlated, and in combination with the correlation between decreased nodal properties (VisI) and disease duration, it indicates that compensatory mechanisms for visual processing in response to the functional decline in the visual I region of NMOSD patients gradually increase. Whether this compensation can effectively improve the clinical symptoms of patients requires further research in the future; (3) the default mode network (DMN). DMN does not directly affect the MON or directly correlate with fatigue but is related to motor preparation. The dynamic interaction between the default network and MON may affect motor task execution abilities (34). Highly active nodes of the default network consume excessive energy, leading to a state of "idleness" fatigue. Similar phenomena have also been found in studies of multiple sclerosis, where a highly active DMN was correlated with fatigue (35). In our study, the efficiency of DMN nodes increased and was negatively correlated with disability level (EDSS scores) and fatigue (MFIS scores), indicating that the default network nodes (AAL26) of NMOSD indirectly contributed to the aforementioned functional changes; and (4) the frontoparietal network (FPN). FPN rapidly accomplishes new tasks through flexible interactions with other control and processing networks. This may be the reason no correlation was found between these brain areas and clinical data in this study. Last, compensatory mechanisms are not uncommon in NMOSD. For example, a study on cerebellar connectivity in NMOSD patients found that increased connectivity in the primary motor module of the cerebellum can reflect specific cortical injury and serve as compensation for patients' motor and sensory functions (4).

In the SVM analysis, we achieved a higher (96.4%) classification accuracy using altered nodal properties of MBNs,

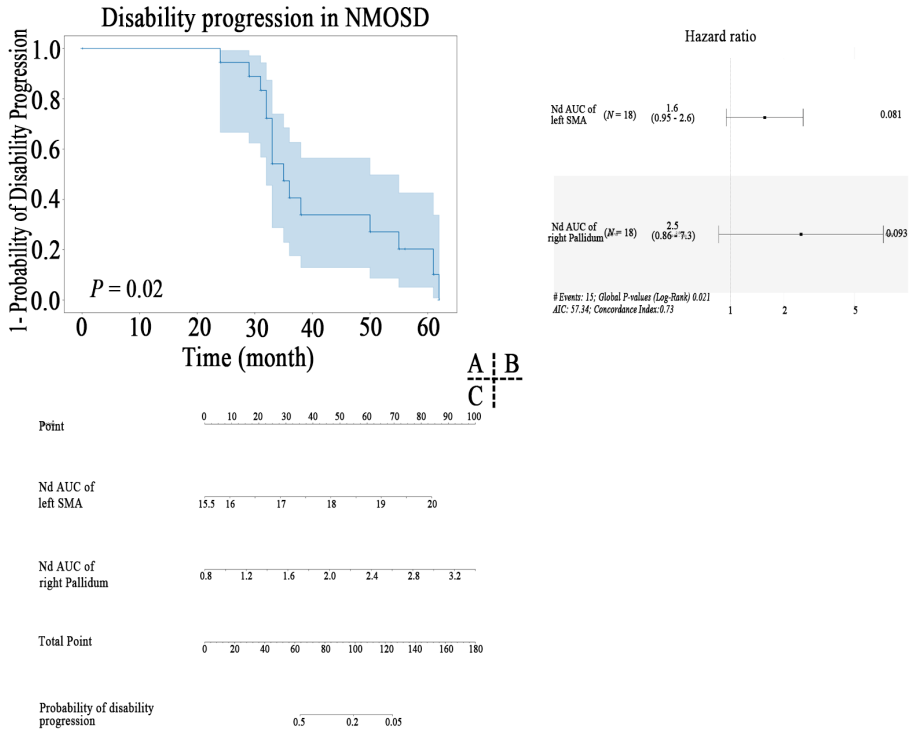

FIGURE 6
Kaplan–Meier survival curve of nodal properties of MBN predicting disability progression in patients with NMOSD **(A)**, the results of the multivariate Cox regression **(B)**, and nomogram **(C)** which were constructed by the significant features.

compared to the classification accuracy (85.7%) of using FBNs, showing that altered nodal properties of MBN were more sensitive in identifying NMOSD from HCs. Our findings support the emerging view that cortical morphological networks, which are crucial in brain function (36),are powerful tools for examining the structural reorganization due to inflammatory and demyelinating damage (33). The morphological network biomarkers have the potential to improve the diagnosis of neurological diseases. Moreover, the altered nodal properties of MBN were directly related to clinical variables, and this relationship was not mediated by functional nodal properties. This underscores the greater sensitivity and clinical significance of topological properties of MBNs compared to functional parameters in NMOSD. These findings bolster the concept that nodal properties of morphological network might serve as a neuroimaging biomarker to assist the clinical diagnosis of mildly disabled NMOSD in the future (12, 33, 36, 37).

Furthermore, in the MBN, increased Nd of left SMA and decreased Nd of right pallidum was predictive of EDSS worsening in NMOSD, which is in line with the idea that brain connectional morphological feature is a composite marker of ageing and a disease-related brain (38). The increased node degree of left SMA side predicts the EDSS worsening, further indicating the presence of pseudoadaptive compensation of supplementary motor area, which is consistent with the hypothesis of the increase of node attributes discussed above. In a recent study of deep learning-derived brain age gap base on morphological MRI, the authors reported brain age gap (5.4 (95% CI 4.3 to 6.5) years) significantly predicted EDSS worsening in patients with NMOSD in the 6 tertiary neurological centers of China cohort (39). Future studies are required to determine the possible causative EDSS worsening factors in individual-scale parameters.

4.3 Limitations

This study had several limitations. First, there was no distinction between patients in the acute phase and the remission phase, and different disease stages or phenotypes may have an impact on brain network topological properties. However, all NMOSD patients in this study had mild disability and mild cognitive impairment. This may explain why the global network properties of the patients remained relatively normal. In future research, it will be important to consider the influence of different disease stages or phenotypes on brain network topological properties. Second, different segmentation templates or network nodes may affect the calculation and comparison of patients' network topological properties. Previous studies have found high consistency between the Harvard-Oxford atlas templates and AAL templates (40). This study also compared different segmentation templates and node correlation methods, and similar results were obtained. Moreover, previous methodological studies have demonstrated their good reproducibility (21, 41).

5 Conclusions

This study suggested that NMOSD patients in a mildly disabled state exhibited compensatory increases in local topological properties to maintain the overall stability of the brain network. Compared to functional networks, the nodal properties of MBNs not only revealed more alterations in NMOSD patients but also showed better correlations with clinical assessments and predicted EDSS worsening.

Data availability statement

The raw data supporting the conclusions of this article will be made available by the authors, without undue reservation.

Ethics statement

The studies involving humans were approved by Medical Ethics Committee of the First Affiliated Hospital of Nanchang University. The studies were conducted in accordance with the local legislation and institutional requirements. The participants provided their written informed consent to participate in this study.

Author contributions

HM: Writing – original draft, Investigation, Formal analysis, Funding acquisition, Visualization. YZ: Writing – review & editing, Data curation, Formal analysis, Visualization. XL: Data curation, Formal analysis, Writing – review & editing. LW: Data curation, Formal analysis, Writing – review & editing. YW: Data curation, Writing – review & editing. XXL: Data curation, Writing – review & editing. LQ: Data curation, Writing – review & editing. GC: Data curation, Writing – review & editing. FZ: Resources, Software, Supervision, Validation, Visualization, Conceptualization, Data curation, Funding acquisition, Writing – original draft.

Funding

The author(s) declare financial support was received for the research, authorship, and/or publication of this article. This study was supported by the National Natural Science Foundation of China (82160331, 81771808), Jiangxi Province Double Thousand Talent Plan (jxsq2023201039), and the Innovation and Entrepreneurship Training Program for College Students of Jiangxi province (202310403075). This project is implemented by the Jiangxi Clinical Research Center for Medical Imaging (20223BCG74001).

Conflict of interest

Author GC was employed by the company Spin Imaging Technology Co., Ltd.

The remaining authors declare that the research was conducted in the absence of any commercial or financial relationships that could be construed as a potential conflict of interest.

Publisher's note

Supplementary material

The Supplementary Material for this article can be found online at: https://www.frontiersin.org/articles/10.3389/fimmu.2024.1345843/full#supplementary-material

References

1. Wingerchuk DM, Brenda B, Bennett JL, Cabre P, Carroll W, Chitnis T, et al. International consensus diagnostic criteria for neuromyelitis optica spectrum disorders. *Neurology* (2015) 85:177–89. doi: 10.1212/WNL.0000000000001729

2. Clarke L, Arnett S, Lilley K, Liao J, Bhuta S, Broadley SA. Magnetic resonance imaging in neuromyelitis optica spectrum disorder. *Clin Exp Immunol* (2021) 206:251–65. doi: 10.1111/cei.13630

3. Carnero Contentti E, Daccach Marques V, Soto de Castillo I, Tkachuk V, Antunes Barreira A, Armas E, et al. Frequency of brain MRI abnormalities in neuromyelitis optica spectrum disorder at presentation: A cohort of Latin American patients. *Mult Scler Relat Disord* (2018) 19:73–8. doi: 10.1016/j.msard.2017.11.004

4. Yang Y, Li J, Li T, Li Z, Zhuo Z, Han X, et al. Cerebellar connectome alterations and associated genetic signatures in multiple sclerosis and neuromyelitis optica spectrum disorder. *J Transl Med* (2023) 21:352. doi: 10.1186/s12967-023-04164-w

5. Yan Z, Wang X, Zhu Q, Shi Z, Chen X, Han Y, et al. Alterations in white matter fiber tracts characterized by automated fiber-tract quantification and their correlations with cognitive impairment in neuromyelitis optica spectrum disorder patients. *Front Neurosci* (2022) 16:904309. doi: 10.3389/fnins.2022.904309

6. Liu Y, Duan Y, He Y, Wang J, Xia M, Yu C, et al. Altered topological organization of white matter structural networks in patients with neuromyelitis optica. *PloS One* (2012) 7:e48846. doi: 10.1371/journal.pone.0048846

7. Han Y, Liu Y, Zeng C, Luo Q, Xiong H, Zhang X, et al. Functional connectivity alterations in neuromyelitis optica spectrum disorder: correlation with disease duration and cognitive impairment. *Clin Neuroradiol* (2020) 30:559–68. doi: 10.1007/s00062-019-00802-3

8. Finke C, Zimmermann H, Pache F, Oertel FC, Chavarro VS, Kramarenko Y, et al. Association of visual impairment in neuromyelitis optica spectrum disorder with visual network reorganization. *JAMA Neurol* (2018) 75:296–303. doi: 10.1001/jamaneurol.2017.3890

9. Rocca MA, Savoldi F, Valsasina P, Radaelli M, Preziosa P, Comi G, et al. Cross-modal plasticity among sensory networks in neuromyelitis optica spectrum disorders. *Mult Scler* (2019) 25:968–79. doi: 10.1177/1352458518778008

10. Bigaut K, Achard S, Hemmert C, Baloglu S, Kremer L, Collongues N, et al. Resting-state functional MRI demonstrates brain network reorganization in neuromyelitis optica spectrum disorder (NMOSD). *PloS One* (2019) 14:e0211465. doi: 10.1371/journal.pone.0211465

11. Pang JC, Aquino KM, Oldehinkel M, Robinson PA, Fulcher BD, Breakspear M, et al. Geometric constraints on human brain function. *Nature* (2023) 618:566–74. doi: 10.1038/s41586-023-06098-1

12. Tian D-C, Xiu Y, Wang X, Shi K, Fan M, Li T, et al. Cortical thinning and ventricle enlargement in neuromyelitis optica spectrum disorders. *Front Neurol* (2020) 11:872. doi: 10.3389/fneur.2020.00872

13. Levy M, Haycox AR, Becker U, Costantino C, Damonte E, Klingelschmitt G, et al. Quantifying the relationship between disability progression and quality of life in patients treated for NMOSD: Insights from the SAkura studies. *Mult Scler Relat Disord* (2022) 57:103332. doi: 10.1016/j.msard.2021.103332

14. Capobianco M, Ringelstein M, Welsh C, Lobo P, deFiebre G, Lana-Peixoto M, et al. Characterization of disease severity and stability in NMOSD: a global clinical record review with patient interviews. *Neurol Ther* (2023) 12:635–50. doi: 10.1007/s40120-022-00432-x

15. Drulovic J, Martinovic V, Basuroski ID, Mesaros S, Mader S, Weinshenker B, et al. Long-term outcome and prognosis in patients with neuromyelitis optica spectrum disorder from Serbia. *Mult Scler Relat Disord* (2019) 36:101413. doi: 10.1016/j.msard.2019.101413

16. Uzawa A, Mori M, Masuda H, Uchida T, Muto M, Ohtani R, et al. Long-term disability progression in aquaporin-4 antibody-positive neuromyelitis optica spectrum disorder: a retrospective analysis of 101 patients. *J Neurol Neurosurg Psychiatry* (2024) 4:jnnp-2023–33266. doi: 10.1136/jnnp-2023-332663

17. Schmidt P, Gaser C, Arsic M, Buck D, Förschler A, Berthele A, et al. An automated tool for detection of FLAIR-hyperintense white-matter lesions in Multiple Sclerosis. *NeuroImage* (2012) 59:3774–83. doi: 10.1016/j.neuroimage.2011.11.032

18. Yan CG, Craddock RC, Zuo XN, Zang YF, Milham MP. Standardizing the intrinsic brain: towards robust measurement of inter-individual variation in 1000 functional connectomes. *Neuroimage* (2013) 80:246–62. doi: 10.1016/j.neuroimage.2013.04.081

19. Zhou F, Wu L, Qian L, Kuang H, Zhan J, Li J, et al. The relationship between cortical morphological and functional topological properties and clinical manifestations in patients with posttraumatic diffuse axonal injury: an individual brain network study. *Brain Topogr* (2023) 36:936–45. doi: 10.1007/s10548-023-00964-x

20. Tzourio-Mazoyer N, Landeau B, Papathanassiou D, Crivello F, Etard O, Delcroix N, et al. Automated anatomical labeling of activations in SPM using a macroscopic anatomical parcellation of the MNI MRI single-subject brain. *Neuroimage* (2002) 15:273–89. doi: 10.1006/nimg.2001.0978

21. Wang H, Jin X, Zhang Y, Wang J. Single-subject morphological brain networks: connectivity mapping, topological characterization and test-retest reliability. *Brain Behav* (2016) 6:e00448. doi: 10.1002/brb3.448

22. Wang J, Wang X, Xia M, Liao X, Evans A, He Y. GRETNA: a graph theoretical network analysis toolbox for imaging connectomics. *Front Hum Neurosci* (2015) 9:386. doi: 10.3389/fnhum.2015.00386

23. Chen Y, Lei D, Cao H, Niu R, Chen F, Chen L, et al. Altered single-subject gray matter structural networks in drug-naïve attention deficit hyperactivity disorder children. *Hum Brain Mapp* (2022) 43(4):1256–64. doi: 10.1002/hbm.25718

24. Li X, Lei D, Niu R, Li L, Suo X, Li W, et al. Disruption of gray matter morphological networks in patients with paroxysmal kinesigenic dyskinesia. *Hum Brain Mapp* (2021) 42:398–411. doi: 10.1002/hbm.25230

25. Kong X-Z, Wang X, Huang L, Pu Y, Yang Z, Dang X, et al. Measuring individual morphological relationship of cortical regions. *J Neurosci Methods* (2014) 237:103–10721. doi: 10.1016/j.jneumeth.2014.09.003

26. Wang L, Zhu Y, Wu L, Zhuang Y, Zeng J, Zhou F. Classification of chemotherapy-related subjective cognitive complaints in breast cancer using brain functional connectivity and activity: a machine learning analysis. *J Clin Med* (2022) 11:2267. doi: 10.3390/jcm11082267

27. Czarnecka D, Oset M, Karlińska I, Stasiołek M. Cognitive impairment in NMOSD-More questions than answers. *Brain Behav* (2020) 10:e01842. doi: 10.1002/brb3.1842

28. Cho EB, Han CE, Seo SW, Chin J, Shin JH, Cho HJ, et al. White matter network disruption and cognitive dysfunction in neuromyelitis optica spectrum disorder. *Front Neurol* (2018) 9:1104. doi: 10.3389/fneur.2018.01104

29. Kim HJ, Paul F, Lana-Peixoto MA, Tenembaum S, Asgari N, Palace J, et al. MRI characteristics of neuromyelitis optica spectrum disorder: an international update. *Neurology* (2015) 84:1165–73. doi: 10.1212/WNL.0000000000001367

30. Yan J, Wang Y, Miao H, Kwapong WR, Lu Y, Ma Q, et al. Alterations in the brain structure and functional connectivity in aquaporin-4 antibody-positive neuromyelitis optica spectrum disorder. *Front Neurosci* (2019) 13:1362. doi: 10.3389/fnins.2019.01362

31. Savoldi F, Rocca MA, Valsasina P, Riccitelli GC, Mesaros S, Drulovic J, et al. Functional brain connectivity abnormalities and cognitive deficits in neuromyelitis optica spectrum disorder. *Mult Scler* (2020) 26:795–805. doi: 10.1177/1352458519845109

32. Wingerchuk DM, Lucchinetti CF. Neuromyelitis optica spectrum disorder. *N Engl J Med* (2022) 387:631–9. doi: 10.1056/NEJMra1904655

33. Fleischer V, Gröger A, Koirala N, Droby A, Muthuraman M, Kolber P, et al. Increased structural white and grey matter network connectivity compensates for functional decline in early multiple sclerosis. *Mult Scler* (2017) 23:432–41. doi: 10.1177/1352458516651503

34. Bazán PR, Biazoli CE Jr., Sato JR, Amaro E Jr. Motor readiness increases brain connectivity between default-mode network and motor cortex: impact on sampling resting periods from fMRI event-related studies. *Brain Connect* (2015) 5:631–40. doi: 10.1089/brain.2014.0332

35. Høgestøl EA, Nygaard GO, Alnæs D, Beyer MK, Westlye LT, Harbo HF. Symptoms of fatigue and depression is reflected in altered default mode network connectivity in multiple sclerosis. *PloS One* (2019) 14:e0210375. doi: 10.1371/journal.pone.0210375

36. Liu Y, Jiang X, Butzkueven H, Duan Y, Huang J, Ren Z, et al. Multimodal characterization of gray matter alterations in neuromyelitis optica. *Mul Scler* (2018) 24:1308–16. doi: 10.1177/1352458517721053

37. Fiala C, Rotstein D, Pasic MD. Pathobiology, diagnosis, and current biomarkers in neuromyelitis optica spectrum disorders. *J Appl Lab Med* (2022) 7(1):305–10. doi: 10.1093/jalm/jfab150

38. Corps J, Rekik I. Morphological brain age prediction using multi-view brain networks derived from cortical morphology in healthy and disordered participants. *Sci Rep* (2019) 9(1):9676. doi: 10.1038/s41598-019-46145-4

39. Wei R, Xu X, Duan Y. Brain age gap in neuromyelitis optica spectrum disorders and multiple sclerosis. *J Neurol Neurosurg Psychiatry* (2023) 94:31–7. doi: 10.1136/jnnp-2022-329680

40. Zhuang Y, Qian L, Wu L, Chen L, He F, Zhang S, et al. Is brain network efficiency reduced in young survivors of acute lymphoblastic leukemia?-evidence from individual-based morphological brain network analysis. *J Clin Med* (2022) 11:5362. doi: 10.3390/jcm11185362

41. Tijms BM, Series P, Willshaw DJ, Lawrie SM. Similarity-based extraction of individual networks from gray matter MRI scans. *Cereb Cortex* (2012) 22:1530–41. doi: 10.1093/cercor/bhr221

frontiers | Frontiers in Immunology

TYPE Original Research
PUBLISHED 30 April 2024
DOI 10.3389/fimmu.2024.1362960

OPEN ACCESS

EDITED BY
Philippe Monnier,
University Health Network (UHN), Canada

REVIEWED BY
David Wagner,
University of Colorado Anschutz Medical Campus, United States
Pablo García De Frutos,
Spanish National Research Council (CSIC), Spain

*CORRESPONDENCE
Domizia Vecchio
domizia.vecchio@med.uniupo.it

†These authors have contributed equally to this work

RECEIVED 29 December 2023
ACCEPTED 03 April 2024
PUBLISHED 30 April 2024

CITATION
D'Onghia D, Colangelo D, Bellan M, Tonello S, Puricelli C, Virgilio E, Apostolo D, Minisini R, Ferreira LL, Sozzi L, Vincenzi F, Cantello R, Comi C, Pirisi M, Vecchio D and Sainaghi PP (2024) Gas6/TAM system as potential biomarker for multiple sclerosis prognosis. *Front. Immunol.* 15:1362960. doi: 10.3389/fimmu.2024.1362960

Gas6/TAM system as potential biomarker for multiple sclerosis prognosis

Davide D'Onghia[1,2†], Donato Colangelo[3,4†], Mattia Bellan[1,2,5], Stelvio Tonello[1,2], Chiara Puricelli[6], Eleonora Virgilio[7], Daria Apostolo[1], Rosalba Minisini[1], Luciana L. Ferreira[1], Leonardo Sozzi[1], Federica Vincenzi[1], Roberto Cantello[7], Cristoforo Comi[8], Mario Pirisi[1,2,5], Domizia Vecchio[4,7*] and Pier Paolo Sainaghi[1,2,4,5]

[1]Department of Translational Medicine, University of Piemonte Orientale (UPO), Novara, Italy, [2]Center for Autoimmune and Allergic Diseases (CAAD), University of Piemonte Orientale (UPO), Novara, Italy, [3]Department of Health Sciences, Pharmacology, University of Piemonte Orientale (UPO), Novara, Italy, [4]Department of Health Sciences, Interdisciplinary Research Center of Autoimmune Diseases (IRCAD), University of Piemonte Orientale (UPO), Novara, Italy, [5]Internal Medicine and Rheumatology Unit, Azienda Ospedaliera Universitaria (AOU) "Maggiore della Carita", Novara, Italy, [6]Department of Health Sciences, Clinical Biochemistry, University of Piemonte Orientale (UPO), Novara, Italy, [7]Department of Translational Medicine, Neurology Unit, Maggiore Della Carità Hospital, University of Piemonte Orientale, Novara, Italy, [8]Department of Translational Medicine, Neurology Unit, S. Andrea Hospital, University of Piemonte Orientale (UPO), Vercelli, Italy

Introduction: The protein growth arrest-specific 6 (Gas6) and its tyrosine kinase receptors Tyro-3, Axl, and Mer (TAM) are ubiquitous proteins involved in regulating inflammation and apoptotic body clearance. Multiple sclerosis (MS) is the most common inflammatory demyelinating disease of the central nervous system leading to progressive and irreversible disability if not diagnosed and treated promptly. Gas6 and TAM receptors have been associated with neuronal remyelination and stimulation of oligodendrocyte survival. However, few data are available regarding clinical correlation in MS patients. We aimed to evaluate soluble levels of these molecules in the cerebrospinal fluid (CSF) and serum at MS diagnosis and correlate them with short-term disease severity.

Methods: In a prospective cohort study, we enrolled 64 patients with a diagnosis of clinical isolated syndrome (CIS), radiological isolated syndrome (RIS) and relapsing–remitting (RR) MS according to the McDonald 2017 Criteria. Before any treatment initiation, we sampled the serum and CSF, and collected clinical data: disease course, presence of gadolinium-enhancing lesions, and expanded disability status score (EDSS). At the last clinical follow-up, we assessed EDSS and calculated MS severity score (MSSS) and age-related MS severity (ARMSS). Gas6 and TAM receptors were determined using an ELISA kit (R&D Systems) and compared to neurofilament (NFLs) levels evaluated with SimplePlex™ fluorescence-based immunoassay.

Results: At diagnosis, serum sAxl was higher in patients receiving none or low-efficacy disease-modifying treatments (DMTs) *versus* patients with high-efficacy DMTs (p = 0.04). Higher CSF Gas6 and serum sAXL were associated with an EDSS <3 at diagnosis (p = 0.04; p = 0.037). Serum Gas6 correlates to a lower MSSS (r^2 = –0.32, p = 0.01). Serum and CSF NFLs were confirmed as disability biomarkers in our cohort according to EDSS (p = 0.005; p = 0.002) and MSSS (r^2 = 0.27, p = 0.03; r^2 = 0.39, p = 0.001). Results were corroborated using multivariate analysis.

10.3389/fimmu.2024.1362960

Conclusions: Our data suggest a protective role of Gas6 and its receptors in patients with MS and suitable severity disease biomarkers.

KEYWORDS

Gas6, TAM receptors, multiple sclerosis, inflammation, biomarker

Introduction

Multiple sclerosis (MS) is an inflammatory demyelinating disease of the central nervous system (CNS) characterized by progressive and irreversible disability with a high impact on patients' quality of life (1). Both inflammatory and neurodegenerative aspects contribute to the disease (2). Inflammation contributes to myelin destruction in the CNS, to damaging of oligodendrocytes (ODs), and activation of astrocytes with neuronal damage (3). It has also been observed that ODs undergo cell death in newly formed lesions, which preludes the appearance of extensive regions of demyelination (4). Growth arrest-specific 6 (Gas6) and its receptors have been shown to play a critical role in innate immune system homeostasis by regulating apoptosis and inflammation (5). Gas6 is a soluble glycoprotein of 75 kDa that belongs to the vitamin K-dependent protein family (6). To exert its biological functions, Gas6 must interact with a specific family of tyrosine kinase receptors, called TAM, consisting of three different receptors: Tyro-3, Axl, and Mer (7). TAM receptors play important roles in cell survival, growth, aggregation and migration, angiogenesis, and control of inflammatory responses, apoptotic cell and membrane engulfment, and phagocytic elimination (8). TAM receptors can be cleaved into their soluble forms (sTyro-3, sAxl, and sMer) by specific proteases, ADAM 10 and 17 (9). These soluble receptors can still bind Gas6 protein retaining their functions in the modulation of inflammation (7). TAM receptors are widely expressed in the nervous system, including ODs, and Gas6/TAMs have been associated with stimulation of OD survival and neuronal remyelination (10). Axl has the highest affinity for Gas6 (11), and the experimental evidence supports a direct role in neuronal myelinization (12). However, few data are available regarding the clinical correlation in MS patients. We aimed to assess the soluble levels of these molecules in the cerebrospinal fluid (CSF) and serum, at the time of MS diagnosis, and evaluate their possible correlations with short-term disease severity.

Materials and methods

Patients

In this observational prospective cohort study, we recruited, between October 2017 and February 2022, 64 patients (43 females) in "Maggiore della Carità" Hospital in Novara, Italy. All patients had a follow-up visit at least 1 year after their diagnosis, between July 2021 and December 2022. The clinical data were acquired twice, both at the diagnosis and at the last follow-up visit. CSF and serum samples were obtained at diagnosis while the patients underwent MS diagnostic work-up. The study's inclusion criteria were the diagnosis of clinical isolated syndrome (CIS), radiological isolated syndrome (RIS), or relapsing–remitting (RR), according to McDonald 2017 (13) at the end of the follow-up.

Ethical committee

All the participants signed an informed consent form. The study protocol was approved by the local Ethical Committee (CE 262/2022) and was conducted in accordance with the Declaration of Helsinki.

Clinical evaluation

Demographic and clinical variables collected at diagnosis were sex, age at onset, clinical course, the presence of gadolinium-enhancing (Gad+) lesions, and disability according to the expanded disability status score (EDSS) (14). Brain and spinal imaging were performed within 3 months from the diagnosis on a 1.5-Tesla MRI with a single dose of Gad. EDSS was used to assess disability and monitor changes over time. This score has been corrected by time-measure using the *MS* severity score (MSSS) (15) and by the age using the age-related MS severity (ARMSS) (16).

Sample collection and biomarker determinations

Cerebrospinal fluid (CSF) was collected through lumbar puncture at diagnosis. CSF was centrifuged at 1,300 rpm for 10 min and stored at −80°C until the analysis. At the time of CSF collection, all patients were treatment naïve (including disease-modifying treatments or DMTs and steroids). Serum was immediately collected by centrifugation at 3,500 rpm for 15 min and stored at −80°C until the analysis time. CSF and serum NFLs were measured with the Simple PlexTM fluorescence-based

10.3389/fimmu.2024.1362960

immunoassay by Bio-Techne with the Ella SimplePlex™ Platform (Bio-Techne s.r.l., Milan, Italy). NFLs were measured using the Human NFL SimplePlex™ Cartridge Kit (Lot no. 21519). All kit components (cartridge, sample diluent SD13, and Wash Buffer A) were provided ready to use, and they were allowed to reach room temperature before use. CSF and serum levels of Gas6 were determined with ELISA technique using a commercial kit (R&D Systems Duo Set Elisa DY6488, McKinley, MN, USA) and following the manufacturer's instructions. Samples were diluted 1:50 in a sample diluent. The optical density at 450 nm was fitted versus a calibration curve prepared with a standard (0–1 ng/ml range), as suggested by the manufacturer. CSF and serum levels of sTyro-3 were determined with the commercially available T ELISA kit (R&D Systems Duo Set Elisa DY6488, McKinley, MN, USA) following the manufacturer's instructions. Samples were diluted 1:5 in a sample diluent. The optical density at 450 nm was fitted versus a calibration curve prepared with a standard (0–4 ng/ml range), as suggested by the manufacturer. The ELISA technique determined CSF and serum levels of sAxl by using a commercial kit (R&D Systems Duo Set Elisa DY6488, McKinley, MN, USA) and following the manufacturer's instructions. Samples were diluted 1:25 in a sample diluent. The optical density at 450 nm was fitted versus a calibration curve prepared with a standard (0–4 ng/ml range), as suggested by the manufacturer. The ELISA technique determined CSF and serum levels of sMer using a commercial kit (R&D Systems Duo Set Elisa DY6488, McKinley, MN, USA) and following the manufacturer's instructions. Samples were diluted 1:2 in a sample diluent. The optical density at 450 nm was fitted versus a calibration curve prepared with a standard (0–10 ng/ml range), as suggested by the manufacturer. Absorbance was recorded using a Victor X4 microplate reader (Perkin Elmer, Waltham, MA, USA).

Statistical analysis

For continuous variables, the measures of centrality and dispersion were medians and interquartile ranges [IQR], and comparisons between groups regarding these variables were performed using the Mann–Whitney U-test and the Kruskal–Wallis test. The Pearson $\chi 2$ was used to analyze the association between categorical variables shown as frequencies (%). Correlations were performed with Spearman's rank correlation coefficient and linear regression for significant predictors in the univariate model. Multivariable regressions were built to identify the variables independently associated with the severity score. The threshold for statistical significance was 0.05 (two tailed). Statistical analyses were performed with Stata statistical software version 17.0 (Stata Corp, 4905 Lakeway Drive College Station, TX, USA), while graphs were created using GraphPad Prism version 9.4.0 (GraphPad Software, La Jolla, CA, USA).

TABLE 1 General features of the study population and their clinical parameters.

Demographics parameters and clinical scores	# of patients
Sex (F/M)	43 (67.19)/ 21 (32.81)
Age (years)	37 [19.0–61.0]
Age at onset (years)	32 [14.0–56.0]
Disease course	
Radiological isolated syndrome	2 (3.12)
Clinical isolated syndrome	3 (4.69)
Relapsing–remitting MS	59 (92.19)
MRI features	
Gadolinium-enhancing lesions	39 (60.94)
Brain lesions >10	36 (56.25)
Spinal lesion (yes)	44 (67.19)
Disability measures	
Switch from first disease-modifying treatments within 1 year	9 (5.7)*
EDSS at diagnosis EDSS < 3 at diagnosis	1.5 [0.0–6.0] 55 (85.94)
EDSS at last follow-up EDSS < 3 at last follow-up	1.5 [0.0–6.5] 56 (87.5)
MSSS at last follow-up	2.85 [0.24–9.59]
ARMSS at last follow-up	3.22 [0.29–8.47]
Biomarkers at diagnosis	
NFLs (pg/ml) Serum CSF	29.55 [12.1–262] 1,590.5 [201–35,824]
Gas 6 (ng/ml) Serum CSF	23.49 [12.26–54.65] 7.76 [1.80–32.75]
sAxl (ng/ml) Serum CSF	29.22 [15.42–231.3] 26.38 [7.9–48.19]
sMer (ng/ml) Serum CSF	2.54 [0.0–55.1] 0.0 [0.0–0.0]
sTyro-3 (ng/ml) Serum CSF	3.54 [1.77–9.63] 3.79 [1.71–6.56]

Continuous variables are presented as medians [IQR] and categorical variables as frequencies (%). CSF, cerebrospinal fluid; OB, oligoclonal bands; EDSS, expanded disability status scale, MSSS, multiple sclerosis severity score; ARMSS, age-related multiple sclerosis severity; NFLs, neurofilaments.
*Of the patients, 3/9 stopped/changed the first DMT for side effects, not for efficacy.

Results

The main features of our 64 patients are reported in Table 1.

Initially, we investigated serum and CSF levels of Gas6 and its receptor. All molecules were detectable except for CSF sMer. Gas6, sAxl, and sMer concentrations resulted moderately higher in the serum than in the CSF, thus showing an opposite trend to NFLs levels that are more elevated in the CSF as largely reported (17). Our data show no statistically significant correlation between serum and CSF concentrations of Gas6, whereas serum and CSF levels of

10.3389/fimmu.2024.1362960

sTyro-3 (p = 0.05), sAxl (p = 0.02), and NFLs (p = 0.0001) were significantly related between the two fluids (sMer was not analyzed since it was undetectable in the CSF) (Figure 1).

We compared the RIS–CIS population to those patients with RRMS and found higher sMer and sTyro-3 serum levels at the diagnosis in the RIS-CIS subgroup (Supplementary Figure 1). No statistically significant results were found in the CSF.

MS treatments and disability

At the end of the follow-up, 7 (11%) patients were receiving no treatment; 37 (58%), a low-efficacy; and 20 (31%), high-efficacy DMTs. Six (9%) patients switched to high-efficacy therapy during the follow up. Instead, 3 (5%) patients stopped/changed the first DMTs for side effects (not for inefficacy). As shown in Figure 2, serum sAxl was higher in those patients who underwent no treatment or on low-efficacy DMTs.

To evaluate disability measures, we divided our patients according to EDSS scores < 3 or ≥ 3 at first and follow-up visit. As shown in Figure 3, we found a higher serum sAxl and CSF Gas6 levels in those patients with EDSS < 3 at diagnosis. As expected, higher NFL levels in the CSF and serum were associated with higher EDSS scores at diagnosis. No significant result associations were observed with the EDSS at follow-up visit (data not shown). Subsequently, we considered disability according to MSSS and

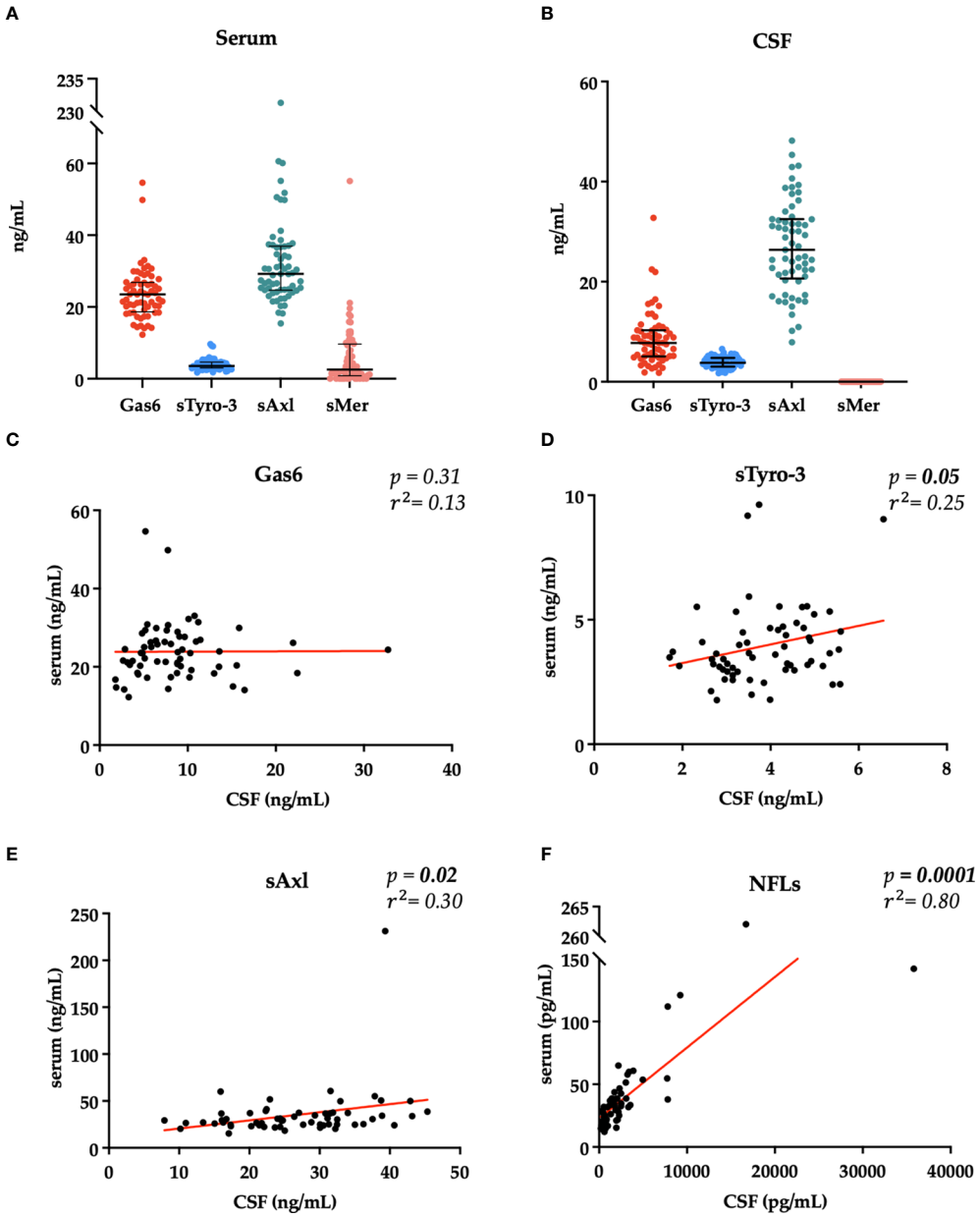

FIGURE 1
Distribution of Gas6 and TAM receptor concentrations in serum **(A)** and CSF **(B)**. Results are shown as medians [IQR]. Spearman's rank correlation between serum and CSF levels of Gas6 **(C)**, sTyro-3 **(D)**, sAxl (**(E)**, and NFLs **(F)** concentrations. r^2, coefficient of correlation; p, p-value.

ARMSS at the last follow-up. As shown in Figure 4, an inverse correlation was found only for serum Gas6 and MSSS. On the other hand, as expected, NFL levels in the serum and CSF directly correlated with MSSS. No other significant correlations were found with ARMSS (Supplementary Figure 2).

We did not find any difference in Gas6 and TAM receptors according to the number of brain, spinal, and gadolinium-enhancing lesions (Supplementary Table 2).

Multivariate analysis

We finally performed multivariate regression models to predict MS disability according to EDSS at diagnosis (Table 2) and MSSS at last follow-up (Table 3). The included independent variables were gender, age, number of lesions, and the other serum biomarkers. We did not find statistically significative predictors in the multivariate analyses for different types of MS and in the type of therapy at follow- up visit (Supplementary Tables 8, 9).

Discussion

In our prospective cohort study, first, we evaluated the CSF and serum Gas6 and TAM receptor levels in MS patients at diagnosis. All biomarkers were detectable, except for sMer that was absent in the CSF, as also previously reported and discussed by our group (18). The absence of sMer could be related to a lower expression in

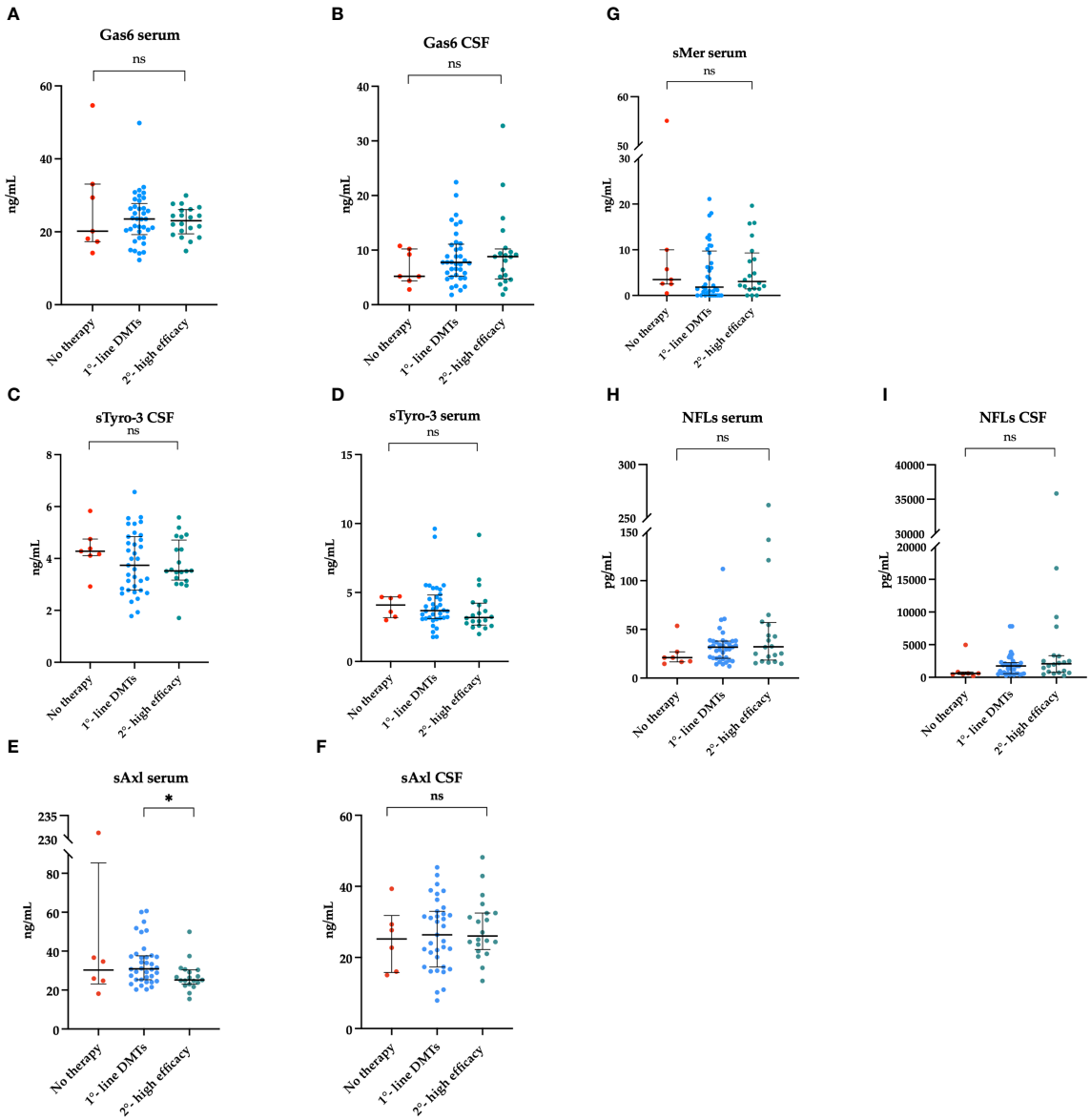

FIGURE 2
Association between Gas6 concentration in the serum **(A)** and CSF **(B)**, sTyro3 concentration in the serum **(C)** and CSF **(D)**, sAxl concentration in the serum **(E)** and CSF **(F)**, sMer concentration in the serum **(G)**, NFLs concentration in the serum **(H)** and CSF **(I)** and the type of therapy at follow-up visit. Results are shown as medians [IQR]. *p = 0.04, ns, not significant.

10.3389/fimmu.2024.1362960

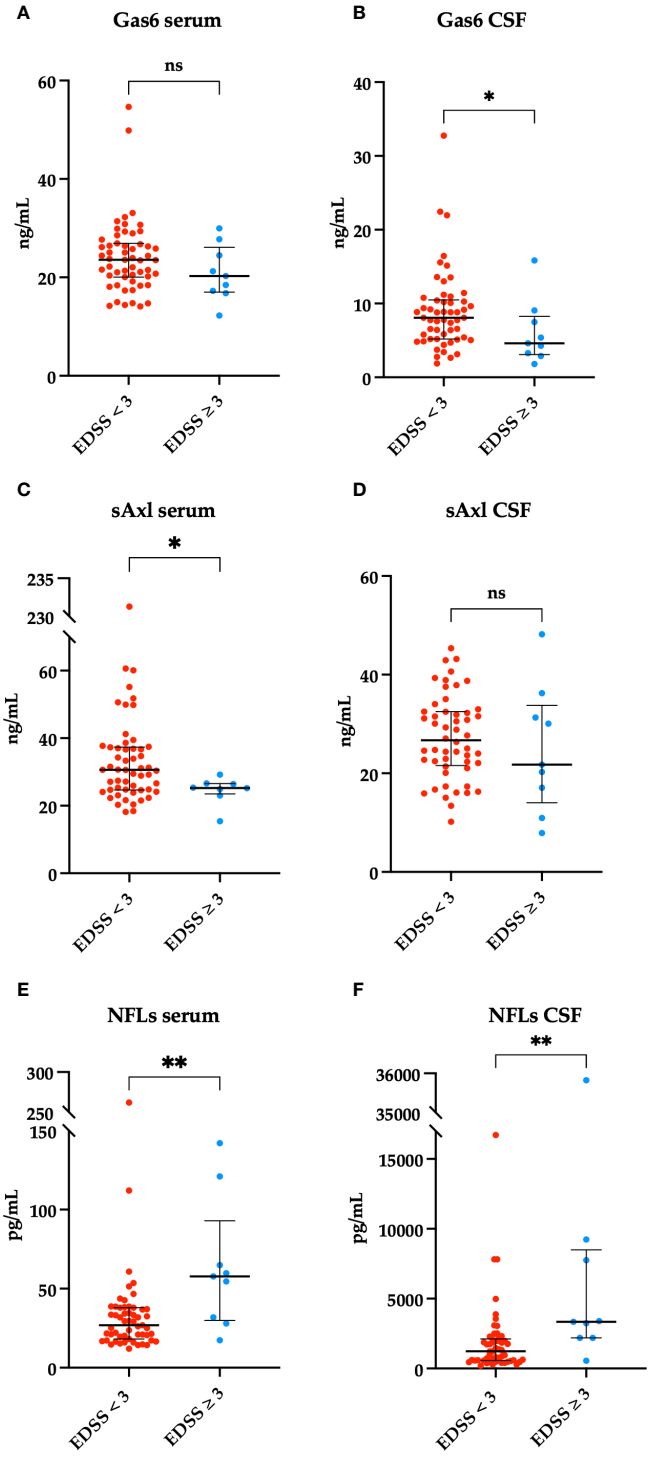

FIGURE 3
Associations between Gas6 levels in the serum and CSF (ng/ml) and < 3 or ≥ 3 EDSS clinical scores on the first visit. *p = 0.04 **(A, B)**. sAxl levels in the serum and CSF (ng/ml) in patients with < 3 or ≥ 3 EDSS clinical scores on the first visit. *p = 0.037 **(C, D)**. Associations between NFLs levels in the serum and CSF (pg/mL) and < 3 or ≥ 3 EDSS clinical scores on the first visit. **p = 0.005, **p = 0.002 **(E, F)**. Results are shown as medians [IQR]. ns, not significant.

the brain compared to sAxl and sTyro-3 (19). Moreover, in the present study, we first compared Gas6 and TAM receptors to NFLs: Gas6, sAxl, and sMer levels resulted higher in the serum than in the CSF, thus showing an opposite trend to that of NFLs (17). A possible role of TAM receptors in MS is related to the clearance of myelin debris for the remyelination process, which can be reduced by ineffective phagocytosis (20), as could happen in the dysregulation of TAM signaling (21). Among the TAM receptors, Tyro-3 could be the main actor in mediating the promyelinating effects of Gas6 during developmental myelination (10).

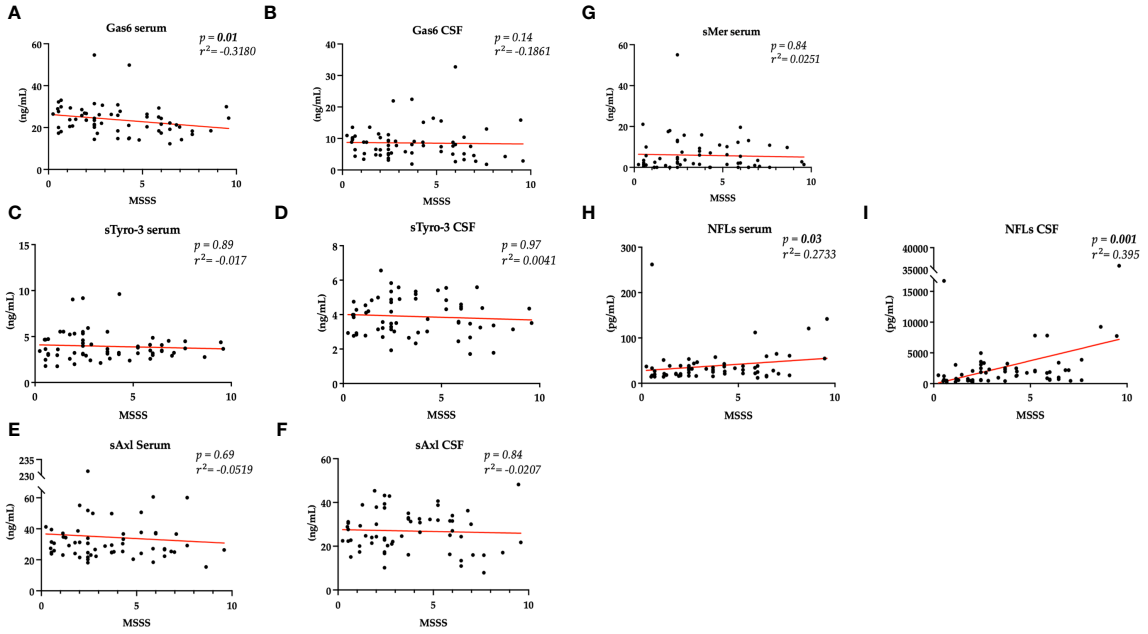

FIGURE 4
Spearman's correlation between MSSS and Gas6 levels in the serum and CSF **(A, B)**, TAM receptors levels in the serum and CSF **(C–G)**, and NFLs levels in the serum and CSF **(H, I)**. r^2 = coefficient of correlation, p = p-value.

Consequently, loss of Tyro-3 causes a delay in myelinization and a reduction in myelin thickness both *in vitro* and *in vivo* (22, 23). Looking at Mer and Axl, they regulate microglial functions (24, 25) and normally drive phagocytosis of apoptotic cells generated during adult neurogenesis (26, 27).

Second, we searched for any association with clinical features at disease diagnosis. Looking at disability at diagnosis, those patients with EDSS score < 3 showed higher levels of CSF Gas6 and serum sAxl levels, whereas, as expected, there was a statistically significant correlation between higher levels of CSF and serum NFLs and EDSS ≥ 3 (28). Our data suggested a role of sAxl to identify those cases with low disability at onset and then treated with low-efficacy DMTs. A possible pathogenic hypothesis is related to the Gas6 and TAM receptors expression in several cell types in the nervous system, including ODs (29). Activation of the Axl receptor by Gas6 induces an intracellular response that promotes oligodendrocyte survival and stimulates the myelination process (30). Nonetheless, hyperactivation of the immune system also contributes to impaired remyelination, as demonstrated in experimental autoimmune encephalomyelitis. In this mouse model, loss of Axl increases

TABLE 2 Multivariate regression model of EDSS < 3 at diagnosis including demographic and severity variables.

Predictor	Coefficient	Standard error	p-value	95% confidence interval
Gas6 serum (ng/mL)	−0.0169	0.0075	**0.029**	−0.0320–−0.0018
Gas6 CSF (ng/mL)	−0.0192	0.0089	**0.037**	−0.0372–−0.0012
sAXL serum (ng/mL)	−0.0026	0.0044	0.55	−0.0112–0.0063
sMer serum (ng/mL)	0.0067	0.0081	0.41	−0.0097–0.0231
sTyro-3 serum (ng/mL)	0.0002	0.0290	0.99	−0.0582–0.0586
NFL serum (pg/mL)	0.0020	0.0011	0.21	−0.0026–0.0044
Age	0.0025	0.0045	0.58	−0.0066–0.0116
Gender	−0.060	0.0936	0.52	−0.2487–0.1279
N° brain lesion >10	0.1444	0.0907	0.11	−0.0381–0.3269
Spinal lesion	0.0985	0.0900	0.28	0.0819–0.2871
Gadolinium enhancing	0.7653	0.6075	0.41	−0.0826–0.2796

In bold are indicated statistically significant results ($p < 0.05$).
After the multivariate analysis, only serum and CSF Gas6 levels (p = 0.029; p = 0.037) resulted as predictors for the disability at the first visit according to EDSS.

TABLE 3 Multivariate regression model of MSSS at last follow-up including demographic and severity variables.

Predictor	Coefficient	Standard error	p-value	95% confidence inte
Gas6 serum (ng/mL)	−0.1577	0.0503	**0.003**	−0.2588–−0.0565
sAXL serum (ng/mL)	0.0317	0.0285	0.27	−0.0256–0.1227
sMer serum (ng/mL)	0.0192	0.0515	0.71	−0.0843–0.1205
sTyro-3 serum (ng/mL)	0.0687	0.1983	0.73	−0.3298–0.4673
NFL serum (pg/mL)	0.0098	0.0078	0.21	−0.0059–0.0257
Age	0.0688	0.0305	**0.029**	0.0074–0.1302
Gender	−0.7116	0.6308	0.26	−1.9793–0.5560
N° brain lesion >10	0.2788	0.5978	0.64	−0.9226–1.4803
Spinal lesion	1.3529	0.6075	**0.035**	0.0970–2.6088
Gadolinium enhancing	0.7653	0.6075	0.41	−0.4555–1.9861

In bold are indicated statistically significant results ($p < 0.05$).
Disability over time according to MSSS was predicted by serum Gas6 (p = 0.003), age, and the presence of spinal lesions.

central nervous system inflammation delaying the removal of myelin debris (12). Furthermore, several studies in Gas6 and Axl-knockout mice showed remyelination abnormalities due to increased microglia activation confirming specific contributions of Gas6/Axl signaling in the remyelination processes. Exposure to toxic cuprizone resulted in axon damage in mutant mice, which is associated with an abnormal inflammatory response due to reduced SOCS expression, suggesting that Gas6/Axl signaling may be important in reducing CNS inflammation and maintaining axon integrity after demyelinating/proinflammatory stimuli (12, 31–35).

Third, a prognostic role over time emerged only for serum Gas6 since lower levels of this biomarker is related to higher MSSS. This result suggests a protective role in MS. As expected, on the contrary, higher CSF and serum NFLs levels are related to higher MSSS score. Gas6 is involved in different cellular processes with anti-inflammatory, neuroprotective, promyelinating properties, and a biomarker for acute disease course. On the other side, our group measured CSF and plasma Gas6 protein during relapses in relation to the clinical features (symptoms) and severity scores as the Kurtzke Functional System (FS) showing the usefulness of Gas6 as a biomarker of an acute disease course (36–39).

Moreover, the Gas6 TAM pathway is involved in viral response, including thus EBV infection (2, 40–42), increasing during a viral infection (7). Gas6 may act as a modulator of inflammation, regulating the immune response and limiting the inflammation and tissue damage associated with viral infection (43). Furthermore, activation of TAM receptors by Gas6 may influence the response of immune cells, including macrophages and dendritic cells, by promoting phagocytosis of infected cells and antigen presentation (44, 45). Viral infection can also influence TAM receptors expression and Gas6 production (46). For instance, during EBV infection, it has been observed that Axl expression can increase in infected cells (47). However, the direct link between Gas6 and EBV still needs several studies to be proven.

With the present work, we focused our attention on prognosis and disability using different clinical scores that better indicate a disease course, such as the MSSS and the ARMSS. Although our study is a pilot analysis with some limitations, like the number of patients involved and the monocentric nature of the recruitment, results are promising and could be extended by the Gas6/TAM levels follow-up during the entire evolution of the pathology.

In conclusion, the Gas6-TAM axis showed a trend to identify those patients that could be considered more "benign." In fact, serum sAxl was higher in those patients with lower disability at onset, and serum Gas6 was higher in patients with lower disability over time.

Our study suggests serum Gas6 as a reliable prognostic biomarker; however, prospective further investigation about the protective role of the Gas6/TAM system role is needed.

Data availability statement

The original contributions presented in the study are included in the article/Supplementary Material. Further inquiries can be directed to the corresponding author.

Ethics statement

The studies involving humans were approved by Ethical Committee (CE 262/2022). The studies were conducted in accordance with the local legislation and institutional requirements. The participants provided their written informed consent to participate in this study.

Author contributions

DD: Conceptualization, Data curation, Formal analysis, Methodology, Visualization, Writing – original draft, Writing – review & editing. DC: Conceptualization, Data curation, Formal

analysis, Investigation, Project administration, Supervision, Writing – original draft, Writing – review & editing. MB: Conceptualization, Data curation, Methodology, Supervision, Writing – original draft, Writing – review & editing, Formal analysis, Project administration. ST: Conceptualization, Data curation, Investigation, Methodology, Supervision, Writing – review & editing, Project administration. CP: Formal analysis, Methodology, Validation, Writing – review & editing. EV: Investigation, Conceptualization, Data curation, Methodology, Project administration, Supervision, Writing – review & editing. DA: Formal analysis, Data curation, Methodology, Writing – original draft, Writing – review & editing. RM: Conceptualization, Project administration, Supervision, Validation, Writing – review & editing. LF: Methodology, Conceptualization, Data curation, Formal analysis, Supervision, Writing – review & editing. LS: Methodology, Writing – review & editing. FV: Methodology, Writing – review & editing. RC: Writing – review & editing, Conceptualization, Data curation, Investigation, Project administration, Supervision, Validation, Visualization, Writing – original draft. CC: Conceptualization, Formal analysis, Investigation, Project administration, Supervision, Validation, Visualization, Writing – original draft, Writing – review & editing. MP: Conceptualization, Data curation, Formal analysis, Methodology, Supervision, Validation, Visualization, Writing – original draft, Writing – review & editing. DV: Conceptualization, Data curation, Formal analysis, Investigation, Methodology, Project administration, Supervision, Visualization, Writing – original draft, Writing – review & editing. PS: Conceptualization, Data curation, Formal analysis, Funding acquisition, Investigation, Methodology, Project administration, Resources, Supervision, Validation, Visualization, Writing – original draft, Writing – review & editing.

Funding

The author(s) declare that no financial support was received for the research, authorship, and/or publication of this article.

Conflict of interest

The authors declare that the research was conducted in the absence of any commercial or financial relationships that could be construed as a potential conflict of interest.

The author(s) declared that they were an editorial board member of Frontiers, at the time of submission. This had no impact on the peer review process and the final decision.

Publisher's note

Supplementary material

The Supplementary Material for this article can be found online at: https://www.frontiersin.org/articles/10.3389/fimmu.2024.1362960/full#supplementary-material

References

1. Garg N, Smith TW. An update on immunopathogenesis, diagnosis, and treatment of multiple sclerosis. *Brain Behav*. (2015) 5(9):e00362. doi: 10.1002/brb3.362

2. Filippi M, Bar-Or A, Piehl F, Preziosa P, Solari A, Vukusic S, et al. Multiple sclerosis. *Nat Rev Dis Prim*. (2018) 4(1):43. doi: 10.1038/s41572-018-0041-4

3. Matute-Blanch C, Brito V, Midaglia L, Villar LM, Garcia-Diaz Barriga G, Guzman de la Fuente A, et al. Inflammation in multiple sclerosis induces a specific reactive astrocyte state driving non-cell-autonomous neuronal damage. *Clin Transl Med*. (2022) 12(5):e837. doi: 10.1002/ctm2.837

4. Goudarzi S, Gilchrist SE, Hafizi S. Gas6 induces myelination through anti-inflammatory IL-10 and TGF-β Upregulation in white matter and glia. *Cells*. (2020) 9. doi: 10.3390/cells9081779

5. Van Der Meer JHM, van der Poll T, Van't Veer C. TAM receptors, Gas6, and protein S: Roles in inflammation and hemostasis. *Blood*. (2014) 123:2460–9. doi: 10.1182/blood-2013-09-528752

6. Manfioletti G, Brancolini C, Avanzi G, Schneider C. The protein encoded by a growth arrest-specific gene (gas6) is a new member of the vitamin K-dependent proteins related to protein S, a negative coregulator in the blood coagulation cascade. *Mol Cell Biol*. (1993) 13:4976–85. doi: 10.1128/MCB.13.8.4976

7. Lemke G, Rothlin CV. Immunobiology of the TAM receptors. *Nat Rev Immunol*. (2008) 8:327–36. doi: 10.1038/nri2303

8. Lu Q, Lemke G. Homeostatic regulation of the immune system by receptor tyrosine kinases of the Tyro 3 family. *Science*. (2001) 293:306–12. doi: 10.1126/science.1061663

9. Tajbakhsh A, Gheibi Hayat SM, Butler AE, Sahebkar A. Effect of soluble cleavage products of important receptors/ligands on efferocytosis: Their role in inflammatory, autoimmune and cardiovascular disease. *Ageing Res Rev*. (2019) 50:43–57. doi: 10.1016/j.arr.2019.01.007

10. Burstyn-Cohen T, Fresia R. TAM receptors in phagocytosis: Beyond the mere internalization of particles. *Immunol Rev*. (2023) 319:7–26. doi: 10.1111/imr.13267

11. Law LA, Graham DK, Di Paola J, Branchford BR. GAS6/TAM pathway signaling in hemostasis and thrombosis. *Front Med*. (2018) 5. doi: 10.3389/fmed.2018.00137

12. Gruber RC, Ray AK, Johndrow CT, Guzik H, Burek D, De Frutos PG, et al. Targeted GAS6 delivery to the CNS protects axons from damage during experimental autoimmune encephalomyelitis. *J Neurosci*. (2014) 34:16320–35. doi: 10.1523/JNEUROSCI.2449-14.2014

13. Thompson AJ, Banwell BL, Barkhof F, Carroll WM, Coetzee T, Comi G, et al. Diagnosis of multiple sclerosis: 2017 revisions of the McDonald criteria. *Lancet Neurol*. (2018) 17:162–73. doi: 10.1016/S1474-4422(17)30470-2

14. Meyer-Moock S, Feng YS, Maeurer M, Dippel FW, Kohlmann T. Systematic literature review and validity evaluation of the Expanded Disability Status Scale (EDSS) and the Multiple Sclerosis Functional Composite (MSFC) in patients with multiple sclerosis. *BMC Neurol*. (2014) 14:58. doi: 10.1186/1471-2377-14-58

15. Kister I, Kantarci OH. Multiple sclerosis severity score: concept and applications. *Mult Scler J*. (2020) 26:548–53. doi: 10.1177/1352458519880125

16. Manouchehrinia A, Westerlind H, Kingwell E, Zhu F, Carruthers R, Ramanujam R, et al. Age Related Multiple Sclerosis Severity Score: Disability ranked by age. *Mult Scler*. (2017) 23:1938–46. doi: 10.1177/1352458517690618

17. Bomont P. The dazzling rise of neurofilaments: Physiological functions and roles as biomarkers. *Curr Opin Cell Biol*. (2021) 68:181–91. doi: 10.1016/j.ceb.2020.10.011

18. Bellan M, Pirisi M, Sainaghi P. The gas6/TAM system and multiple sclerosis. *Int J Mol Sci*. (2016) 17:1807. doi: 10.3390/ijms17111807

19. Pierce AM, Keating AK. TAM receptor tyrosine kinases: Expression, disease and oncogenesis in the central nervous system. *Brain Res*. (2014) 1542:206–20. doi: 10.1016/j.brainres.2013.10.049

20. Mahad DH, Trapp BD, Lassmann H. Pathological mechanisms in progressive multiple sclerosis. *Lancet Neurol.* (2015) 14(2):183–93. doi: 10.1016/S1474-4422(14)70256-X

21. Tondo G, Perani D, Comi C. TAM receptor pathways at the crossroads of neuroinflammation and neurodegeneration. *Dis Markers.* (2019) 2019:2387614. doi: 10.1155/2019/2387614

22. Gilchrist SE, Pennelli GM, Hafizi S. Gas6/tam signalling negatively regulates inflammatory induction of gm-csf in mouse brain microglia. *Cells.* (2021) 10(12):3281. doi: 10.3390/cells10123281

23. Lutz AB, Chung WS, Sloan SA, Carson GA, Zhou L, Lovelett E, et al. Schwann cells use TAM receptor-mediated phagocytosis in addition to autophagy to clear myelin in a mouse model of nerve injury. *Proc Natl Acad Sci U S A.* (2017) 114:E8072–80. doi: 10.1073/pnas.1710566114

24. Gilchrist SE, Goudarzi S, Hafizi S. Gas6 inhibits toll-like receptor-mediated inflammatory pathways in mouse microglia *via* axl and mer. *Front Cell Neurosci.* (2020) 14:576650. doi: 10.3389/fncel.2020.576650

25. Fourgeaud L, Traves PG, Tufail Y, Leal-Bailey H, Lew ED, Burrola PG, et al. TAM receptors regulate multiple features of microglial physiology. *Nature.* (2016) 532:240–4. doi: 10.1038/nature17630

26. Weinger JG, Omari KM, Marsden K, Raine CS, Shafit-Zagardo B. Up-regulation of soluble Axl and Mer receptor tyrosine kinases negatively correlates with Gas6 in established multiple sclerosis lesions. *Am J Pathol.* (2009) 175:283–93. doi: 10.2353/ajpath.2009.080807

27. Wu H, Zheng J, Xu S, Fang Y, Wu Y, Zeng J, et al. Mer regulates microglial/macrophage M1/M2 polarization and alleviates neuroinflammation following traumatic brain injury. *J Neuroinflamm.* (2021) 18:1–20. doi: 10.1186/s12974-020-02041-7

28. Benkert P, Meier S, Schaedelin S, Manouchehrinia A, Yaldizli Ö, Maceski A, et al. Serum neurofilament light chain for individual prognostication of disease activity in people with multiple sclerosis: a retrospective modelling and validation study. *Lancet Neurol.* (2022) 21:246–57. doi: 10.1016/S1474-4422(22)00009-6

29. Binder MD, Kilpatrick TJ. TAM receptor signalling and demyelination. *NeuroSignals.* (2009) 17:277–87. doi: 10.1159/000231894

30. Goudarzi S, Rivera A, Butt AM, Hafizi S. Gas6 promotes oligodendrogenesis and myelination in the adult central nervous system and after lysolecithin-induced demyelination. *ASN Neuro.* (2016) 8(5):1759091416668430. doi: 10.1177/1759091416668430

31. Binder MD, Cate HS, Prieto AL, Kemper D, Butzkueven H, Gresle MM, et al. Gas6 deficiency increases oligodendrocyte loss and microglial activation in response to cuprizone-induced demyelination. *J Neurosci.* (2008) 28:5195–206. doi: 10.1523/JNEUROSCI.1180-08.2008

32. Tutusaus A, Marí M, Ortiz-Pérez JT, Nicolaes GAF, Morales A, García de Frutos P. Role of vitamin K-dependent factors protein S and GAS6 and TAM receptors in SARS-coV-2 infection and COVID-19-associated immunothrombosis. *Cells.* (2020) 9(10):2186. doi: 10.3390/cells9102186

33. Paolino M, Penninger JM. The role of TAM family receptors in immune cell function: Implications for cancer therapy. *Cancers (Basel).* (2016) 8(10):97. doi: 10.3390/cancers8100097

34. Ray AK, Dubois JC, Gruber RC, Guzik HM, Gulinello ME, Perumal G, et al. Loss of Gas6 and Axl signaling results in extensive axonal damage, motor deficits, prolonged neuroinflammation, and less remyelination following cuprizone exposure. (2017) 65(12):2051–69. doi: 10.1002/glia.23214

35. Tsiperson V, Li X, Schwartz GJ, Raine CS, Shafit-Zagardo B. GAS6 enhances repair following cuprizone-induced demyelination. *PloS One.* (2010) 5. doi: 10.1371/journal.pone.0015748

36. Vago JP, Amaral FA, van de Loo FAJ. Resolving inflammation by TAM receptor activation. *Pharmacol Ther.* (2021) 227:107893. doi: 10.1016/j.pharmthera.2021.107893

37. Shafit-Zagardo B, Gruber RC, DuBois JC. The role of TAM family receptors and ligands in the nervous system: From development to pathobiology. *Pharmacol Ther.* (2018) 188:97–117. doi: 10.1016/j.pharmthera.2018.03.002

38. Akkermann R, Aprico A, Perera AA, Bujalka H, Cole AE, Xiao J, et al. The TAM receptor Tyro3 regulates myelination in the central nervous system. *Glia.* (2017) 65:581–91. doi: 10.1002/glia.23113

39. Sainaghi PP, Collimedaglia L, Alciato F, Molinari R, Sola D, Ranza E, et al. Growth arrest specific gene 6 protein concentration in cerebrospinal fluid correlates with relapse severity in multiple sclerosis. *Mediators Inflamm.* (2013) 2013:406483. doi: 10.1155/2013/406483

40. Bjornevik K, Cortese M, Healy BC, Kuhle J, Mina MJ, Leng Y, et al. MULTIPLE SCLEROSIS Longitudinal analysis reveals high prevalence of Epstein-Barr virus associated with multiple sclerosis. (2022) 375(6578):296–301. doi: 10.1126/science.abj8222

41. Wieland L, Schwarz T, Engel K, Volkmer I, Krüger A, Tarabuko A, et al. Epstein-barr virus-induced genes and endogenous retroviruses in immortalized B cells from patients with multiple sclerosis. *Cells.* (2022) 11(22):3619. doi: 10.3390/cells11223619

42. Yang J, Hamade M, Wu Q, Wang Q, Axtell R, Giri S. Current and future biomarkers in multiple sclerosis. *Int J Mol Sci.* (2022) 23(11):5877. doi: 10.3390/ijms23115877

43. Morizono K, Chen ISY. Role of phosphatidylserine receptors in enveloped virus infection. *J Virol.* (2014) 88:4275–90. doi: 10.1128/JVI.03287-13

44. Grabiec AM, Goenka A, Fife ME, Fujimori T, Hussell T. Axl and MerTK receptor tyrosine kinases maintain human macrophage efferocytic capacity in the presence of viral triggers. *Eur J Immunol.* (2018) 48:855–60. doi: 10.1002/eji.201747283

45. Bellan M, Cittone MG, Tonello S, Rigamonti C, Castello LM, Gavelli F, et al. Gas6/TAM system: A key modulator of the interplay between inflammation and fibrosis. *Int J Mol Sci.* (2019) 20(20):5070. doi: 10.3390/ijms20205070

46. Tonello S, Rizzi M, Matino E, Costanzo M, Casciaro GF, Croce A, et al. Baseline plasma gas6 protein elevation predicts adverse outcomes in hospitalized COVID-19 patients. *Dis Markers.* (2022) 2022:1568352. doi: 10.1155/2022/1568352

47. Lemke G. Biology of the TAM receptors. *Cold Spring Harb Perspect Biol.* (2013) 5(11):a009076. doi: 10.1101/cshperspect.a009076

frontiers | Frontiers in Immunology

TYPE Original Research
PUBLISHED 30 April 2024
DOI 10.3389/fimmu.2024.1350837

OPEN ACCESS

EDITED BY
Shougang Guo,
Shandong Provincial Hospital, China

REVIEWED BY
Takao Kiriyama,
Nara Medical University, Japan
Hsiuying Wang,
National Yang Ming Chiao Tung University, Taiwan

*CORRESPONDENCE
Takahiro Iizuka
takahiro@med.kitasato-u.ac.jp

RECEIVED 06 December 2023
ACCEPTED 25 March 2024
PUBLISHED 30 April 2024

CITATION
Iizuka M, Nagata N, Kanazawa N, Iwami T, Nagashima M, Nakamura M, Kaneko J, Kitamura E, Nishiyama K, Mamorita N and Iizuka T (2024) H-intensity scale score to estimate CSF GluN1 antibody titers with one-time immunostaining using a commercial assay.
Front. Immunol. 15:1350837.
doi: 10.3389/fimmu.2024.1350837

H-intensity scale score to estimate CSF GluN1 antibody titers with one-time immunostaining using a commercial assay

Masaki Iizuka[1], Naomi Nagata[1], Naomi Kanazawa[1], Tomomi Iwami[1], Makoto Nagashima[1], Masaaki Nakamura[1], Juntaro Kaneko[1], Eiji Kitamura[1], Kazutoshi Nishiyama[1], Noritaka Mamorita[2] and Takahiro Iizuka[1]*

[1]Department of Neurology, Kitasato University School of Medicine, Sagamihara, Japan, [2]Department of Medical Informatics, Kitasato University School of Allied Health Sciences, Sagamihara, Japan

Introduction: Anti-NMDA receptor encephalitis is an autoimmune disorder caused by autoantibodies (abs) against the conformational epitope on GluN1 subunits. GluN1-abs have been determined with cell-based assay (CBA) co-expressing GluN1/GluN2 subunits. However, commercial fixed CBA expressing only GluN1 subunit has increasingly been used in clinical practice. The ab titers can be determined with serial dilutions, but its clinical significance remains unclear. We aimed to develop an H-intensity scale (HIS) score to estimate GluN1-ab titers in cerebrospinal fluid (CSF) with one-time immunostaining using both commercial CBA and immunohistochemistry and report its usefulness. "H" is the initial of a patient with high CSF GluN1-ab titers (1:2,048).

Methods: We first determined the reliability of CBA in 370 patients with suspected autoimmune encephalitis by comparing the results between commercial CBA and established assay in Dalmau's Lab. Then, we made positive control panels using the patient H's CSF diluted in a fourfold serial dilution method (1:2, 1:8, 1:32, 1:128, 1:512, and 1:2,048). Based on the panels, we scored the intensity of ab reactivity of 79 GluN1-ab-positive patients' CSF (diluted at 1:2) on a scale from 0 to 6 (with ≥1 considered positive). To assess inter-assay reliability, we performed immunostaining twice in 21 patients' CSF. We investigated an association between the score of CSF obtained at diagnosis and the clinical/paraclinical features.

Results: The sensitivity and specificity of CBA were 93.7% (95% CI: 86.0–97.3) and 98.6% (95% CI: 96.5–99.5), respectively. Linear regression analysis showed a good agreement between the scores of the first and second assays. Patients with a typical spectrum, need for mechanical ventilation support, autonomic symptoms/central hypoventilation, dyskinesias, speech dysfunction, decreased

level of consciousness, preceding headache, ovarian teratoma, and CSF leukocyte count >20 cells/μL had a higher median HIS score than those without, but HIS score was not associated with sex, age at onset, or seizure. HIS score at diagnosis had a significant effect on 1-year functional status.

Discussion: The severity of disease and four of the six core symptoms were associated with higher GluN1-ab titers in CSF at diagnosis, which may play a role in poor 1-year functional status. An incomplete phenotype can be attributed to low CSF GluN1-ab titers.

KEYWORDS

NMDA receptor encephalitis, immunohistochemistry, autoantibodies, cell-based assay, tissue-based assay

1 Introduction

Autoimmune encephalitis (AE) is defined as a form of encephalitis that occurs as a result of a brain-specific immune response, and it usually associates with autoantibodies (abs) against a neuronal or glial cell surface antigen (1). Anti-NMDA receptor (NMDAR) encephalitis is one of the most common AE characterized by viral prodrome followed by memory or psychobehavioral alterations, seizures, decreased level of consciousness, dyskinesias, speech dysfunction, autonomic symptoms, and central hypoventilation or a combination of these symptoms (2–4). Anti-NMDAR encephalitis is caused by abs against the conformational epitope on the extracellular amino terminal domain of the GluN1 subunit (GluN1-abs) (5). A definite diagnosis requires confirmation of the presence of GluN1-abs in cerebrospinal fluid (CSF) with appropriate assay (6).

The GluN1-abs have been determined with live or fixed cell-based assay (CBA) co-expressing GluN1/GluN2 subunits of the NMDAR in the research laboratory (1–4). However, in clinical practice, commercial fixed CBA expressing only GluN1 subunit has increasingly been used. Ab titers can be determined with ELISA (7) or serial dilutions in the commercial laboratory for a fee, but serial dilutions result in an increase in the cost, making it difficult to determine ab titers in many patients in clinical practice. Previous studies (7–10) reported an association between CSF GluN1-ab titers at diagnosis and some of the clinical features, but its clinical significance remains unclear.

To resolve these issues, we aimed to develop an intensity-based scale score to estimate CSF ab titers without serial dilutions and assessed whether the score of CSF obtained at diagnosis is associated with certain clinical and paraclinical features of this disorder. We named the score as "H-intensity scale (HIS) score", in which the "H" is the initial of a patient whose CSF containing high ab titers (1:2,048) was used to make positive control panels to score the intensity of ab reactivity. We used the name "HIS score" after consent from the patient H who had achieved full recovery.

2 Materials and methods

2.1 Patient selection and antibody measurement

First, we retrospectively reviewed the clinical information of 710 patients with suspected AE or related disorder who underwent testing for neuronal surface (NS)-abs between January 1, 2007 and September 30, 2023. Among those, 470 (66.2%) patients' CSF/sera were referred from other 163 hospitals to Kitasato University to examine NS-abs. The detailed clinical information was provided from each physician to TI (a principal investigator). The inclusion criteria of this cohort are as follows: AE or related neurological disorder is highly suspected based on clinical assessment; detailed clinical information is available for review by TI, including the mode of onset of symptoms, past history, family history, regular medications, neurologic examination, neuropsychological assessment, laboratory test results (blood, CSF, electro-encephalography, brain or spinal MRIs, and body CT), and subsequent clinical course and outcome when available; and written informed consent is obtained from the patients or their proxies.

In all patients, NS-abs were measured at the laboratory of Josep Dalmau (Dalmau's Lab at University of Pennsylvania, Philadelphia, or IDIBAPS Hospital Clinic, Barcelona) because of it being one of the most advanced research laboratories, where many of the novel NS-abs have been identified since the first discovery of NMDAR-abs in 2007 (2). NS-abs were determined with previously established assays, such as rat brain immunohistochemistry (IHC) adapted to NS

10.3389/fimmu.2024.1350837

antigens and CBA (2, 11–18). Live neurons were also added when needed to determine the presence of NS-abs. The NS antigens examined included the NMDAR, α-amino-3-hydroxy-5-methyl-4-isoxazolepropionic acid receptor (AMPAR), γ-aminobutyric acid A receptor (GABAaR), γ-aminobutyric acid B receptor (GABAbR), glutamate kainate receptor subunit 2 (GluK2), metabotropic glutamate receptor 5 (mGluR5), metabotropic glutamate receptor 1 (mGluR1), dipeptidyl peptidase-like protein 6 (DPPX), contactin-associated protein-like 2 (Caspr2), leucine-rich glioma-inactivated 1 (LGI1), neurexin 3, or glycine receptor (GlyR). These antigens were examined based on the clinical phenotypes and/or immunoreactivity pattern on in-house IHC. Abs against myelin oligodendrocyte glycoprotein (MOG), aquaporin-4 (AQP4), or glial fibrillary acidic proteins (GFAP) were also examined in CSF and/or serum with established CBA (19), when being clinically or radiologically suspected, or based on immunoreactivity pattern on in-house or commercial IHC.

We also retrospectively examined NS-abs in the archived CSF at Kitasato University in appropriately half of the patients with commercial fixed CBA for NMDAR or others, commercial rat brain IHC, and/or in-house IHC adapted to NS antigens, as previously reported elsewhere (20).

2.2 Part I (reliability of commercial fixed CBA expressing only GluN1 subunit)

In part I, we included 370 patients whose residual archived samples of the CSF identical to one examined at Dalmau's Lab were available for this study (Figure 1). GluN1-abs were examined with a commercial kit (EUROIMMUN AG, product no.: FA 111m-3, Lübeck, Germany) at Kitasato University to evaluate the reliability of the commercial CBA. The kit consists of four biochips per field, containing the NMDAR (only GluN1 subunits)-transfected cells, control-transfected cells, hippocampus, and cerebellum, as previously reported (20).

In this study, we evaluated the intensity of ab reactivity of the CSF diluted at 1:2 instead of non-diluted CSF because we usually use CSF diluted at 1:2 for screening of NS-abs (20) on in-house IHC or to determine estimated CSF ab titers; otherwise, we followed the instruction of the company with indirect immunofluorescence assay (IIFA). The ab reactivity on CBA and IHC was evaluated with an Olympus BX53 fluorescence microscope equipped with a DP80 digital camera, CellSence Dimension1.8 imaging Software (Olympus, Japan). Green fluorescence was detected using a fluorescein-isothiocyanate filter (excitation: 470–495 nm,

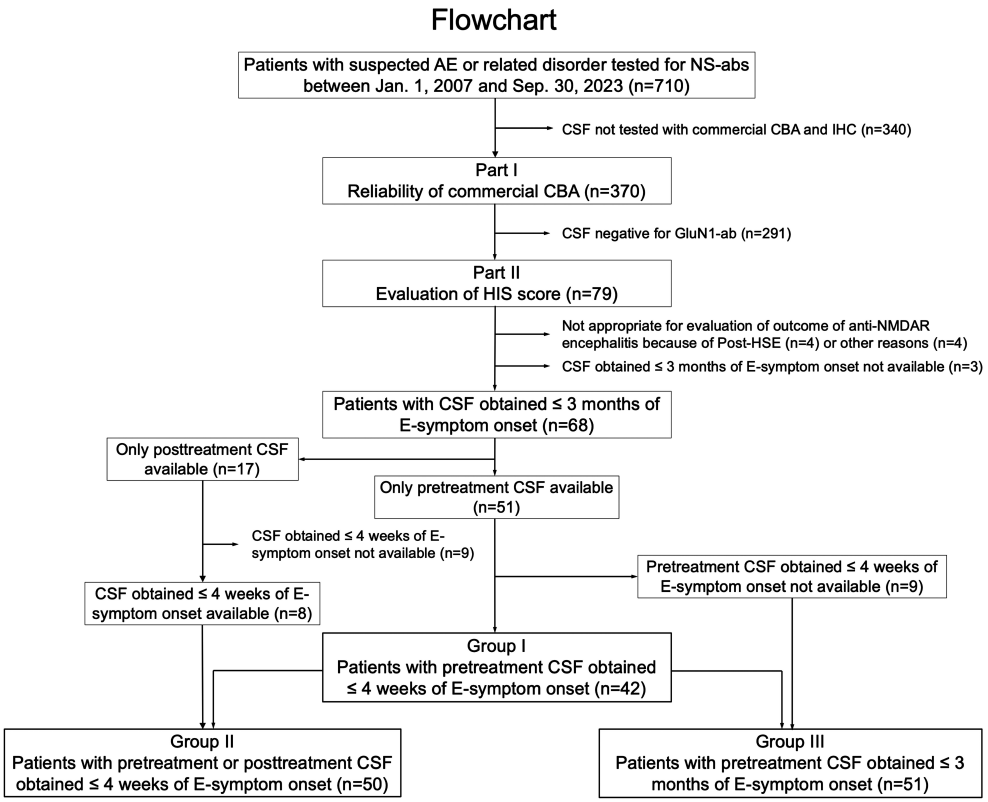

FIGURE 1
Flowchart. This figure shows a diagram of the study conducted. In part I, the reliability of a commercial fixed cell-based assay (CBA) expressing only GluN1 subunits was investigated, while in part II, the clinical significance of an H-intensity scale (HIS) score was evaluated in three overlapping groups. The number of patients is shown in parentheses. AE, autoimmune encephalitis; ab, antibodies; E-symptom, encephalitis symptom (see Text); NS, neuronal surface; post-HSE, autoimmune post-herpes simplex encephalitis.

emission: 510–505 nm, and dichroic: 505 nm; U-FBNA, Olympus, Japan).

Ab reactivity to commercial fixed CBA was initially evaluated by three authors (NN, NK, and TI) independently and was finally determined by agreement of the authors. GluN1-ab-positivity or negativity was determined based on the results performed at Dalmau's Lab, and the sensitivity and the specificity of the commercial CBA were calculated.

2.3 Part II (evaluation of HIS score)

2.3.1 Development of positive control panels

To make positive control panels, we first selected patient H who presented with a typical spectrum of anti-NMDAR encephalitis, whose CSF ab titers were thought to be highest among patients who had been examined with the commercial CBA.

Patient H's CSF was diluted in a fourfold serial dilution method (1:2, 1:8, 1:32, 1:128, 1:512, and 1:2,048) to make the positive control panels, in which we started with CSF diluted at 1:2. The patient's CSF ab titers were determined by fourfold serial dilutions; the ab reactivity remained positive at 1:2,048 under ×10 or ×20 objective lens (Figure 2A) but was negative at 1:8,192. Accordingly, the CSF ab titers were determined to be 1:2,048 as the greatest dilution at which a detectable positive result is still obtained with the fourfold serial dilution method.

We made a pair of positive control panels to score the intensity of ab reactivity (Figures 2A, B for CBA and IHC, respectively). A series of photographs was taken with the Olympus BX53 fluorescence microscope in several settings by adjusting the ISO/Exposure as follows: in panel A, the photographs were taken under the two settings of ISO/Exposure (1,600/500 ms and 800/500 ms) when viewing the slide under ×4, ×10, and ×20 objective lens. In panel B, the photographs were taken under the three settings of ISO/Exposure adjusted for each magnification of the objective lens as follows: 1,600/500 ms for ×4, 800/500 ms for ×10, and 400/500 ms for ×20, respectively. We used these several ISO/Exposure settings because it is difficult to score based on a single setting due to concomitant halation caused by the reactivity of antinuclear antibodies when present.

2.3.2 Scoring of the intensity of antibody reactivity

We scored the intensity of ab reactivity of the individual patients' CSF diluted at 1:2 on a scale from 0 to 6 (with ≥1 considered positive) visually based on the positive control panels. Through this scoring strategy, CSF ab titers can be estimated as follows: when the intensity of a patient's CSF diluted at 1:2 is nearly identical to the score 6 (intensity of patient H's CSF diluted at 1:2), the CSF ab titers can be estimated to be approximately 1:2,048 because patient H's CSF ab titers are 1:2,048. In other words, "the

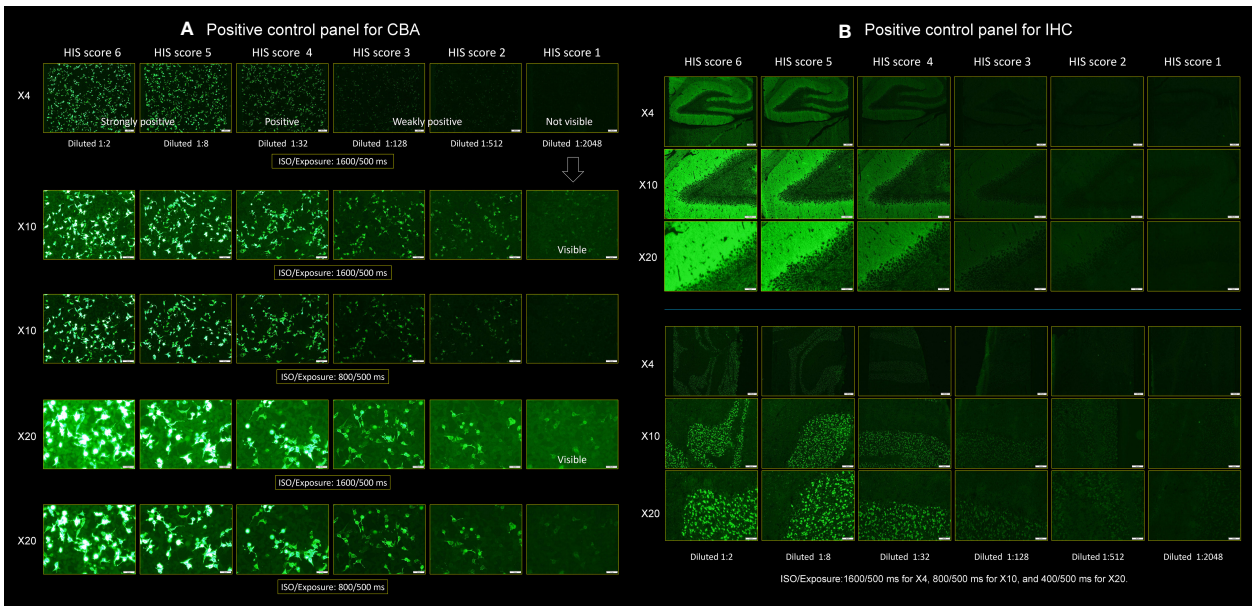

FIGURE 2
Positive control panels for CBA and IHC. This figure shows a pair of positive control panels. Each panel was made using the cerebrospinal fluid (CSF) of a "patient H" having ab titers of 1:2,048, which was diluted in a fourfold serial dilution method, ranging from 1:2, 1:8, 1:32, 1:128, and 1:512 to 1:2,048 to score the individual patient's CSF. **(A)** Positive control panel for CBA and **(B)** positive control panel for IHC (upper: hippocampus, lower: cerebellum). A series of photographs was taken in several settings by adjusting the ISO/Exposure. In **(A)**, the photographs were taken under the two settings of ISO/Exposure (1,600/500 and 800/500 ms) when viewing the slide under ×4, ×10, and ×20 objective lens. In **(B)**, the photographs were taken under the three settings of ISO/Exposure adjusted for each magnification of the objective lens as follows: 1,600/500 ms for ×4, 800/500 ms for ×10, and 400/500 ms for ×20, respectively (see text). CBA, cell-based assay; HIS, H-intensity scale; IHC, immunohistochemistry.

intensity identical to the score 6" means that the patient's CSF would be positive when the CSF is diluted five times in a fourfold serial dilution method (at 1: 2,048) but would be negative when being diluted six times (at 1:8,192). When the intensity of a patient's CSF diluted at 1:2 is scored 3, it means that the patient's CSF would still be positive when being diluted two times in a fourfold serial dilution method (at 1:32) but would be negative when being diluted three times (at 1:128), indicating that the estimated titers are 1:32. The intensity of ab reactivity that appeared higher than the score 6 was also scored 6 in this study. Accordingly, it can be considered as follows: the scores 6, 5, 4, 3, 2, and 1 correspond to estimated titers of 1:2,048 or more, 1:512, 1:128, 1:32, 1:8, and 1:2, respectively when CSF diluted at 1:2 is used. When no apparent reactivity was seen even when viewing under a ×20 objective lens, the score was considered to be 0.

HIS score was first determined by four authors (MI, NN, NK, and TI) independently and was finally determined by agreement of the authors on a scale from 0 to 6; however, when considered to be appropriate, a score of 0.5, 1.5, 2.5, 3.5, or 4.5 was given, but no sample scored 5.5 was seen in our cohort.

2.3.3 Inter-assay reliability

We performed immunostaining twice in 21 patients' CSF samples, which were selected from 79 GluN1-ab-positive patients in order to see an agreement of the score on each assay at different score levels (range, 0–6). The agreement between the scores of the first and second assay was evaluated using linear regression analysis.

2.3.4 Evaluation of clinical features and HIS score of CSF obtained at diagnosis

In this study, we defined "pretreatment CSF" as CSF obtained before initiation of immunotherapy, while "posttreatment CSF" was defined as CSF after initiation of immunotherapy. We scored the intensity of CSF obtained from 79 patients (54 female, 68.3%), median age at onset 31 years (range, 12–74 years), whose CSF tested positive for GluN1-abs at Dalmau Lab. After reasonable exclusion of 11 patients (Figure 1), we assessed the score in the following three groups: group I was the primary group (n = 42), in which pretreatment CSF obtained within 4 weeks of encephalitis symptom (E-symptom) onset was available. The time from E-symptom onset to CSF collection was median 7 days (range, -1 to 28 days). We also assessed in the other two groups: group II (n = 50, with CSF obtained within 4 weeks of E-symptom onset regardless of pretreatment or posttreatment CSF) and group III (n = 51, with pretreatment CSF obtained within 3 months of E-symptom onset) (Figure 1). The subjects in group I were also included in groups II and III. The time from E-symptom onset to CSF collection in groups II and III was median 9 days (range, -1 to 28 days) and median 10 days (range, -1 to 90 days), respectively.

In general, it is ideal to evaluate pretreatment CSF to exclude a potential effect of immunotherapy on CSF ab titers at diagnosis. In a clinical setting, however, the pretreatment CSF is not always available. Furthermore, CSF ab titers may not immediately decline after initiation of immunotherapy due to sustained high disease activity. Therefore, we investigated the score in group II, including posttreatment CSF obtained during the acute stage. We also investigated the score in group III to include a small group of patients whose symptoms gradually developed beyond 4 weeks of E-symptom onset.

Immunotherapy included first-line therapy [intravenous high-dose methylprednisolone (IVMP), immunoglobulins, and plasma exchanges], second-line therapy (intravenous cyclophosphamide and rituximab), or other immunosuppressive drugs. E-symptoms were defined as those directly attributed to encephalitis, such as [1] abnormal (psychiatric) behavior or cognitive dysfunction (memory or psychobehavioral alterations), [2] speech dysfunction, [3] seizures, [4] movement disorder, dyskinesias, or rigidity/abnormal postures, [5] decreased level of consciousness, or [6] autonomic symptoms/central hypoventilation, which are listed as six core symptoms in the diagnostic criteria for anti-NMDAR encephalitis (6). Headache or fever that developed before E-symptom onset was not included in E-symptoms but was regarded as a preceding symptom. The clinical phenotype was evaluated by the sum of the number of the six core symptoms; a typical spectrum was defined as a manifestation with four or more core symptoms, while an incomplete phenotype was defined as a manifestation with three or fewer core symptoms, in which "isolated psychosis" is included.

We evaluated an association between the HIS score and a variety of clinical and paraclinical features, including sex, age at onset, the presence of tumor, preceding headache or fever, core symptoms, CSF total leukocyte count, CSF leukocyte count >5 cells/μL or >20 cells/μL, detection of oligoclonal bands (OCBs), elevated IgG index (≥0.74), brain MRI features suggestive of encephalitis, need for mechanical ventilation support, anti-NMDAR encephalitis one-year functional status (NEOS) score (21), worst functional status within 3 months of E-symptom onset, and 1-year functional status. The 1-year functional status was measured by modified Rankin Scale (mRS), in which good status was defined as mRS 0–2, while poor status was defined as mRS 3–6. Worst functional status was also measured by mRS. We defined brain MRI features suggestive of encephalitis as increased T2/FLAIR signal highly restricted to one or both medial temporal lobes or in multifocal areas involving gray matter, white matter, or both compatible with demyelination or inflammation, as defined in the possible AE diagnostic criteria (6).

2.4 Standard protocol approvals, registrations, and patient consents

The study was approved by the Institutional Review Board of Kitasato University (B20-280). Written informed consent was obtained from the patients or their proxies.

2.5 Statistical analysis

Statistical analyses were performed using JMP, version 17.0.0 (SAS Institute Inc.). Fisher exact test was performed for a comparison of categorical variables, and Wilcoxon test was used for continuous variables. Wilcoxon test with Bonferroni correction was used to compare worst mRS and NEOS score within each

group. Spearman's rank correlation was used to examine the relationship between continuous variables, but the inter-score agreement between the first and second assay was evaluated using linear regression analysis. Nominal logistic regression models were used to determine an association between HIS score at diagnosis and 1-year functional status or need for mechanical ventilation support. The statistical significance was set at $p < 0.05$. The sensitivity and the specificity of the commercial IHC were also determined with two-way contingency table analysis using JMP.

3 Results

3.1 Part I. Sensitivity and specificity of commercial fixed CBA

False-negative and false-positive results were seen in five of 79 ab-positive patients (6.3%) and four of 291 ab-negative patients (1.4%), respectively (Table 1). Although CSF ab titers were not determined at Dalmau's Lab, according to the report, none of the five false-negative patients had high CSF ab titers: weakly positive in three (#1, 2, and 3), mildly positive in one (#4), and extremely very low in one (#5). These patients' clinical phenotypes were also different from a typical spectrum of anti-NMDAR encephalitis: multifocal demyelinating syndrome (#1, later diagnosed with multiple sclerosis based on the subsequent course of the disease and the absence of GluN1-abs in the follow-up CSF), isolated seizures (#2), autoimmune post-herpes simplex encephalitis (#3), new-onset nonconvulsive status epilepticus (#4), and GlyR-ab-positive progressive encephalomyelitis with rigidity and myoclonus (#5).

In the four false-positive patients, HIS score was low (range, 1–1.5; estimated titers, 1:2–1:4), and their clinical features were inconsistent with anti-NMDAR encephalitis. Their final diagnosis included leptomeningeal metastasis of embryonal carcinoma ($n = 1$), overlapping NS-ab-negative encephalitis and MOG-ab-negative demyelinating syndrome ($n = 1$), GFAP-ab-positive encephalitis ($n = 1$), and probable neurodegenerative dementia with titin- and AchR-ab-positive myasthenia gravis ($n = 1$).

TABLE 1 Results of GluN1 antibody testing.

	GluN1-antibody positive at Dalmau Lab (n = 79)	GluN1-antibody negative at Dalmau Lab (n = 291)
GluN1-antibody positive on commercial CBA (n=78)	True positive (n=74)	False positive (n=4)
GluN1-antibody negative on commercial CBA (n=292)	False negative (n=5)	True negative (n=287)

GluN1 antibodies were examined with commercial fixed CBA (EUROIMMUN AG, product No: FA 111m-3, Lübeck, Germany) (see Text) using CSF diluted at 1:2. The positivity or negativity of GluN1 antibodies was determined based on the results performed at the laboratory of Josep Dalmau (Barcelona).

The sensitivity and the specificity of the commercial CBA were 93.7% (95% CI: 86.0–97.3) and 98.6% (95% CI: 96.5–99.5), respectively. The positive predictive value and negative predictive value were 94.9% (95% CI: 87.5–98.0) and 98.3% (95% CI: 96.1–99.3), respectively.

3.2 Part II. Clinical features, HIS score, inter-assay reliability, and clinical significance

3.2.1 Clinical and paraclinical features in each group

The clinical and paraclinical features are summarized in Table 2. These features overlapped among the three groups because of the overlapping subjects. Female patients account for 73%–74% with a median age at onset of approximately 30 years. Preceding headache and fever were seen in 53%–56% and 47%–52% of patients, respectively. A typical spectrum was seen in 68%–69%. Among the six core symptoms, memory or psychobehavioral alterations were most frequently seen, followed by seizures,

TABLE 2 Clinical and paraclinical features in each group.

	Group I (n=42)	Group II (n=50)	Group III (n=51)
Female, n (%)	31 (73.8)	37 (74.0)	37 (72.5)
Age at onset (y), median (IQR, range)	30.5 (21.8-38.3, 14-66)	29.5 (20.8-37, 14-66)	31.0 (24-39, 14-72)
CSF obtained within 4 weeks of E-symptoms[1] onset, n (%)	42 (100)	50 (100)	42 (82.4)
From E-symptom onset to CSF collection (days), median (IQR, range)	7 (5-13, -1[2]-28)	9 (5-14, -1[2]-28)	10 (5-18, -1[2]-90)
Pretreatment CSF, n (%)	42 (100%)	42 (84%)	51 (100%)
Headache that preceded E-symptom onset, n (%)	22/40 (55.0)	27/48 (56.3)	26/49 (53.1)
Fever that preceded E-symptom onset, n (%)	22 (52.4)	25 (50.0)	24 (47.1)
Typical spectrum[3] (≥ 4 of 6 core symptoms), n (%)	29 (69.0)	34 (68.0)	35 (68.6)
Abnormal (psychiatric) behavior or cognitive dysfunction, n (%)	41 (97.6)	48 (96.0)	50 (98.0)
Speech dysfunction, n (%)	27 (64.3)	34 (68.0)	30 (58.8)
Seizures, n (%)	34 (81.0)	41 (82.0)	41 (80.4)
Movement disorder, dyskinesias, or rigidity/abnormal postures, n (%)	27 (64.3)	32 (64.0)	30 (58.8)
Decreased level of consciousness, n (%)	32 (76.2)	37 (74.0)	38 (74.5)

(Continued)

10.3389/fimmu.2024.1350837

TABLE 2 Continued

	Group I (n=42)	Group II (n=50)	Group III (n=51)
Autonomic symptoms/ central hypoventilation, n (%)	27 (64.3)	32 (64.0)	29 (56.9)
Need for mechanical ventilation support, n (%)	24 (57.1)	29 (58.0)	26 (51.0)
Brain MRI features suggestive of encephalitis, n (%)	19 (45.2)	23 (46.0)	20 (39.2)
CSF leukocyte count (/μL), median (IQR, range)	40 (14.8-122.3, 1-567)	43 (14.8-133, 1-567)	30 (12-105, 0-567)
CSF leukocyte count > 5 cells/μL, n (%)	39 (92.9)	47 (94.0)	44 (86.3)
CSF leukocyte count > 20 cells/μL, n (%)	29 (69.0)	34 (68.0)	31 (60.8)
Detection of oligoclonal bands, n (%)	27/37 (73.0)	32/44 (72.7)	28/45 (62.2)
Elevated IgG index (≥0.74), n (%)	13/39 (33.3)	15/46 (32.6)	14/47 (29.8)
Presence of tumor including teratoma, n (%)	19[4] (45.2)	25[5] (50.0)	24[6] (47.1)
Presence of ovarian teratoma in female patients, n (%)	16/31 (51.6)	22/37 (59.5)	18/37 (48.6)
High NEOS score (4-5), n (%)	9 (21.4)	10 (20.0)	10 (19.6)
Worst functional status (mRS 5-6)[7], n (%)	34 (81.0)	40 (80.0)	42 (82.4)[8]
Poor one-year functional status, n (%)	10/39 (25.6)	10/47 (21.3)	13/45 (28.9)
First-line immunotherapy, n (%)	41 (97.6)	49 (98.0)	49 (96.1)
Second-line immunotherapy, n (%)	22 (52.4)	26 (52.0)	24 (47.1)
Lack of clinical improvement within 4 weeks after treatment, n (%)	23/41 (56.1)	27/49 (55.1)	27/50 (54.0)
HIS score at diagnosis, median (IQR, range)	4 (3-6, 0-6)	4 (3-5.3, 0-6)	4 (3-5, 0-6)

Group I is a primary group, in which pretreatment CSF obtained within 4 weeks of E-symptom onset is available. Group II is a second group, in which CSF obtained within 4 weeks of E-symptom onset regardless of pretreatment or posttreatment CSF is available. Group III is a third group, in which pretreatment CSF obtained within 3 months of E-symptom onset is available. The subjects in Group I are all included in Groups II and III (see text).
[1]E-symptoms: encephalitis symptoms; [2] In one patient, CSF obtained one day before E-symptom onset was used; [3]Typical spectrum is defined as a manifestation with four or more of the six core symptoms of anti-NMDAR encephalitis (see Text); [4]Tumors included ovarian teratoma (n=16, 84.2%), suspected small cell lung cancer (SCLC) (n=1), esophageal carcinoma (n=1) and thyroid cancer (n=1). [5]Tumors included ovarian teratoma (n=22, 88.0%), suspected SCLC (n=1), esophageal cancer (n=1), and thyroid cancer (n=1). [6]Tumors included ovarian teratoma (n=18, 75.0%), suspected SCLC (n=1), SCLC (n=1), esophageal cancer (n=1), thyroid cancer (n=1), breast cancer (n=1) and large ovarian cyst (no teratoma was found pathologically) (n=1). [7]Worst functional status within 3 months of E-symptom onset; [8]One patient with SCLC who died within 3 months of E-symptom onset is included.

decreased level of consciousness, dyskinesias or associated movement disorders, speech dysfunction, and autonomic symptoms/central hypoventilation (Table 2). Mechanical ventilation support was needed in 51%–58%. Brain MRI features suggestive of encephalitis was seen in 39%–46%, CSF pleocytosis (>5 cells/μL) in 86%–94%, CSF pleocytosis (>20 cells/μL) in 61%–69%, OCBs in 62%–73%, and elevated IgG index in 30%–33%. Tumors were seen in 45%–50%; among those, ovarian teratoma (OT) was most frequent (49%–60% of female patients). High NEOS score (4 to 5) was seen in 20%–21%, while worst functional status (mRS 5 to 6) was observed in 80%–82%. Poor 1-year functional outcome was found in 21%–29%. First-line and second-line immunotherapy were used in 96%–98% and 47%–52%, respectively. Approximately 55% of patients did not show a clinical improvement within 4 weeks after initiation of immunotherapy or tumor removal. The HIS score in each group is also shown.

3.2.2 HIS score at diagnosis in each group

HIS score at diagnosis is shown in Figure 3. In 79 ab-positive patients (Figure 3A), the HIS score was median 3.5 (interquartile range, IQR: 2.5–4.5; range, 0–6); five patients (6.3%) who scored 0 are false-negative (Table 1), but these samples are considered to have low or extremely low titers (see "Result"). Two of the five false-negative patients (#2 and 4) were also included in all three groups (Figures 3B–D). The median HIS score was 4 in each group, indicating that median CSF ab titers were estimated to be approximately 1:128.

3.2.3 Inter-assay reliability of HIS score

There was a good agreement between the scores of the first and second assays (β = 0.9657, 95% CI = 0.9120–1.0195, p <.0001, α = 0.1044, 95% CI = -0.0876–0.2965, p = 0.2692, R^2 = 0.9867; Supplementary Figure S1).

3.2.4 Clinical significance of HIS score at diagnosis

In group I, the median HIS score was not associated with sex, age at onset (Figure 4A), or CSF total leukocyte count (Figure 4B), but it was higher in patients with a typical spectrum than in those with an incomplete phenotype (p <.0001) (Table 3). The median HIS score was also higher in patients with a need for mechanical ventilation support (p <.0001), autonomic symptoms/central hypoventilation (p = 0.0002), dyskinesias (p = 0.0004), speech dysfunction (p = 0.0010), decreased level of consciousness (p = 0.0012), preceding headache (p = 0.0161), OT (p = 0.0211), and CSF leukocyte count > 20 cells/μL (p = 0.0278) than in those without, but there was no difference between patients with and without memory or psychobehavioral alterations, seizure, tumors, preceding fever, MRI features suggestive of encephalitis, CSF leukocyte count >5 cells/μL, OCB-detection, or elevated IgG index.

The median HIS score was higher in patients with mRS of 5 than in those with mRS of 4 (p = 0.0120) or mRS of 3 (p = 0.0181) (Figure 4C). The median HIS score was also higher in patients with a high NEOS score (4 to 5) than in those with a low NEOS score (0

10.3389/fimmu.2024.1350837

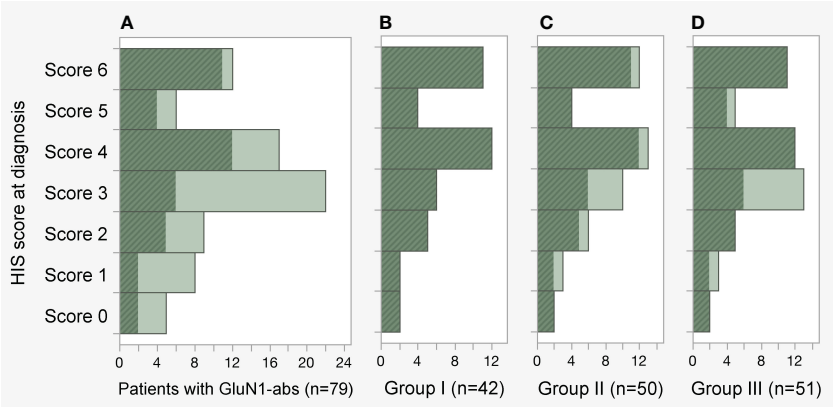

FIGURE 3
Distribution of H-intensity scale (HIS) score. **(A–D)** The HIS score in the 79-ab-positive patients, groups I, II and III was median 3.5 (IQR 2.5–4.5, range 0–6), 4 (IQR 3–6, range 0–6), 4 (IQR 3–5.3, range 0–6), and 4 (IQR 3–5, range 0–6), respectively. Note that the HIS score was determined using pretreatment cerebrospinal fluid (CSF) obtained within 4 weeks of E-symptom onset in group I **(B)**, CSF obtained within 4 weeks of E-symptom onset regardless of pretreatment or posttreatment CSF in group II **(C)**, and pretreatment CSF obtained within 3 months of E-symptom onset in group III **(D)**. Patients included in group I are shown with a diagonal stripe pattern in dark color. In the panels, patients who scored 4.5, 3.5, 2.5, and 1.5 were included in the histogram scored 4, 3, 2, and 1, respectively. abs, antibodies; E-symptom, encephalitis symptom; IQR, interquartile range.

to 1) ($p = 0.0012$) or NEOS score 2 ($p = 0.0008$) (Figure 4D) and was higher in patients with need for ICU admission than in those without ($p < .0001$) and in patients who received second-line immunotherapy than in those who did not ($p = 0.0500$). The median HIS score was also higher in patients without clinical improvement within 4 weeks after initiation of treatment than in those with clinical improvement ($p = 0.0016$, Table 3). Such patients, who did not show clinical improvement within 4 weeks after initiation of treatment, more frequently received second-line immunotherapy than those who did ($p = 0.0005$, Figure 4E). Patients with a high NEOS score (4 to 5) had more frequently poor 1-year functional status than those with low NEOS score 2 ($p = 0.0010$) or score of 0 to 1 ($p = 0.0023$) (Figure 4F).

A logistic regression analysis revealed that HIS score at diagnosis had a mild but significant effect on 1-year functional status ($p = 0.0231$) (Figure 4G). However, there was no difference in 1-year functional status between patients with second-line immunotherapy and those without [13/21 (61.9%) vs. 16/18 (88.9%), $p = 0.0740$, not shown]. It was also shown that HIS score at diagnosis had also a significant effect on need for mechanical ventilation support ($p = 0.0029$), with a probability of 17% of mechanical ventilation support on score 3, 59% on score 4, and 91% on score 5, respectively (Figure 4H); a similar effect was seen in groups II and III (Supplementary Figures S2F, S3F).

Among the three groups, most of the results were similar, but there were a few differences (Table 3). In group II, the median HIS score was higher in patients with OCB-detection than in those without ($p = 0.0477$), while HIS score had a significant effect on 1-year functional outcome ($p = 0.0126$, Supplementary Figure S2E), as did in group I. In group III, the median HIS score was higher not only in patients with OCB-detection ($p = 0.0069$) but also in patients with elevated IgG index ($p = 0.0432$) than in those without (Table 3). In group III, HIS score did not have a significant effect on 1-year functional outcome ($p = 0.0582$, Supplementary Figure S3E). There was no association between the use of second-line immunotherapy and 1-year functional status in either group II ($p = 0.0786$) or III ($p = 0.5136$) (data not shown).

4 Discussion

This study demonstrates the following findings: (1) the commercial fixed CBA is a reliable assay with high sensitivity and high specificity, even when CSF diluted at 1:2 is used; (2) a good inter-assay agreement was seen; (3) HIS score at diagnosis was higher in patients with a typical spectrum of anti-NMDAR encephalitis, dyskinesias or associated movement disorders, decreased level of consciousness, autonomic symptoms/central hypoventilation, speech dysfunction, preceding headache, need for mechanical ventilation support, worst functional status (mRS 5 to 6), high NEOS score (4 to 5), OT, or CSF leukocyte count >20 cells/μL than those without, (4) the HIS score at diagnosis may be used to predict a probability of need for mechanical ventilation support, (5) higher GluN1-ab titers in CSF obtained at diagnosis may play a role in poor 1-year functional status, and (6) an incomplete phenotype can be attributed to low CSF ab titers.

We have developed this score to estimate CSF ab titers with one-time immunostaining and conducted this study to clarify whether (1) the score of the CSF obtained at diagnosis is associated with clinical/paraclinical features and (2) the HIS score can be used as a marker to predict the subsequent course of disease. The HIS score does not provide CSF ab titers directly measured by ELISA or using serial dilutions, but this strategy provides estimated CSF ab titers as an HIS score, ranging from 1:2 (score 1), 1:8 (score 2), 1:32 (score 3), 1:128 (score 4), and 1:512 (score 5) to 1:2,048 or more (score 6). The estimated CSF ab titers are close to those measured in a fourfold serial dilution method. The HIS score can be

10.3389/fimmu.2024.1350837

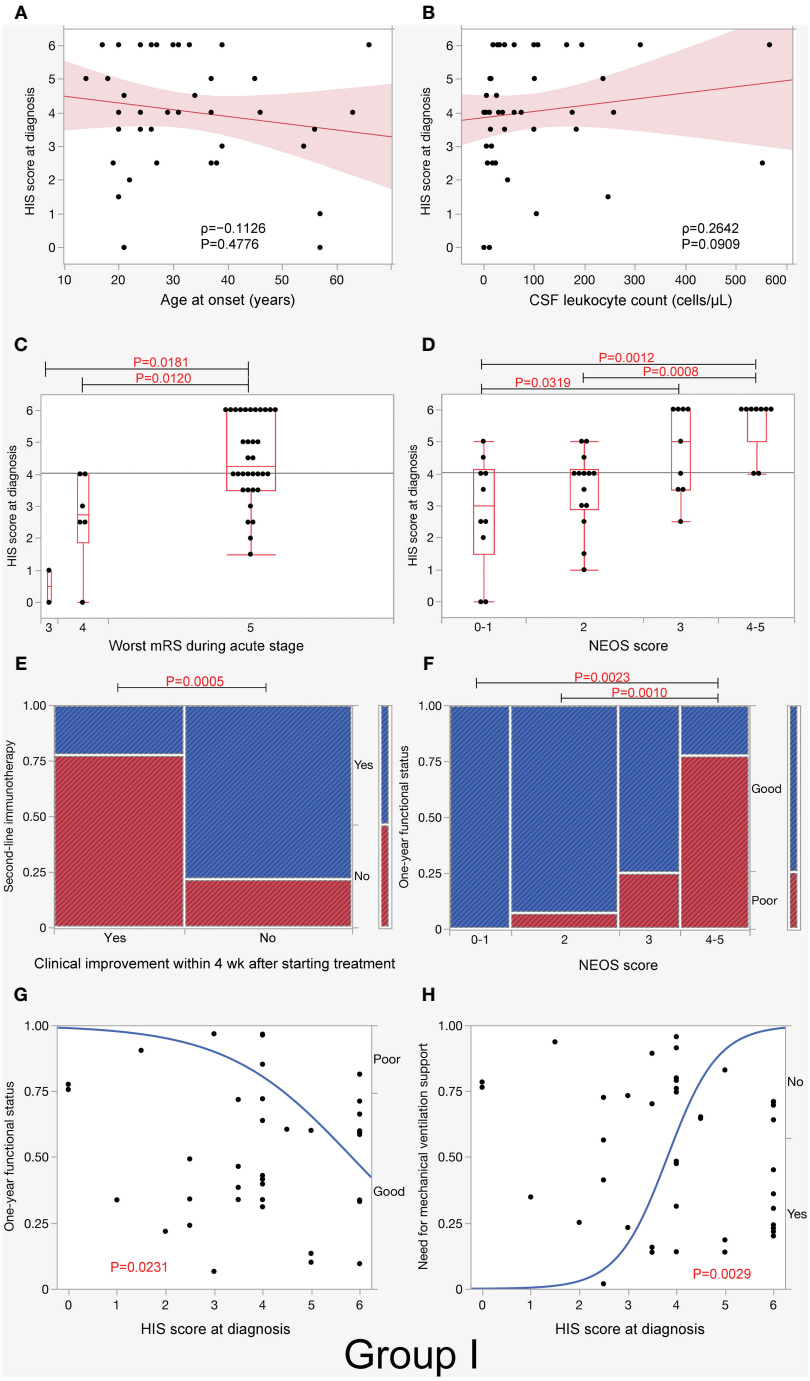

FIGURE 4
H-intensity scale (HIS) score and clinical/paraclinical features in group I. This figure shows an association between HIS score and clinical/paraclinical data, including age at onset **(A)**, CSF leukocyte count **(B)**, worst functional status within 3 months of E-symptom onset **(C)**, NEOS score **(D)**, use of second-line immunotherapy in patients with and without clinical improvement within 4 weeks after starting treatment **(E)**, 1-year functional status **(F, G)**, and need for mechanical ventilation support **(H)** in group I. Note that HIS score was higher in patients with worst functional status (mRS 5) **(C)** or high NEOS score (4 to 5) **(D)** than in those without, while HIS score had a significant effect on both 1-year functional status and need for mechanical ventilation support. In **(A, B)**, the red line represents the regression line, and the light red area represents the 95% CI of the line. In **(C, D)**, boxplots depict median and interquartile range with whiskers extending to minimum and maximum values. E-symptom, encephalitis symptom.

used as a marker not only of a disease activity but also of 1-year functional status, but individual laboratories have to make their own positive control panels. The ideal positive control patient's CSF ab titers are unclear, but we used patient H's CSF having ab titers of 1:2,048 and developed the visually distinguishable six-grade positive control panels.

After starting this study, however, we received another patient's CSF, which revealed intense reactivity far beyond that of patient H's

10.3389/fimmu.2024.1350837

TABLE 3 Median HIS score (IQR, range) in each group.

	Group I	p value	Group II	p value	Group III	p value
Sex						
Female	4 (3.5-7, 0-6)	0.1854	4 (3.3-6, 0-6)	0.0746	4 (3.5-6, 0-6)	0.1548
Male	4 (2.5-4.5, 0-6)		3.5 (1.5-4.3, 0-6)		3.5 (2.9-4.1, 0-6)	
Clinical phenotype[1]						
Typical spectrum (≥ 4 of 6 core symptoms)	5 (4-6, 1.5-6)	<.0001	4.5 (3.9-6, 1-6)	<.0001	4.5 (3.5-6, 1.5-6)	<.0001
Incomplete phenotype (< 4 core symptoms)	2.5 (1.5-3.8, 0-4)		2.8 (2-3.4, 0-4)		2.8 (1.3-3.5, 0-4)	
Abnormal (psychiatric) behavior or cognitive dysfunction						
Yes	4 (3.3-6, 0-6)	0.2572	4 (3-5.8, 0-6)	0.0833	4 (3.4-5, 0-6)	0.2418
No	2.5 (2.5, 2.5)		2.3 (2-2.5, 2-2.5)		2.5 (2.5, 2.5)	
Speech dysfunction						
Yes	4.5 (4-6, 2.5-6)	0.0010	4 (3.5-6, 1-6)	0.0019	4.5 (3.9-6, 2.5-6)	0.0001
No	3 (1.5-4, 0-6)		3 (1.6-4, 0-6)		3.5 (1.8-3.8, 0-6)	
Seizures						
Yes	4 (3.4-6, 0-6)	0.0841	4 (3-6, 0-6)	0.1153	4 (3.5-6, 0-6)	0.1360
No	3.5 (2.6-4, 1-5)		3.5 (2.8-4, 1-5)		3.5 (2.1-4.3, 1-5)	
Movement disorders[2]						
Yes	5 (4-6, 1.5-6)	0.0004	4.5 (3.5-6, 1-6)	0.0002	4.8 (3.5-6, 1.5-6)	<.0001
No	3 (2-4, 0-5)		3 (2-4, 0-5)		3.5 (2.3-4, 0-5)	
Decreased level of consciousness						
Yes	4.5 (3.6-6, 1.5-6)	0.0012	4 (3.5-6, 1-6)	0.0004	4 (3.5-6, 1.5-6)	0.0003
No	2.8 (0.8-4, 0-4)		3 (1.5-3.8, 0-4)		3 (1-3.8, 0-4)	
Autonomic symptoms/central hypoventilation						
Yes	5 (4-6, 1.5-6)	0.0002	4.8 (3.5-6, 1-6)	0.0001	5 (3.5-6, 1.5-6)	0.0001
No	3 (2-4, 0-4)		3 (2-4, 0-4)		3.5 (2.4-4, 0-4)	
Need for mechanical ventilation support						
Yes	5 (4-6, 2.5-6)	<.0001	5 (4-6, 1-6)	<.0001	5 (4-6, 2.5-6)	<.0001
No	3 (1.9-4, 0-4)		3 (2-4, 0-4)		3.5 (2.3-4, 0-5)	
Headache that preceded E-symptom onset						
Yes	4.8 (4-6, 1.5-6)	0.0161	4.5 (3.5-6, 1-6)	0.0137	4.5 (3.5-6, 1.5-6)	0.0067
No	3.5 (2.4-4.3, 0-6)		3.5 (2.3-4, 0-6)		3.5 (2.5-4, 0-6)	
Fever that preceded E-symptom onset						
Yes	4.3 (2.5-6, 0-6)	0.7103	4 (2.5-6, 0-6)	0.7529	4.3 (2.8-6, 0-6)	0.2972
No	4 (3.1-5, 0-6)		4 (3-5, 0-6)		3.5 (3-4, 0-6)	
Brain MRI features suggestive of encephalitis						
Yes	4 (3.1-6, 0-6)	0.7781	4 (3-6, 0-6)	0.9843	4 (3.3-6, 0-6)	0.5412
No	4.3 (2.5-5.3, 0-6)		4 (2.5-5, 0-6)		3.8 (2.9-5, 0-6)	
CSF leukocyte count > 5 cells/μL						
Yes	4 (3-6, 0-6)	0.2854	4 (3-6, 0-6)	0.3957	4 (3.1-5.8, 0-6)	0.0758
No	4 (0-4, 0-4)		4 (0-4, 0-4)		3.5 (1-4, 0-4)	
CSF leukocyte count > 20 cells/μL						
Yes	4 (3.5-6, 1-6)	0.0278	4 (3.5-6, 1-6)	0.0089	4 (3.5-6, 1-6)	0.0028
No	3.5 (2.5-4.3, 0-5)		3.3 (2.1-4, 0-5)		3.5 (2.6-4, 0-5)	
Detection of oligoclonal bands						
Yes	4 (3.5-6, 1-6)	0.0847	4 (3.5-6, 1-6)	0.0477	4 (3.5-6, 1-6)	0.0069
No	3.3 (1.5-4.6, 0-6)		3 (2.1-4.4, 0-6)		3.5 (2.3-4, 0-6)	
Elevated IgG index						
Yes	5 (3.8-6, 1-6)	0.1537	5 (3.5-6, 1-6)	0.0616	5 (1.3-6, 1-6)	0.0432
No	4 (2.9-5, 0-6)		4 (3-4.5, 0-6)		3.5 (3-4.5, 0-6)	
Systemic tumors including ovarian teratoma						
Yes	5 (3.5-6, 0-6)	0.0538	4 (3.5-6, 0-6)	0.0602	4.3 (3.5-6, 0-6)	0.0869
No	4 (2.5-6, 0-6)		4 (2.5-4.3, 0-6)		3.5 (3-4, 0-6)	
Ovarian teratoma						
Yes	5 (4-6, 2-6)	0.0211*	4.3 (3.5-6, 2-6)	0.0331*	4.8 (3.5-6, 2-6)	0.0170*
No	4 (2.5-4.7, 0-6)		3.8 (2.5-4.4, 0-6)		3.5 (2.8-4.3, 0-6)	

(Continued)

10.3389/fimmu.2024.1350837

TABLE 3 Continued

	Group I	p value	Group II	p value	Group III	p value
Clinical improvement ≤ 4 weeks of treatment initiation						
No	5 (4-6, 1.5-6)	0.0016	5 (3.5-6, 1-6)	0.0008	5 (3.5-6, 1-6)	0.0014
Yes	3.8 (2.4-4.1, 0-5)		3.3 (2.4-4, 0-5)		3.5 (2.5-4, 0-5)	
Need for ICU admission						
Yes	5 (4-6, 2.5-6)	<.0001	5 (4-6, 1-6)	<.0001	5 (3.8-6, 2.5-6)	<.0001
No	3 (1.8-4, 0-4)		3 (2-4, 0-4)		3.3 (1.9-4, 0-4)	
Second-line immunotherapy						
Yes	4 (4-6, 1.5-6)	0.0500	4 (3.9-6, 1.5-6)	0.0108	4 (3.6-6, 1.5-6)	0.0212
No	3.5 (2.5-5, 0-6)		3.3 (2.1-4.9, 0-6)		3.5 (2.5-5, 0-6)	

Group I is a primary group, in which pretreatment CSF obtained within 4 weeks of E-symptom onset is available. Group II is a second group, in which CSF obtained within 4 weeks of E-symptom onset regardless of pretreatment or posttreatment CSF is available. Group III is a third group, in which pretreatment CSF obtained within 3 months of E-symptom onset is available.
[1]Typical spectrum is defined as a manifestation with four or more of the six core symptoms, while forme fruste is defined as an incomplete manifestation with three or fewer core symptoms.
[2]Movements disorders including dyskinesias or rigidity/abnormal postures. *P value was assessed in all patients including male patients.
CSF, cerebrospinal fluid; E-symptom, encephalitis symptoms.

CSF. The CSF ab titers were determined to be 1:32,768 in a fourfold serial dilution method. If we revised the positive control panels using this exceptionally high ab titer CSF, we could have developed a pair of eight-grade positive control panels (estimated CSF ab titers, 1:2–1:32,768). However, we did not revise the panels because it is likely to be difficult to recognize visually subtle difference in intensity between the scores 6 and 7 as well as 7 and 8, and we did not find out a clinical value that it is better to distinguish patients with extremely high CSF ab titers (>1:2,048) from those with CSF ab titers of 1:2,048. On the other hand, it is still possible to estimate CSF ab titers using these positive control panels even when a patient's CSF ab titers are >1:2,048 through additional one-time immunostaining using the patient's CSF diluted at 1:8,192. When the patient's CSF diluted at 1:8,192 is scored 2, the CSF ab titers can be estimated to be approximately 1:32,768 because "the score 2" means that the patient's diluted CSF would still be positive when being diluted one time in a fourfold serial dilution (diluted at 1:32,768) but would be negative when being diluted twice (diluted at 1:131,072), indicating that the CSF ab titers are estimated to be approximately 1:32,768.

Among the six core symptoms, HIS score was not associated with memory or psychobehavioral alterations or seizures. In our cohort, 96%–98% of patients presented with memory or psychobehavioral alterations. Accordingly, it was statistically difficult to compare the HIS score between those with and without memory or psychobehavioral alterations because of the too small sample size in one arm, whereas seizures were seen in 80%–82% of patients but less frequently than memory or psychobehavioral alterations. We did not find a significant difference in HIS score between patients with and without seizures. On bedside examination, it is often difficult to distinguish epileptic seizure from non-epileptic seizure or seizure from paroxysmal movement disorders, particularly in unresponsive patients with anti-NMDAR encephalitis. In most of them, these symptoms occur concurrently or one after another and are often indiscernible (3). Seizure was more frequently reported by referring physicians than dyskinesias or associated movement disorders (80%–82% vs. 59%–64%). Given the presence of a significant association between movement disorders and HIS score in all groups, high CSF ab titers play an important role in "dyskinesias or associated movement disorders" than in "seizure". The ambiguity of the term "seizures" and its indiscernibility from paroxysmal movement disorders may lead to a lack of significant relationship between HIS score and seizures.

Memory or psychobehavioral alterations were not associated with HIS score; however, it is important to note that prominent psychobehavioral alterations are almost always seen in the early stage, and HIS score was significantly lower in patients with an incomplete phenotype than in those with a typical spectrum, indicating that "isolated psychosis" can be attributed to low CSF ab titers. It is also extremely important in such low-ab-positive patients with an incomplete phenotype to perform IHC adapted to NS antigens or live neurons to exclude false positive results and prevent unnecessary repeated immunotherapies in patients with a primary psychiatric disorder or non-immune-mediated epilepsy (22).

Regarding an association with a tumor, approximately half of the patients were found to have tumors (mostly OT); OT was found in approximately 50%–60% of female patients (Table 2). We found that the median HIS score was higher in patients with OT than in those without in all three groups, but it was not significantly higher in patients with tumors (when cancers were included; Table 2) than in those without in any group. The results of this study support the previous observation (8) that CSF ab titers were higher in patients with teratoma than in those without teratoma. It is suggested that teratoma plays an important role in ab production though NMDAR expressed in the nervous tissue contained in the teratoma, which are taken up by antigen-presenting cells and are presented to the immune system (23) or through ectopic germinal center formation in the teratoma (24).

We also investigated a possible association between HIS score and paraclinical findings. The HIS score was not associated with either OCB-detection or elevated IgG index in group I, but OCB-detection in groups II and III, and elevated IgG index in group III. In our cohort, OCBs were detected in two-thirds of the patients and elevated IgG index in one-third (Table 2). In group II, posttreatment CSF obtained after initiation of IVMP are included in 16% of patients; despite this, the HIS score was higher in patients with OCB-detection than those without. As intrathecal ab synthesis has been demonstrated in anti-NMDAR encephalitis (25), it is

reasonable to think that high CSF ab titers are, in part, attributed to intrathecal ab synthesis, but elevated IgG index might be less sensitive than OCB-detection in terms of a biomarker of intrathecal ab synthesis. We also investigated an association between the HIS score and CSF leukocyte count in three variables: CSF total leukocyte count and CSF leukocyte count >5 cells/μL or >20 cells/μL. Among those, only CSF leukocyte count >20 cells/μL, which is an independent predictor for outcome in NEOS score (21), showed a significant association in all three groups. Brain MRI features suggestive of encephalitis was seen in 39%–46% of the patients, but the HIS score was not associated with MRI abnormalities, suggesting that factors other than high CSF ab titers, such as concurrent abs against MOG, AQP4, GFAP (19, 26), or other surface antigens not identified, or T-cell-mediated injury may contribute to MRI abnormalities. These glial surface antibodies were concurrently detected in some of the patients, including those with abnormal MRI findings but were not examined in all patients in our cohort. Extreme delta blush pattern was seen in some of the patients, but we did not investigate an association between the HIS score and EEG abnormalities because the EEG recorded during the course of the disease is not fully available for review.

The HIS score at diagnosis was higher in patients with high NEOS score (4 to 5), worst functional status (mRS 5 to 6), and need for mechanical ventilation support than those without in all three groups, and it had a significant effect on 1-year functional status in groups I and II, but not in group III. These data suggest that high CSF ab titers, particularly in the CSF obtained within 4 weeks of E-symptom onset, determine a disease severity and play an important role in the subsequent course of disease. These results are not inconsistent with the previous observations that high NEOS score (4 to 5) is associated with poor 1-year functional status (21), and high CSF ab titers are associated with poor functional outcome (7, 8). Accordingly, higher CSF ab titers at diagnosis are considered to play an important role in poor 1-year functional status but may not be a sole factor contributing to poor outcome. In most of the cases, CSF ab titers usually decline with time after initiation of immunotherapy, and functional recovery is associated with a reduction in CSF ab titers (7, 8); however, approximately 20% of cases are refractory to immunotherapy. In such refractory cases, sustained high CSF ab titers have been reported (8). Therefore, sustained high ab titers are likely to be a more important factor contributing to poor long-term functional status than the initial high ab titers.

In our cohort, we did not find a positive effect of the use of second-line immunotherapy on 1-year functional status in any group. However, patients who were treated with second-line immunotherapy exhibited a more frequently poor response to initial treatment than those who were not treated. Furthermore, the median CSF ab titers at diagnosis were higher in patients who were treated with second-line immunotherapy than in those who were not treated. Accordingly, the lack of positive effect on 1-year functional status does not exclude the efficacy of second-line immunotherapy.

This study has limitations because of it being a retrospective study, having a small sample size, and having analysis based on estimated CSF ab titers without serial dilutions. EEG findings are not included in this study. GFAP, MOG, and AQP4 abs were examined in some but not in all patients. Chronological changes in the HIS score are not included in the analysis. Despite these limitations, we showed an association between estimated CSF ab titers at diagnosis through the HIS score and some of the clinical/paraclinical features, disease severity, and 1-year functional status. A nominal logistic model may also help to predict a probability of need for mechanical ventilation support (Figure 4H, Supplementary Figures S2F, S3F). This strategy is relatively easy to determine CSF ab titers with only one-time immunostaining without serial dilutions at a low cost, can be used in clinical practice at any laboratory when minimum equipment for IIFA is available, and provides clinicians with important clues regarding this devastating but potentially reversible AE.

Data availability statement

The original contributions presented in the study are included in the article/Supplementary Material. Further inquiries can be directed to the corresponding author.

Ethics statement

The studies involving humans were approved by Institutional Review Boards of Kitasato University (B20-280). The studies were conducted in accordance with the local legislation and institutional requirements. Written informed consent for participation in this study was provided by the participants' legal guardians/next of kin. The animal study was approved by Animal Experimentation and Ethics Committee of the Kitasato University School of Medicine (2023–069). The study was conducted in accordance with the local legislation and institutional requirements.

Author contributions

MI: Conceptualization, Data curation, Investigation, Methodology, Writing – original draft, Writing – review & editing. NN: Conceptualization, Data curation, Investigation, Methodology, Writing – review & editing. NK: Conceptualization, Data curation, Investigation, Methodology, Writing – review & editing. TIw: Data curation, Writing – review & editing. MNag: Data curation, Writing – review & editing. MNak: Data curation, Writing – review & editing. JK: Data curation, Writing – review & editing. EK: Data curation, Writing – review & editing. KN: Data curation, Writing – review & editing. NM: Data curation, Formal analysis, Methodology, Writing – review & editing. TIi: Conceptualization, Data curation, Formal analysis, Funding acquisition, Investigation, Methodology, Project administration, Resources, Supervision, Visualization, Writing – original draft, Writing – review & editing.

Funding

The author(s) declare financial support was received for the research, authorship, and/or publication of this article. The authors declare that this study was supported in part by a research support from Astellas Pharma Inc (TIi), but the funder was not involved in the study design, collection, analysis, interpretation of data, the writing of this article or the decision to submit it for publication.

Acknowledgments

The authors particularly thank Professor Josep Dalmau in Institut d´Investigació Biomèdica August Pi I Sunyer (IDIBAPS), Barcelona, Spain, for examining antibodies against extensive neuronal surface and synaptic proteins, glial surface or GFAP, at the laboratory of Josep Dalmau. They are grateful to all participants and physicians for their contribution to this study.

Conflict of interest

The authors declare that the research was conducted in the absence of any commercial or financial relationships that could be construed as a potential conflict of interest.

Publisher's note

Supplementary material

The Supplementary Material for this article can be found online at: https://www.frontiersin.org/articles/10.3389/fimmu.2024.1350837/full#supplementary-material

SUPPLEMENTARY FIGURE 1
Inter-assay reliability. H-intensity scale score was determined twice in 21 patients' cerebrospinal fluid samples with different GluN1 antibody titers that scored from 0 to 6. This figure reveals a good agreement between the scores of the first and second assays.

SUPPLEMENTARY FIGURE 2
H-intensity scale (HIS) score and clinical/paraclinical features in group II. HIS score was higher in patients with worst functional status within 3 months of E-symptom onset **(A)** and a high NEOS score (4 to 5) **(B)** than in those without. Second-line immunotherapy was more frequently used in patients who did not show clinical improvement within 4 weeks after starting treatment than in those who did **(C)**. Patients with a high NEOS score (4 to 5) more frequently had a poor 1-year functional status **(D)**. HIS score at diagnosis **(E)** had a significant effect on both 1-year functional status and need for mechanical ventilation support **(F)** (see Table 2). In **(A, B)**, boxplots depict median and interquartile range with whiskers extending to minimum and maximum values. E-symptom, encephalitis symptom.

SUPPLEMENTARY FIGURE 3
H-intensity scale (HIS) score and clinical/paraclinical features in group III. HIS score was higher in patients with worst functional status within 3 months of E-symptom onset **(A)** and a high NEOS score (4 to 5) **(B)** than in those without. Second-line immunotherapy was more frequently used in patients who did not show clinical improvement within 4 weeks after starting treatment than in those who did **(C)**. Patients with a high NEOS score (4 to 5) more frequently had a poor 1-year functional status compared with those without **(D)**. HIS score at diagnosis **(E)** did not have a significant effect on 1-year functional status in group III, but it had on need for mechanical ventilation support **(F)** (see Table 2). In **(A, B)**, boxplots depict median and interquartile range with whiskers extending to minimum and maximum values. E-symptom, encephalitis symptom.

References

1. Dalmau J, Graus F. *Autoimmune Encephalitis and Related Disorders of the Nervous System*. Cambridge: Cambridge University Press (2022). doi: 10.1017/9781108696722

2. Dalmau J, Tüzün E, Wu HY, Masjuan J, Rossi JE, Voloschin A, et al. Paraneoplastic anti-N-methyl-D-aspartate receptor encephalitis associated with ovarian teratoma. *Ann Neurol*. (2007) 61:25–36. doi: 10.1002/ana.21050

3. Iizuka T, Sakai F, Ide T, Monzen T, Yoshii S, Iigaya M, et al. Anti-NMDA receptor encephalitis in Japan: long-term outcome without tumor removal. *Neurology*. (2008) 70:504–11. doi: 10.1212/01.wnl.0000278388.90370.c3

4. Dalmau J, Gleichman AJ, Hughes EG, Rossi JE, Peng X, Lai M, et al. Anti-NMDA-receptor encephalitis: case series and analysis of the effects of antibodies. *Lancet Neurol*. (2008) 7:1091–8. doi: 10.1016/S1474-4422(08)70224-2

5. Gleichman AJ, Spruce LA, Dalmau J, Seeholzer SH, Lynch DR. Anti-NMDA receptor encephalitis antibody binding is dependent on amino acid identity of a small region within the GluN1 amino terminal domain. *J Neurosci*. (2012) 32:11082–94. doi: 10.1523/JNEUROSCI.0064-12.2012

6. Graus F, Titulaer MJ, Balu R, Benseler S, Bien CG, Cellucci T, et al. A clinical approach to diagnosis of autoimmune encephalitis. *Lancet Neurol*. (2016) 15:391–404. doi: 10.1016/S1474-4422(15)00401-9

7. Dalmau J, Lancaster E, Martinez-Hernandez E, Rosenfeld MR, Balice-Gordon R. Clinical experience and laboratory investigations in patients with anti-NMDAR encephalitis. *Lancet Neurol*. (2011) 10:63–74. doi: 10.1016/S1474-4422(10)70253-2

8. Gresa-Arribas N, Titulaer MJ, Torrents A, Aguilar E, McCracken L, Leypoldt, et al. Antibody titres at diagnosis and during follow-up of anti-NMDA receptor encephalitis: a retrospective study. *Lancet Neurol*. (2014) 13:167–77. doi: 10.1016/S1474-4422(13)70282-5

9. Cai MT, Zheng Y, Wang S, Lai QL, Fang GL, Shen CH, et al. Clinical relevance of cerebrospinal fluid antibody titers in anti-N-Methyl-d-Aspartate receptor encephalitis. *Brain Sci*. (2021) 12:4. doi: 10.3390/brainsci12010004

10. Hümmert MW, Jendretzky KF, Fricke K, Gingele M, Ratuszny D, Möhn N, et al. The relevance of NMDA receptor antibody-specific index for diagnosis and prognosis in patients with anti-NMDA receptor encephalitis. *Sci Rep*. (2023) 13:12696. doi: 10.1038/s41598-023-38462-6

11. Lai M, Hughes EG, Peng X, Zhou L, Gleichman AJ, Shu H, et al. AMPA receptor antibodies in limbic encephalitis alter synaptic receptor location. *Ann Neurol*. (2009) 65:424–34. doi: 10.1002/ana.21589

12. Lancaster E, Lai M, Peng X, Hughes E, Constantinescu R, Raizer J, et al. Antibodies to the GABA(B) receptor in limbic encephalitis with seizures: case series and characterisation of the antigen. *Lancet Neurol*. (2010) 9:67–76. doi: 10.1016/S1474-4422(09)70324-2

13. Lai M, Huijbers MG, Lancaster E, Graus F, Bataller L, Balice-Gordon R, et al. Investigation of LGI1 as the antigen in limbic encephalitis previously attributed to potassium channels: a case series. *Lancet Neurol*. (2010) 9:776–85. doi: 10.1016/S1474-4422(10)70137-X

14. Lancaster E, Huijbers MG, Bar V, Boronat A, Wong A, Martinez-Hernandez E, et al. Investigations of caspr2, an autoantigen of encephalitis and neuromyotonia. *Ann Neurol.* (2011) 69:303–11. doi: 10.1002/ana.22297

15. Boronat A, Gelfand JM, Gresa-Arribas N, Jeong HY, Walsh M, Roberts K, et al. Encephalitis and antibodies to dipeptidyl-peptidase-like protein-6, a subunit of Kv4.2 potassium channels. *Ann Neurol.* (2013) 73:120–8. doi: 10.1002/ana.23756

16. Petit-Pedrol M, Armangue T, Peng X, Bataller L, Cellucci T, Davis R, et al. Encephalitis with refractory seizures, status epilepticus, and antibodies to the GABAA receptor: a case series, characterisation of the antigen, and analysis of the effects of antibodies. *Lancet Neurol.* (2014) 13:276–86. doi: 10.1016/S1474-4422(13)70299-0

17. Martinez-Hernandez E, Ariño H, McKeon A, Iizuka T, Titulaer MJ, Simabukuro MM, et al. Clinical and immunologic investigations in patients with stiff-person spectrum disorder. *JAMA Neurol.* (2016) 73:714–20. doi: 10.1001/jamaneurol.2016.0133

18. Landa J, Guasp M, Míguez-Cabello F, Guimarães J, Mishima T, Oda F, et al. GluK2 encephalitis study group. Encephalitis with autoantibodies against the glutamate kainate receptors GluK2. *Ann Neurol.* (2021) 90:101–17. doi: 10.1002/ana.26098

19. Martinez-Hernandez E, Guasp M, García-Serra A, Maudes E, Ariño H, Sepulveda M, et al. Clinical significance of anti-NMDAR concurrent with glial or neuronal surface antibodies. *Neurology.* (2020) 94:e2302–e10. doi: 10.1212/WNL.0000000000009239

20. Nagata N, Kanazawa N, Mitsuhata T, Iizuka M, Nagashima M, Nakamura M, et al. Neuronal surface antigen-specific immunostaining pattern on a rat brain immunohistochemistry in autoimmune encephalitis. *Front Immunol.* (2023) 13:1066830. doi: 10.3389/fimmu.2022.1066830

21. Balu R, McCracken L, Lancaster E, Graus F, Dalmau J, Titulaer MJ. A score that predicts 1-year functional status in patients with anti-NMDA receptor encephalitis. *Neurology.* (2019) 92:e244–52. doi: 10.1212/WNL.0000000000006783

22. Flanagan EP, Geschwind MD, Lopez-Chiriboga AS, Blackburn KM, Turaga S, Binks S, et al. Autoimmune encephalitis misdiagnosis in adults. *JAMA Neurol.* (2023) 80:30–9. doi: 10.1001/jamaneurol.2022.4251

23. Dalmau J. NMDA receptor encephalitis and other antibody-mediated disorders of the synapse: The 2016 Cotzias Lecture. *Neurology.* (2016) 87:2471–82. doi: 10.1212/WNL.0000000000003414

24. Al-Diwani A, Theorell J, Damato V, Bull J, McGlashan N, Green E, et al. Cervical lymph nodes and ovarian teratomas as germinal centres in NMDA receptor-antibody encephalitis. *Brain.* (2022) 145:2742–54. doi: 10.1093/brain/awac088

25. Martinez-Hernandez E, Horvath J, Shiloh-Malawsky Y, Sangha N, Martinez-Lage M, Dalmau J. Analysis of complement and plasma cells in the brain of patients with anti-NMDAR encephalitis. *Neurology.* (2011) 77:589–93. doi: 10.1212/WNL.0b013e318228c136

26. Titulaer MJ, Höftberger R, Iizuka T, Leypoldt F, McCracken L, Cellucci T, et al. Overlapping demyelinating syndromes and anti–N-methyl-D-aspartate receptor encephalitis. *Ann Neurol.* (2014) 75:411–28. doi: 10.1002/ana.24117

Frontiers in Immunology

Explores novel approaches and diagnoses to treat immune disorders.

The official journal of the International Union of Immunological Societies (IUIS) and the most cited in its field, leading the way for research across basic, translational and clinical immunology.

Discover the latest Research Topics

See more →

Frontiers

Avenue du Tribunal-Fédéral 34
1005 Lausanne, Switzerland
frontiersin.org

Contact us

+41 (0)21 510 17 00
frontiersin.org/about/contact